

Imperial College London  
Department of Life Sciences

# Ionic liquid pretreatment of lignocellulosic biomass

Agnieszka Brandt

Thesis submitted as partial fulfilment of the  
requirements for the degree of Doctor of Philosophy of  
Imperial College London  
2007-2011

## Declaration

The work described in this thesis was carried out at Imperial College London between October 2007 and November 2010. The entire body of work is my own unless expressly stated to the contrary and has not been submitted previously for a degree at this or any other university.

## Statement of copyright

The copyright of this thesis rests with the author. No quotation from it should be published without the prior written consent of the author and information derived from it should be appropriately acknowledged.

---

## Acknowledgments

First of all, I want to thank my supervisors Dr. David Leak, Prof. Tom Welton and Dr. Richard Murphy for their helpful supervision, inspirational advice and warm personal interaction. I believe we made excellent use of the fact that the Biology and Chemistry buildings are located shoulder by shoulder. I also would like to thank the people from the Porter Institute for the funding and providing the platform that brought us together.

This thesis would not be the same without the valuable contributions of Alistair McIntosh and Hemal Bosamia who worked hard on the methyl carbonate synthesis and Julian Gianuzzi who performed initial saccharification experiments.

I wish to extend my thanks to all colleagues in the Welton, Murphy and Leak group, past and present for help and company. A major thank-you goes to Heiko, best lunch buddy on campus and Über-colleague. It was a great experience to work with Dr. Jason Hallett. I must thank him for uncounted inspiring discussions about basically anything - including science. I am indebted to Dr. Michael Ray for his continued support by running the biomass laboratory, sharing his wisdom and protocols and giving a hand on many occasions. I also owe thanks to James Mansfield for looking after the HPLC system in the fermentation lab, which provided data for so many figures in this thesis. I would like to thank Tom Wells, Andy, Trang, Georgina, Syareeda, Lorna, Azri and Matthew for assembling into a supportive and very international chemistry family. At the Murphy lab, Nick and Lucy (Lei) were always there to help and give advice. At the Leak lab, I would like to thank Nicky, Bryn, Rochelle, Alex and Jeremy, who always made me feel welcome, although I mostly came to steal things.

I would like to thank my mum and dad for their support throughout my life. They instilled a desire in me to try my best and the belief that continued hard work will make things happen. Many people helped keeping up the spirits and prevented me from over-working by saying, cooking or organising pleasant things. Examples are my big brother

Rene, Antje, my flatmates Franzi and Monica. In addition, the people from Badminton and members of the IC choir, who helped extending my fitness, vocal abilities and sometimes restoring my sanity.

Another list would include everyone, who paved the path that led me into the jungle that is science: various teachers, the Röpke family, Heidi Reinholz, and a few wonderful supervisors such as the duo Vladimir and Wolfgang from TU Munich and Reinhard, Nada and Mirjam from the MPI in Martinsried.

I want to thank my ~~fiancé~~ *husband* Clifford, who did not mind listening to my excited gibberish about ionic liquids on a daily basis. I am immensely happy that we are continuing our collaboration and very enthusiastic about starting our future. Love you lots!

Last but not least I must thank the Micky Maus magazines I used to read when I was little. They are the earliest known supporters of my save the planet attitude and indirectly responsible for quite a lot of this.

---

## Publications

Part of the work presented in this thesis has been published in the peer-reviewed literature and/or has been patented:

- Brandt, A.; Hallett, J. P.; Leak, D. J.; Murphy, R. J.; Welton, T., The effect of the ionic liquid anion in the pretreatment of pine wood chips. *Green Chemistry* **2010**, *12* (4), 672-679.
- Brandt, A.; Ray, M. J.; To, T. Q.; Leak, D. J.; Murphy, R.; Welton, T., Ionic liquid pretreatment of lignocellulosic biomass with ionic liquid water mixtures. *Green Chemistry* **2011**, *13*, 2489-2499
- Brandt, A.; Welton, T.; Leak, D. J.; Murphy R. J., Ionic liquids for pretreating lignocellulosic biomass; GB 1021319.7, filed on 15/12/2010

## Abstract

This thesis is concerned with the thermal treatment of lignocellulosic biomass using ionic liquids for the purpose of comminution *via* dissolution, for fractionating the biological composite and for obtaining aqueous solutions of carbohydrate monomers from the pulp *via* enzymatic hydrolysis. A major focus was the relationship between the choice of the anion and the effectiveness of the treatment.

The synthesis of a range of 1-butyl-3-methylimidazolium ionic liquids with strongly hydrogen-bond basic anions was accomplished. Selected, process-relevant physicochemical properties were measured, such as the Kamlet-Taft solvent polarity, hygroscopicity and thermal stability. It was shown that 1-butyl-3-methylimidazolium acetate is not stable at 120°C, while other ionic liquids e.g. 1-butyl-3-methylimidazolium hydrogen sulfate exhibit very good long-term thermal stability. It was shown that hydrogen-bond basic 1-butyl-3-methylimidazolium ionic liquids attract more than stoichiometric quantities of water when exposed to air, suggesting that ionic liquid pretreatment under anhydrous conditions is difficult to achieve.

Dissolution of air-dried wood chips in 1-butyl-3-methylimidazolium ionic liquids was attempted. It was shown that the large particle size and the moisture contained in the biomass hamper complete dissolution. The hydrogen-bond basicity of the ionic liquid, described by the Kamlet-Taft parameter  $\beta$ , was correlated with the ability to expand as well as partially and anisotropically dissolve wood chips.

Pretreatment of lignocellulosic biomass with 1-butyl-3-methylimidazolium methyl sulfate, 1-butyl-3-methylimidazolium hydrogen sulfate and 1-butyl-3-methylimidazolium methanesulfonate was explored and high saccharification yields were reported. It was found that successful application of methyl sulfate and hydrogen sulfate ionic liquids requires addition of water and that comparatively high water contents are tolerated. Fractionation of lignocellulose into an insoluble cellulose fraction, a solubilised hemicellulose fraction and a lignin containing precipitate was achieved. The influence of water content, pretreatment

time and biomass type on the enzymatic saccharification yield and the extent of hemicellulose solubilisation, hydrolysis and dehydration were examined.

# Table of contents

<b>Declaration .....</b>	<b>1</b>
<b>Acknowledgments .....</b>	<b>2</b>
<b>Publications.....</b>	<b>4</b>
<b>Abstract .....</b>	<b>5</b>
<b>List of Abbreviations .....</b>	<b>14</b>
<b>List of Figures .....</b>	<b>17</b>
<b>List of Tables.....</b>	<b>25</b>
<b>List of Schemes .....</b>	<b>26</b>
<b>Thesis overview .....</b>	<b>27</b>
<b>Objectives.....</b>	<b>28</b>
<b>1 Introduction .....</b>	<b>30</b>
1.1 The energy challenge.....	30
1.2 Biorefinery .....	32
1.3 Biorefinery feedstocks.....	33
1.3.1 First generation feedstocks .....	33
1.3.2 Second generation feedstocks.....	33
1.4 The chemical composition of wood .....	35
1.4.1 Cellulose.....	36
1.4.2 Hemicellulose .....	38
1.4.3 Lignin.. ..	38
1.4.4 Lignin-carbohydrate complexes .....	42
1.5 The structure of wood.....	43
1.6 Lignocellulosic energy crops.....	44



---

1.6.1	Miscanthus x giganteus (perennial grass).....	44
1.6.2	Pine (softwood) .....	46
1.6.3	Willow (hardwood).....	47
<b>1.7</b>	<b>Pretreatment of lignocellulosic biomass .....</b>	<b>48</b>
1.7.1	Existing pretreatment methods.....	49
1.7.2	Degradation reactions of sugars .....	52
1.7.2.1	Degradation of pentoses .....	53
1.7.2.2	Degradation of hexoses .....	54
1.7.3	Pseudo-lignins.....	55
1.7.4	The optimal pretreatment process.....	55
<b>1.8</b>	<b>Ionic liquids .....</b>	<b>57</b>
1.8.1	The structure of ionic liquids and implications for their melting point ....	57
1.8.2	Properties of ionic liquids and applications <sup>70</sup> .....	59
<b>2</b>	<b>Synthesis of hydrophilic ionic liquids.....</b>	<b>61</b>
<b>2.1</b>	<b>Introduction .....</b>	<b>61</b>
2.1.1	Acid base combination .....	61
2.1.2	Synthesis with halide intermediates .....	62
2.1.2.1	Purification of starting materials .....	63
2.1.2.2	Quaternisation .....	63
2.1.2.3	Purification of ionic liquid precursor .....	63
2.1.2.4	Ion metathesis.....	64
2.1.2.5	Purification of the ionic liquid product.....	65
2.1.3	Direct alkylation and transesterification.....	65
2.1.4	Ion exchange with silver salts.....	66
2.1.5	Ion metathesis with ion exchange resins.....	67
2.1.6	Methyl carbonate route.....	68
<b>2.2</b>	<b>Materials and Methods.....</b>	<b>70</b>
2.2.1	Reagents .....	70
2.2.2	Instrumentation.....	70
2.2.3	Ionic liquid synthesis .....	70
2.2.3.1	1-Butyl-3-methylimidazolium chloride, [C <sub>4</sub> C <sub>1</sub> im]Cl .....	70
2.2.3.2	1-Butyl-3-methylimidazolium bromide, [C <sub>4</sub> C <sub>1</sub> im]Br.....	71
2.2.3.3	1-Butyl-3-methylimidazolium acetate, [C <sub>4</sub> C <sub>1</sub> im][MeCO <sub>2</sub> ].....	71
2.2.3.4	1-Butyl-3-methylimidazolium dicyanamide, [C <sub>4</sub> C <sub>1</sub> im][N(CN) <sub>2</sub> ].....	72
2.2.3.5	1-Butyl-3-methylimidazolium dimethyl phosphate, [C <sub>4</sub> C <sub>1</sub> im][Me <sub>2</sub> PO <sub>4</sub> ]....	73
2.2.3.6	1-Butyl-3-methylimidazolium methyl sulfate, [C <sub>4</sub> C <sub>1</sub> im][MeSO <sub>4</sub> ].....	74
2.2.3.7	1,1-Butylmethylpyrrolidinium acetate [C <sub>4</sub> C <sub>1</sub> py][MeCO <sub>2</sub> ] .....	74
2.2.3.8	1-Butyl-3-methylimidazolium methyl carbonate, [C <sub>4</sub> C <sub>1</sub> im][MeCO <sub>3</sub> ] .....	75
2.2.3.9	1-Butyl-3-methylimidazolium methanesulfonate, [C <sub>4</sub> C <sub>1</sub> im][MeSO <sub>3</sub> ] .....	75

---

2.2.3.10	1-Butyl-3-methylimidazolium hydrogen sulfate, [C <sub>4</sub> C <sub>1</sub> im][HSO <sub>4</sub> ]	76
2.2.3.11	1-Ethyl-3-methylimidazolium-4-carboxylate, [C <sub>2</sub> C <sub>1</sub> im-4-COO], and 1-ethyl-3-methylimidazolium-5-carboxylate, [C <sub>2</sub> C <sub>1</sub> im-5-COO]	77
2.2.3.12	1-Ethyl-3-methylimidazolium methyl carbonate, [C <sub>2</sub> C <sub>1</sub> im][MeCO <sub>3</sub> ]	77
<b>2.3</b>	<b>Results and Discussion</b>	<b>79</b>
2.3.1	Failure of ion metathesis in dichloromethane in the case of strongly hydrogen-bonding ionic liquids	79
2.3.2	Direct alkylation	81
2.3.3	Ion metathesis using silver salts	82
2.3.4	Methyl carbonate route	84
2.3.4.1	Synthesis and purification of the precursor	84
2.3.4.2	Anion metathesis with methyl carbonate salts	90
2.3.4.3	Summary of the methyl carbonate route	91
2.3.5	Synthesis of [C <sub>4</sub> C <sub>1</sub> im][HSO <sub>4</sub> ] by hydrolysis	93
<b>2.4</b>	<b>Summary</b>	<b>93</b>
<b>3</b>	<b>Solvent polarity of hydrophilic ionic liquids</b>	<b>94</b>
<b>3.1</b>	<b>Introduction</b>	<b>94</b>
3.1.1	Kamlet-Taft solvent polarity	94
3.1.1.1	Polarisability ( $\pi^*$ )	95
3.1.1.2	Hydrogen-bond basicity ( $\beta$ )	96
3.1.1.3	Hydrogen-bond acidity ( $\alpha$ )	97
3.1.1.4	The Kamlet-Taft parameters of ionic liquids	99
3.1.2	Ionic liquid stability	100
3.1.3	Hygroscopicity of ionic liquids	102
<b>3.2</b>	<b>Materials and Methods</b>	<b>104</b>
3.2.1	Materials	104
3.2.2	Karl Fischer titration	104
3.2.3	Determination of ionic liquid hygroscopicity	104
3.2.4	Spectroscopy	104
3.2.5	Measurement of Kamlet-Taft parameters	105
3.2.6	Measuring the Kamlet-Taft parameters of ionic liquids with a melting point above room temperature	105
3.2.7	Thermogravimetric analysis	106
3.2.8	Kugelrohr distillation of [C <sub>4</sub> C <sub>1</sub> py][MeCO <sub>2</sub> ]	106
<b>3.3</b>	<b>Results and Discussion</b>	<b>107</b>
3.3.1	Kamlet-Taft parameters of hydrophilic ionic liquids	107
3.3.1.1	Accuracy of Kamlet-Taft values	107
3.3.2	Practical considerations for the use of Reichhardt's dye	108
3.3.2.1	The effect of moisture on the Kamlet-Taft values	109

---

3.3.2.2	Thermochromism of solvatochromic dyes.....	109
3.3.3	Kamlet-Taft parameters of hydrophilic ionic liquids.....	110
3.3.3.1	The effect of hydrophilic anions on the Kamlet-Taft polarity of ionic liquids .....	111
3.3.4	The effect of hydrophilic anions on the hydrogen-bonding between ..... cations and anions .....	113
3.3.4.1	The effect of salt impurities on the polarity parameters .....	114
3.3.5	Physical properties that are affected by the hydrogen-bond basicity of the anion.....	115
3.3.5.1	Effect on the water-miscibility.....	115
3.3.5.2	Hygroscopicity of ionic liquids .....	116
3.3.5.3	Ionic liquid stability at elevated temperatures .....	119
3.3.5.4	Decomposition mechanism for [C <sub>4</sub> C <sub>1</sub> pyrr][MeCO <sub>2</sub> ] .....	122
<b>3.4</b>	<b>Summary .....</b>	<b>123</b>
<b>4</b>	<b>Literature review: Solubilisation and pretreatment of lignocellulosic biomass with ionic liquids.....</b>	<b>125</b>
4.1	Solubility of cellulose in ionic liquids .....	125
4.2	Solubility of lignocellulose in ionic liquids.....	126
4.3	Energy requirements for grinding lignocellulosic biomass.....	127
4.4	Selective extraction of lignocellulose components during ionic liquid pretreatment.....	128
4.4.1	The effect of ionic liquid pretreatment on the composition of lignocellulosic biomass.....	129
4.4.2	Interactions of ionic liquids and lignin.....	130
4.5	Carbohydrates in ionic liquids.....	132
4.5.1	Carbohydrate depolymerisation .....	132
4.5.1.1	Chemical depolymerisation in ionic liquids.....	132
4.5.1.2	Enzymatic saccharification.....	134
4.5.2	Other reactions of sugars in ionic liquids.....	135
<b>5</b>	<b>The impact of the ionic liquid anion on the swelling and dissolution of wood chips .....</b>	<b>137</b>
5.1	Materials and Methods.....	137
5.1.1	Preparation of wood chips.....	137
5.1.2	Swelling experiments .....	138
5.1.3	Dissolution of pine flour .....	139
5.1.4	Pine chip processing .....	139
5.2	Results and Discussion.....	141
5.2.1	Experimental design.....	141
5.2.2	Swelling and dissolution of pine wood chips .....	143

5.2.3	The influence of moisture on the disintegration of pine chips .....	148
5.2.4	The influence of the anion basicity .....	150
5.2.5	The influence of the pretreatment temperature .....	153
5.2.6	Wood chip regeneration .....	156
5.2.7	The effect of the biomass type .....	158
<b>5.3</b>	<b>Summary .....</b>	<b>160</b>
<b>6</b>	<b>Pretreatment of lignocellulosic biomass with ionic liquid water mixtures.....</b>	<b>162</b>
<b>6.1</b>	<b>Materials and Methods.....</b>	<b>162</b>
6.1.1	Materials.....	162
6.1.2	Enhanced liquid uptake of Miscanthus chips at 80°C .....	163
6.1.3	Determination of biomass moisture content.....	163
6.1.4	Ionic liquid pretreatment and isolation of pretreated pulp.....	164
6.1.5	Lignin isolation.....	164
6.1.6	Enzymatic saccharification .....	165
6.1.7	Determination of extractives.....	165
6.1.8	Compositional analysis.....	166
6.1.9	Calculating the delignification.....	166
6.1.10	Quantification of solubilised sugars and furfurals.....	166
6.1.11	Ionic liquid treatment of cellulose .....	167
<b>6.2</b>	<b>Results and Discussion .....</b>	<b>168</b>
6.2.1	Treatment of Miscanthus chips with [C <sub>4</sub> C <sub>1</sub> im][MeSO <sub>4</sub> ] .....	168
6.2.2	Design of pretreatment experiment .....	170
6.2.3	The notation for ionic liquid water mixtures .....	172
6.2.4	Miscanthus composition .....	172
6.2.5	Sugar yields after pretreatment of Miscanthus with 1-butyl-3-methylimidazolium methyl sulfate water mixtures .....	173
6.2.6	The impact of the solid loading.....	175
6.2.7	The influence of the wash solvent on biomass recovery and fractionation .....	176
6.2.8	Lignin precipitation and the impact of the wash solvent on the yield... ..	180
6.2.9	Recycling of [C <sub>4</sub> C <sub>1</sub> im][MeSO <sub>4</sub> ].....	183
6.2.10	Enzymatic digestibility after pretreatment with [C <sub>4</sub> C <sub>1</sub> im][HSO <sub>4</sub> ]-water mixtures.....	184
6.2.11	Biomass composition after pretreatment with [C <sub>4</sub> C <sub>1</sub> im][MeSO <sub>4</sub> ] and [C <sub>4</sub> C <sub>1</sub> im][HSO <sub>4</sub> ]-water mixtures .....	185
6.2.12	Precipitate yield from [C <sub>4</sub> C <sub>1</sub> im][HSO <sub>4</sub> ] water mixtures.....	187
6.2.13	The time dependency of the saccharification yield.....	187
6.2.14	Solubilised sugars and sugar degradation products .....	189
6.2.15	The influence of the ionic liquid anion .....	194

---

6.2.15.1	The effect of the anion on the composition .....	195
6.2.15.2	The effect of the anion on the enzymatic digestibility.....	196
6.2.15.3	The effect of the anion on the sugar solubilisation and the generation of furfurals . .....	198
6.2.15.4	The effect of the anion on the lignin recovery .....	199
6.2.16	The effect of the Kamlet-Taft parameter $\beta$ on the saccharification yield ... ..	201
6.2.17	The effect of the lignocellulose type: pretreatment of willow and pine with [C <sub>4</sub> C <sub>1</sub> im][HSO <sub>4</sub> ] <sub>80%</sub> and [C <sub>2</sub> C <sub>1</sub> im][MeCO <sub>2</sub> ] <sub>80%</sub> .....	202
6.2.17.1	The composition of willow and pine before and after pretreatment.....	202
6.2.17.2	The effect of the biomass type on the glucose yield .....	203
6.2.17.3	The effect of the biomass type on the concentration of solubilised sugars and furfurals .....	205
6.2.17.4	The effect of the biomass type on the delignification and the lignin recovery .....	206
6.2.18	Pretreatment of Miscanthus and willow chips with [C <sub>4</sub> C <sub>1</sub> im][HSO <sub>4</sub> ] <sub>80%</sub> .....	207
6.2.19	Treatment of cellulose with [C <sub>4</sub> C <sub>1</sub> im][HSO <sub>4</sub> ]and [C <sub>4</sub> C <sub>1</sub> im][MeSO <sub>4</sub> ] .....	209
<b>6.3</b>	<b>Summary .....</b>	<b>212</b>
<b>7</b>	<b>General summary, outlook and conclusions.....</b>	<b>214</b>
<b>7.1</b>	<b>The importance of (ligno)cellulose solubility in ionic liquid pretreatment .....</b>	<b>214</b>
<b>7.2</b>	<b>Comparison with other pretreatment options .....</b>	<b>215</b>
7.2.1	Advantages of using ionic liquids .....	215
7.2.2	Disadvantages/challenges of ionic liquid pretreatment .....	216
<b>7.3</b>	<b>Comparison of different ionic liquids.....</b>	<b>218</b>
<b>7.4</b>	<b>A putative ionic liquid process .....</b>	<b>219</b>
<b>7.5</b>	<b>Further work .....</b>	<b>222</b>
7.5.1	Ionic liquid synthesis .....	222
7.5.2	Stability of dialkylimidazolium acetate ionic liquids .....	223
7.5.3	Ionic liquid pretreatment .....	223
7.5.3.1	Optimisation of ionic liquid composition .....	223
7.5.3.2	Hemicellulose recovery .....	223
7.5.3.3	Optimising other process variables .....	224
7.5.3.4	Investigation of separations involving ionic liquids and biomass .....	224
7.5.3.5	Grinding after ionic liquid pretreatment .....	224
7.5.3.6	Characterisation of soluble carbohydrate oligomers .....	224
7.5.3.7	Determining the yield of organic acids .....	225
7.5.3.8	Characterisation of isolated lignin .....	225
<b>7.6</b>	<b>Over-all conclusions .....</b>	<b>225</b>

<b>8</b>	<b>References.....</b>	<b>229</b>
----------	------------------------	------------

## List of Abbreviations

[C <sub>4</sub> C <sub>1</sub> im]	1-Butyl-3-methylimidazolium
[C <sub>2</sub> C <sub>1</sub> im]	1-Ethyl-3-methylimidazolium
[C <sub>4</sub> C <sub>1</sub> pyrr]	N,N-butylmethylpyrrolidinium
[MeCO <sub>2</sub> ]	Acetate
[OTf]	Trifluoromethanesulfonate, triflate
[N(Tf) <sub>2</sub> ]	Bis(trifluoromethylsulfonyl)imide, bisimide
[N(CN) <sub>2</sub> ]	Dicyanamide
[MeSO <sub>4</sub> ]	Methyl sulfate
[Me <sub>2</sub> PO <sub>4</sub> ]	Dimethyl phosphate
[MeSO <sub>3</sub> ]	Methanesulfonate
[MeCO <sub>3</sub> ]	Methyl carbonate
[HSO <sub>4</sub> ]	Hydrogen sulfate
HMF	5-(Hydroxymethyl)furfural
DMSO	Dimethyl sulfoxide
D <sub>2</sub> O	Deuterated water
iPrOH	Isopropyl alcohol, propan-2-ol
{ <sup>1</sup> H}	Proton-decoupled
NMR	Nuclear magnetic resonance
HPLC	High performance liquid chromatography
ATR	Attenuated total reflection
IR	Infrared
UV/Vis	Ultraviolet and visible light
TGA	Thermogravimetric analysis

LSIMS	Liquid secondary ion mass spectrometry
ESI	Electrospray ionisation
Vol%	Volume percent
Wt%	Weight percent
ODW	Oven-dried weight
$T_{\text{onset}}$	Onset temperature of decomposition
RD	Reichhardt's dye
$\alpha$	Kamlet-Taft parameter for hydrogen bond donation capacity
$\beta$	Kamlet-Taft parameter for hydrogen bond acceptor capacity
$\pi^*$	Kamlet-Taft parameter for dipolarity/polarisability
$\bar{\nu}$	Wavenumber (in $\text{cm}^{-1}$ )
$\text{pK}_a$	Acid dissociation constant at logarithmic scale
pH	Proton activity in solution at logarithmic scale
$\text{cm}^{-1}$	Number of wave lengths per centimetre, inverse centimetre
min	Minute
h	Hour
ppm	Parts per million (weight/weight)
ml	Millilitre
mol	Mole
mmol	Millimole



---

M	Moles/litre
l	Litre
g	Gram
Hz, MHz	Hertz, Mega hertz
°C	Degree centigrade
m/z	Mass-to-charge ratio
Calc.	Calculated
max.	Maximum
$\Delta\nu$	Enhanced solvatochromic shift
$\beta$ -O-4	Common ether bond between two lignin subunits

## List of Figures

Figure 1: Global surface temperature anomalies over the past 130 years. <sup>2</sup> .....	30
Figure 2: Current and predicted world energy consumption. The energy consumption is projected to grow by 48% by 2035 (in $10^{15}$ J). <sup>3</sup> .....	31
Figure 3: Energy consumption in the EU-27 until 2006, allocated to various sectors. The transportation sector consumed just under a third of the total energy. <sup>4</sup> .....	32
Figure 4: Biological, thermal and chemical route to biofuels and renewable chemicals (adapted from Pickett <i>et al.</i> <sup>5</sup> ).....	33
Figure 5: Structural arrangement of the major components in the cell walls of lignocellulosic biomass <sup>7</sup> .....	34
Figure 6: Conversion of first generation and second generation feedstocks <i>via</i> the biological route. ....	35
Figure 7: Glucose, the monomer of cellulose with $\alpha$ (a) and $\beta$ (b) confirmation at the anomeric carbon. ....	36
Figure 8: Stretched chain conformation of cellulose (a) and helical conformation of $\alpha$ -amylose in starch (b) <sup>14</sup> .....	36
Figure 9: Covalent linkages and hydrogen bonding in crystalline cellulose <sup>16</sup> .....	37
Figure 10: The hexoses and pentoses typically found in hemicellulose. ....	38
Figure 11: Structure of arabino-4- O-methylglucuronoxylan, a hemicellulose found in softwood (adapted from <sup>18</sup> ).....	38
Figure 12: The three monolignols from which lignin is synthesised. The monomers vary in the substitution at the C-3 and C-5 ring positions (adapted from <sup>18</sup> ). ....	39
Figure 13: Lignin distribution in the cell corner middle lamella (CCML) and the outer secondary cell wall (S1). The lignin in the S1 wall appears to be aligned to the cellulose fibrils. The picture was obtained with transmission microscopy of <i>Pinus radiata</i> wood after permanganate staining. Scale bar 440 nm. <sup>21</sup> .....	40
Figure 14: Lignin fragment with various C-O and C-C linkages typically present in native lignin <sup>24</sup> .....	41
Figure 15: Lignin-carbohydrate complexes in involving ferulic acid.....	42
Figure 16: Ferulic acid dimer cross link.....	43
Figure 17: Lignin distribution in lignified cell walls of <i>Pinus radiata</i> visualised by confocal fluorescence microscopy (160 x 160 $\mu\text{m}$ ). The lignin autofluorescence at 350 nm was excited. The empty voids (green arrow), the cellulose and lignin containing cell walls (red arrow) and the cellulose free middle lamella (blue arrow) are marked. Brighter areas show the high lignin concentration in the middle lamella. <sup>20</sup> .....	44

- Figure 18: *Miscanthus* plants at the University of Illinois.<sup>31</sup> ..... 45
- Figure 19: Cross-section of a *Miscanthus* culm. The outer ring and the pith are visible, as well as the vascular bundles (own photo)..... 45
- Figure 21: Cross section of a willow showing the bark, fibre cells, the vessels involved in nutrient transport and longitudinal ray cells.<sup>33</sup> Scale bar = 1 mm ..... 47
- Figure 22: A wood chip excised from a *Salix sp.* branch. Scale bar =10 mm..... 47
- Figure 23: Hexose and pentose degradation products obtained under acidic conditions: 5-Hydroxymethylfurfural (HMF, left) and 2-furaldehyde (right). ..... 50
- Figure 24: Time profile of cellulose hydrolysis at 200°C in dilute sulfuric acid (0.05 M). The concentrations of various compounds was examined.<sup>62</sup> Abbreviations: GLC, Glucose; FA, Formic acid; LA, Levulinic acid; HMF, Hydroxymethylfurfural, FUR, Furfural..... 55
- Figure 25: Common cations used in modern ionic liquids ..... 58
- Figure 26: Selection of anions used in modern ionic liquids..... 59
- Figure 27: Ion metathesis of [C<sub>4</sub>C<sub>1</sub>im]Cl with Li[NTf<sub>2</sub>] to obtain [C<sub>4</sub>C<sub>1</sub>im][NTf<sub>2</sub>] in dichloromethane. Lower phase: solid inorganic salt phase. Upper phase: dichloromethane with dissolved ionic liquid..... 64
- Figure 28: Synthesis of [C<sub>4</sub>C<sub>1</sub>im][MeCO<sub>2</sub>] in aqueous solution using an ion exchange resin. .... 68
- Figure 29: <sup>1</sup>H-NMR spectrum of [C<sub>4</sub>C<sub>1</sub>im][MeSO<sub>3</sub>] after ion metathesis with [C<sub>4</sub>C<sub>1</sub>im]Cl and sodium methanesulfonate (in DMSO-d<sub>6</sub>). The integral of the peak (1.94) at 2.31 ppm, assigned to the methyl group on the anion, is only 65% of the expected value. Peaks that were not integrated are caused by residual ethyl acetate and dichloromethane (spectrum recorded by Nur Hasyareeda Hassan). ..... 80
- Figure 30: Products found after reaction of 1-butylimidazole with dimethyl carbonate at 180°C for 24 h without methanol (only one regioisomer is depicted). .. 85
- Figure 31: <sup>1</sup>H-NMR spectrum of the solid product obtained after reaction of 1-ethylimidazole with dimethyl carbonate containing 1-ethyl-3-methylimidazolium-4-carboxylate and 1-ethyl-3-methylimidazolium-5-carboxylate (in D<sub>2</sub>O)..... 87
- Figure 32: <sup>1</sup>H NMR spectrum of the crude product from the reaction of 1-butylimidazole with dimethyl carbonate in methanol. Displayed is the region of the ring proton signals. Three large peaks (and their <sup>13</sup>C satellites) give evidence of the formation of 1,3-dialkylimidazolium cations. Residual butylimidazole is present, as well as small quantities of carboxylated and over-alkylated product..... 88

- Figure 33:  $^1\text{H-NMR}$  spectrum of recrystallised product from the synthesis of  $[\text{C}_4\text{C}_1\text{im}][\text{MeCO}_3]$  in  $\text{DMSO-d}_6$ . The sample was prepared in a glove box and the  $\text{DMSO-d}_6$  was taken from a freshly opened ampoule..... 89
- Figure 34:  $^1\text{H-NMR}$  spectrum of product crystals before (red) and after (blue) addition of water (in  $\text{DMSO-d}_6$ ). ..... 89
- Figure 35: The  $\pi^*$  dye *N,N*-diethyl-4-nitroaniline ..... 95
- Figure 36: The  $\beta$  dye 4-nitroaniline and its homomorphic  $\pi^*$  dye ..... 96
- Figure 37: The  $\alpha$  dye 2,6-diphenyl-4-(2,4,6-triphenylpyridinium)phenoxide or Reichhardt's dye ..... 97
- Figure 38: 4-nitroanisole, an alternative  $\pi^*$  probe ..... 98
- Figure 39: Determining  $T_{\text{onset}}$  of two ionic liquids by fitting tangents to the decomposition curves. .... 101
- Figure 40: Kamlet-Taft parameters of dry hydrophilic 1-butyl-3-methylimidazolium ionic liquids. The parameter  $\beta$  varies widely, while  $\pi^*$  and  $\alpha$  are only slightly affected by the nature of the anion..... 112
- Figure 41: The influence of anion basicity of 1-butyl-3-methylimidazolium ionic liquids on the apparent hydrogen-bond acidity of the ionic liquid: the Kamlet-Taft  $\beta$  parameters of various ionic liquids were correlated with the position of the peak maximum of Reichhardt's dye. A negative correlation can be observed. .... 112
- Figure 42: Possible cause of the reduction of the  $\alpha$  value with increasing hydrogen-bond basicity of the anion. A: Weakly hydrogen-bonding anions let Reichhardt's dye with its phenoxide oxygen coordinate to the C-2 proton. B: Strongly hydrogen-bonding anions displace the dye from C-2 position and thus reduce the apparent hydrogen-bond acidity. .... 113
- Figure 43: Correlation between the Kamlet-Taft parameter  $\beta$  of 1-butyl-3-methylimidazolium ionic liquids and the  $^1\text{H-NMR}$  chemical shift of the proton attached to carbon C-2 of the cation (in  $\text{DMSO-d}_6$ ). The higher the anion basicity was the larger was the chemical shift.  $R^2$  of the regression line is 0.978 and the p-value  $2 \cdot 10^{-4}$ . .... 114
- Figure 44: Moisture uptake by 1-butyl-3-methylimidazolium acetate monitored with ATR-IR spectroscopy. The uptake of water from the air is evidenced by an emerging broad band between  $3200\text{ cm}^{-1}$  and  $3500\text{ cm}^{-1}$ . Pink: dry ionic liquid (6500 ppm, 0.07 water molecules per ion pair), blue: 15 min, black: 45 min, red: 75 min. .... 117
- Figure 45: ATR-IR bands of the O-H stretching vibrations in moist  $[\text{C}_4\text{C}_1\text{im}][\text{MeSO}_4]$  (red),  $[\text{C}_4\text{C}_1\text{im}][\text{MeSO}_3]$  (blue),  $[\text{C}_4\text{C}_1\text{im}]\text{Br}$  (black) and  $[\text{C}_4\text{C}_1\text{im}]\text{Cl}$  (pink). ..... 118
- Figure 46: Correlation between the Kamlet-Taft  $\beta$  parameter of dry 1-butyl-3-methylimidazolium ionic liquids with the number of water

molecules per ion pair when the ionic liquids are equilibrated with air. The fit of the trend line is $R^2=0.966$ .....	119
Figure 47: Long-term stability of hydrophilic ionic liquids at 120°C .....	120
Figure 48: Decomposition of [C <sub>4</sub> C <sub>1</sub> im][MeCO <sub>2</sub> ] at 120°C and first derivative of the mass loss (red line) .....	121
Figure 49: Dissolution of beech powder in [C <sub>2</sub> C <sub>1</sub> im][MeCO <sub>2</sub> ] <sup>151</sup> .....	127
Figure 50: Schematic depiction of a pine chip with 3 growth rings. Definition of lengths a (tangential), b (radial) and c (axial) relative to growth rings. ...	142
Figure 51: Wood chips used for swelling experiments: pine (left), willow (middle) and <i>Miscanthus</i> (right) .....	142
Figure 52: Swelling of pine chips incubated in distilled water at 90°C in the 3 directions defined in Figure 50. ....	143
Figure 53: Swelling of pine chips treated at 120°C with: a [C <sub>4</sub> C <sub>1</sub> im][OTf], b [C <sub>4</sub> C <sub>1</sub> im][N(CN) <sub>2</sub> ], c [C <sub>4</sub> C <sub>1</sub> im][MeCO <sub>2</sub> ]. The expansion is relative to length .....	145
Figure 54: Wood chips (pine, <i>Miscanthus</i> , willow) immersed in [C <sub>4</sub> C <sub>1</sub> im][MeCO <sub>2</sub> ]. Top: before pretreatment. Bottom: after 70 min pretreatment at 120°C.	147
Figure 55: Dry pine specimens treated at 120°C for 15 h with [C <sub>4</sub> C <sub>1</sub> im][Me <sub>2</sub> PO <sub>4</sub> ] (left), [C <sub>4</sub> C <sub>1</sub> im][MeCO <sub>2</sub> ] (middle) and [C <sub>4</sub> C <sub>1</sub> im]Cl (right). The specimen in the middle is a meshed pine chip. ....	149
Figure 56: The water content of [C <sub>4</sub> C <sub>1</sub> im][MeCO <sub>2</sub> ] during the swelling of a dried willow chip at 120°C determined by Karl Fischer titration. ....	150
Figure 57: Swelling of pine chips after immersion in various 1-butyl-3-methylimidazolium ionic liquids. The relative expansion in tangential direction ( $a/a_0$ ) is shown, which is the ratio between the length after swelling ( $a$ ) and the length before immersion of the chips in ionic liquid ( $a_0$ ). The expansion shown was measured after 35 h incubation at 120°C. ....	151
Figure 58: Correlation of pine chip swelling and dissolution in the tangential (a), radial (b) and axial (c) direction in 1-butyl-3-methylimidazolium ionic liquids at 120°C with the Kamlet-Taft parameter $\beta$ . Expansion and shrinkage at 3 time-points is shown. Anions 1- [OTf], 2 - [N(CN) <sub>2</sub> ], 3 - [MeSO <sub>4</sub> ], 4 - [Me <sub>2</sub> PO <sub>4</sub> ], 5 - [MeCO <sub>2</sub> ]. $R^2 = 0.760$ and $p = 0.054$ for the regression line shown for $a/a_0$ . ....	152
Figure 59: Expansion of pine chips immersed in 1-butyl-3-methylimidazolium ionic liquids at various temperatures (60, 90 and 120°C) in the direction tangential to the growth rings. The expansion depends on the ionic liquid and the temperature. ....	155
Figure 60: Pine chip regeneration in methanol after 18 h treatment with [C <sub>4</sub> C <sub>1</sub> im][MeCO <sub>2</sub> ] .....	156

Figure 61: The dimensions of pine chips over the course of ionic liquid pretreatment with [C <sub>4</sub> C <sub>1</sub> im][MeCO <sub>2</sub> ] at 120°C followed by regeneration and washing in methanol, drying and incubation with cellulose and hemicellulose hydrolysing enzymes.....	157
Figure 62: Swelling profile of a willow chip immersed in [C <sub>4</sub> C <sub>1</sub> im][MeCO <sub>2</sub> ] containing 1.2 wt% moisture at 120°C.....	159
Figure 63: Swelling profile of a <i>Miscanthus</i> chip immersed in [C <sub>4</sub> C <sub>1</sub> im][MeCO <sub>2</sub> ] containing 1.2 wt% moisture. ....	159
Figure 65: The uptake of various 1-butyl-3-methylimidazolium ionic liquids and water into <i>Miscanthus</i> chips at 80°C. Ionic liquid anions (left to right): acetate, methyl sulfate, triflate, dicyanamide, bis(trifluoromethylsulfonyl)imide, dimethyl phosphate .....	168
Figure 66: Images of <i>Miscanthus</i> wood dissolved in wet [C <sub>4</sub> C <sub>1</sub> im][MeSO <sub>4</sub> ] using light transmission microscopy. Left: outer part with fibre cells; right: parenchyma cells. Scale bar corresponds to 100 µm.....	169
Figure 67: Capped glass tubes used for the ionic liquid pretreatment of ground lignocellulosic biomass: <i>Miscanthus</i> (left), willow (middle) and pine (right). ....	170
Figure 68: <i>Miscanthus</i> flour after pretreatment with [C <sub>4</sub> C <sub>1</sub> im][MeSO <sub>4</sub> ]. Left: pretreated at 120°C for 6 h with pure ionic liquid (experiment performed by Julian Giannuzzi). Right: pretreated at 120°C for 22 h with 80/20 vol% ionic liquid water mixtures after washing.....	171
Figure 69: The experimental setup for pretreatment of <i>Miscanthus</i> flour with [C <sub>4</sub> C <sub>1</sub> im][MeSO <sub>4</sub> ] water mixtures.....	172
Figure 70: Saccharification yields after 22 h/120°C pretreatment of ground <i>Miscanthus</i> with [C <sub>4</sub> C <sub>1</sub> im][MeSO <sub>4</sub> ] water mixtures. ....	173
Figure 71: Saccharification samples after completed enzyme hydrolysis of untreated and pretreated <i>Miscanthus</i> . Complete solubilisation of the fibrous biomass was achieved after pretreatment and only a fine brown residue was left behind (right vial). Pretreatment conditions: [C <sub>4</sub> C <sub>1</sub> im][MeSO <sub>4</sub> ] <sub>80%</sub> at 120°C for 22 h. ....	175
Figure 72: Saccharification yields obtained after ionic liquid pretreatment of ground <i>Miscanthus</i> at various solid loadings. Conditions: [C <sub>4</sub> C <sub>1</sub> im][MeSO <sub>4</sub> ] <sub>80%</sub> , 22 h, 120°C, saccharification time was 48 h. ....	176
Figure 73: Ionic liquid pretreatment liquor diluted with methanol. ....	177
Figure 74: Influence of wash solvent on the biomass recovery after pretreatment with [C <sub>4</sub> C <sub>1</sub> im][MeSO <sub>4</sub> ] <sub>80%</sub> for 22 h at 120°C. All experiments were performed in triplicate, except for the washing with acetone. ....	178
Figure 75: ATR-IR spectra of <i>Miscanthus</i> pulp recovered after a pretreatment with [C <sub>4</sub> C <sub>1</sub> im][MeSO <sub>4</sub> ] <sub>80%</sub> for 22 h at 120°C. Wash solvents: water (pink),	

methanol (green), acetone (black), isopropanol (red) and ethanol (blue). .....	178
Figure 76: ATR-IR spectrum of ground <i>Miscanthus</i> : untreated (black), pretreated with [C <sub>4</sub> C <sub>1</sub> im][MeSO <sub>4</sub> ] <sub>80%</sub> at 120°C and washed with isopropanol (blue) and pretreated and Soxhlet extracted with isopropanol (red). ....	179
Figure 77: Influence of the wash solvent on the saccharification yield. Pretreatment with [C <sub>4</sub> C <sub>1</sub> im][MeSO <sub>4</sub> ] <sub>80%</sub> was performed at 120°C for 22 h, the saccharification for 48 h. ....	180
Figure 78: Elemental composition of fractions after exhaustive solvent washing with isopropanol. The carbon content was the highest in the precipitate, which is attributed to the lower abundance of oxygenated carbon in lignin. ....	181
Figure 79: AT-IR spectrum of precipitate isolated from a [C <sub>4</sub> C <sub>1</sub> im][HSO <sub>4</sub> ] <sub>80%</sub> liquor after treatment of ground <i>Miscanthus</i> at 120°C for 22 h upon dilution with water (black line). The precipitate was washed with water and dried prior to the analysis. For comparison, the AT-IR spectrum of a reference lignin (alkali lignin, Aldrich) was recorded (red line). ....	181
Figure 80: Lignin yield after application of various solvent for separating solid and liquid fractions. Water was used for the precipitation ([C <sub>4</sub> C <sub>1</sub> im][MeSO <sub>4</sub> ] <sub>80%</sub> , 120°C, 22 h). ....	182
Figure 81: Ratio of cation to [MeSO <sub>4</sub> ] <sup>-</sup> anions in the ionic liquid recovered after pretreatment of <i>Miscanthus</i> in ionic liquid/water mixtures for 22 h at 120°C. ....	184
Figure 82: Saccharification of <i>Miscanthus</i> pulp after pretreatment with [C <sub>4</sub> C <sub>1</sub> im][HSO <sub>4</sub> ] water and [C <sub>4</sub> C <sub>1</sub> im][MeSO <sub>4</sub> ] water mixtures. The conditions were 120°C and 13 h or 22 h pretreatment time, respectively. ....	185
Figure 83: Effect of pretreatment with [C <sub>4</sub> C <sub>1</sub> im][MeSO <sub>4</sub> ] <sub>80%</sub> and [C <sub>4</sub> C <sub>1</sub> im][HSO <sub>4</sub> ] <sub>80%</sub> at 120°C on the composition of ground <i>Miscanthus</i> for various lengths of time. ....	186
Figure 84: Lignin recovery after pretreatment with [C <sub>4</sub> C <sub>1</sub> im][HSO <sub>4</sub> ] water mixtures at 120°C for 13 h. ....	187
Figure 85: Mass loss during pretreatment with [C <sub>4</sub> C <sub>1</sub> im][MeSO <sub>4</sub> ] <sub>80%</sub> or [C <sub>4</sub> C <sub>1</sub> im][HSO <sub>4</sub> ] <sub>80%</sub> liquors at 120°C. ....	188
Figure 86: Time course study of saccharification and lignin yields obtained from ground <i>Miscanthus</i> . Pretreatment with [C <sub>4</sub> C <sub>1</sub> im][MeSO <sub>4</sub> ] <sub>80%</sub> and [C <sub>4</sub> C <sub>1</sub> im][HSO <sub>4</sub> ] <sub>80%</sub> mixtures was performed at 120°C for up to 26 h. ....	189
Figure 87: Sugar monomers (hemicellulose sugars and glucose) in [C <sub>4</sub> C <sub>1</sub> im][HSO <sub>4</sub> ] <sub>80%</sub> and [C <sub>4</sub> C <sub>1</sub> im][MeSO <sub>4</sub> ] <sub>80%</sub> pretreatment liquors released from <i>Miscanthus</i> during pretreatment at 120°C. ....	190
Figure 88: Amount of furfural and 5-hydroxymethylfurfural found in the pretreatment liquor (per biomass). The data were collected after lignin precipitation. .	191

- Figure 89: Amount of sugar monomers and furfurals dissolved in the ionic liquid liquor  $[\text{C}_4\text{C}_1\text{im}][\text{HSO}_4]_{80\%}$  or  $[\text{C}_4\text{C}_1\text{im}][\text{MeSO}_4]_{80\%}$ . Samples were taken immediately after the pretreatment, before the lignin precipitation. .... 193
- Figure 90: The impact of pretreatment with 80/20% dialkylimidazolium ionic liquid water mixtures on the composition of *Miscanthus*. The anions are ordered according to their  $\beta$  parameter (high values on the left). The cation was 1-butyl-3-methylimidazolium, except for  $[\text{C}_2\text{C}_1\text{im}][\text{MeCO}_2]$ . .... 195
- Figure 91: Anion effect of saccharification yields after pretreatment with 80/20% mixtures of 1,3-dialkylimidazolium ionic liquid and water at 120°C for 22 h. Yields were determined after 96 h of saccharification. The cation was  $[\text{C}_4\text{C}_1\text{im}]^+$ , with exception of  $[\text{C}_2\text{C}_1\text{im}][\text{MeCO}_2]$ . .... 196
- Figure 92: Concentrations of solubilised sugars and sugar dehydration products in 80 vol% ionic liquid liquors after pretreatment of *Miscanthus*. .... 199
- Figure 93: The influence of the anion of 1,3-dialkylimidazolium ionic liquids on the delignification and the lignin yield. *Miscanthus* flour was pretreated with ionic liquid water mixtures at 120°C for 22 h. The ionic liquid cation was  $[\text{C}_4\text{C}_1\text{im}]^+$ , except in  $[\text{C}_2\text{C}_1\text{im}][\text{MeCO}_2]$ . .... 200
- Figure 94: *Miscanthus* lignin precipitated from the pretreatment liquor. Left: after 22 h from  $[\text{C}_4\text{C}_1\text{im}][\text{HSO}_4]_{80\%}$ ; middle: after 22 h from  $[\text{C}_4\text{C}_1\text{im}][\text{MeSO}_3]_{80\%}$ ; right: after 2 h from  $[\text{C}_4\text{C}_1\text{im}][\text{HSO}_4]_{80\%}$ . .... 200
- Figure 95: The Kamlet-Taft  $\beta$  parameter of the pure ionic liquid plotted against the glucose yield after enzymatic saccharification of the pulp after pretreatment with 80/20vol% ionic liquid water mixtures at 120°C for 22 h. A correlation between the glucose yield and the Kamlet-Taft parameter, which represents the hydrogen-bond basicity of the ionic liquid anion, cannot be established. .... 201
- Figure 96: Correlation between lignin removal and hemicellulose content in *Miscanthus* pulp after pretreatment with 1,3-dialkylimidazolium ionic liquids and the enzymatic cellulose digestibility. .... 202
- Figure 97: Composition of willow and pine flour before and after pretreatment with  $[\text{C}_4\text{C}_1\text{im}][\text{HSO}_4]_{80\%}$  and  $[\text{C}_2\text{C}_1\text{im}][\text{MeCO}_2]_{80\%}$ . .... 203
- Figure 98: Glucose yield after enzymatic hydrolysis of various feedstocks pretreated with  $[\text{C}_4\text{C}_1\text{im}][\text{HSO}_4]_{80\%}$  at 120°C for 22 h (96 h saccharification). .... 204
- Figure 99: Enzymatic saccharification of various lignocellulose pulps obtained after pretreatment with  $[\text{C}_4\text{C}_1\text{im}][\text{HSO}_4]_{80\%}$  at 120°C for 22 h. .... 205
- Figure 100: Sugar monomers and furfurals found in the  $[\text{C}_4\text{C}_1\text{im}][\text{HSO}_4]_{80\%}$  pretreatment liquor after pretreatment of various lignocellulose feedstocks at 120°C for 22 h. .... 206
- Figure 101: Delignification and recovery of lignin after pretreatment of various feedstocks with 80/20% ionic liquid/water mixtures at 120°C for 22 h. The



---

pretreatment liquors were [C<sub>4</sub>C<sub>1</sub>im][HSO<sub>4</sub>]<sub>80%</sub> and [C<sub>2</sub>C<sub>1</sub>im][MeCO<sub>2</sub>]<sub>80%</sub>.  
Only one sample per measurement was processed. Misc: *Miscanthus*. 207

Figure 102: *Miscanthus* and willow chips pretreated with [C<sub>4</sub>C<sub>1</sub>im][HSO<sub>4</sub>]<sub>80%</sub> at 120°C  
for 22 h. .... 208

Figure 103: Air-dried willow chips before and after [C<sub>4</sub>C<sub>1</sub>im][HSO<sub>4</sub>]<sub>80%</sub> pretreatment at  
120°C for 22 h. .... 208

Figure 104: Saccharification of *Miscanthus* and willow chips after pretreatment with  
[C<sub>4</sub>C<sub>1</sub>im][HSO<sub>4</sub>]<sub>80%</sub> for 22 h at 120°C. .... 209

Figure 105: Regenerated cellulose pretreated in 80% and 100% [C<sub>2</sub>C<sub>1</sub>im][MeCO<sub>2</sub>]  
(left). Note the voluminous cellulose flakes in the 80% sample. Cellulose in  
undiluted [C<sub>4</sub>C<sub>1</sub>im][HSO<sub>4</sub>] (right). The dark colour of 100% samples is a  
sign of cellulose degradation. .... 210

Figure 106: Enzymatic saccharification of Avicel cellulose after treatment with pure  
1,3-dialkylimidazolium ionic liquids and 80/20% ionic liquid/water mixtures  
at 120°C for 22 h. The yield was determined after a 48 h saccharification.  
..... 211

Figure 107: Suggested pretreatment process using ionic liquids that fractionate  
biomass. .... 221

## List of Tables

Table 1: E factors in various segments of the chemical industry <sup>64</sup> .....	56
Table 2: Solubility of silver halides in water at 25°C <sup>88</sup> .....	66
Table 3: Suitability of ion metathesis for the synthesis of pure 1-butyl-3-methylimidazolium ionic liquids .....	81
Table 4: Kamlet-Taft parameters of selected non-protic imidazolium and pyrrolidinium ionic liquids. The values shaded in dark grey show the effect on $\alpha$ upon changing the cation. Values shaded light grey show the impact on $\beta$ when the anion is varied. <sup>113</sup> .....	100
Table 5: $T_{0.01/10}$ and $T_{\text{onset}}$ of various ionic liquids (in °C) <sup>120</sup> .....	102
Table 6: Kamlet-Taft parameters reported by different members of the Welton group in per-reviewed publications (standard deviation in brackets).....	107
Table 7: Position of peak maxima of 4-nitroaniline (NA) and <i>N,N</i> -diethyl-4-nitroaniline (DNA) in reference solvents used to calculate $\beta$ and $\pi^*$ . Units are $10^3 \text{ cm}^{-1}$ .....	108
Table 8: Effect of moisture on the Kamlet-Taft parameters of $[\text{C}_4\text{C}_1\text{im}][\text{Me}_2\text{PO}_4]$ .....	109
Table 9: Thermochromatic effect on Kamlet-Taft parameters of $[\text{C}_4\text{C}_1\text{im}][\text{OTf}]$ ,.....	110
Table 10: Kamlet-Taft parameters of hydrophilic 1-butyl-3-methylimidazolium ionic liquids (standard deviation in brackets) using the probes 4-nitroaniline, <i>N,N</i> -diethyl-4-nitroaniline and Reichhardt's dye. The values were determined at 25°C with dried ionic liquids, unless stated otherwise. ....	111
Table 11: Influence of the Kamlet-Taft $\beta$ value on the water miscibility.....	116
Table 12: Moisture content of 1-butyl-3-methylimidazolium ionic liquids exposed to air .....	119
Table 13: Decomposition temperatures of selected ionic liquids.....	122
Table 14 Literature reports of lignin and hemicellulose removal by $[\text{C}_2\text{C}_1\text{im}][\text{MeCO}_2]$ pretreatment.....	130
Table 15: Saccharification yields from ionic liquid pretreated biomass reported in the literature. Glu: glucose, Xyl: Xylose.....	135
Table 16: Classification of ionic liquids according to their impact on wood chips....	147
Table 17: Weight changes of a pine chip before and after treatment with $[\text{C}_4\text{C}_1\text{im}][\text{MeCO}_2]$ (oven-dried weight, ODW).....	157
Table 18: Studies that have used methylsulfate based ionic liquids for biomass....	169
Table 19: Solubility of cellulose in 1,3-dialkylimidazolium ionic liquids containing methyl sulfate, hydrogen sulfate and acetate anions; the solubility in dried ionic liquid (IL) and ionic liquid mixed with 20 vol% water was investigated. ....	210

## List of Schemes

Scheme 1: Combination of two lignin radicals to form a $\beta$ -O-4 bond, followed by the quenching of the quinone methide intermediate with a nucleophile such as water (R = H). If R-OH is part of another lignin fragment or carbohydrate, a branching $\alpha$ -O-4 ether bond is formed (adapted from <sup>23</sup> ). .....	41
Scheme 2: Acid-catalysed dehydration of D-xylose to furfural. The mechanism shown proceeds <i>via</i> a cyclic intermediate. <sup>60</sup> .....	53
Scheme 3: Acid catalysed conversion of cellulose to levulinic acid <i>via</i> glucose, fructose and HMF.....	54
Scheme 4: Quaternisation of a tertiary amine with a haloalkane to yield a halide ionic liquid.....	63
Scheme 5: Synthesis of 1-butyl-3-methylimidazolium methyl carbonate in methanol.....	68
Scheme 6: Decomposition of the methyl carbonate anion upon addition of an acid HA. ....	69
Scheme 7: Synthesis of 1-butyl-3-methylimidazolium hydrogen sulfate.....	81
Scheme 8: Synthesis of 1-butyl-3-methylimidazolium dimethyl phosphate.....	81
Scheme 9: Formation of a 1,3-dialkylimidazolium carbene under basic aprotic conditions.....	85
Scheme 10: Nucleophilic attack of 1-butyl-3-methylimidazolium carbene on dimethyl carbonate; both carboxylation or methylation can occur .....	86
Scheme 11: Dehydration of [C <sub>4</sub> C <sub>1</sub> im][HCO <sub>3</sub> ] to 1-butyl-3-methylimidazolium-2-carboxylate.....	90
Scheme 12: Formation of 1-butyl-3-methylimidazolium-2-carboxylate from [C <sub>4</sub> C <sub>1</sub> im][MeCO <sub>3</sub> ] under reduced pressure.....	90
Scheme 13: Complexation of residual butylimidazole by sulfuric acid .....	91
Scheme 14: Synthesis of 1-butyl-3-methylimidazolium hydrogen sulfate by hydrolysis .....	93
Scheme 15: Reversible decomposition of [C <sub>4</sub> C <sub>1</sub> pyrr][MeCO <sub>2</sub> ] at elevated temperatures and <i>in vacuo</i> .....	123
Scheme 16: Dehydration of the lignin model compound guaiacylglycerol- $\beta$ -guaiacyl ether in ionic liquids. <sup>162</sup> .....	131
Scheme 17: Condensation of glucose with a 1,3-dialkylimidazolium cation under basic conditions.....	136
Scheme 18: Equilibrium between methyl sulfate and hydrogen sulfate at elevated temperatures in the presence of water and methanol .....	183
Scheme 19: Putative sulfation of cellulose in [C <sub>4</sub> C <sub>1</sub> im][HSO <sub>4</sub> ] .....	212

## Thesis overview

Improving the processing of woody biomass into fuels and/or chemicals is currently an important challenge. The use of novel pretreatment technologies such as ionic liquids could reduce energy consumption for pre-processing and make the use of lignocellulose more economically viable and environmentally friendly. This work seeks to explore the use of ionic liquids for biomass fractionation to enable an evaluation of this relatively novel application of ionic liquids.

The problem was approached by selecting three types of lignocellulosic biomass representative of the most important feedstock groups (grasses, hardwood and softwood) and subjecting them to treatment with ionic liquids. Furthermore, after surveying the literature, it was decided that comparative studies using a wider range of ionic liquids were needed to better understand which chemical features should be incorporated into ionic liquid designed for pretreating lignocellulosic biomass. The enormous number of possible ionic liquids required to make a careful selection. It was decided that the role of the anion should be investigated in more detail. The number of candidate anions was further narrowed down after surveying the literature on carbohydrate and lignin solubility in ionic liquids and picking the ones that exhibited high activity. As controls, ionic liquids with anions that are expected to have little impact on the biomass were also used in the experiments. 1-Butyl-3-methylimidazolium, a popular cation exhibiting high stability and typically yielding low-melting liquids, was selected to be paired with these anions. The literature on the synthesis of the candidate ionic liquids was surveyed and the routes that achieve reasonable purities and sufficient quantities were used. The experience with the various synthetic methods is accounted in this work.

In an attempt to better mimic industrial conditions the use of wood chips was explored. The vast majority of studies have used and still use by the time of printing milled and oven-dried biomass. Therefore part of this study was dedicated to the dissolution of air-dried wood chips in ionic liquids. The effect of various ionic liquids on the dissolution of these

wood chips was tested. A quantitative correlation between chip expansion/swelling and the ionic liquids' hydrogen-bond basicity was found. This confirms that the anion plays a prominent role in the solubilisation of the major components of lignocellulose and that this also applies to chips. However, it is shown that the reduced surface area of chip-sized biomass and the moisture introduced by the biomass reduces the speed of the dissolution and prevents softening of more recalcitrant biomass chips such as pine and willow.

Another important set of findings was the successful application of ionic liquids with anions that were not known to be useful for isolating cellulose from woody biomass and which have lower hydrogen-bond basicity than the previously used ionic liquids. This adds new candidates to the range of ionic liquids known to be useful in lignocellulose fractionation which have improved properties such as high thermal stability and high water tolerance. Another important set of results is concerned with the effect of anion acidity, showing distinct effects on the extent of cellulose purification that can be achieved by ionic liquids. In addition, the anion acidity was shown to have a very pronounced effect on the rate of hemicellulose hydrolysis and conversion of the monomeric hemicellulose sugars into furfurals. Degradation was primarily seen in ionic liquids with acidic anions, while basic anions slowed the hydrolysis of the hemicellulose and inhibited the generation of furfurals.

## Objectives

- Select a range of ionic liquids which have shown potential in biomass processing
- Synthesise these ionic liquids in sufficiently pure form
- Characterise the ionic liquids to ensure product purity
- Determine the solvent polarity parameters according to Kamlet and Taft
- Investigate industrially relevant physical properties of these ionic liquids, such as stability at temperatures

relevant to thermal pretreatment and moisture uptake from air (hygroscopicity)

- Thermally pretreat a representative range of lignocellulosic biomass feedstocks in the presence of these ionic liquids
- Design experiments with the intention to increase the industrial viability of ionic liquid pretreatment whenever or the use of ionic liquid water mixtures
- Characterise impacts of the ionic liquid treatment (*e.g.* physical disintegration, enzymatic sugar release, biomass composition, fractionation of biomass components)
- Relate impact of ionic liquid pretreatment with ionic liquid composition and physical properties (particularly solvent polarity)
- Qualitatively assess the usefulness of the investigated ionic liquids
- Suggest a working model for a potential ionic liquid based pretreatment and fractionation process

# 1 Introduction

## 1.1 The energy challenge

Fossil resources such as coal, gas and oil are cheap and abundant feedstocks and currently the preferred resources for the generation of energy and the production of materials. However, the combustion of these fossil resources results in the release of carbon dioxide into the atmosphere. This carbon dioxide has been sequestered over millions of years of photosynthetic activity. It is now generally accepted that the increase of the carbon dioxide concentration is linked to the rise of the global average surface temperature (Figure 1).<sup>1</sup> Evidence has also accumulated that the higher surface temperature has an effect on the climate, locally and globally.<sup>1</sup>

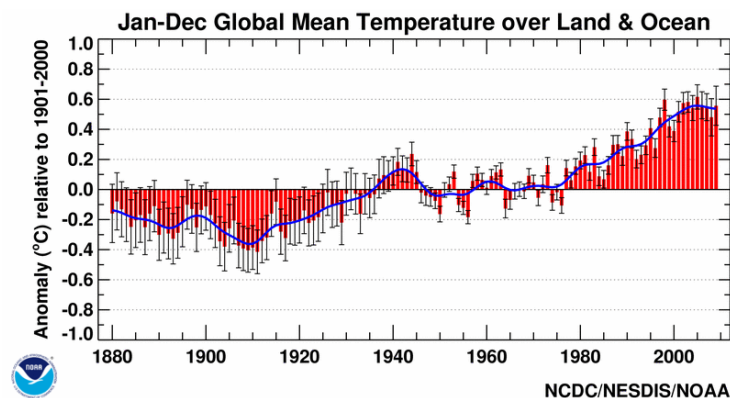


Figure 1: Global surface temperature anomalies over the past 130 years.<sup>2</sup>

The overwhelming portion of the currently produced energy is generated by burning fossil resources. In addition, it is projected that the world-wide demand for energy in the form of liquid fuels, electricity and heat will increase by almost 50% over the next 25 years (Figure 2), while fossil feedstock reserves will decrease.

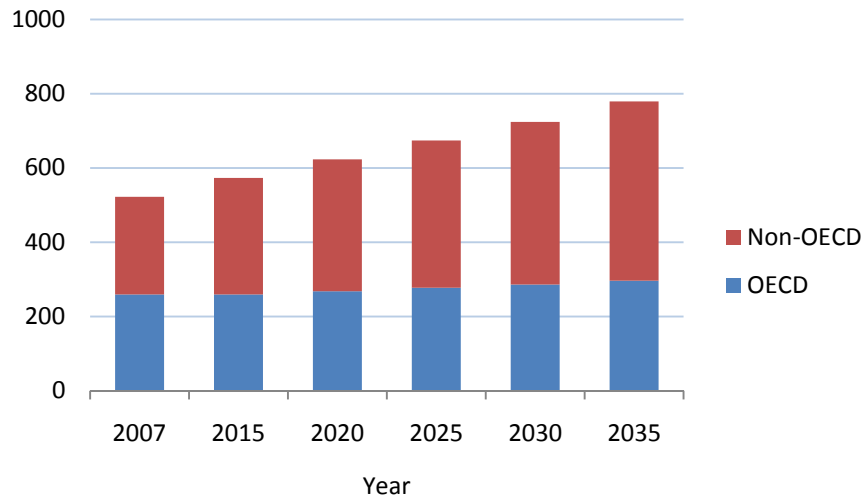


Figure 2: Current and predicted world energy consumption. The energy consumption is projected to grow by 48% by 2035 (in  $10^{15}$  J).<sup>3</sup>

The development of renewable energy technologies, which are fuelled directly or indirectly by incident sunlight, could help meeting the rising demand for energy while reducing the amount of green house gases emitted into the atmosphere. Most of the currently available renewable energy technologies, such as wind, hydro, photovoltaic, tidal and wave technology as well as anaerobic digestion of agricultural wastes generate only electricity. Although electricity is a substantial part of the energy mix, almost a third of the energy is consumed in the transportation sector (Figure 3). This sector is currently almost entirely reliant on liquid fossil fuels such as gasoline, diesel and kerosene. In addition, the majority of chemicals are produced from the same petroleum feedstocks. Renewable alternatives to liquid fossil fuels are liquefied hydrogen generated by electrolysis of water with renewable electricity and methanol generated by artificial photosynthesis, technologies which are still under development.



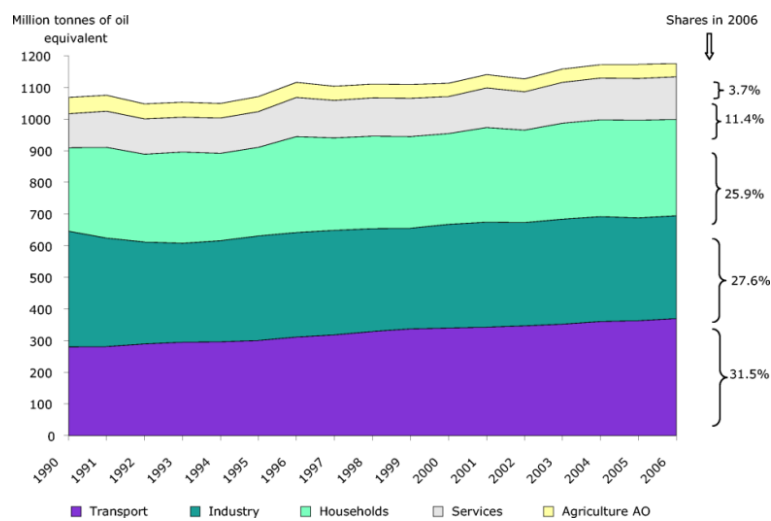


Figure 3: Energy consumption in the EU-27 until 2006, allocated to various sectors. The transportation sector consumed just under a third of the total energy.<sup>4</sup>

## 1.2 Biorefinery

A variety of processes, collectively called oil refineries, is applied to fractionate and refine crude fossil oil. Oil refineries supply the majority of liquid fuels and the raw materials for the production of most chemicals. However, the oil feedstock is projected to decline rapidly over the next decades and a substitute may be required in less than 20 years. Non-fossilised plant biomass could be a carbon-neutral alternative and supply a range of biofuels and biochemicals *via* the so-called biorefinery (Figure 4).

If the biorefineries are implemented carefully, they may be able to contribute to meet future energy and material needs in a sustainable way.<sup>5</sup> Apart from climate change mitigation, the biorefinery also has the potential to enhance local energy security and improve rural development.<sup>5</sup>

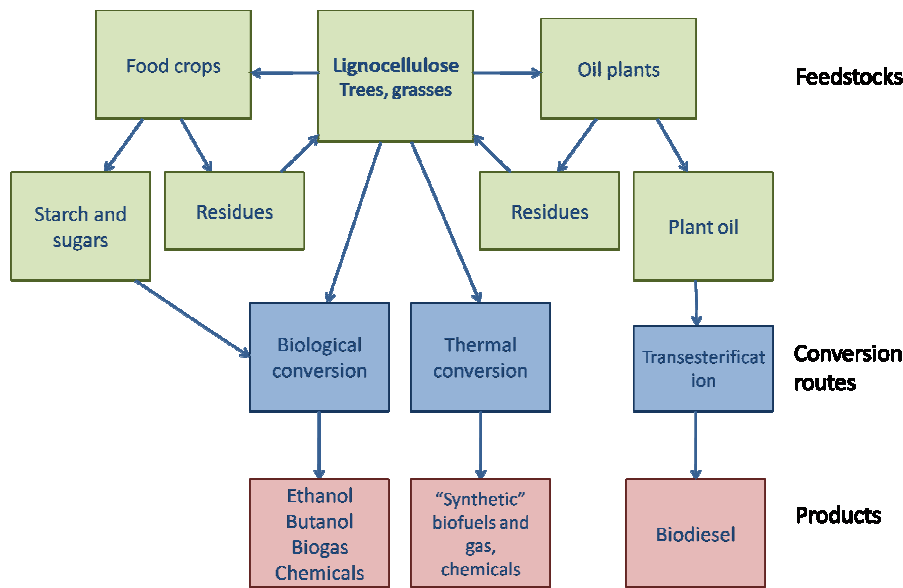


Figure 4: Biological, thermal and chemical route to biofuels and renewable chemicals (adapted from Pickett *et al.*<sup>5</sup>)

## 1.3 Biorefinery feedstocks

### 1.3.1 First generation feedstocks

Currently, biofuels are made from edible components of food crops, such as sucrose, starch and vegetable oils. Their advantage is that it is relatively easy to bring these so-called first-generation feedstocks into a form that can be fermented by microorganisms.

Brazilian sugar cane ethanol can save 80% of greenhouse gas emissions (compared to gasoline) with current technology,<sup>5</sup> but other options such as corn ethanol provide only modest savings (around 20%).<sup>6</sup> The production of fuels from edible biomass also competes with food production and might diminish CO<sub>2</sub> savings by releasing sequestered carbon during land use change.<sup>6</sup>

### 1.3.2 Second generation feedstocks

Lignocellulose is the material that the cell walls of woody plants are made of and is a so-called second generation feedstock. It is a

composite material, with three biopolymers making up the majority of the material: cellulose, hemicellulose and lignin. Cellulose and hemicellulose are polymeric carbohydrates while lignin is an aromatic ether-linked polymer (Figure 5). Their chemical structure of the components will be discussed in greater detail on page 35 and thereafter. In addition, lignocellulose contains smaller amounts of inorganic compounds, proteins and extractives such as waxes and lipids. The exact composition of lignocellulose depends on the species, the plant tissue and the growth conditions.

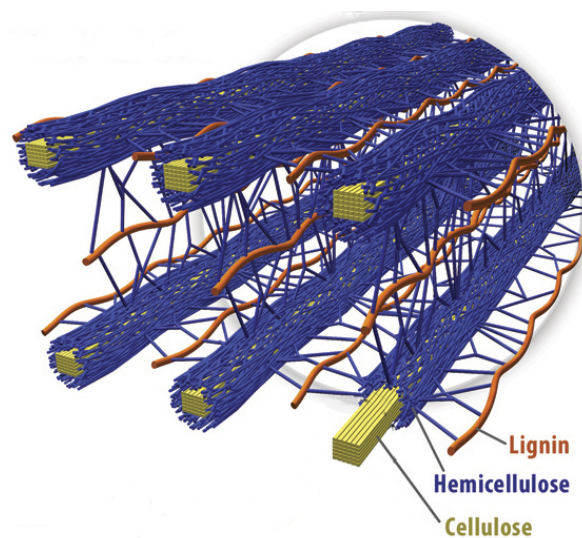


Figure 5: Structural arrangement of the major components in the cell walls of lignocellulosic biomass<sup>7</sup>

Lignocellulosic biomass is the most abundant plant material on the planet. It will be available in much higher quantities and at lower cost than first-generation substrates.<sup>8</sup> In addition, it is projected that lignocellulose utilisation will provide much higher CO<sub>2</sub> emission savings.<sup>9</sup>

Lignocellulosic biomass can be obtained from various sources: agricultural and forest residues, municipal waste such as organic and paper waste and dedicated biofuel crops. Dedicated biofuel crops have the advantage of high yields. Growing wheat, one of the major food crops world-wide, affords only ca. 5 t ha<sup>-1</sup> of wheat straw residue,<sup>10</sup> while 10-30 dry tons per hectare and year can be produced when growing biofuel crops like *Miscanthus*, willow and poplar (these crops will be described in more detail later).<sup>11</sup> The higher yields per area mean that

less land needs to be dedicated to non-food applications, improving the coexistence of biofuel production and food security. It has been estimated that the US could produce enough lignocellulosic feedstock to substitute 30% of their liquid transport fuels with biofuels.<sup>8</sup> The major obstacle is that the technology for processing lignocellulosic material into low-cost fuels and chemicals is not mature yet.<sup>12</sup>

Lignocellulose can be refined *via* a thermochemical route (gasification and pyrolysis) or a biological route. The biological route utilises the carbohydrates contained in lignocellulose, which make up 70-80 wt% of the matter. In order to access the carbohydrates in the biomass, a pretreatment step is required (Figure 6).

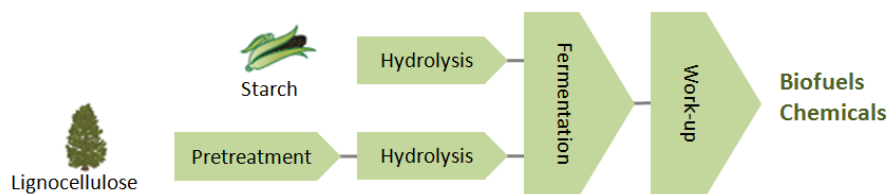


Figure 6: Conversion of first generation and second generation feedstocks *via* the biological route.

A number of process steps are required to obtain a product *via* the biological route: feedstock comminution, pretreatment, conditioning (*e.g.* detoxification and neutralisation), hydrolysis of the polysaccharides, fermentation of sugars and product recovery (often by distillation). The pretreatment step accounts for an important fraction of the energy requirement of the biological route.<sup>13</sup>

## 1.4 The chemical composition of wood

In order to overcome the resistance of lignocellulosic biomass towards deconstruction, an understanding of its architecture, its composition and the chemical linkages is required. In the following sections describe the major components of lignocellulose in more detail.

### 1.4.1 Cellulose

Cellulose is a linear polymer consisting solely of glucose. It is typically the most abundant component in lignocellulose. Although the exact composition of different biomass feedstocks varies significantly, the cellulose content is usually in the range 35-50 wt%. The glucopyranosyl monomers are linked by 1-4- $\beta$  glycosidic bonds.

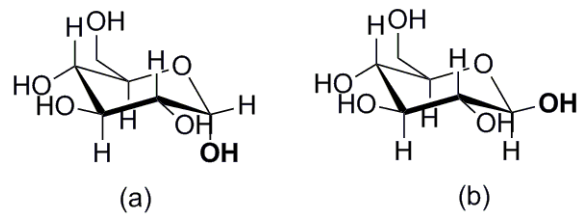


Figure 7: Glucose, the monomer of cellulose with  $\alpha$  (a) and  $\beta$  (b) confirmation at the anomeric carbon.

The  $\beta$  configuration (Figure 7) at the anomeric carbons gives rise to a stretched chain conformation (Figure 8). This is in contrast to  $\alpha$ -amylose a polymer that occurs in starch and has a helical shape due to the  $\alpha$  configuration at the anomeric carbon of its glucose subunits.

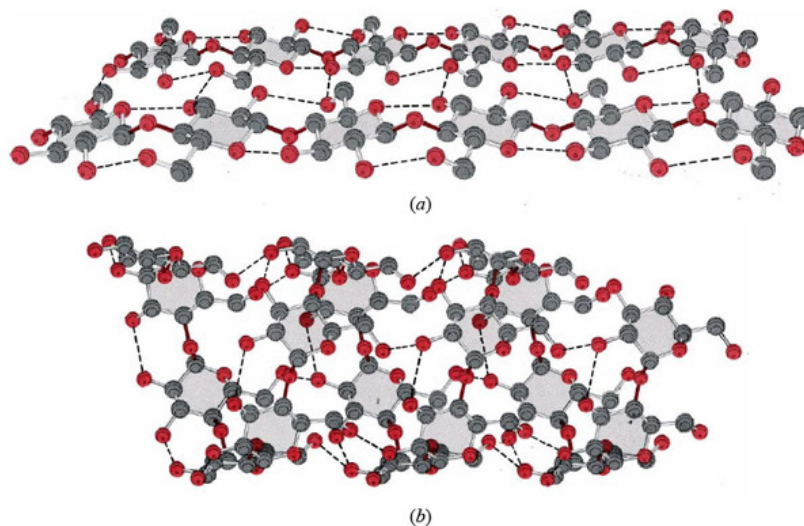


Figure 8: Stretched chain conformation of cellulose (a) and helical conformation of  $\alpha$ -amylose in starch (b)<sup>14</sup>

The linear conformation of cellulose enables packing of numerous cellulose strands into crystalline fibrils. In cellulose, three hydrogen bonds per glucosyl subunit occur, two intramolecular hydrogen bonds

and one intermolecular hydrogen bond (Figure 9). Cellulose is the lignocellulosic polymer with the highest degree of polymerisation in lignocellulose, the number of glucosyl units in one polymer strand being typically around 10 000 or higher.<sup>15</sup> Glucose is water-soluble, however, the large molecular weight, the intermolecular hydrogen-bonding and the tight packing of cellulose strands render cellulose insoluble in water and most solvents.

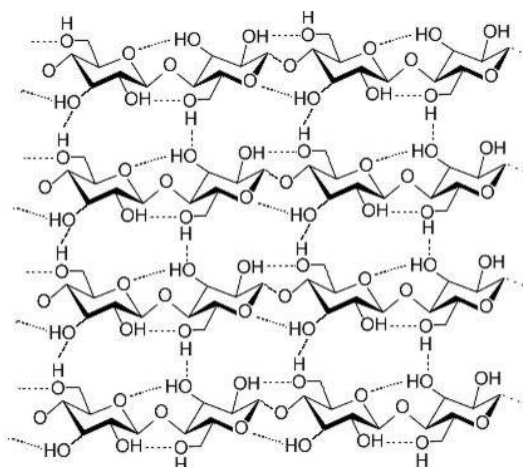


Figure 9: Covalent linkages and hydrogen bonding in crystalline cellulose<sup>16</sup>

The parallel synthesis of 36 glucan strands by a membrane bound protein complex called cellulose synthetase ensures the arrangement into crystalline fibrils during biosynthesis (although less ordered regions are also found in these fibrils).<sup>17</sup> Such fibrils are the backbone of the cell wall, giving strength and stiffness to plant cell walls. The highly ordered cellulose structure found in cellulose fibrils can be perturbed by dissolving cellulose in certain solvents and then precipitating it. Amorphous cellulose is more susceptible to hydrolysis than the crystalline counterpart.

The cellulose portion in lignocellulosic biomass is of major interest as it can be depolymerised to glucose, which can be fed to a wide range of fermentative microorganisms for the production of renewable fuels and chemicals.

### 1.4.2 Hemicellulose

Hemicellulose is a group of carbohydrate polymers and makes up around 25 wt% of the biomass.<sup>18</sup> The strand are of lower molecular weight than cellulose (degree of polymerisation around 100-200). A variety of pentose and hexose sugars can be found in hemicellulose: glucose, xylose, mannose, galactose and arabinose (Figure 10).

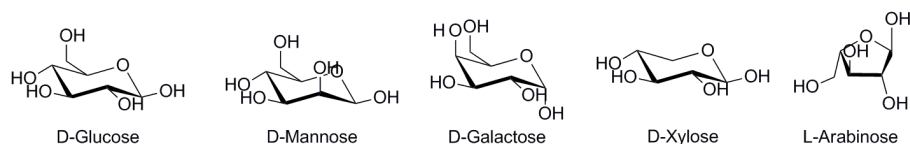


Figure 10: The hexoses and pentoses typically found in hemicellulose.

Hemicellulose polymers are often branched and may be decorated with functionalities such as acetyl and methyl groups, cinnamic, glucuronic and galacturonic acids (Figure 11).

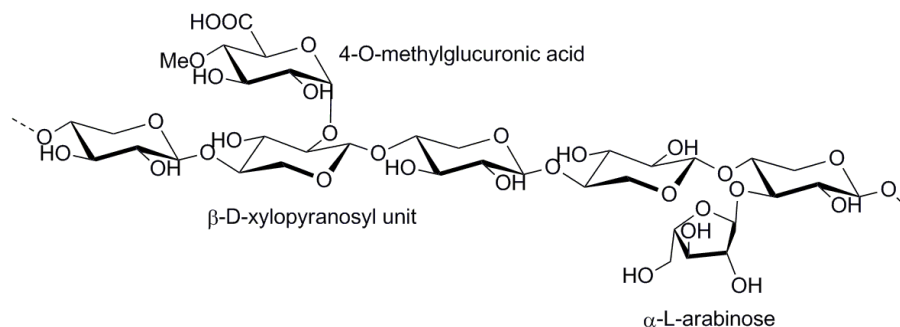


Figure 11: Structure of arabino-4-O-methylglucuronoxylan, a hemicellulose found in softwood (adapted from <sup>18</sup>)

Hemicellulose binds non-covalently to cellulose and acts as a matrix material, holding together the cellulose fibrils. The most common hemicellulose sugar in grasses and hardwood is xylose. In softwood, mannose is the major hemicellulose sugar.<sup>18</sup> Due to its amorphous nature, hemicellulose is more susceptible to chemical hydrolysis than cellulose, an aspect that is exploited by many pretreatment operations.

### 1.4.3 Lignin

Lignin is an aromatic water-insoluble polymer and deposited after growth has ceased. It provides water-proofing and reinforcement. During

cell wall formation it is built from up to three monomers: coniferyl, sinapyl and *para*-coumaryl alcohol (Figure 12).

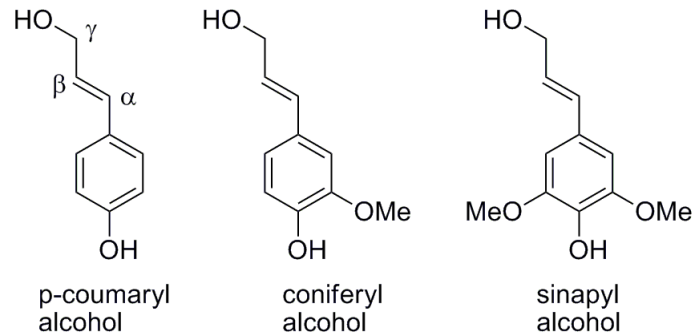


Figure 12: The three monolignols from which lignin is synthesised. The monomers vary in the substitution at the C-3 and C-5 ring positions (adapted from <sup>18</sup>).

The monomers are synthesised by the plant cell and secreted into the surrounding space (apoplast), where they are polymerised by oxidative radical polymerisation. The process is called lignification and is mediated by enzymes.<sup>19</sup> Lignification occurs after formation of the primary cell wall has ceased, encrusting the cellulose fibrils and the hemicellulose matrix. The composition and content of lignin differs between softwood, hardwood and grasses. The distribution of lignin within the cell wall material also varies. While the lignin is aligned parallel to the cellulose fibrils in parts of the cell wall, it forms a dense and uniform matrix in the middle lamella.<sup>20</sup>



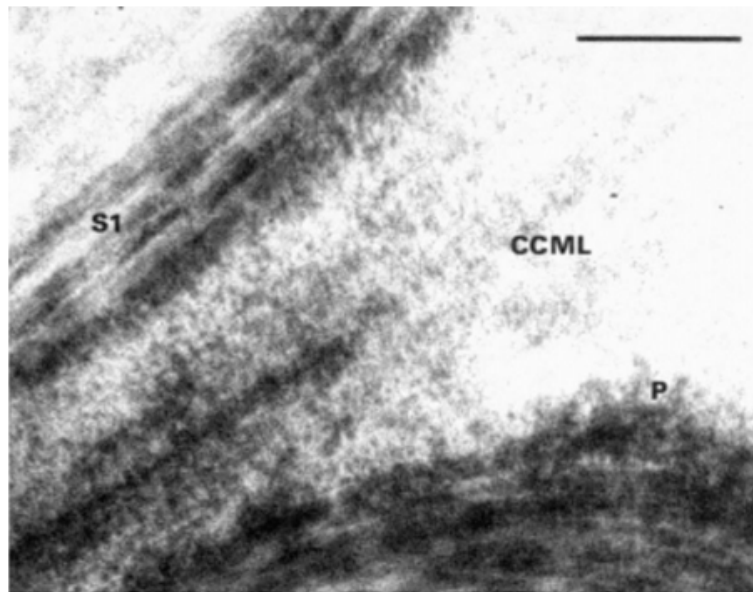
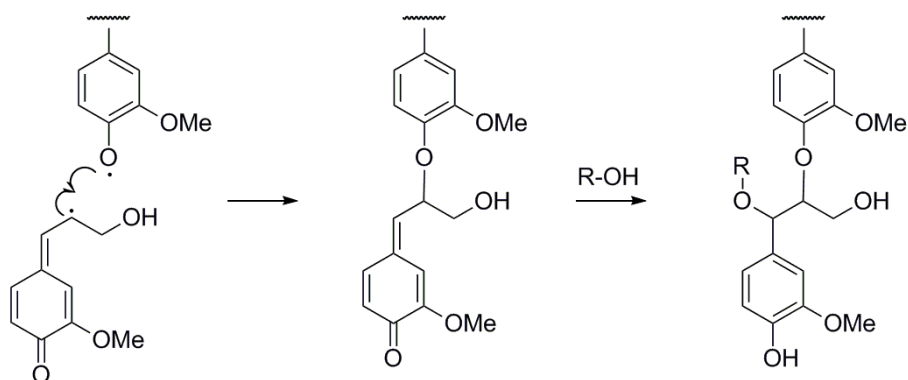


Figure 13: Lignin distribution in the cell corner middle lamella (CCML) and the outer secondary cell wall (S1). The lignin in the S1 wall appears to be aligned to the cellulose fibrils. The picture was obtained with transmission microscopy of *Pinus radiata* wood after permanganate staining. Scale bar 440 nm.<sup>21</sup>

During lignification, the monolignols are transformed into radicals by  $\cdot\text{H}$  abstraction, and subsequently undergo polymerisation (Scheme 1). The process is initiated by enzymes that reside in the apoplast. The final lignin polymer contains a wide range of linkages. The most common linkage is the  $\beta\text{-O-4}$  ether bond. Roughly 50% of all inter-subunit bonds are of this type.<sup>22</sup> The  $\beta\text{-O-4}$  ether bonds lead to a linear elongation of the polymer. If the quinone methide intermediate reacts with a nucleophile other than water, an  $\alpha\text{-O-4}$  ether bond is formed (Scheme 1). This bond can lead to lignin branching or to cross-linking of lignin with carbohydrate polymers.



Scheme 1: Combination of two lignin radicals to form a  $\beta$ -O-4 bond, followed by the quenching of the quinone methide intermediate with a nucleophile such as water ( $R = H$ ). If R-OH is part of another lignin fragment or carbohydrate, a branching  $\alpha$ -O-4 ether bond is formed (adapted from<sup>23</sup>).

Other C-O and C-C linkages are also formed in lower abundance during radical polymerisation. The most common linkages are depicted in Figure 14.

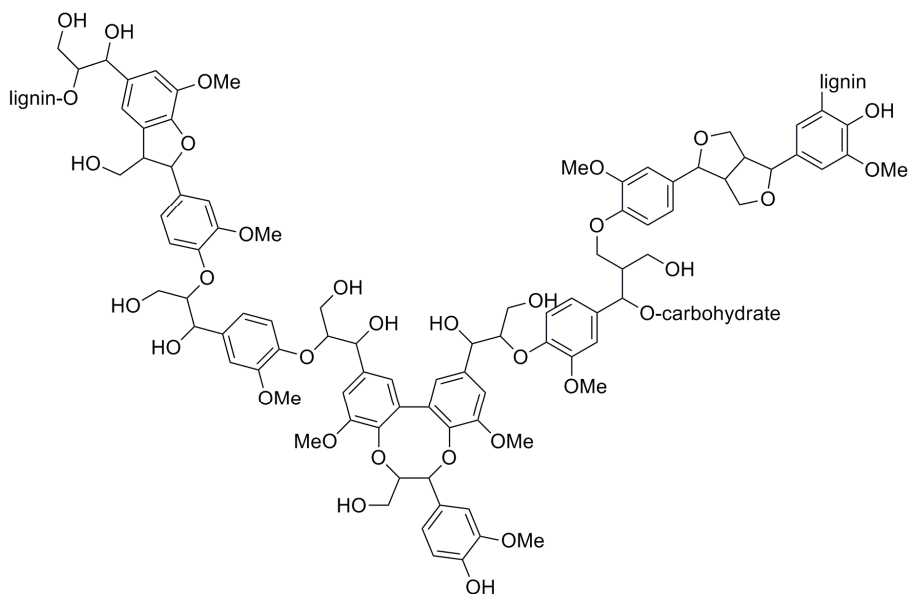


Figure 14: Lignin fragment with various C-O and C-C linkages typically present in native lignin<sup>24</sup>

The presence of the lignin crust has been identified as one of the major obstacles for an energy-efficient pretreatment process.<sup>13</sup> Most chemical pretreatment operations modify lignin by hydrolysing its ether bonds, but few physically remove it from the pulp. Lignin that has been freed from the cell wall matrix is soluble in basic aqueous solutions and some organic solvents. It can also become water-soluble through chemical

modification, as in the case of the liginosulfonates produced during sulfite pulping.

Native lignin not only prevents access of carbohydrate hydrolases to their substrates, but residual lignin can also cause unproductive binding of cellulases which leads to the use of high enzyme loadings.<sup>15</sup> Lignin can also be a source of compounds inhibitory to hydrolases and fermentative organisms, such a syringyl aldehyde and vanillic acid.<sup>25</sup>

#### 1.4.4 Lignin-carbohydrate complexes

Cellulose, hemicellulose and lignin are not only entangled, but also covalently cross-linked. The cross-links between carbohydrates and lignin are termed lignin-carbohydrate complexes. In grasses, these complexes are often mediated by ferulic acid (Figure 15). Ferulic acid is attached to the hemicellulose (arabinoxylan) *via* ester bonds. The ester bond is preformed intracellularly and the feruloylated arabinoxylan fragment exported through the cell membrane.<sup>26</sup> During lignification, the ferulic acid participates in the radical polymerisation with its aromatic portion.<sup>27</sup> This is why a significant portion of the ferulic acid is not liberated upon cleavage of the ester bond between hemicellulose and ferulic acid.<sup>23</sup>

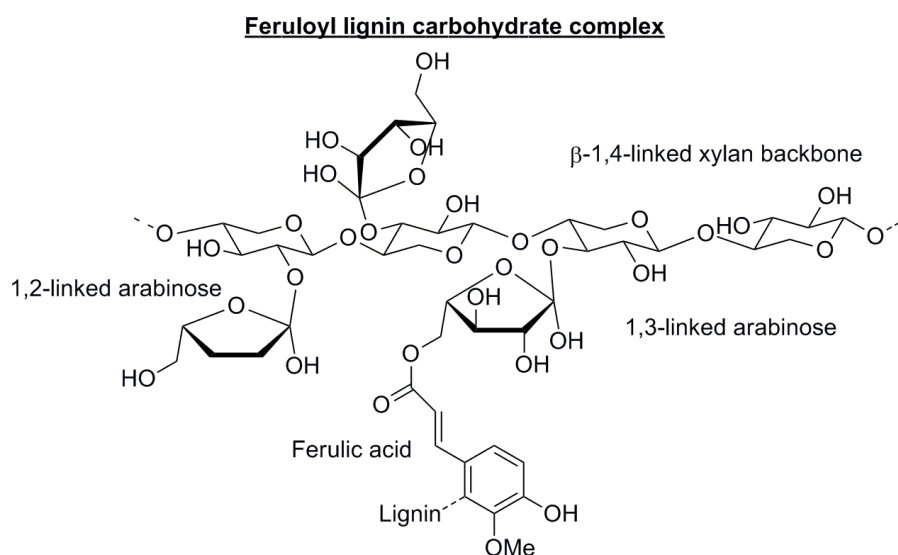


Figure 15: Lignin-carbohydrate complexes in involving ferulic acid

Some feruloyl substituents dimerise hemicellulose chains (Figure 16). The extent of cross-linking *via* lignin-carbohydrate complexes has been correlated with increased cell wall rigidity and resistance to enzymatic digestion.<sup>28</sup>

In softwood and hardwood, direct complexes between lignin and carbohydrates are present.<sup>29</sup> It is thought they are formed during lignification, when the hydroxyl groups of carbohydrates react with the ketone methide intermediates, as shown in Scheme 1.

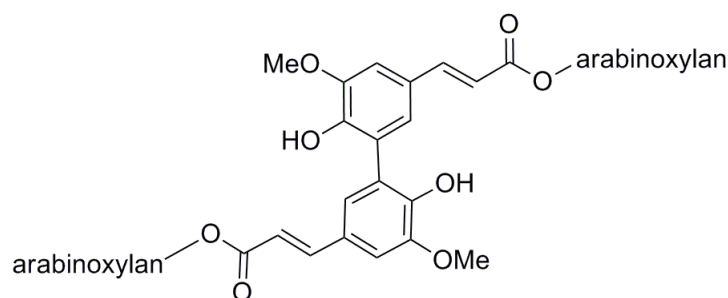


Figure 16: Ferulic acid dimer cross link

## 1.5 The structure of wood

Lignocellulosic biomass is synthesised by plants. The plant cells surround themselves with walls made from lignocellulosic material, creating a porous light-weight structure to support and protect them.<sup>18</sup> In trees, most living cells disappear when they reach maturity, while the cell walls remain to continue supporting the tree structurally.

The cells in woody tissue are elongated and mostly orientated in the axial direction. This makes wood an anisotropic material. The cells are often connected *via* tiny channels (pits and perforation plates). The perforated cells create long channels that enable transport of nutrients and water between roots and leaves. Several cell types can be found in wood which differ in shape, cell wall polymer content and in function. There are a few cells which oriented in the radial direction to enhance structural rigidity and reduce swelling in this direction. The size and shape of the pores varies considerably for different biomass types.

In between the cell walls is a lumen called the middle lamella. It is devoid of cellulose fibrils but rich in hemicellulose. This matrix holds the

individual cell walls together. In mature woody tissue, the middle lamella also contains lignin (Figure 17).

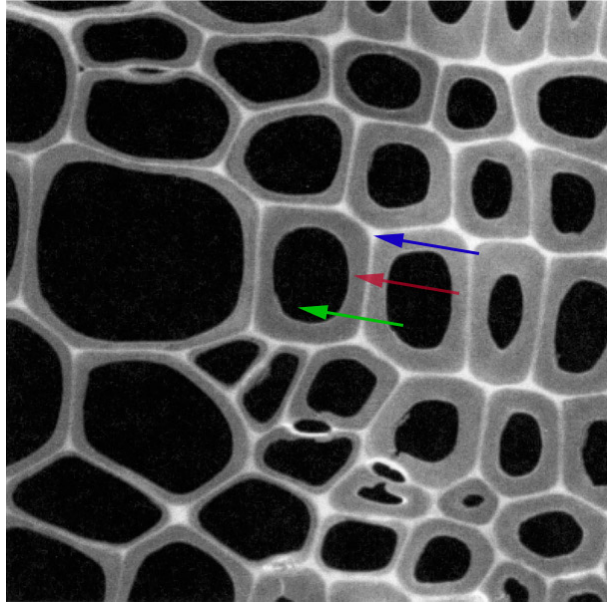


Figure 17: Lignin distribution in lignified cell walls of *Pinus radiata* visualised by confocal fluorescence microscopy (160 x 160  $\mu\text{m}$ ). The lignin autofluorescence at 350 nm was excited. The empty voids (green arrow), the cellulose and lignin containing cell walls (red arrow) and the cellulose free middle lamella (blue arrow) are marked. Brighter areas show the high lignin concentration in the middle lamella.<sup>20</sup>

## 1.6 Lignocellulosic energy crops

There are three major groups of lignocellulosic biomass: Hardwood, softwood and grass biomass. Three lignocellulosic substrates were used in this work, which were selected to represent the major types of lignocellulosic crops and are suitable for UK climate and soil conditions.

### 1.6.1 *Miscanthus x giganteus* (perennial grass)

*Miscanthus x giganteus* is a tall perennial grass.<sup>30</sup> It is a triploid sterile hybrid of *Miscanthus sinensis* and *Miscanthus sacchariflorus*. The plant consists of a root system (rhizome) and a stem with long leaves.



Figure 18: *Miscanthus* plants at the University of Illinois.<sup>31</sup>

The stem consists of several internodes. Cross sections reveal a rigid outer ring with thicker cell walls and pith consisting of thin cell walls (Figure 19). The pith acts as a foam core, while the outer ring gives stability against compression and tension. Grass stems are axially symmetric and stem growth occurs at the tip only.

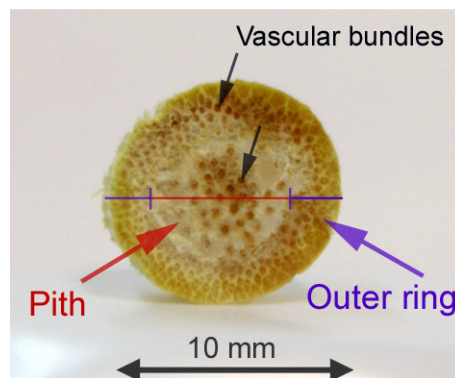


Figure 19: Cross-section of a *Miscanthus* culm. The outer ring and the pith are visible, as well as the vascular bundles (own photo).

At the end of a growth season, *Miscanthus* translocates mineral nutrients from the over-ground part into the rhizome. The dry culms can be harvested in winter and used for biofuel production, while the nutrient-rich rhizome remains in the soil and will produce new shoots in the next growth period.

*M. x giganteus* is a promising energy crop. High biomass yields, in the area of 10-30 tons per hectare and year ( $\text{t}\cdot\text{ha}^{-1}\cdot\text{y}^{-1}$ ) have been reported, particularly in warmer climate.<sup>11</sup> *Miscanthus* can be harvested annually for many years, reducing maintenance efforts. The translocation of nutrients into the rhizome reduces the requirement for fertiliser.<sup>32</sup> Moreover, there are no pests currently known for *M. x giganteus*.<sup>12</sup>

### 1.6.2 Pine (softwood)

Softwood has a largely uniform microscopic structure (Figure 17), due to the high abundance of one cell type, the so-called tracheids.<sup>18</sup> Fir, spruce and pine are examples of softwood species.

Unlike grasses, softwood trees (and hardwood trees) grow in the axial direction, increasing the stem height, and in the radial direction, increasing the stem diameter. In wood from temperate regions, annual rings are formed due to the seasonal change of growth conditions.

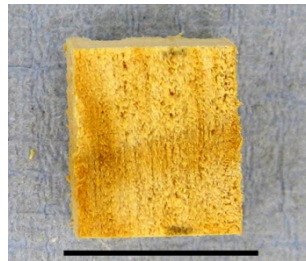


Figure 20: Wood chip excised from a pine tree trunk with one growth ring running from left to right. Scale bar = 10 mm (own photo)

The early-wood formed in summer has thinner cell walls and larger pores, in contrast to the denser late-wood formed at the end of the growth period. The difference between the cell walls in early and late wood can be seen in Figure 17.

Over 100 pine species belong to the genus *Pinus*. Fast-growing and tall pine species are among the most important commercial trees, grown in large plantations for their timber and wood-pulp. It is projected that currently unused softwood resources such as forest thinning, logging, timber mill and urban wood residues will be part of the biorefinery feedstock base.<sup>8</sup>

### 1.6.3 Willow (hardwood)

Hardwoods have a more complex structure than softwood, containing large water-conducting pores or vessels which are surrounded by narrower fibre cells (Figure 21).<sup>18</sup>

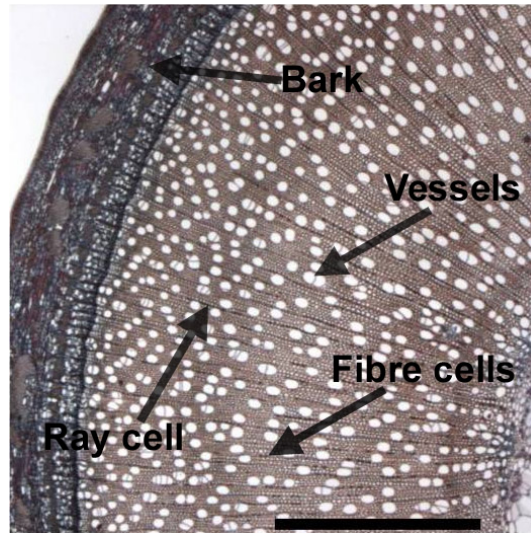


Figure 21: Cross section of a willow showing the bark, fibre cells, the vessels involved in nutrient transport and longitudinal ray cells.<sup>33</sup> Scale bar = 1 mm

Willows (genus *Salix*) are a group of about 400 hardwood species. Willows take root from cuttings and grow fast. Some species, especially *S. viminalis* and its hybrids can be maintained as short rotation coppice. Branches are harvested every 3-5 years. Willow is largely undomesticated, so breeding and genotype selection may significantly improve biomass yield to up to 30 tons per hectare and year.<sup>34</sup>

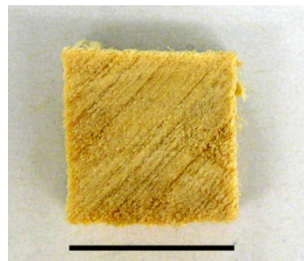


Figure 22: A wood chip excised from a *Salix* sp. branch. Scale bar =10 mm.



## 1.7 Pretreatment of lignocellulosic biomass

In order to produce chemicals from lignocellulose *via* fermentation, the carbohydrates must be provided in a soluble form that can be readily metabolised by fermenting microorganisms.

The primary goal of any pretreatment is to overcome the structural and chemical features that limit the release of carbohydrates.<sup>13</sup> The majority of processes concentrate on the cellulose portion. To gain access to the cellulose fibrils, the lignin-hemicellulose shield must be broken up. The cellulose can be subsequently hydrolysed in a separate saccharification step. The saccharification may be catalysed by chemicals<sup>35</sup> or enzymes<sup>15</sup>.

Historically, the focus of lignocellulose treatment was the production of a cellulose-enriched pulp for the manufacture of paper and fibre board. Aspects such as high material yield or fibre strength are paramount in paper production. With the advent of biorefineries, the focus is shifting towards obtaining a maximum amount of low molecular carbohydrate fragments in fermentable quality and in a cost and energy efficient manner. There are a range of effects that can be brought about by pretreatment operations:

- Lignin modification/redistribution/solubilisation
- Deacetylation of hemicellulose
- Hydrolysis of lignin-carbohydrate linkages
- Hemicellulose hydrolysis
- Particle size reduction
- Reduction of cellulose crystallinity

A purely physical pretreatment such as coarse grinding increases the surface area but does not result in high carbohydrate release, because it does not interfere with the chemical resistance features of lignocellulose. Milling to the size of individual fibres is more successful, because the lignin shield is mechanically removed.<sup>36</sup> However, the energy requirement for such grinding surpasses the energy content in the

fermentation product.<sup>37</sup> Therefore, the chemical (or biological) alteration of the lignocellulosic matrix is a more promising approach. Chemical pretreatment options use solvents, mostly water and are often catalysed by acid or base.<sup>13</sup>

Herbaceous plants are usually less resistant to chemical pretreatment than hardwoods and particularly softwood.<sup>38</sup> The high resistance of softwood is attributed to their less reactive lignin, which contains fewer  $\alpha$ -ether linkages, less reactive  $\beta$ -O-4 ether linkages and a higher tendency to lignin recondensation.<sup>39</sup>

### 1.7.1 Existing pretreatment methods

Brief descriptions of the most common pretreatment operations are presented in the following paragraphs. A detailed literature review of biomass pretreatment with ionic liquids is presented in chapter 4.

*Kraft pulping:* The currently most widely used lignocellulose treatment process is the alkaline Kraft process for the production of paper.<sup>40</sup> In Kraft pulping, the lignocellulosic biomass is cooked in aqueous sodium hydroxide and sodium hydrogen sulfide at 130-180°C for several hours to solubilise most of the lignin and part of the hemicellulose. The lignin and hemicellulose containing liquor is concentrated and burned for energy generation and to aid regeneration of the sulfide (which is partially converted to sulfate during the pulping).

*Aqueous acid pretreatment:* Dilute acid pretreatment uses sulfuric or hydrochloric acid at a concentration of 0.5-5% and at temperatures between 160 and 220°C. Sometimes the liquor is also acidified with SO<sub>2</sub> gas, which diffuses quickly into the biomass and produces sulfurous acid. An advantage of acid treatments is their speed (usually minutes) and the low cost of the chemicals. Application of aqueous acid results in the cleavage of glycosidic bonds and of  $\alpha$ - and  $\beta$ -ether bonds in lignin. While a shorter pretreatment mostly releases the labile hemicellulose fraction, a longer pretreatment will also hydrolyse the cellulose fraction. However, the acid treatment will cause conversion of carbohydrate

monomers into degradation products such as 5-hydroxymethylfurfural (HMF) and 2-furaldehyde (furfural).

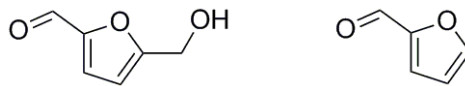


Figure 23: Hexose and pentose degradation products obtained under acidic conditions: 5-Hydroxymethylfurfural (HMF, left) and 2-furaldehyde (right).

This reduces the yield and produces compounds which are toxic to microorganisms (details on the formation of these compounds in section 1.7.2.1 on page 53). Because a significant fraction of the sugars are released into the pretreatment liquor, the liquor is conditioned by raising the pH with lime to be able to use this solubilised fraction. This adds cost and creates a waste stream. The lignin is redistributed on the cellulose fibrils and remains attached to them as tiny droplets, due to its poor solubility in aqueous acid.<sup>41</sup> This can be regarded as delignification on a microscopic scale. However, the residual lignin binds cellulase enzymes non-productively.<sup>25, 42, 43</sup> Another drawback of dilute acid treatment is the corrosive nature of the pretreatment liquor requiring the use of expensive equipment.

Hot water and steam explosion also fall under the category of dilute acid pretreatment, as the pH of the liquor drops during the pretreatment. The pH decrease is due to the high temperature, which increases the self-ionisation of water, and the release of acids from the biomass (autocatalysis). Addition of sodium bisulfite to the liquor can help to improve the digestibility of more recalcitrant softwood.<sup>44</sup> Bisulfite salts have been used extensively for pulping in paper production in the past. Sulfonation at the  $\alpha$ - and  $\gamma$ -positions of the lignin subunits makes the lignin fragments water-soluble, which assists in generating a highly enriched cellulose pulp.<sup>45</sup> However, pollution of the atmosphere with SO<sub>2</sub>, resulting in acid rain, has been a major reason for the decline of sulfite pulping.

A special case is the use of concentrated acids, e.g. sulfuric acid. Concentrated acids can decrystallise cellulose. Concentrated acid treatment is typically a two-stage process.<sup>46</sup> Initially, cellulose is decrystallised at low temperature and atmospheric pressure, followed by

dilution with water and a second treatment at around 100°C, which leads to the hydrolysis of the carbohydrate polymers. The carbohydrates are separated from the acid by membrane separation or chromatography. The acid is recovered and recycled. A process using concentrated phosphoric acid (COSLIF) has also been proposed, with recovery of an amorphous cellulose fraction. A separate lignin fraction can be obtained after extraction with acetone.<sup>47</sup>

*Organosolv pretreatment:* This treatment uses mixtures of an organic solvent, most commonly ethanol, and water for lignocellulose treatment at high temperature and pressure.<sup>48, 49</sup> Sulfuric acid is usually added to enhance the effectiveness of the treatment. Organosolv pretreatment has been demonstrated for hardwood (e.g. poplar)<sup>50</sup> softwood (e.g. pine)<sup>51</sup> and grasses (*Miscanthus*)<sup>52</sup>. The main effects are the hydrolysis and solubilisation of part of the lignin and part of the hemicellulose. The lignin can be precipitated by diluting the liquor with water. Organosolv lignin is regarded as a high quality lignin and can enhance the economic attractiveness of the organosolv process. A main drawback of this pretreatment is loss of the volatile organic solvent. This increases cost and the risk of pollution and explosion.<sup>48</sup> Generation of fermentation inhibitors (furfurals) is also a problem in organosolv pretreatment.

*Alkaline pretreatment:* Pretreatment under alkaline conditions results in the depolymerisation and solubilisation of lignin, hydrolysis of ester bonds and swelling of the cellulose fibrils.<sup>53</sup> Enzyme loadings are lower than in acid-catalyzed processes, because more lignin is removed and the cellulose is less crystalline. The generation of sugar degradation products is avoided in base pretreatment. Lime pretreatment requires long incubation times (hours rather than minutes) and more expensive chemicals than acids. However, temperature and pressure are lower and the equipment for basic treatments is less expensive than the equipment for acid treatment.

*Ammonia based pretreatment:* Ammonia pretreatment uses a volatile base as catalyst. Ammonia-based pretreatment technologies seem to work well on herbaceous biomass, but are currently not very effective on wood.<sup>54</sup> The basic pH prevents sugar degradation and thus reduces

sugar losses and post-pretreatment conditioning. Any residual ammonia can serve as a nitrogen source for fermentative organisms. The volatility of ammonia is beneficial for recovery, although losses must be avoided. Ammonia is also a considerable hazard to workers and the environment due to the use of volatile ammonia under high pressure. *Ammonia fibre expansion (AFEX)* uses 100% anhydrous ammonia under pressure which is rapidly released. The ammonia swells and decrystallises cellulose and alters the structure of lignin. The sudden decompression that follows the pretreatment reduces the particle size. After the treatment the ammonia is recondensed and recycled. An advantage of AFEX is the use of high biomass loadings. The hemicellulose recovery is high, because it is not washed away. *Ammonia recycling percolation (ARP)* applies 10-15% aqueous solutions of ammonia at elevated temperatures (around 180°C).<sup>55</sup> It causes delignification, hemicellulose hydrolysis and reduction of cellulose crystallinity.

*Biological pretreatment:* Microorganisms have developed the capability to break-down the lignocellulosic matrix under ambient conditions using a varied set of enzymes. The process is slow, however, controlled inoculation with suitable fungal strains could be combined with storage, yielding feedstock with improved accessibility without much extra energy input.<sup>5</sup>

A variety of other factors can affect the pretreatment efficiency. For example, the cropping time influences the sugar recovery from *Miscanthus*.<sup>56</sup> Plant breeding and genetic engineering has been envisaged to create crops that are more sensitive to pretreatment.<sup>57</sup> However, it is possible that there will be limits, as plant resilience against natural impacts such as adverse weather or diseases could be impaired when the cell walls are too fragile.

### 1.7.2 Degradation reactions of sugars

As mentioned earlier, many pretreatment operations use acid catalysis. However, acidic conditions promote the formation of substances that are inhibitory to fermentative organisms. The most prominent inhibitors are 2-furaldehyde (furfural) and 5-(hydroxymethyl)furfural (HMF), which are

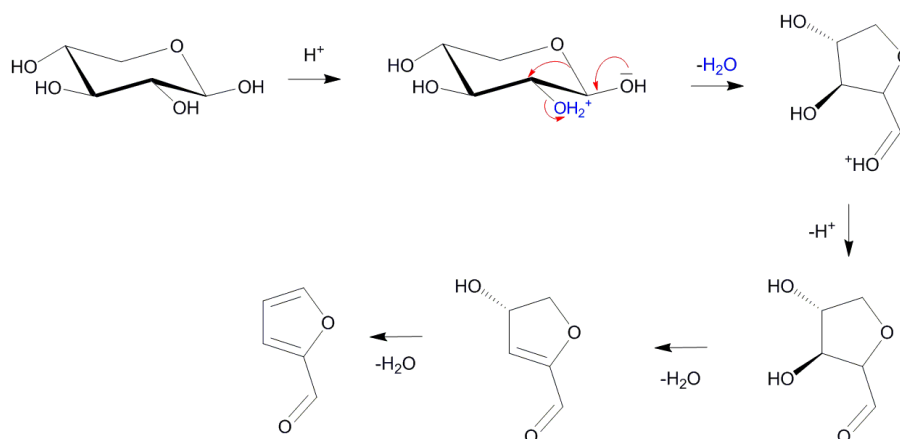
derived from pentose and hexose sugars, respectively. They are also undesired because they lower the sugar yields. However, conversion into furfurals may be desired, because they can serve as platform chemicals which can be transformed into a variety of polymers and liquid fuels, but then high yields and a selective conversion are required.<sup>58, 59</sup>

### 1.7.2.1 Degradation of pentoses

Furfural is formed under acidic conditions as a product of xylose and arabinose dehydration. Two reaction pathways have been suggested, *via* an open-chain or a cyclic intermediate (as shown in Scheme 2).<sup>60</sup> Three molecules of water are removed from the pentose during transformation into furfural.

The rate of xylose disappearance in aqueous acids is proportional to the  $H^+$  concentration and exponentially proportional to the temperature.<sup>61</sup> At 230°C, xylose is consumed within a few minutes, but at 180°C the conversion takes hours (without changing the acid concentration).

Batch yields of furfural from xylan are significantly lower than 100% (often <60%). This is due to side reactions such as furfural condensation, a reaction between furfural and an intermediate of furfural formation. Another side reaction is resinification, a reaction of furfural with itself, resulting in polymer formation.<sup>61</sup>

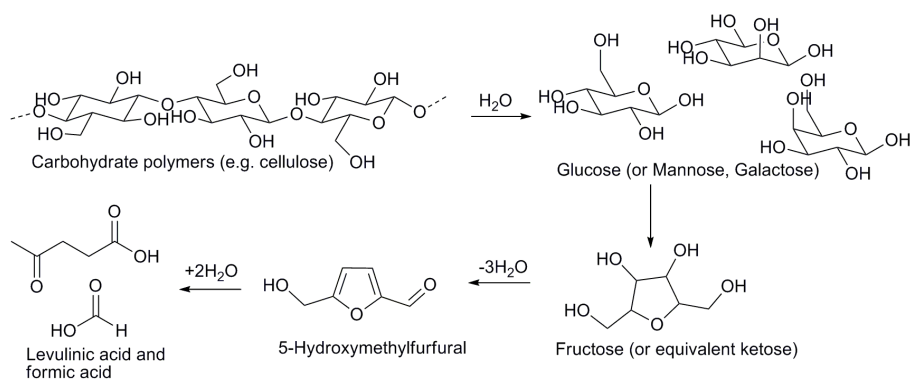


Scheme 2: Acid-catalysed dehydration of D-xylose to furfural. The mechanism shown proceeds *via* a cyclic intermediate.<sup>60</sup>

### 1.7.2.2 Degradation of hexoses

Hexoses also undergo dehydration under acidic conditions and 5-(hydroxymethyl)furfural (HMF) is formed. Fructose reacts readily, because it is a ketose and therefore mainly in the furanose form. This conformation is the immediate precursor for the dehydration sequence. Aldoses such as glucose, mannose and galactose require isomerisation into a ketose *via* an enediol intermediate before they can undergo dehydration. This transformation is called Lobry-de-Bruyn-van-Ekenstein transformation and can be acid or base-catalysed.

HMF is not stable in aqueous solution, and will decompose to levulinic acid and formic acid with the addition of two molecules of water. The reaction sequence starting from cellulose through to levulinic acid is shown in Scheme 3. The scheme does not show the pathways that lead to the formation of insoluble degradation products.



Scheme 3: Acid catalysed conversion of cellulose to levulinic acid *via* glucose, fructose and HMF

The concentrations of the intermediate and products during acid-catalysed conversion of cellulose into acids are shown in Figure 24.

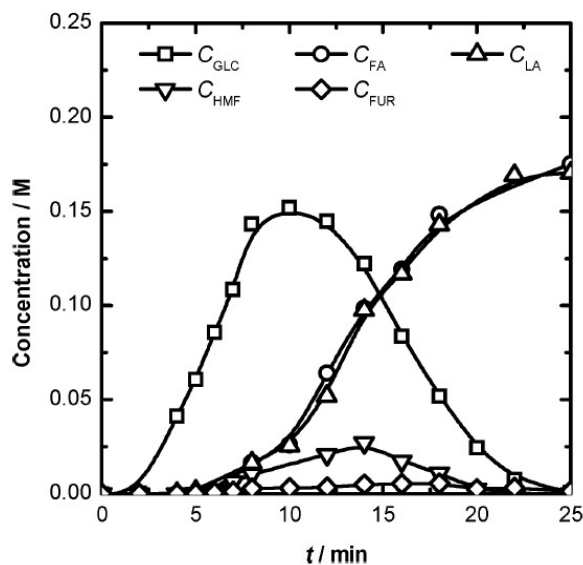


Figure 24: Time profile of cellulose hydrolysis at 200°C in dilute sulfuric acid (0.05 M). The concentrations of various compounds was examined.<sup>62</sup> Abbreviations: GLC, Glucose; FA, Formic acid; LA, Levulinic acid; HMF, Hydroxymethylfurfural, FUR, Furfural

### 1.7.3 Pseudo-lignins

The insoluble sugar degradation products are called humins or pseudo-lignin. The term pseudo-lignin is used because in standard quantitative analytical methods these compounds are quantified as lignin (Klason lignin, see section 4.4). The formation of pseudo-lignins reduces the sugar yields and limits the yields of furfural,<sup>61</sup> HMF or levulinic acid. Attempts have been made to overcome this limitation. The yield of furfural can be improved by distilling it from the broth during the reaction. The HMF yield is improved by extracting it into an organic solvent phase during the reaction.<sup>63</sup> Levulinic acid yields can be improved by reducing the amount of starting material, lowering the temperature and increasing the acid concentration.<sup>62</sup>

### 1.7.4 The optimal pretreatment process

Because a biorefinery will produce bulk chemicals such as fuels and platform chemicals, energy input, waste streams and the environmental impact need to be very low. The Environmental (E) factor is a Green Chemistry metric that summarises waste generation, solvent losses and



fuel requirement of a process into one number.<sup>64</sup> A low E factor indicates that the process by which a compound is made is very material-efficient. The E factors for oil refinery products and bulk chemicals are very low compared to the E factors of fine chemicals or pharmaceuticals (Table 1). The E factor of biorefinery products must be equally low to be sustainable and cost-competitive.

Table 1: E factors in various segments of the chemical industry<sup>64</sup>

Industry segment	Product tonnage	E Factor (kg waste/kg product)
Oil Refining	$10^6$ - $10^8$	<0.1
Bulk chemicals	$10^4$ - $10^6$	<1-0.5
Fine chemicals	$10^2$ - $10^4$	5->50
Pharmaceuticals	$10$ - $10^3$	25>100

The ideal pretreatment operation should be applicable to a wide range of feedstocks. Energy-intensive upstream-processing, such as feedstock drying and fine milling should not be required. For the pretreatment process, high solid-to-liquid ratios (>20 wt%) must be achieved.<sup>37</sup> The pretreatment times should be short. If chemicals are used, they should be inexpensive and used in low quantities or they should be recycled easily and efficiently. The risk of environmental pollution and health hazards to workers should be minimal, e.g. by applying reasonable operating pressures and using less toxic/volatile/corrosive chemicals. The reactor should be constructed from inexpensive material and a minimum number of unit operations should be required to reduce investment cost. The need for down-stream conditioning (such as neutralisation and removal unwanted of side-products) should be minimal or absent avoiding the generation of waste. The usage of water should be limited or the water cycled efficiently. Low enzyme loadings should be required (preferably 90% digestion in less than 3 days at 10 Filter paper units (FPU) per gram of cellulose).<sup>65</sup> The glucose yield should be >90% and the concentration of sugars in the syrup fed to microorganisms should be high (more than 10% weight per volume).

## 1.8 Ionic liquids

Ionic liquids are salts that are liquid at or close to room temperature. The salts that are liquid at room temperature are called ambient or room-temperature ionic liquids. The recent surge of interest in ionic liquids can be credited to the discovery of air and water stable room-temperature ionic liquids in the early 1990s.<sup>66</sup> This new development made it possible to handle ionic liquids in a similar fashion to molecular solvents.

### 1.8.1 *The structure of ionic liquids and implications for their melting point*

Ionic substances are often solid, due to the strong coulombic forces between the positively charged cations and the negatively charged anions. The inorganic salt NaCl melts at 801°C, for example. Therefore, in order to obtain low melting salts, the ability to form ordered structures must be sufficiently disturbed. Important factors for the low melting points of ionic liquids are the bulkiness and the low symmetry of both cations and anions and the charge delocalisation over more than one atom.

Modern ionic liquids contain organic cations, usually quaternised aromatic and aliphatic ammonium ions. Alkylphosphonium and alkylsulfonium cations are also in use. A representative selection of common cations is shown in Figure 25. Ionic liquid cations often have lengthy names, therefore a notation of the form  $[C_nC_m(C_oC_p)x(yz)]$  will be adopted throughout this thesis. The subscripted C signifies an alkyl chain. The subscripts n and m denote the length of these alkyl chains (all methylene units plus the terminal methyl group). The one or two letter abbreviations symbolised by x(yz) define the cation core. The cation core can be a single atom or a more elaborate, often heterocyclic, structure. Examples are x=N for nitrogen, xy=im for imidazolium, x=pyr for pyridinium and xy=pyrr for pyrrolidinium. Up to 4 alkyl chains can be attached to the cation core.

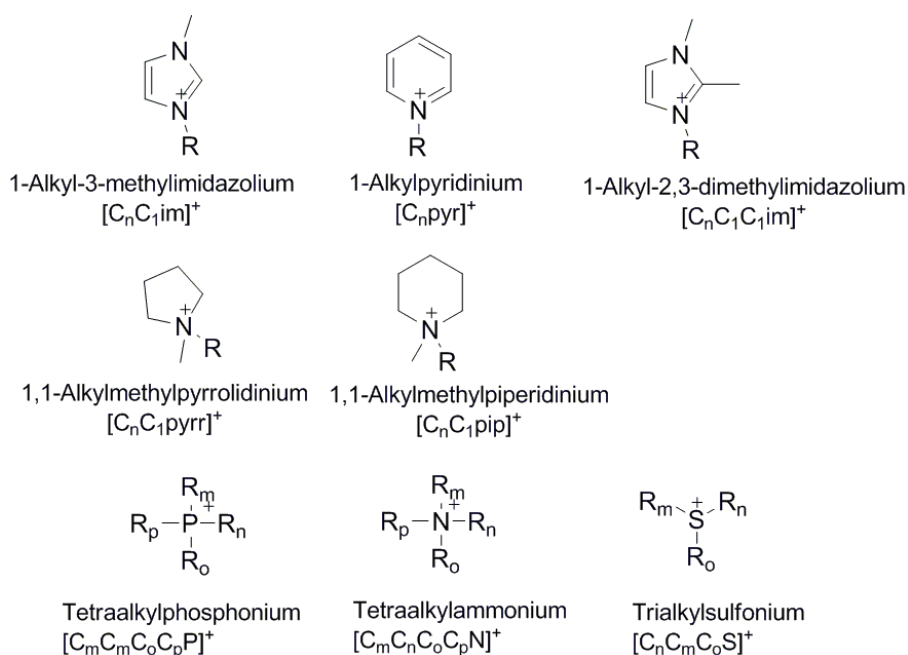


Figure 25: Common cations used in modern ionic liquids

The positive charge is usually delocalised over several atoms, particularly in aromatic cations.<sup>67</sup> An important contribution to lowering the melting point of salts comes from the alkyl chains, which introduce rotational degrees of freedom that are active at low temperature.<sup>68</sup> For cations with more than one alkyl group, differing lengths of alkyl chains result in a reduced symmetry and also contribute to a lower melting point. In addition, the cation cores shown in Figure 25 can be modified, for example by substituting hydrogen atoms with methyl groups or with alkyl chains that are branched or bear functionalities, such as hydroxy, cyano or sulfonic acid groups.

Ionic liquid anions are either inorganic or organic (Figure 26). With the exception of halide anions, the negative charge is usually distributed over several atoms. Many anions are substituted with fluorine atoms, such as trifluoromethanesulfonate or tetrafluoroborate. Fluorination also has a positive effect on the ionic liquid stability.<sup>69</sup> The lipophilic character of fluorinated alkyl groups and their ability to withdraw electron density from the rest of the anion reduces the hydrogen-bonding and thus the melting point.<sup>69</sup>

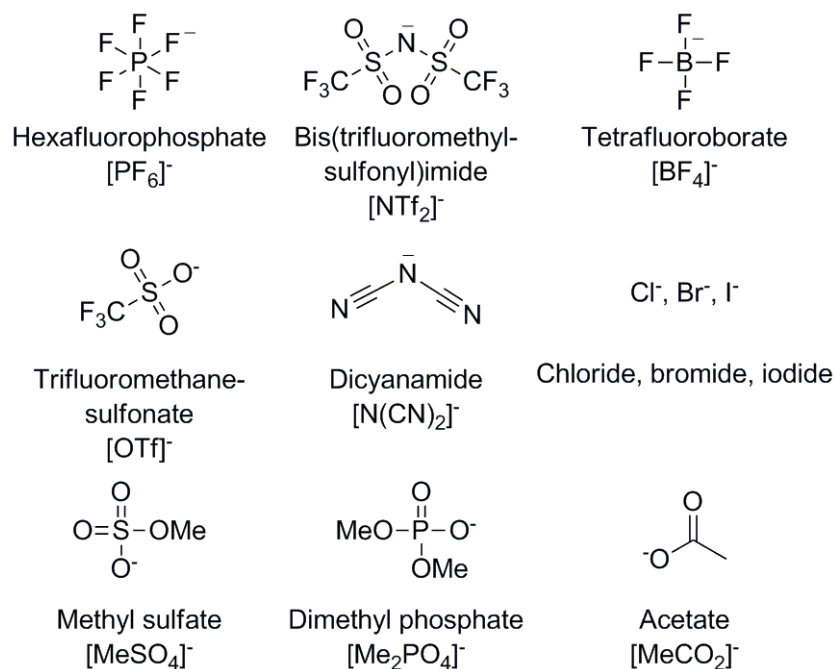


Figure 26: Selection of anions used in modern ionic liquids

### 1.8.2 Properties of ionic liquids and applications<sup>70</sup>

Ionic liquids have found a wide range of applications.<sup>71</sup> They are used as electrolytes in electrochemical processes, as solvents or solvent additives in chemical and biocatalytic reactions, in separation processes and as lubricants. They have also recently been employed in biomass processing.<sup>72</sup>

When ionic liquids have made or are expected to make a positive impact in the area of chemistry or engineering, it is usually due to a number of specific properties, which will be discussed briefly.

1. Ionic liquids are liquids that normally entirely comprised of ions. This enables the use of ionic solvents in organic synthetic reactions. The use of ionic solvents allows enhanced stabilisation of charged transition states in organic reactions<sup>73</sup> and the separation of ion pairs. This can potentially alter reactivities and selectivities observed in molecular solvents.
2. Ionic liquids are concentrated low-viscosity room-temperature electrolytes. They have a larger electrochemical window than

molecular solvents and allow electrochemical transformations that are not possible otherwise.

3. Ionic liquids have no appreciable vapour pressure over a large temperature range. This means that solvent emissions can be prevented, improving solvent recovery and reducing the hazard of toxic fumes escaping into the surroundings. The extremely low vapour pressure also results in a very low flammability over a large temperature range. The low volatility of ionic liquids allows new separation processes. Volatile products can be removed by distillation while the solvent is left behind, and catalyst/solvent systems can be recycled as a whole.
4. The liquid range of many ionic liquids extends to high temperatures and reactions requiring high temperatures can be carried out without the use of pressure equipment.
5. The physical and chemical properties of ionic liquid solvents can be finely tuned by selecting appropriate ion combinations. The large number of possible ion combinations and functionalisations makes this class of solvents extremely diverse. Using mixtures of ionic liquids extends the range of accessible properties.
6. Ionic liquids are highly polar solvents, yet, they can be non-coordinating. This enables transition metal catalysis in a range of polar solvents. Ionic liquids can also be modified to bear catalytically active functionalities.
7. The unusual miscibility behaviour of ionic liquids makes them a non-aqueous polar alternative to water in new systems with more than two phases.

## 2 Synthesis of hydrophilic ionic liquids

### 2.1 Introduction

A review of the early literature on biomass processing with ionic liquids at the beginning of this project showed that the ionic liquid anion had an important effect on the solvation of biomolecules.

For example, it had been shown that cellulose was soluble in ionic liquids containing anions such as chloride or acetate,  $[\text{MeCO}_2]^-$ , but not tetrafluoroborate  $[\text{BF}_4]^-$  or hexafluorophosphate  $[\text{PF}_6]^-$ .<sup>74</sup> An investigation of the solubility of a lignin preparation in dialkylimidazolium ionic liquids had shown that lignin dissolved in large quantities in ionic liquids with trifluoromethanesulfonate,  $[\text{OTf}]^-$ , and methyl sulfate,  $[\text{MeSO}_4]^-$ , anions.<sup>75</sup>

These ionic liquids are water-miscible. However, the standard synthetic procedure used in the Welton group has been optimised for water-immiscible or poorly water-miscible ionic liquids (see section 2.1.2). Therefore other available synthetic approaches had to be surveyed. The requirement was that the product ionic liquids should be of very good purity and colourless. Another requirement was that they could be obtained in sufficient quantities, because experiments involving biomass often require more material than is needed for spectroscopic or kinetic studies.

This chapter describes why the traditional synthesis procedure is not applicable to the ionic liquids of interest. The materials and methods section details the synthetic procedures that were selected and the results section accounts the experience gained with the various synthetic approaches.

#### 2.1.1 *Acid base combination*

Ionic liquids can be made from a Brønsted acid and a Brønsted base. Appropriate amounts of acid and base are mixed together in

stoichiometric quantities. The ionic liquid is formed when a proton from the acid is transferred onto the base. The extent of proton transfer depends on the nature of the acid and base and the position of the proton transfer equilibrium.<sup>76</sup> Many of these ionic liquids are mixtures of acid, base and the ionic liquid. The synthesis and application of acid-base ionic liquids were not in the scope of the project, so their synthesis will not be treated in more detail.

### 2.1.2 *Synthesis with halide intermediates*

This traditional synthetic route has been widely used for the synthesis of a variety of ionic liquids and produces hydrophobic and moderately hydrophilic ionic liquids of excellent purity. The method is used with some of the most popular anions, such as trifluoromethanesulfonate ([OTf]), tetrafluoroborate, [BF<sub>4</sub>], or bis(trifluoromethylsulfonyl)imide ([NTf<sub>2</sub>]). The synthesis consists of five steps:<sup>77</sup>

- Purification of starting materials
- Quaternisation of the amine (sulfone, phosphine)
- Purification of ionic liquid precursor
- Ion metathesis
- Purification of ionic liquid product

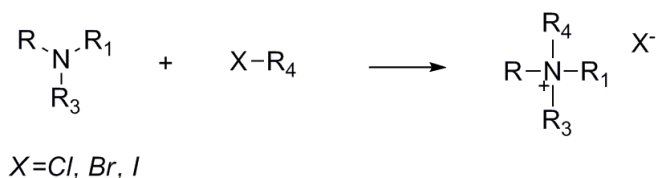
Impurities can have a great impact on the performance of an ionic liquid.<sup>78</sup> Distillation, a powerful purification method for molecular solvents is not applicable due to the negligible vapour pressures of most ionic liquids. Several alternative purification steps are part of the ionic liquid synthesis protocol to compensate for this. All the steps mentioned above are carried out carefully if the ionic liquid is used for research purposes. It is unlikely that commercial suppliers of ionic liquids invest as much effort into the synthesis to be able to sell ionic liquid at competitive prices. Therefore commercial ionic liquids prepared by this method will contain varying degrees of impurities and are rarely colourless.

### 2.1.2.1 Purification of starting materials

The starting materials, usually an amine or a phosphine and the alkylating agent must be dry and colourless. Unless high-purity, anhydrous starting materials can be purchased, they need to be distilled, after drying with an appropriate drying agent.

### 2.1.2.2 Quaternisation

The quaternisation reaction is an alkylation reaction using a suitable alkylating agent, typically chloro-, bromo- or iodoalkanes. Chloroalkanes are preferred alkylating agents, because chloride salts are less soluble in organic solvents than bromide salts and more hydrophilic. This will be an advantage in the subsequent ion exchange and washing steps.



Scheme 4: Quaternisation of a tertiary amine with a haloalkane to yield a halide ionic liquid.

The quaternisation can be performed in a variety of solvents, as long as they dissolve the reactants. The choice of solvent will affect the reaction rate.<sup>79</sup> Ethyl acetate and toluene are commonly used. A solvent is required because the reaction is exothermic and the solvent helps to dissipate the reaction heat. Moreover, the halide precursors are usually solid up to around 70°C, so stirring the reaction mix without a solvent would become increasingly difficult due to the increasing viscosity.

The hygroscopicity of the halide salts is so strong, that these solids turn into liquid salt-water mixtures within minutes when exposed to air. Exclusion of water is also required to enable purification through recrystallisation. In order to keep the water content low, the reaction is performed under a nitrogen atmosphere using Schlenk technique.<sup>80</sup>

### 2.1.2.3 Purification of ionic liquid precursor

Once the quaternisation reaction is completed, residual reactants need to be removed. This can be achieved by washing the precursor with a



solvent that dissolves the reactants but not the ionic liquid, e.g. ethyl acetate. This option is available for both solid and liquid ionic liquids. If a solid precursor is contaminated with large quantities of reactants and a very high purity is required, recrystallisation from a suitable solvent might be necessary, e.g. with acetonitrile. The recrystallisation also removes colour. Residual solvents and volatile reactants are removed by applying mild heat under vacuum.

#### 2.1.2.4 Ion metathesis

In many cases the final ionic liquid will contain an anion that is not chloride and the halide anion needs to be exchanged against the desired anion. The traditional ion exchange reaction has been optimised by our group and others.<sup>80</sup> The procedure exploits the high solubility of ionic liquids in dichloromethane, while the solubilities of inorganic salts such as lithium (or sodium) chloride are low. A slight excess of ionic liquid precursor is dissolved in dichloromethane and stirred with a lithium or sodium salt of the desired anion, usually for 1-2 days to ensure that the equilibrium state is reached. Figure 27 shows an exemplary ion metathesis for the synthesis of  $[\text{C}_4\text{C}_{1}\text{im}][\text{NTf}_2]$ . The halide crystals are filtered off to yield the crude product dissolved in dichloromethane.

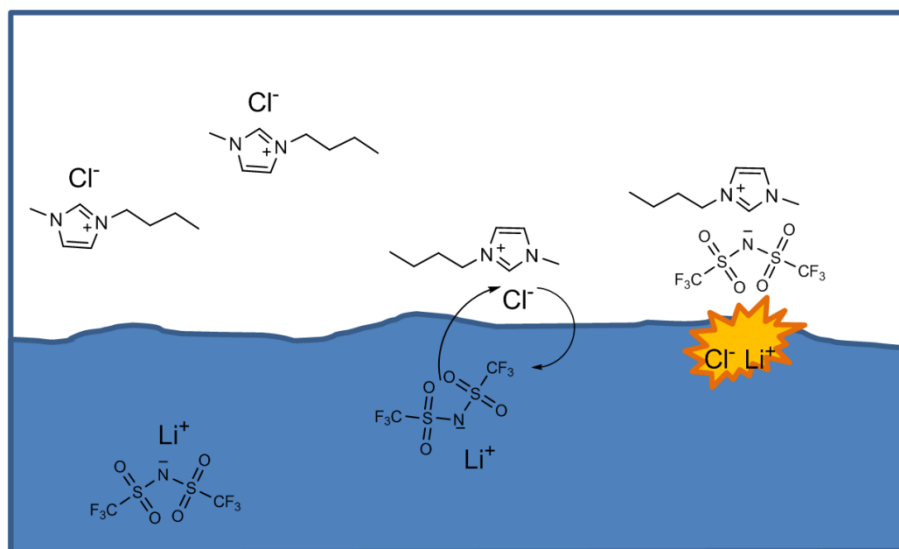


Figure 27: Ion metathesis of  $[\text{C}_4\text{C}_{1}\text{im}]\text{Cl}$  with  $\text{Li}[\text{NTf}_2]$  to obtain  $[\text{C}_4\text{C}_{1}\text{im}][\text{NTf}_2]$  in dichloromethane. Lower phase: solid inorganic salt phase. Upper phase: dichloromethane with dissolved ionic liquid.

#### 2.1.2.5 Purification of the ionic liquid product

After the ion exchange, the dichloromethane phase contains the ionic liquid product, but also substantial amounts of ionic impurities. The major impurity is the ionic liquid precursor; however, lithium salts will also be present. These impurities must be removed by washing. The wash solvent is water, which is not miscible with dichloromethane and can solubilise the impurities. Care must be taken if the product ionic liquid is also water-soluble, such as  $[\text{C}_4\text{C}_1\text{im}][\text{OTf}]$ . Only small amounts of wash water must be used, to reduce losses. The washing step is finished when addition of silver nitrate to the wash water does not result in the formation of a visible silver halide precipitate.

Ionic liquids are colourless, but they can become coloured during synthesis or use. Unless the development of colour is accompanied by degradation, the coloured impurities do not interfere with the application.<sup>81</sup> However, if the ionic liquids are used for spectroscopic measurements, a high level of transparency is required. For example, the measurement of Kamlet-Taft solvent polarity requires UV/Vis-transparent ionic liquids.

As mentioned earlier, colour can be removed from starting materials by distillation or from solid ionic liquids by recrystallisation. Decolourisation of liquid product ionic liquids can often be achieved by filtration through charcoal.<sup>81</sup> However, this method is only recommended for ionic liquids with less basic anions such as  $[\text{NTf}_2]^-$ ,  $[\text{BF}_4]^-$  or  $[\text{PF}_6]^-$ , but not for strongly hydrogen-bonding anions.<sup>81</sup>

#### 2.1.3 *Direct alkylation and transesterification*

The alkylation of amines, phosphines or sulfones with alkylating agents other than alkyl halides can also be used to make ionic liquids. This route is called direct alkylation and is the primary method for making alkylsulfates<sup>82</sup> and dialkylphosphates<sup>83</sup>. It is also sometimes used for the synthesis of alkylsulfonates<sup>84</sup>, trifluoroacetates<sup>85, 86</sup> and trifluoromethanesulfonates<sup>85</sup>. The advantage of ionic liquids obtained by direct alkylation is that they are cheap and halogen-free.

Contamination with colour may be a problem with this route, particularly if very reactive alkylating agents, such as dimethyl sulfate or methyl trifluoromethanesulfonate, are used. To minimise colour formation, cooling during the alkylation reaction is recommended. Many alkylating agents are also prone to react with water and contamination with acidic impurities may occur. Therefore the starting materials must be thoroughly dried and the use of excess alkylating agent avoided.

The half-ester anions such as alkyl sulfates and dialkyl phosphates have the propensity to hydrolyse in the presence of water, which may also introduce acid into the ionic liquid. On the other hand the half-ester structure provides the opportunity to modify the anion easily and cheaply: other, longer chain esters can be obtained by transesterification.<sup>87</sup> However, traces of acid catalyst might be present in the product ionic liquid, restricting the application of ionic liquids synthesised by transesterification to acid-tolerant processes.

Ionic liquids that are obtained by direct alkylation can also be used as intermediates for ion exchange, analogous to the way halide precursors are used. For example, ionic liquids based on the methanesulfonate anion have been used as precursors.<sup>84</sup>

#### 2.1.4 Ion exchange with silver salts

Silver salts have been used for the ion metathesis for a long time. The first synthesis of "air and water stable" ionic liquids used silver salts to exchange iodide in  $[\text{C}_2\text{C}_1\text{im}]\text{I}$ , and synthesise ionic liquids such as 1-ethyl-3-methylimidazolium nitrate,  $[\text{C}_2\text{C}_1\text{im}][\text{NO}_3]$ , or  $[\text{C}_2\text{C}_1\text{im}][\text{MeCO}_2]$ .<sup>66</sup> The metathesis with silver salts exploits the poor solubility of silver halides in aqueous or alcoholic solutions (Table 2). The solubility of AgCl in water is lower than  $2 \cdot 10^{-5}$  mol/l. The solubility of AgBr and AgI is even lower, due to the less favourable hydration of larger halide anions.

Table 2: Solubility of silver halides in water at 25°C<sup>88</sup>

---

	Solubility in mol/l
AgCl	$1.3 \times 10^{-5}$
AgBr	$7.1 \times 10^{-7}$
AgI	$1.3 \times 10^{-8}$

---

The precursor is dissolved in water and the respective silver salt is added in stoichiometric amounts. The silver halide crystals are removed by filtration. If the silver salt of the anion is not commercially available, it can be synthesised from  $\text{AgNO}_3$  and the respective sodium salt, provided the product silver salt is sparingly soluble in water (which most silver salts are). Drawbacks of this synthesis route are the possibility of residual silver ions remaining in the product and the high cost of silver salts.

### 2.1.5 *Ion metathesis with ion exchange resins*

Ion exchange resins are polymeric materials that are functionalised with charged groups and can be used to exchange the ionic liquid anion. The resins used for preparative anion exchange contain quaternary ammonium groups.<sup>89</sup> The mobile phase is often water, but can also be an organic molecular solvent. Initially, the anion exchange resin is loaded with the desired anion by flushing the resin with a concentrated solution of its sodium salt. When the column has been loaded and washed, a solution of the ionic liquid precursor is passed through the column, during which it exchanges its halide anions with the anions coordinated to the charged groups of the resin (Figure 28). The existence of a large number of microequilibria on the resin ensures that the exchange is driven to completion.

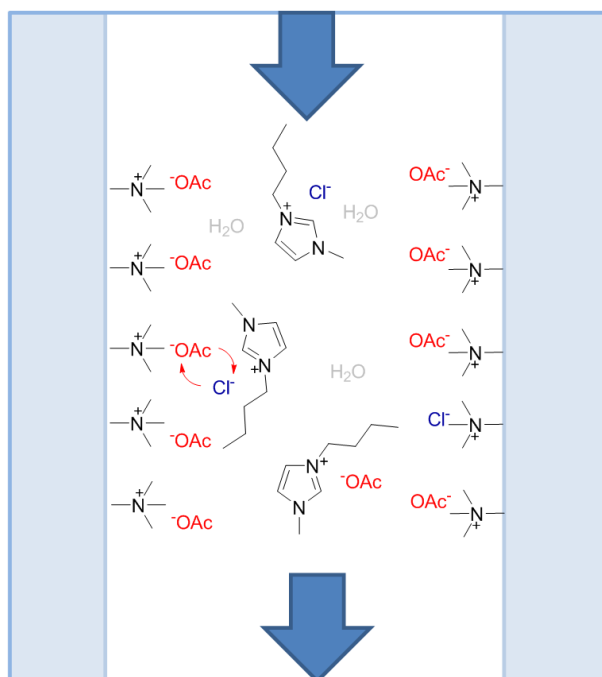
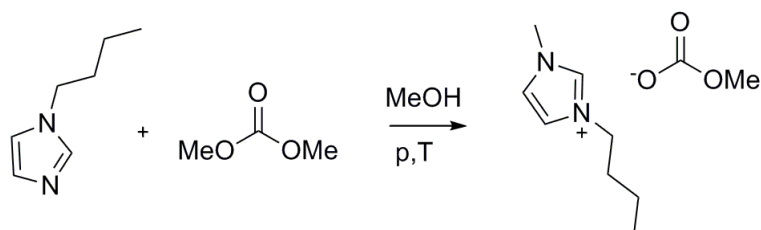


Figure 28: Synthesis of  $[C_4C_1im][MeCO_2]$  in aqueous solution using an ion exchange resin.

This route yields pure and transparent ionic liquids. The halide content is typically reduced to below detection limit.<sup>90</sup> The drawback of this method is the use of large quantities of resin and solvent, which results in a limited product volume per batch, dictated by the capacities of research laboratory equipment. Not more than 10-20 ml ionic liquid are synthesised in one batch and the procedure is lengthy and labour-intensive.

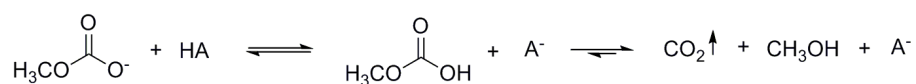
### 2.1.6 Methyl carbonate route

A route that has recently become popular uses dimethyl carbonate as the alkylating agent (Scheme 5).<sup>91, 92</sup> The use of the methyl carbonate intermediate is greener than the halide precursor for three reasons.



Scheme 5: Synthesis of 1-butyl-3-methylimidazolium methyl carbonate in methanol

Firstly, dimethyl carbonate is non-toxic, while many alkylating agents are carcinogens.<sup>93</sup> Secondly, the alkylation with dimethyl carbonate and the subsequent ion exchange are carried out without the use of the decidedly non-green solvent dichloromethane. Thirdly, the methyl carbonate precursor allows ion exchange with simple acids instead of alkali or silver salts. This is due to the acid-lability of the methyl carbonate anion, which will decompose to methanol and carbon dioxide upon addition of acid (Scheme 6). The  $pK_a$  of methyl carbonic acid is 5.6,<sup>94</sup> so any acid with a lower  $pK_a$  will react readily, leaving its corresponding base as the new anion.



Scheme 6: Decomposition of the methyl carbonate anion upon addition of an acid HA.

The alkylation with dimethyl carbonate needs to be performed in pressure reactors, because the reaction temperature is higher than the boiling point of both solvent ( $T_b(\text{methanol}) = 65^\circ\text{C}$ ) and alkylating agent ( $T_b(\text{dimethyl carbonate}) = 90^\circ\text{C}$ ). A solvent-free synthesis of  $[\text{C}_n\text{C}_1\text{im}][\text{MeCO}_3]$  ( $n = 2, 4$ ) has been reported.<sup>95</sup>

In this project, the methyl carbonate route was explored for the synthesis of  $[\text{C}_4\text{C}_1\text{im}][\text{MeSO}_3]$  and  $[\text{C}_4\text{C}_1\text{im}][\text{HSO}_4]$ . Moreover, the purification of 1-butyl-3-methylimidazolium methyl carbonate ( $[\text{C}_4\text{C}_1\text{im}][\text{MeCO}_3]$ ) was investigated, which has not been studied before.

## 2.2 Materials and Methods

### 2.2.1 Reagents

All reagents were purchased from Sigma-Aldrich, Fisher or VWR. 1-Methylimidazole and 1-butylimidazole were dried with potassium hydroxide pellets and distilled under vacuum. 1-Chlorobutane and 1-bromobutane were distilled over phosphorous pentoxide, P<sub>2</sub>O<sub>5</sub>. Dimethyl sulfate was distilled over calcium oxide. Trimethyl phosphate, silver acetate, sodium dicyanamide and silver nitrate were used as received. Ethyl acetate and acetonitrile were dried over CaH<sub>2</sub>. Toluene was distilled over sodium (with benzophenone as moisture indicator). 1,1-Butylmethylpyrrolidinium bromide was synthesised by Juan Manuel Pérez Arlandis. 1-Butyl-3-methylimidazolium methyl sulfate (Basionic AC01) for the synthesis of 1-butyl-3-methylimidazolium hydrogen sulfate was purchased from Sigma-Aldrich.

### 2.2.2 Instrumentation

Liquid secondary ion mass spectrometry (LSIMS) was performed on a Micromass AutoSpec Premier. Electrospray ionisation (ESI) mass spectra were recorded on a Micromass LCT Premier instrument. <sup>1</sup>H-NMR and <sup>13</sup>C-NMR spectra (proton-decoupled) were recorded with a Bruker 400 MHz spectrometer. Chemical shifts are reported in ppm (relative to tetramethylsilane) and coupling constants are given in Hz. Elemental analysis was carried out by the London Metropolitan University Service. The pressure reactors were from Parr Instruments Ltd equipped with stainless vessels (250-600 ml internal volume).

### 2.2.3 Ionic liquid synthesis

#### 2.2.3.1 1-Butyl-3-methylimidazolium chloride, [C<sub>4</sub>C<sub>1</sub>im]Cl

Chlorobutane (288 ml, 2.87 mol) was mixed with 200 ml ethyl acetate. 1-Methylimidazole (200 ml, 2.53 mol) was added dropwise. The mixture was stirred at 45°C for 14 days. The two-phase mixture was cooled to

-20°C until the product crystallised. The liquid was removed, the crystals washed with ethyl acetate and recrystallised in acetonitrile. The white crystals were dried and stored in the glove box for further use. Yield: 55.9%

$^1\text{H-NMR}$  (400 MHz, DMSO- $d_6$ )  $\delta$ : 9.53 (1H, s, CH-2), 7.89 (1H, s, CH-4), 7.81 (1H, s, CH-5), 4.21 (2H, t, N-CH $_2$ -), 3.88 (3H, s, N-CH $_3$ ), 1.77 (2H, m, N-CH $_2$ CH $_2$ -), 1.24 (2H, m, N-(CH $_2$ ) $_2$ CH $_2$ CH $_3$ ), 0.89 (3H, t, N(CH $_2$ ) $_3$ CH $_3$ ) ppm.  $^{13}\text{C}\{^1\text{H}\}$ -NMR (100 MHz, CDCl $_3$ )  $\delta$ : 137.83 (s, C-2), 123.67 (s, C-4), 121.98 (s, C-5), 49.69 (s, N-CH $_2$ CH $_2$ -), 36.47 (s, N-CH $_3$ ), 32.11 (s, CH $_2$ CH $_2$ CH $_2$ -), 19.38 (s, -(CH $_2$ ) $_2$ CH $_2$ CH $_3$ ), 13.37 (s, -CH $_2$ CH $_3$ ) ppm. Elemental analysis (calc.): %C=54.87 (55.01), %H=8.79 (8.66), %N=15.95 (16.04).

#### 2.2.3.2 1-Butyl-3-methylimidazolium bromide, [C $_4$ C $_1$ im]Br

1-Methylimidazole (100 ml, 1.27 mol) was mixed with 100 ml ethyl acetate. 1-Bromobutane (143 ml, 1.33 mol) was added dropwise. The mixture was stirred at room temperature overnight. The temperature was raised to 35°C and the emulsion stirred for 4 days and then cooled to -20°C to crystallise the product. The product was recrystallised in acetonitrile; the white crystals were dried and stored in the glove box. Yield: 78.4%

$^1\text{H-NMR}$  (400 MHz, DMSO- $d_6$ )  $\delta$ : 9.34 (1H, s, CH-2), 7.87 (1H, s, CH-4), 7.79 (1H, s, CH-5), 4.20 (2H, t, N-CH $_2$ -), 3.88 (3H, s, N-CH $_3$ ), 1.77 (2H, m, N-CH $_2$ -CH $_2$ -), 1.25 (2H, m, N-CH $_2$ -CH $_2$ -CH $_2$ -), 0.89 (3H, t, N-CH $_2$ -CH $_2$ -CH $_2$ -CH $_3$ ) ppm.  $^{13}\text{C}\{^1\text{H}\}$ -NMR (100 MHz, DMSO- $d_6$ )  $\delta$ : 137.00 (s, C-2), 124.02 (s, C-4), 122.72 (s, C-5), 48.88 (s, N-CH $_2$ (CH $_2$ ) $_2$ CH $_3$ ), 36.24 (s, N-CH $_3$ ), 31.84 (s, N-CH $_2$ CH $_2$ CH $_2$ CH $_3$ ), 19.21 (s, N-(CH $_2$ ) $_2$ CH $_2$ CH $_3$ ), 13.75 (s, N(CH $_2$ ) $_3$ CH $_3$ ) ppm. Elemental analysis (calc.): %C=43.75 (43.85), %H=6.87 (6.90), %N=12.71 (12.78).

#### 2.2.3.3 1-Butyl-3-methylimidazolium acetate, [C $_4$ C $_1$ im][MeCO $_2$ ]

[C $_4$ C $_1$ im]Br (130.2 g, 0.594 mol) and silver acetate (99.7 g, 0.597 mol) was transferred into a 500 ml conical flask. The flask was covered with aluminium foil to reduce photo degradation of silver bromide. 250 ml



distilled water was added and the suspension stirred overnight. The yellowish precipitate was filtered off. An aqueous 2 mol/L solution of  $[C_4C_1im]Br$  was added dropwise. The addition was stopped when precipitate formation ceased and a subsequent test for silver ions with dilute HCl was negative. The solution was placed in the continuous extractor and extracted with ethyl acetate for 16 h. The water was removed with the rotary evaporator and the ionic liquid dried to completion under vacuum at 60°C. Yield: 84.8%

$^1H$ -NMR (400 MHz, DMSO- $d_6$ )  $\delta$ : 10.17 (1H, s,  $CH-2$ ), 7.91 (1H, s,  $CH-4$ ), 7.83 (1H, s,  $CH-5$ ), 4.20 (2H, t,  $N-CH_2-$ ), 3.88 (3H, s,  $N-CH_3$ ), 1.75 (2H, m,  $N-CH_2-CH_2-$ ), 1.58 (3H, m,  $O_2C-CH_3$ ), 1.22 (2H, m,  $N-CH_2-CH_2-CH_2-$ ), 0.87 (3H, t,  $N-CH_2-CH_2-CH_2-CH_3$ ) ppm.  $^{13}C\{^1H\}$ -NMR (100 MHz, DMSO- $d_6$ )  $\delta$ : 173.59 (s,  $COO^-$ ), 137.04 (s, C-2), 124.02 (s, C-4), 122.27 (s, C-5), 48.41 (s,  $N-CH_2(CH_2)_2CH_3$ ), 35.76 (s,  $N-CH_3$ ), 31.33 (s,  $N-CH_2CH_2CH_2CH_3$ ), 18.74 (s,  $N-(CH_2)_2CH_2CH_3$ ), 13.27 (s,  $N(CH_2)_3CH_3$ ) ppm.  $m/z$  (LSIMS+): 139 (100%)  $[C_4C_1im]^+$ , 337 (14%)  $[(C_4C_1im)_2CH_3CO_2]^+$ .  $m/z$  (LSIMS-): 59 (100%)  $[CH_3CO_2]^-$ , 119 (61%)  $[(CH_3CO_2)_2H]^-$ , 257 (68%)  $[(CH_3CO_2)_2(C_4C_1im)]^-$ , 455 (28%)  $[(C_4C_1im)_2(CH_3CO_2)_3]^-$ . Elemental analysis (calc.): %C=60.63 (60.58), %H=9.13 (9.15), %N=13.96 (14.13).

#### 2.2.3.4 1-Butyl-3-methylimidazolium dicyanamide, $[C_4C_1im][N(CN)_2]$

Silver nitrate (71.3 g, 0.42 mol) was dissolved in 150 ml distilled water at 40°C. Sodium dicyanamide (39.2 g, 0.44 mol) was dissolved in 150 ml distilled water at 40°C and the silver nitrate solution was added slowly. The suspension was stirred for 1 h. The precipitate was filtered off and washed with 100 ml distilled water. The solid was dried at 80°C.  $[C_4C_1im]Br$  (76.4 g, 0.349 mol) was dissolved in 50 ml of distilled water. The  $[C_4C_1im]Br$  solution was added to a stirred suspension of silver dicyanamide (63.9 g, 0.367 mol) in 100 ml distilled water. The suspension was stirred overnight in a flask covered with aluminium foil. The precipitate was removed by filtration. A sample was taken and a drop of dilute HCl solution added, the absence of precipitate indicated that the concentration of silver ions was below detection limit. The

product was extracted into dichloromethane by continuous extraction for 3 days. The solvent was removed and the ionic liquid dried to completion. A second extraction of the water phase for 5 days yielded more  $[\text{C}_4\text{C}_1\text{im}][\text{N}(\text{CN})_2]$ . The product was a clear, slightly greenish liquid. Combined yield: 71.6%

$^1\text{H-NMR}$  (400 MHz,  $\text{DMSO-d}_6$ )  $\delta$ : 9.10 (1H, s, *CH*-2), 7.75 (1H, s, *CH*-4), 7.68 (1H, s, *CH*-5), 4.17 (2H, t, *N-CH*<sub>2</sub>-), 3.85 (3H, s, *N-CH*<sub>3</sub>), 1.77 (2H, m, *N-CH*<sub>2</sub>-*CH*<sub>2</sub>-), 1.26 (2H, m, *N-CH*<sub>2</sub>-*CH*<sub>2</sub>-*CH*<sub>2</sub>-), 0.89 (3H, t, *N-CH*<sub>2</sub>-*CH*<sub>2</sub>-*CH*<sub>2</sub>-*CH*<sub>3</sub>) ppm.  $^{13}\text{C}\{^1\text{H}\}$ -NMR (100 MHz,  $\text{DMSO-d}_6$ )  $\delta$ : 136.96 (s, *C*-2), 124.02 (s, *C*-4), 122.68 (s, *C*-5), 199.55 (s, *NCNCN*) 49.00 (s, *N-CH*<sub>2</sub>(*CH*<sub>2</sub>)<sub>2</sub>*CH*<sub>3</sub>), 36.17 (s, *N-CH*<sub>3</sub>), 31.80 (s, *N-CH*<sub>2</sub>*CH*<sub>2</sub>*CH*<sub>2</sub>*CH*<sub>3</sub>), 19.32 (s, *N-(CH*<sub>2</sub>)<sub>2</sub>*CH*<sub>2</sub>*CH*<sub>3</sub>), 13.65 (s, *N(CH*<sub>2</sub>)<sub>3</sub>*CH*<sub>3</sub>) ppm. *m/z* (LSIMS+): 139 (100%)  $[\text{C}_4\text{C}_1\text{im}]^+$ , 344 (8%)  $[(\text{C}_4\text{C}_1\text{im})_2(\text{N}(\text{CN})_2)]^+$ . *m/z* (LSIMS-): 66 (100%)  $[\text{N}(\text{CN})_2]$ . Elemental analysis (calc.): %C=56.06 (58.51), %H=7.21 (7.37), %N=31.36 (34.12).

#### 2.2.3.5 1-Butyl-3-methylimidazolium dimethyl phosphate, $[\text{C}_4\text{C}_1\text{im}][\text{Me}_2\text{PO}_4]$

1-Butylimidazole (112.5 g, 0.905 mol) was mixed with 100 ml ethyl acetate. Trimethyl phosphate (126.8 g, 0.905 mol) was added dropwise. The mixture was stirred at 80°C for 20 h. 50 ml distilled water were added. The solution was placed in the continuous extractor and extracted with toluene for 16 hours in order to remove excess reactants. The aqueous phase was isolated, the water was removed *in vacuo* and the ionic liquid dried to completion at 120°C. The product was a clear, colourless, oily liquid. Yield: 76.5%

$^1\text{H-NMR}$  (400 MHz,  $\text{DMSO-d}_6$ )  $\delta$ : 9.92 (1H, s, *CH*-2), 8.05 (1H, s, *CH*-4), 7.94 (1H, s, *CH*-5), 4.22 (2H, t, *N-CH*<sub>2</sub>-), 3.91 (3H, s, *N-CH*<sub>3</sub>), 3.32 (6H, d, *H*<sub>3</sub>*C-O-P*), 1.75 (2H, m, *N-CH*<sub>2</sub>-*CH*<sub>2</sub>-), 1.21 (2H, m, *N-CH*<sub>2</sub>-*CH*<sub>2</sub>-*CH*<sub>2</sub>-), 0.84 (3H, t, *N-CH*<sub>2</sub>-*CH*<sub>2</sub>-*CH*<sub>2</sub>-*CH*<sub>3</sub>) ppm.  $^{13}\text{C}\{^1\text{H}\}$ -NMR (100 MHz,  $\text{DMSO-d}_6$ )  $\delta$ : 137.73 (*C*-2), 124.07 (*C*-4), 122.78 (*C*-5), 51.70 (d, *H*<sub>3</sub>*C-O-P*) 48.81 (*N-CH*<sub>2</sub>(*CH*<sub>2</sub>)<sub>2</sub>*CH*<sub>3</sub>), 36.00 (*N-CH*<sub>3</sub>), 31.90 (*N-CH*<sub>2</sub>*CH*<sub>2</sub>*CH*<sub>2</sub>*CH*<sub>3</sub>), 19.22 (*N-(CH*<sub>2</sub>)<sub>2</sub>*CH*<sub>2</sub>*CH*<sub>3</sub>), 13.69 (*N(CH*<sub>2</sub>)<sub>3</sub>*CH*<sub>3</sub>) ppm. *m/z* (LSIMS+): 139 (100%)  $[\text{C}_4\text{C}_1\text{im}]^+$ , 403  $[(\text{C}_4\text{C}_1\text{im})_2\text{Me}_2\text{PO}_4]^+$ ; *m/z* (LSIMS-): 125 (100%)

[Me<sub>2</sub>PO<sub>4</sub>]<sup>-</sup>. Elemental analysis (calc.): %C=28.75 (28.64), %H=3.66 (3.61), %N=9.89 (10.02).

#### 2.2.3.6 1-Butyl-3-methylimidazolium methyl sulfate, [C<sub>4</sub>C<sub>1</sub>im][MeSO<sub>4</sub>]

N-butylimidazole (143 ml, 1.09 mol) was mixed with 200 ml toluene and the mixture cooled to 0°C. Dimethyl sulfate (103 ml, 1.09 mol) was added drop-wise while stirring. The stirring was continued for 1 h at room temperature. The top phase was decanted and the lower phase washed three times with 50 ml toluene. The ionic liquid was dried under vacuum. The product was a colourless, viscous liquid. Yield: 70.8%

<sup>1</sup>H-NMR (400 MHz, DMSO-d<sub>6</sub>) δ: 9.12 (1H, s, CH-2), 7.79 (1H, s, CH-4), 7.71 (1H, s, CH-5), 4.17 (2H, t, N-CH<sub>2</sub>-), 3.86 (3H, s, N-CH<sub>3</sub>), 3.41 (3H, s, H<sub>3</sub>C-O-S), 1.76 (2H, m, N-CH<sub>2</sub>-CH<sub>2</sub>-), 1.24 (2H, m, N-CH<sub>2</sub>-CH<sub>2</sub>-CH<sub>2</sub>-), 0.87 (3H, t, N-CH<sub>2</sub>-CH<sub>2</sub>-CH<sub>2</sub>-CH<sub>3</sub>) ppm. <sup>13</sup>C{<sup>1</sup>H}-NMR (100 MHz, DMSO-d<sub>6</sub>) δ: 137.04 (s, C-2), 124.02 (s, C-4), 122.72 (s, C-5), 53.41 (s, H<sub>3</sub>C-O-S) 48.92 (s, N-CH<sub>2</sub>(CH<sub>2</sub>)<sub>2</sub>CH<sub>3</sub>), 36.09 (s, N-CH<sub>3</sub>), 31.84 (s, N-CH<sub>2</sub>CH<sub>2</sub>CH<sub>2</sub>CH<sub>3</sub>), 19.20 (s, N-(CH<sub>2</sub>)<sub>2</sub>CH<sub>2</sub>CH<sub>3</sub>), 13.66 (s, N(CH<sub>2</sub>)<sub>3</sub>CH<sub>3</sub>) ppm. m/z (LSIMS<sup>+</sup>): 139 (100%) [C<sub>4</sub>C<sub>1</sub>im]<sup>+</sup>, 389 (4%) [(C<sub>4</sub>C<sub>1</sub>im)<sub>2</sub>MeSO<sub>4</sub>]<sup>+</sup>. m/z (LSIMS<sup>-</sup>): 111 (100%) [MeSO<sub>4</sub>]<sup>-</sup>, 361 (3%) [(C<sub>4</sub>C<sub>1</sub>im)(MeSO<sub>4</sub>)<sub>2</sub>]<sup>-</sup>. Elemental analysis (calc.): %C=43.22 (43.18), %H=7.29 (7.25), %N=11.19 (11.27).

#### 2.2.3.7 1,1-Butylmethylpyrrolidinium acetate [C<sub>4</sub>C<sub>1</sub>py][MeCO<sub>2</sub>]

1-Butyl-1-methylpyrrolidinium bromide (10.0 g, 45.0 mmol) was dissolved in 5 ml distilled water in an Erlenmeyer flask covered with aluminium foil to prevent photo degradation of the silver bromide. Silver acetate (8.35 g, 50.0 mmol) was washed into the flask using distilled water. The volume was about 100 ml. The emulsion was stirred for a minimum of 1 h. The precipitate was removed by filtration through a Buchner funnel. The excess silver acetate was titrated with a 2 mol/L solution of [C<sub>4</sub>C<sub>1</sub>py]Br (2.22 g in 5 ml H<sub>2</sub>O) using a burette. The solution was stirred gently. Three drops of titrant were added at a time. A fine precipitate of silver bromide formed near surface. After the precipitate settled, more titrant was added until precipitate formation ceased. The

solvent was removed and the remaining liquid dried under high vacuum and 70°C until it was a viscous liquid. Yellowish crystals formed upon cooling to room temperature. Yield: *not determined*

$^1\text{H-NMR}$  (400 MHz, DMSO- $d_6$ )  $\delta$ : 3.54 (4H, m), 3.40 (2H, m), 3.03 (3H, s), 2.05 (4H, m), 1.66 (2H, m), 1.53 (3H, s) 1.29 (2H, m), 0.90 (3H, t) ppm.  $^{13}\text{C}\{^1\text{H}\}$ -NMR (100 MHz, DMSO- $d_6$ )  $\delta$ : 172.90, 63.65, 62.99, 47.60, 26.69, 25.42, 21.45, 19.79, 13.98 ppm. Elemental analysis (calc.): %C = 62.72 (65.63), %H = 11.38 (11.52), %N = 6.73 (6.96).

#### 2.2.3.8 1-Butyl-3-methylimidazolium methyl carbonate, [C<sub>4</sub>C<sub>1</sub>im][MeCO<sub>3</sub>]

1-Butylimidazole (50.0 ml, 0.380 mol) and dimethyl carbonate (42 ml, 0.495 mol) and 100 ml methanol was charged into a 300 ml stainless steel pressure reactor with Teflon lining and stir bar. The mixture was heated to 140°C and heated for 24 h, after which a yellowish solution containing the product was obtained. Conversion: 98%

$^1\text{H-NMR}$  (400 MHz, DMSO- $d_6$  capillary)  $\delta$ : 9.87 (1H, s, CH-2), 8.32 (1H, s, CH-5), 8.24 (1H, s, CH-5), 4.81 (2H, t, N-CH<sub>2</sub>-), 4.49 (3H, s, N-CH<sub>3</sub>), 3.98 (6H, d, H<sub>3</sub>C-OCO<sub>2</sub>), 2.39 (2H, m, N-CH<sub>2</sub>-CH<sub>2</sub>-), 1.87 (2H, m, N-CH<sub>2</sub>-CH<sub>2</sub>-CH<sub>2</sub>-), 1.46 (3H, t, N-CH<sub>2</sub>-CH<sub>2</sub>-CH<sub>2</sub>-CH<sub>3</sub>) ppm.  $^{13}\text{C}\{^1\text{H}\}$ -NMR (100 MHz, DMSO- $d_6$ )  $\delta$ : 157.92 (COOCH<sub>3</sub>), 137.43 (C-2), 123.92 (C-5), 122.62 (C-4), 51.67 (H<sub>3</sub>C-OCO<sub>2</sub>) 48.89 (N-CH<sub>2</sub>(CH<sub>2</sub>)<sub>2</sub>CH<sub>3</sub>), 35.72 (N-CH<sub>3</sub>), 31.87 (N-CH<sub>2</sub>CH<sub>2</sub>CH<sub>2</sub>CH<sub>3</sub>), 19.15 (N-(CH<sub>2</sub>)<sub>2</sub>CH<sub>2</sub>CH<sub>3</sub>), 13.30 (N(CH<sub>2</sub>)<sub>3</sub>CH<sub>3</sub>) ppm. m/z (LSIMS<sup>+</sup>): 139 (100%) [C<sub>4</sub>C<sub>1</sub>im]<sup>+</sup>, 321 (5%) [(C<sub>4</sub>C<sub>1</sub>im-COO)(C<sub>4</sub>C<sub>1</sub>im)]<sup>+</sup>, 353 (5%) [(C<sub>4</sub>C<sub>1</sub>im)<sub>2</sub>MeCO<sub>3</sub>]<sup>+</sup>. m/z (LSIMS<sup>-</sup>): 75 (100%) [MeCO<sub>3</sub>]<sup>-</sup>, 107 (18%) [MeCO<sub>3</sub>·MeOH]<sup>-</sup>, 181 (30%) [C<sub>4</sub>C<sub>1</sub>im-COO - H<sup>+</sup>]<sup>-</sup>, 213 (35%) [C<sub>4</sub>C<sub>1</sub>im-COO·MeOH - H<sup>+</sup>]<sup>-</sup>, 289 (25%) [(C<sub>4</sub>C<sub>1</sub>im)(MeCO<sub>3</sub>)<sub>2</sub>]<sup>-</sup>.

#### 2.2.3.9 1-Butyl-3-methylimidazolium methanesulfonate, [C<sub>4</sub>C<sub>1</sub>im][MeSO<sub>3</sub>]

Methanesulfonic acid (33.73 g, 351 mmol) was added to a stirred crude product mixture containing 351 mmol 1-butyl-3-methylimidazolium methyl carbonate. Vigorous gas formation was observed. The solution was dried *in vacuo* until the product crystallised. The salt was recrystallised twice

from acetonitrile, washed with ethyl acetate and dried under reduced pressure. The product was a white solid with a melting point of 72°C. Yield: 70%

$^1\text{H-NMR}$  (400 MHz, DMSO- $d_6$ )  $\delta$ : 9.28 (1H, s, CH-2), 7.82 (1H, s, CH-5), 7.75 (1H, s, CH-4), 4.18 (2H, t, N-CH $_2$ -), 3.87 (3H, s, N-CH $_3$ ), 2.34 (3H, s, H $_3$ C-SO $_3$ ), 1.77 (2H, m, N-CH $_2$ -CH $_2$ -), 1.26 (2H, m, N-(CH $_2$ ) $_2$ -CH $_2$ -), 0.90 (3H, t, N-(CH $_2$ ) $_3$ -CH $_3$ ) ppm.  $^{13}\text{C}\{^1\text{H}\}$ -NMR (100 MHz, DMSO- $d_6$ )  $\delta$ : 137.15 (C-2), 124.08 (C-5), 122.74 (C-4), 48.88 (N-CH $_2$ (CH $_2$ ) $_2$ CH $_3$ ), 40.25 (H $_3$ C-SO $_3$ ) 36.14 (N-CH $_3$ ), 31.83 (N-CH $_2$ CH $_2$ CH $_2$ CH $_3$ ), 19.22 (N-(CH $_2$ ) $_2$ CH $_2$ CH $_3$ ), 13.72 (N(CH $_2$ ) $_3$ CH $_3$ ) ppm.  $m/z$  (LSIMS $^+$ ): 139 (100%) [C $_4$ C $_1$ im] $^+$ , 373 (5%) [(C $_4$ C $_1$ im) $_2$ MeSO $_3$ ] $^+$ .  $m/z$  (LSIMS $^-$ ): 95 (100%) [MeSO $_3$ ] $^-$ , 329 (10%) [(C $_4$ C $_1$ im)(MeSO $_3$ ) $_2$ ] $^-$ , 563 (4%) [(C $_4$ C $_1$ im) $_2$ (MeSO $_3$ ) $_3$ ] $^-$ . Elemental analysis (calc.): %C = 45.96 (46.13), %H = 7.92 (7.74), %N = 11.84 (11.86).

#### 2.2.3.10 1-Butyl-3-methylimidazolium hydrogen sulfate, [C $_4$ C $_1$ im][HSO $_4$ ]

1-Butyl-3-methylimidazolium methyl sulfate (Basionic AC01, Sigma-Aldrich) (170.67 g, 682 mmol) was mixed with 25 ml distilled water in a round-bottomed flask with vertical Graham condenser and a horizontal Liebig condenser on top. The mixture was heated to reflux for 24 h. The temperature of the cooling water in the Graham condenser was maintained at 65°C using a temperature-controlled circulator. The Liebig condenser was cooled with tap water. The ionic liquid was dried *in vacuo* at 45°C. The product was a very viscous yellowish liquid.

$^1\text{H-NMR}$  (400 MHz, DMSO- $d_6$ )  $\delta$ : 9.22 (1H, s, CH-2), 9.01 (1H, s, HSO $_4$ ) 7.82 (1H, s, CH-5), 7.74 (1H, s, CH-4), 4.18 (2H, t, N-CH $_2$ -), 3.87 (3H, s, N-CH $_3$ ), 2.34 (3H, s, H $_3$ C-SO $_3$ ), 1.73 (2H, m, N-CH $_2$ -CH $_2$ -), 1.20 (2H, m, N-(CH $_2$ ) $_2$ -CH $_2$ -), 0.82 (3H, t, N-(CH $_2$ ) $_3$ -CH $_3$ ) ppm.  $^{13}\text{C}\{^1\text{H}\}$ -NMR (100 MHz, DMSO- $d_6$ )  $\delta$ : 137.18 (C-2), 123.98 (C-5), 122.74 (C-4), 48.84 (N-CH $_2$ (CH $_2$ ) $_2$ CH $_3$ ), 36.06 (N-CH $_3$ ), 31.88 (N-CH $_2$ CH $_2$ CH $_2$ CH $_3$ ), 19.16 (N-(CH $_2$ ) $_2$ CH $_2$ CH $_3$ ), 13.64 (N(CH $_2$ ) $_3$ CH $_3$ ) ppm.  $m/z$  (LSIMS $^+$ ): 139 (100%) [C $_4$ C $_1$ im] $^+$ .  $m/z$  (LSIMS $^-$ ): 97 (100%) [MeSO $_3$ ] $^-$ , 333 (2%)

$[(C_4C_1im)(MeSO_3)_2]$ . Elemental analysis (calc.): %C=43.22 (43.18), %H=7.29 (7.25), %N=11.19 (11.27).

2.2.3.11 1-Ethyl-3-methylimidazolium-4-carboxylate,  $[C_2C_1im-4-COO]$ , and 1-ethyl-3-methylimidazolium-5-carboxylate,  $[C_2C_1im-5-COO]$

1-Ethylimidazole (50.0 ml, 0.517 mol) and dimethyl carbonate (120 ml, 1.44 mol) were charged into a 300 ml stainless steel pressure reactor with Teflon lining and overhead stirrer. The reaction was heated at 140°C for 4 h and subsequently at 100°C for 20 h. The precipitate was washed with ethyl acetate, recrystallised in acetonitrile and dried *in vacuo*. The product was a white crystalline solid, consisting of two regioisomers of the zwitterion (81.5%  $[C_2C_1im-4-COO]$  and 18.5%  $[C_2C_1im-5-COO]$ ). The isomers were not separated.

$[C_2C_1im-5-COO]$ :  $^1H$ -NMR (400 MHz,  $D_2O$ )  $\delta$ : 8.60 (1H, s,  $CH_2$ ), 7.60 (1H, s,  $CH_5$ ), 4.39 (2H, q,  $N-CH_2$ ), 3.76 (3H, s,  $N-CH_3$ ), 1.33 (3H, t,  $N-CH_2-CH_3$ ) ppm.  $^{13}C\{^1H\}$ -NMR (100 MHz,  $D_2O$ )  $\delta$ : 163.53 ( $-COO$ ), 137.13 (C-2), 130.73 (C-4), 126.53 (C-5), 44.08 ( $N-CH_2-CH_3$ ), 35.60 ( $N-CH_3$ ), 15.03 ( $N-CH_2-CH_3$ ) ppm.

$[C_2C_1im-4-COO]$ :  $^1H$ -NMR (400 MHz,  $D_2O$ )  $\delta$ : 8.60 (1H, s,  $CH_2$ ), 7.68 (1H, s,  $CH_4$ ), 4.10 (2H, q,  $N-CH_2$ ), 3.89 (3H, s,  $N-CH_3$ ), 1.38 (3H, t,  $N-CH_2-CH_3$ ) ppm.  $^{13}C\{^1H\}$ -NMR (100 MHz,  $D_2O$ )  $\delta$ : 163.53 ( $-COO$ ), 137.13 (C-2), 130.73 (C-4), 124.79 (C-5), 44.89 ( $N-CH_2-CH_3$ ), 35.60 ( $N-CH_3$ ), 14.22 ( $N-CH_2-CH_3$ ) ppm.

m/z (ESI<sup>+</sup>): 155 (100%)  $[(C_2C_1im-COO)H]^+$ , 309 (5%)  $[(C_2C_1im-COO)_2H]^+$ , 331 (12%)  $[(C_2C_1im-COO)_2Na]^+$ , 485 (5%)  $[(C_2C_1im-COO)_3Na]^+$ , 639 (5%)  $[(C_2C_1im-COO)_4Na]^+$ , 793 (2%)  $[(C_2C_1im-COO)_5Na]^+$ .

2.2.3.12 1-Ethyl-3-methylimidazolium methyl carbonate,  $[C_2C_1im][MeCO_3]$

1-Ethylimidazole (25 ml, 0.259 mol), dimethyl carbonate (24 ml, 0.285 mol) and 50 ml methanol were charged into a 300 ml stainless steel pressure reactor with Teflon lining and overhead stirrer. The reaction

mixture was heated at 120°C for 82 h. The product solution was an amber-coloured solution. The product was not isolated. Conversion: 86%

$^1\text{H-NMR}$  (400 MHz, DMSO- $d_6$  capillary)  $\delta$ : 9.78 (1H, s, *CH*-2), 8.18 (1H, s, *CH*-5), 8.08 (1H, s, *CH*-4), 4.64 (2H, q, N-*CH*<sub>2</sub>-), 4.31 (3H, s, N-*CH*<sub>3</sub>), 3.76 (3H, s, (C(O)O*CH*<sub>3</sub>)), 1.81 (3H, t, N-*CH*<sub>2</sub>-*CH*<sub>3</sub>) ppm.  $^{13}\text{C}\{^1\text{H}\}$ -NMR (100 MHz, DMSO- $d_6$  capillary)  $\delta$ : 159.37 (COO*CH*<sub>3</sub><sup>-</sup>), 137.32 (C-2), 124.04 (C-5), 122.44 (C-4), 51.68 (COO*CH*<sub>3</sub><sup>-</sup>), 44.83 (N-*CH*<sub>2</sub>-*CH*<sub>3</sub>), 35.51 (N-*CH*<sub>3</sub>), 15.02 (N-*CH*<sub>2</sub>-*CH*<sub>3</sub>) ppm.

## 2.3 Results and Discussion

### 2.3.1 *Failure of ion metathesis in dichloromethane in the case of strongly hydrogen-bonding ionic liquids*

The applicability of ion metathesis using halide containing precursors and alkali metal salts relies on two principles:

- The ion exchange is considerably in favour of the new anion
- Residual precursor and salt impurities can be washed away with water.

Both requirements are easily met when synthesising hydrophobic ionic liquids such as  $[\text{C}_4\text{C}_1\text{im}][\text{NTf}_2]$  or  $[\text{C}_4\text{C}_1\text{im}][\text{PF}_6]$ . The ionic liquid  $[\text{C}_4\text{C}_1\text{im}][\text{NTf}_2]$  can be synthesised in water, as the product spontaneously forms a separate layer.<sup>84</sup> For ionic liquids that have moderately hydrogen-bonding anions, it is still possible to use the halide route, although the product may be water-miscible. In this case, the ion exchange needs to be carried out in an organic solvent and the washing steps need to be carried out carefully. The complete water-miscibility of the product ionic liquid means that with each washing step a significant amount of product partitions into the wash water, reducing the yield. Dried reagents and solvents must be used to optimise the metathesis. An example is the synthesis of  $[\text{C}_4\text{C}_1\text{im}][\text{OTf}]$ .<sup>80</sup>

However, when the anion's hydrogen-bonding strength is even higher, the synthesis *via* the halide route will not lead to a pure ionic liquid. The metathesis reaction will reach equilibrium with a mixture of precursor and product anions in the dichloromethane phase. This is illustrated by Figure 29 which shows the  $^1\text{H-NMR}$  spectrum after an attempted synthesis of  $[\text{C}_4\text{C}_1\text{im}][\text{MeSO}_3]$  *via* the halide route (with courtesy of Nur Syareeda Hassan). Equimolar quantities of  $[\text{C}_4\text{C}_1\text{im}]\text{Cl}$  and  $\text{Na}[\text{MeSO}_3]$  were stirred in dry dichloromethane for 3 days, the ionic liquid partially dried and an  $^1\text{H-NMR}$  spectrum recorded. The peak integral of the C-2 proton was compared to the peak integral of the methyl group on the anion. The integral of the methyl group was significantly lower than expected, showing that 45% of the anions were chloride ions.



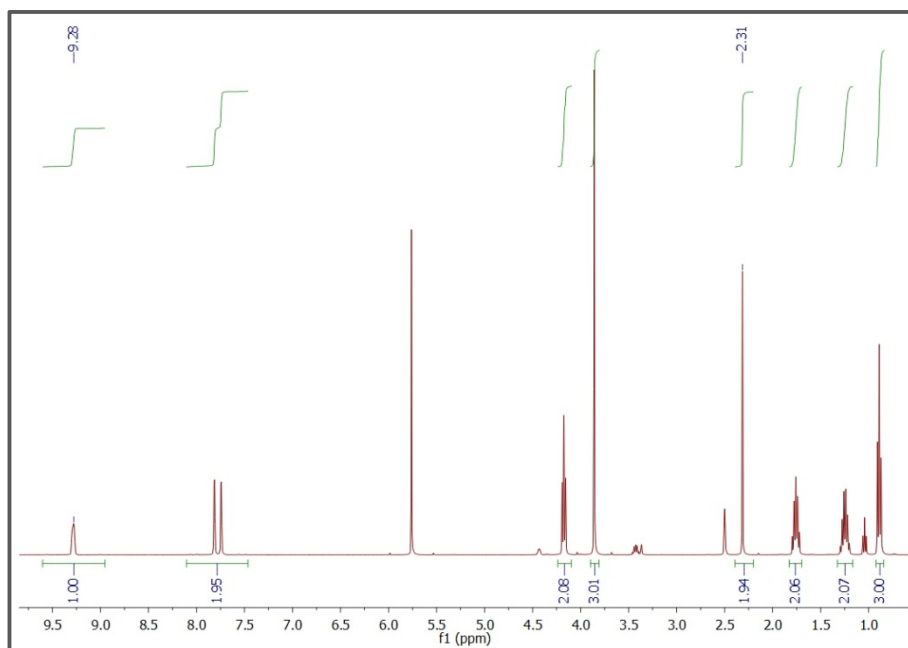


Figure 29:  $^1\text{H-NMR}$  spectrum of  $[\text{C}_4\text{C}_1\text{im}][\text{MeSO}_3]$  after ion metathesis with  $[\text{C}_4\text{C}_1\text{im}]\text{Cl}$  and sodium methanesulfonate (in  $\text{DMSO-d}_6$ ). The integral of the peak (1.94) at 2.31 ppm, assigned to the methyl group on the anion, is only 65% of the expected value. Peaks that were not integrated are caused by residual ethyl acetate and dichloromethane (spectrum recorded by Nur Hasyareeda Hassan).

The product to halide ratio could be improved by repeating the metathesis reaction with fresh batches of alkali metal salt until the chloride content is sufficiently reduced. However, this will produce large quantities of salt waste, while the halide impurities will not be completely eliminated.

The increased hydrogen-bonding basicity of the anion also results in a stronger hydrogen-bonding interaction with water.<sup>96</sup> This will impede the washing step, because the product ionic liquid will be washed out together with the precursor. This problem was encountered when the dichloromethane phase containing the crude  $[\text{C}_4\text{C}_1\text{im}][\text{MeSO}_3]$  was subjected to washing. No product ionic liquid was left in the dichloromethane phase after the wash was completed. The synthesis of ionic liquids with strongly hydrogen-bonding cations faces similar problems, for example when the cation is functionalised with a hydroxyl or sulfonic acid group. The failure of the washing step for 1-hydroxyethyl-3-methylimidazolium trifluoromethanesulfonate,  $[\text{HOC}_3\text{C}_1\text{im}][\text{OTf}]$ , has been recently reported by our group.<sup>97</sup>

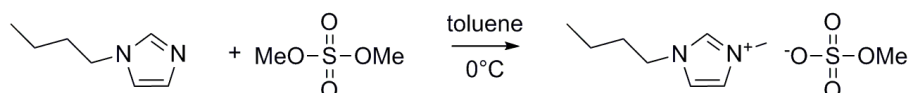
A summary of the suitability for ion metathesis is presented in Table 3. The ionic liquids required for this project belong to group 3. To obtain group 3 ionic liquids in high purity, alternative routes had to be used.

Table 3: Suitability of ion metathesis for the synthesis of pure 1-butyl-3-methylimidazolium ionic liquids

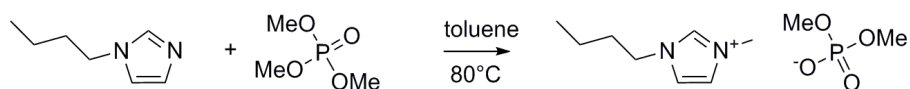
	Water miscibility	Suitability for ion metathesis in DCM	Ionic liquid anion
Group 1	no	yes	[NTf <sub>2</sub> ] <sup>-</sup> , [PF <sub>6</sub> ] <sup>-</sup>
Group 2	yes	yes	[OTf] <sup>-</sup> , [BF <sub>4</sub> ] <sup>-</sup>
Group 3	yes	no	[MeSO <sub>3</sub> ] <sup>-</sup> , [N(CN) <sub>2</sub> ] <sup>-</sup> , [MeCO <sub>2</sub> ] <sup>-</sup>

### 2.3.2 Direct alkylation

Direct alkylation was used to obtain the ionic liquids 1-butyl-3-methylimidazolium methylsulfate, [C<sub>4</sub>C<sub>1</sub>im][MeSO<sub>4</sub>], (Scheme 7) and 1-butyl-3-methylimidazolium dimethyl phosphate, [C<sub>4</sub>C<sub>1</sub>im][Me<sub>2</sub>PO<sub>4</sub>]. It is a straightforward and fast synthesis and has been accomplished following literature procedures.<sup>82, 83</sup> Dimethyl sulfate alkylated 1-butylimidazole at 0°C with good yields, while the alkylation with trimethyl phosphate required elevated temperatures.



Scheme 7: Synthesis of 1-butyl-3-methylimidazolium hydrogen sulfate



Scheme 8: Synthesis of 1-butyl-3-methylimidazolium dimethyl phosphate

The purification was achieved by washing away excess alkylating agent and unreacted 1-butylimidazole. The purification of [C<sub>4</sub>C<sub>1</sub>im][Me<sub>2</sub>PO<sub>4</sub>] turned out to be more laborious. The presence of residual trimethyl phosphate induced miscibility with organic wash solvents that were not expected to be miscible with ionic liquids, e.g. toluene or diethyl ether. Knowing that the ionic liquid was water-miscible,

water was added which helped to separate the ionic liquid from the organic solvent. However, the high affinity of trimethyl phosphate to the ionic liquid-water phase still made it difficult to remove the trimethyl phosphate by simple two-phase extraction. This problem was overcome by using a continuous extraction of the trimethyl phosphate from the ionic liquid water phase into a toluene phase. Recently, dilution with the solvent (toluene) was also successfully applied to aid phase separation (personal communication Heiko Niedermeyer).

### 2.3.3 Ion metathesis using silver salts

$[\text{C}_4\text{C}_1\text{im}][\text{N}(\text{CN})_2]$  was synthesised from  $[\text{C}_4\text{C}_1\text{im}]\text{Br}$  and silver dicyanamide,  $\text{Ag}[\text{N}(\text{CN})_2]$  using a literature procedure.<sup>98</sup> Silver dicyanamide is not commercially available and was therefore synthesised from sodium dicyanamide and silver nitrate, exploiting the limited water-solubility of silver dicyanamide. The ionic liquid was synthesised by adding the silver dicyanamide to an aqueous solution of  $[\text{C}_4\text{C}_1\text{im}]\text{Br}$ . The ion exchange was driven by the formation of  $\text{AgBr}$ , which has a lower solubility than  $\text{Ag}[\text{N}(\text{CN})_2]$ . The product was a colourless free-flowing liquid.

Unfortunately, the ionic liquid was contaminated with residual sodium dicyanamide which had been carried over from the silver dicyanamide synthesis. The impurity was detected by ESI mass spectroscopy. Therefore the option of further purification was explored. Purification of  $[\text{C}_4\text{C}_1\text{im}][\text{N}(\text{CN})_2]$  was attempted by extracting the ionic liquid from an aqueous phase into dichloromethane using continuous extraction. The continuous extraction helped to reduce the sodium ion content. However, elemental analysis results of the purified  $[\text{C}_4\text{C}_1\text{im}][\text{N}(\text{CN})_2]$  still significantly deviated from the expected values. This suggests that the synthesis of the silver dicyanamide requires improvement and contamination with sodium ions must be avoided. Additional extraction steps for the  $[\text{C}_4\text{C}_1\text{im}][\text{N}(\text{CN})_2]$  could also improve the final purity.

An analogous route was used for the synthesis of  $[\text{C}_4\text{C}_1\text{im}][\text{MeCO}_2]$ . Silver acetate is commercially available. It is also relatively soluble ( $\approx 1$  g/100 ml) in water. Therefore ion exchange was attempted in

dichloromethane. It was speculated that this would decrease the solubility of silver acetate. However, it turned out that the silver ions are highly soluble in dichloromethane in the presence of  $[\text{C}_4\text{C}_1\text{im}]\text{Br}$ .

This can be explained by the formation of a silver carbene complex. Formation of such a complex was supported by mass spectroscopy. The mass spectrum (LSIMS) exhibited a peak at  $m/z = 245$  (and 247), which is the mass of one silver atom (105 and 107) combined with one 1-butyl-3-methylimidazolium ion lacking a proton (138). In the  $^{13}\text{C}$ -NMR spectrum of the supernatant the 1-butyl-3-methylimidazolium ylidene was also detected. Its C-2 peak was shifted down-field to 185 ppm (compared to 140 ppm for the C-2 peak in the cation). The  $^1\text{H}$ -NMR spectrum showed the presence of a species that lacked the signal of the proton attached to C-2.

Silver N-heterocyclic carbene complexes are known in the literature and can be formed *via* a number of routes. They can be synthesised using free carbene that has been generated beforehand or synthesised by *in-situ* deprotonation of the imidazolium salt. This usually involves silver oxide,  $\text{AgO}$ , which acts as the base and the silver donor.<sup>99</sup> In the present case, the acetate anion seems to be able to act as reversible proton acceptor, driving the formation of the silver imidazolium-ylidene complex. A high relative stability of the carbene acetic acid complex in  $[\text{C}_2\text{C}_1\text{im}][\text{MeCO}_2]$ , even in the absence of silver, has been recently suggested computationally.<sup>100</sup>

The increased solubility of silver acetate in the presence of imidazolium cations was not seen when methanol or water were used as solvents. To obtain a high purity ionic liquid the synthesis was completed with a titration procedure. For the main ion exchange, silver acetate was used in slight excess. When completed, aqueous  $[\text{C}_4\text{C}_1\text{im}]\text{Br}$  was added drop-wise until precipitate formation stopped, ensuring that an equimolar ratio of  $[\text{C}_4\text{C}_1\text{im}]^+$  cations and acetate anions were present. The ion exchange with silver acetate in water yielded colourless ionic liquid of very good purity in a 150 ml quantity. The ionic liquid  $[\text{C}_4\text{C}_1\text{pyrr}][\text{MeCO}_2]$ , 1-butyl-1-methylpyrrolidinium acetate, was synthesised from 1-butyl-1-

methylpyrrolidinium bromide and silver acetate using an analogous procedure.

### 2.3.4 Methyl carbonate route

#### 2.3.4.1 Synthesis and purification of the precursor

For the synthesis of the ionic liquids  $[\text{C}_4\text{C}_1\text{im}][\text{MeSO}_3]$  and  $[\text{C}_4\text{C}_1\text{im}][\text{HSO}_4]$ , it had been envisaged to use the relatively new, acid-labile  $[\text{C}_4\text{C}_1\text{im}][\text{MeCO}_3]$  precursor. Methanesulfonic acid and sulfuric acid are commercially available in high purity and at low cost, so the challenge was to obtain the precursor in high purity and to perform the ion exchange accurately.

Initially it was decided to follow a procedure that used excess alkylating agent with no added solvent. The feasibility of a solvent-free alkylation was supported by a published procedure which claimed to synthesise 1-ethyl-3-methylimidazolium acetate and 1-butyl-3-methylimidazolium acetate using dimethyl carbonate in 96% yield.<sup>95</sup> The procedure advised reacting the N-alkylimidazole with 1.2 equivalents of dimethyl carbonate in the presence of acidic aluminium oxide as catalyst at 210°C for 2 h. We decided to modify the conditions slightly, using a lower temperature (180°C) and running the reaction for longer (24 h). However, in our hands the solvent-free synthesis failed, although it provided insight into the mechanism and limitations of the alkylation of alkylimidazole with dimethyl carbonate and is therefore presented here.

The pressure in the reactor had increased during the reaction to over 10 bar even after cooling to room temperature, suggesting the formation of gas. The product was a darkly coloured viscous liquid. The extraction of the product with diethyl ether, as detailed in the literature procedure,<sup>95</sup> could not be achieved. Instead, only small quantities of unreacted 1-butylimidazole were isolated.

A positive ESI mass spectrum of the product solution revealed that the solution contained a mixture of cations (Figure 30). The 1-butyl-3-methylimidazolium cation ( $m/z = 139$ ) was the principal product, however cations with one and two additional methyl groups ( $m/z = 153$  and  $167$ )

were also present. The mass spectrum also suggested the presence of a substantial amount of carboxylated cations ( $m/z = 183$ ) and carboxylated cations with an additional methyl group ( $m/z = 197$ ).

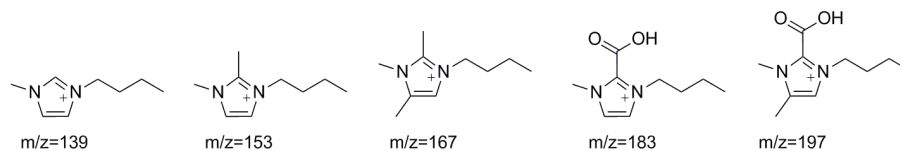
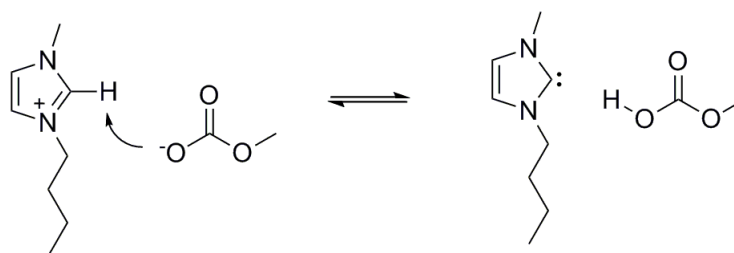


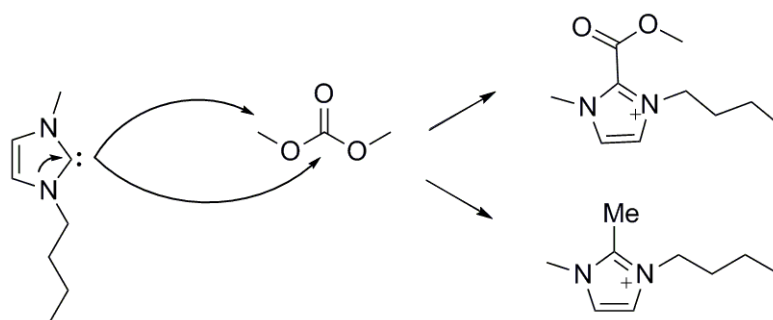
Figure 30: Products found after reaction of 1-butylimidazole with dimethyl carbonate at 180°C for 24 h without methanol (only one regioisomer is depicted).

The mass spectrum suggested that not only formation of the ionic liquid cation was accomplished but over-alkylation and carboxylation took place. The only nucleophilic centre of 1-butylimidazole is the nitrogen atom with the lone pair. The additional alkylations and the carboxylation can be explained with the formation of reactive carbene intermediates. The formation of dialkylimidazolium carbenes usually requires very strong bases. For example stable carbenes can be created permanently *via* reduction with potassium, lithium or lithium aluminium hydride ( $\text{LiAlH}_4$ ) under aprotic conditions.<sup>101</sup> At elevated temperature and pressure, a weak base such as the methyl carbonate anion ( $pK_b = 6.5$ ) seems to be capable of deprotonating the cation at its most acidic site, the carbon at position 2 (Scheme 9). The decomposition of methyl carbonic acid into methanol and carbon dioxide would drive the formation of carbene and also explain the pressure rise during the reaction.



Scheme 9: Formation of a 1,3-dialkylimidazolium carbene under basic aprotic conditions

The result of the deprotonation is a nucleophilic heterocarbene that can react with available electrophiles such as excess dimethyl carbonate (Scheme 10).



Scheme 10: Nucleophilic attack of 1-butyl-3-methylimidazolium carbene on dimethyl carbonate; both carboxylation or methylation can occur

After performing these experiments, a publication by Rogers *et al.* was retrieved describing the synthesis of 1,3-dimethylimidazolium-2-carboxylate from 1-methylimidazole in excess dimethyl carbonate. The reaction had been carried out at a lower temperature than applied in this study (24 h at 120°C) explaining the higher selectivity obtained by these researchers.<sup>102</sup>

Improved selectivity was also obtained in this study when reacting 1-ethylimidazole with dimethyl carbonate at 120°C, this time without the alumina, which appeared to be not required for the reaction. A solid product was isolated which was identified as a mixture of 1-ethyl-3-methylimidazolium-4-carboxylate and 1-ethyl-3-methylimidazolium-5-carboxylate. In the mixture, 80% of the ylide was the 4-carboxylate and 20% was the 5-carboxylate. The <sup>1</sup>H-NMR spectrum of the mixture is depicted in Figure 31.

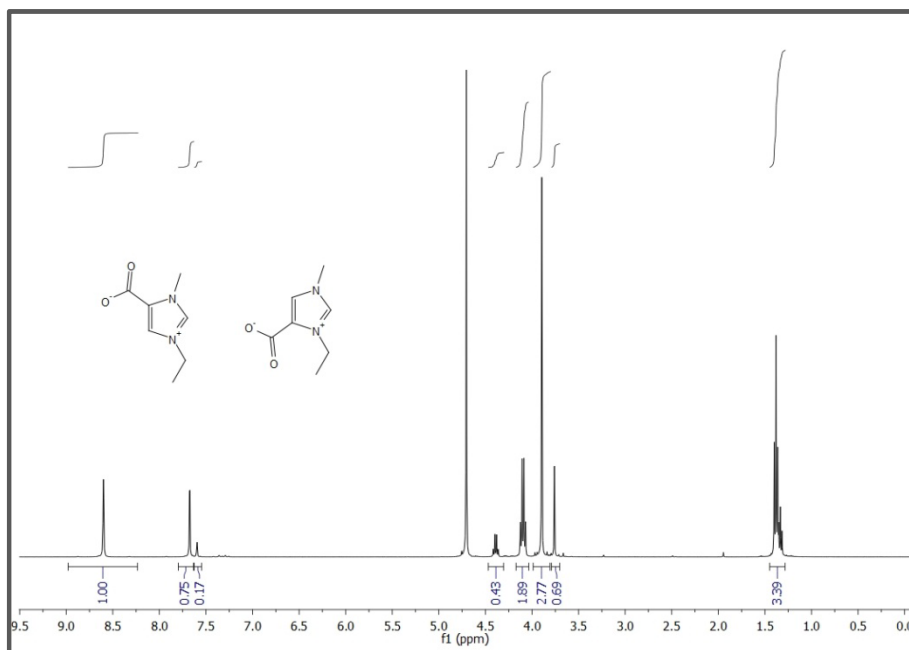


Figure 31:  $^1\text{H-NMR}$  spectrum of the solid product obtained after reaction of 1-ethylimidazole with dimethyl carbonate containing 1-ethyl-3-methylimidazolium-4-carboxylate and 1-ethyl-3-methylimidazolium-5-carboxylate (in  $\text{D}_2\text{O}$ ).

It is reported in the literature that dialkylimidazolium-4-carboxylate is the thermodynamically most stable isomer of the three possible zwitterions and thus the 4-carboxylate will be the most abundant isomer, if isomerisation is possible.<sup>103</sup> The synthesis of 1,3-dimethylimidazolium-4-carboxylate has been patented by BASF AG using a solvent-free method.<sup>104</sup> It has been suggested that the 4-carboxylate and 5-carboxylate are formed from dialkylimidazolium-2-carboxylates in the solid state by transferring carboxylate groups between two neighbouring,  $\pi$ -stacked zwitterions.<sup>105</sup> As this project was not concerned with the synthesis of zwitterions, the solvent-free route was not pursued further.

Subsequent syntheses were performed in methanol as reported by MSci students Alistair McIntosh and Hemal Bosamia, and by other literature sources.<sup>97, 106</sup> The conversion of 1-butylimidazole into  $[\text{C}_4\text{C}_1\text{im}][\text{MeCO}_3]$  at  $140^\circ\text{C}$  for 24 h was 90% or higher and side-products were only formed in minor quantities (Figure 32).



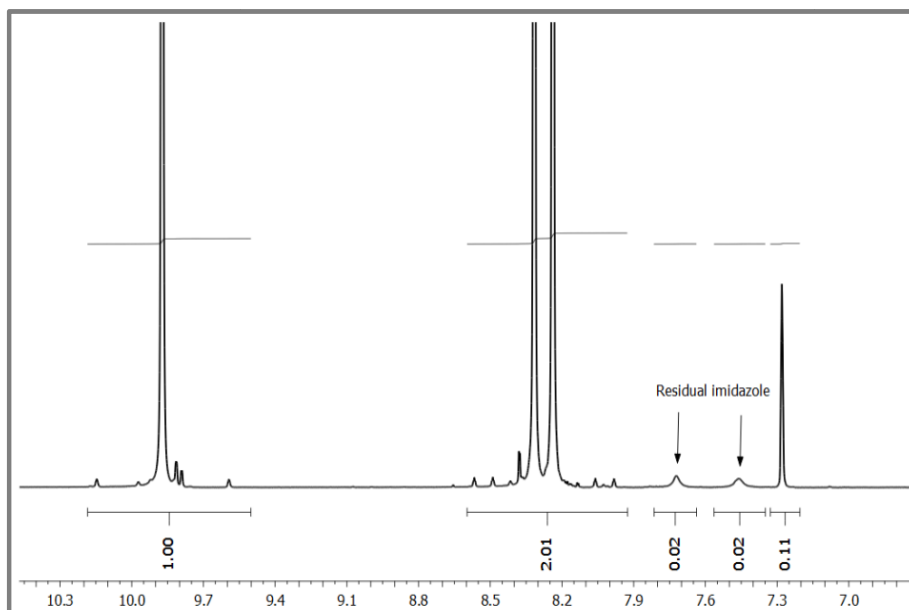


Figure 32:  $^1\text{H}$  NMR spectrum of the crude product from the reaction of 1-butylimidazole with dimethyl carbonate in methanol. Displayed is the region of the ring proton signals. Three large peaks (and their  $^{13}\text{C}$  satellites) give evidence of the formation of 1,3-dialkylimidazolium cations. Residual butylimidazole is present, as well as small quantities of carboxylated and over-alkylated product.

Following this, the purification of the methyl carbonate precursor was investigated. The application of a sequence of washing steps with ethyl acetate and a recrystallisation in acetonitrile was envisaged, analogous to the purification used for the traditional halide precursors.

The methanol was evaporated and white-yellowish crystals were isolated, which were washed and recrystallised. Interestingly, the purified dried crystals were not a single product but a mixture of  $[\text{C}_4\text{C}_1\text{im}][\text{HCO}_3]$  and 1-butyl-3-methylimidazolium-2-carboxylate. Both compounds were identified by  $^1\text{H}$ -NMR and mass spectrometry (Figure 33).

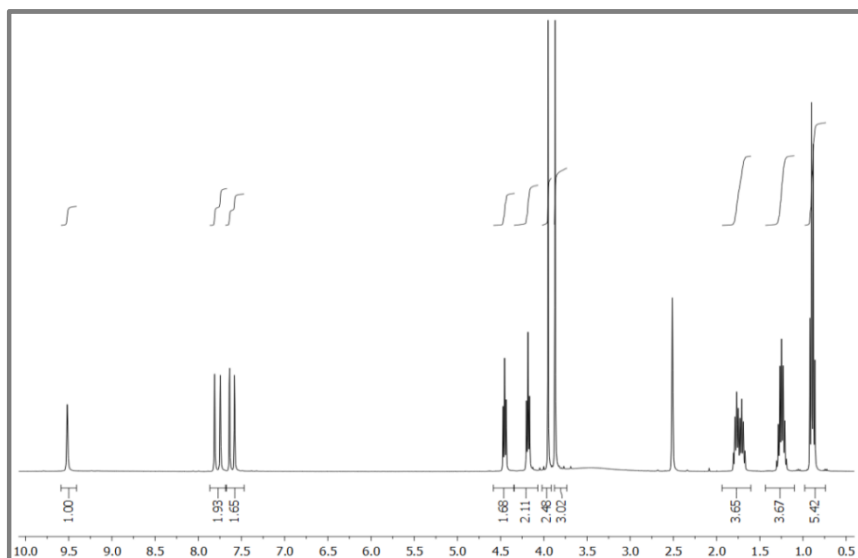


Figure 33:  $^1\text{H-NMR}$  spectrum of recrystallised product from the synthesis of  $[\text{C}_4\text{C}_1\text{im}][\text{MeCO}_3]$  in  $\text{DMSO-d}_6$ . The sample was prepared in a glove box and the  $\text{DMSO-d}_6$  was taken from a freshly opened ampoule.

While characterising the product mixture, it was noted that different preparations of the same sample contained varying quantities of ionic liquid and zwitterions. For clarification, a sample was prepared in the glove box using  $\text{DMSO-d}_6$  from a freshly opened ampoule and its  $^1\text{H-NMR}$  spectrum was recorded. This sample contained a larger fraction of 1-butyl-3-methylimidazolium-2-carboxylate. When a drop of water was added to the NMR sample, the ratio drastically changed in favour of  $[\text{C}_4\text{C}_1\text{im}][\text{HCO}_3]$  (Figure 34).

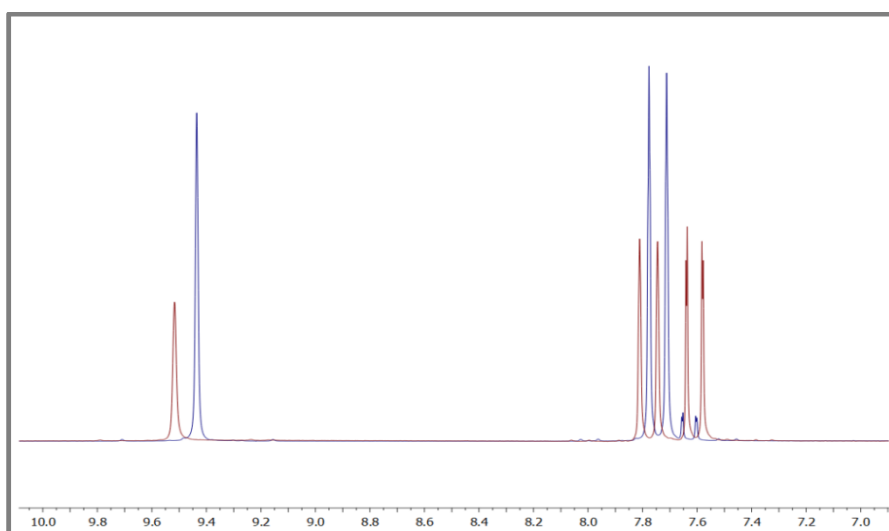
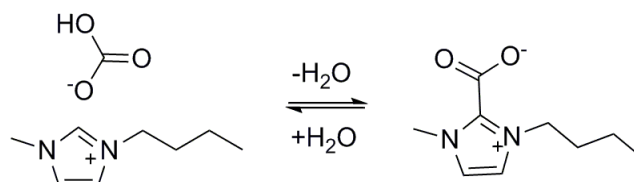
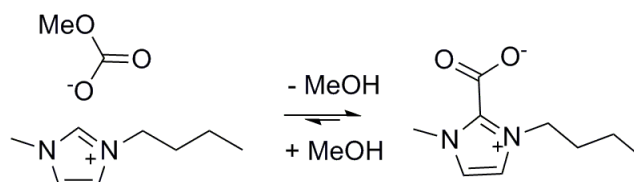


Figure 34:  $^1\text{H-NMR}$  spectrum of product crystals before (red) and after (blue) addition of water (in  $\text{DMSO-d}_6$ ).

This indicates that  $[\text{C}_4\text{C}_1\text{im}][\text{HCO}_3]$  converts to the zwitterion upon drying (Scheme 11) and reverts back when hydrated, which has also been noted by others.<sup>107</sup> Likewise, the conversion of  $[\text{C}_4\text{C}_1\text{im}][\text{MeCO}_3]$  into 1-butyl-3-methylimidazolium-2-carboxylate is driven by the removal of methanol under reduced pressure (Scheme 12).



Scheme 11: Dehydration of  $[\text{C}_4\text{C}_1\text{im}][\text{HCO}_3]$  to 1-butyl-3-methylimidazolium-2-carboxylate



Scheme 12: Formation of 1-butyl-3-methylimidazolium-2-carboxylate from  $[\text{C}_4\text{C}_1\text{im}][\text{MeCO}_3]$  under reduced pressure

This sensitivity of the carbonate based precursor towards drying complicates the correct execution of the anion exchange step, because a mixture of chemical species with different molecular masses may be used. For a clean metathesis, a strict 1:1 ratio of precursor and acid is required. Errors in weighing would result in contamination with excess acid or unreacted precursor.

#### 2.3.4.2 Anion metathesis with methyl carbonate salts

The purity of the product ionic liquid is affected by the accuracy of acid addition. Otherwise excess acid or residual precursor will be present in the product, which should be removed. The case of  $[\text{C}_4\text{C}_1\text{im}][\text{MeSO}_3]$  will be presented, where purification is possible, but also the synthesis of the ionic liquid  $[\text{C}_4\text{C}_1\text{im}][\text{HSO}_4]$ , where it is not possible.

##### 2.3.4.2.1 Synthesis of $[\text{C}_4\text{C}_1\text{im}][\text{MeSO}_3]$

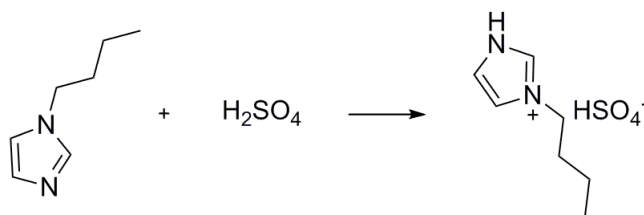
The ionic liquid 1-butyl-3-methylimidazolium methanesulfonate was anticipated to be liquid at room temperature, based on reports of earlier

PhD students. However, during drying of the ionic liquid, crystallisation of substance was observed, which was identified as  $[\text{C}_4\text{C}_1\text{im}][\text{MeSO}_3]$ . The solid was recrystallised twice in acetonitrile and yielded pure white crystals with a melting point of  $72^\circ\text{C}$ . The commercial supplier BASF reports a melting point of  $75\text{--}80^\circ\text{C}$  for  $[\text{C}_4\text{C}_1\text{im}][\text{MeSO}_3]$ , which is in good agreement with the melting point measured in this study. Since product was a solid and could be recrystallised, it is concluded that direct alkylation may have been a less laborious way to obtain this ionic liquid.

#### 2.3.4.2.2 Synthesis of $[\text{C}_4\text{C}_1\text{im}][\text{HSO}_4]$

The synthesis of  $[\text{C}_4\text{C}_1\text{im}][\text{HSO}_4]$  from  $[\text{C}_4\text{C}_1\text{im}][\text{MeCO}_3]$  and sulfuric acid was also attempted. A problem was encountered when the acid was added in a concentrated form. The acid not only reacted with the methyl carbonate anion but also with the solvent, creating a mixture of hydrogen sulfate and methyl sulfate anions. This problem was overcome by using dilute (5 M) sulfuric acid.

However, the use of crude  $[\text{C}_4\text{C}_1\text{im}][\text{MeCO}_3]$  solution in methanol turned out to be of limited value, too. It was discovered that residual 1-butylimidazole would form complexes with sulfuric acid and the protic hydrogen sulfate anions (Scheme 13). The complexes were strong enough to resist removal of 1-butylimidazole with organic solvents. Therefore it is advised to remove unreacted alkyimidazole from the precursor before the anion exchange with the acid.



Scheme 13: Complexation of residual butylimidazole by sulfuric acid

#### 2.3.4.3 Summary of the methyl carbonate route

The following insights were gained during the exploration of the synthesis of ionic liquids by the methyl carbonate route.

#### 2.3.4.3.1 Synthesis

The ionic liquid precursor  $[C_nC_m\text{im}][\text{MeCO}_3]$  can only be synthesised using a protic solvent, e.g. methanol. Otherwise, a mixture of ionic liquids and zwitterions is obtained. Over-alkylation of the cation may also be observed under solvent-free conditions.

Carboxylation and over-alkylation are problems associated with the imidazolium cation, but should not be a problem with aliphatic cations such as tetraalkylammonium, tetraalkylphosphonium and dialkylpyrrolidinium.<sup>91</sup> Permethylated imidazolium cations should also be unreactive. It seems that the methyl carbonate route may be more suited for the synthesis of ionic liquids with cations other than 1,3-dialkylimidazolium. Successful syntheses of various precursors with methanol and without solvent have been published recently.<sup>91</sup>

#### 2.3.4.3.2 Purification

- $[C_nC_m\text{im}][\text{MeCO}_3]$  is converted into dialkylimidazolium-2-carboxylate when removing methanol *in vacuo*
- The dialkylimidazolium-2-carboxylate can be purified using recrystallisation in acetonitrile
- Dialkylimidazolium-2-carboxylate can convert to  $[C_nC_m\text{im}][\text{HCO}_3]$  if it is hydrated
- Under certain conditions, the kinetically favourable dialkylimidazolium-2-carboxylates rearrange to the thermodynamically more stable dialkylimidazolium-4-carboxylates and 5-carboxylates

#### 2.3.4.3.3 Ion exchange with acids

- $[C_nC_m\text{im}][\text{MeCO}_3]$ ,  $[C_nC_m\text{im}][\text{HCO}_3]$  and dialkylimidazolium-2-carboxylates are acid-labile and will convert to a dialkylimidazolium ionic liquid upon addition of an appropriate acid.
- If the product is a solid, it can be purified by recrystallisation. Purification of the precursor is not

necessary in this case. The recrystallisation will not only remove impurities from the alkylation but also excess acid from the ion exchange step.

### 2.3.5 Synthesis of $[C_4C_1im][HSO_4]$ by hydrolysis

The synthesis of 1-butyl-3-methylimidazolium hydrogen sulfate was finally accomplished by hydrolysing  $[C_4C_1im][MeSO_4]$  (Scheme 14). The set-up was a simplified fractional distillation. A mixture of  $[C_4C_1im][MeSO_4]$  and water was heated to reflux, while the temperature of the cooling water was maintained at 70°C, so the methanol could evaporate. A second condenser liquefied the methanol to prevent the release of toxic vapours. Commercial  $[C_4C_1im][MeSO_4]$  was used in order to obtain large quantities of  $[C_4C_1im][HSO_4]$  in a short time.



Scheme 14: Synthesis of 1-butyl-3-methylimidazolium hydrogen sulfate by hydrolysis

The hydrolysis route has the advantage of ensuring that a strictly stoichiometric amount of acidic protons is present. The drawback was that around 5% residual methyl sulfate anions were still present that could not be removed even after extended reaction times.

## 2.4 Summary

The synthesis of a range of hydrophilic ionic liquid was accomplished using various synthetic methodologies, particularly direct alkylation, the silver salt route and the methyl carbonate route. For the first time, purification of the 1,3-dialkylimidazolium methyl carbonate salt has been investigated. It was found that recrystallisation can be used improve the purity of the salt and reduce or even remove colour.

## 3 Solvent polarity of hydrophilic ionic liquids

### 3.1 Introduction

#### 3.1.1 Kamlet-Taft solvent polarity

The solvent has a huge impact on the solubility of solutes as well as on the rate and the selectivity of chemical reactions. The large number of available solvents has spurred the development of tools that help to predict the most suitable solvent.

An attempt to classify solvents and their effects on solutes is the concept of polarity. A large range of probes has been applied, based on solvatochromism, NMR chemical shifts, chemical equilibria and reaction rates.<sup>108</sup> Although it would be practical, the multitude of possible solvent solute interactions such as electrostatic attraction/repulsion, hydrogen-bonding, polarisation and dispersion cannot be described adequately by only one parameter. A solution to the problem was the introduction of polarity scales using several parameters.

A solvatochromic solvent polarity scale with three descriptors was devised by Kamlet and Taft in the 1970s.<sup>109-111</sup> Various molecules were selected that have UV/Vis absorption bands that are particularly sensitive to the solvent environment. It was shown that the shift of the peak maximum can be correlated with certain aspects of the solvent solute interaction.

Out of the many solvent-solute interactions, the three most significant for solvation were selected. Each interaction is represented by one Kamlet-Taft parameters. The general polarisation/polarisability is represented by the parameter  $\pi^*$  ("pi star"). The two other properties are the ability to donate hydrogen-bonds to a solute, represented by the  $\alpha$  ("alpha") parameter, and the ability to accept hydrogen-bonds from a solute, represented by the parameter  $\beta$  ("beta"). The parameters are

defined in a way that a strong interaction will result in a high value of the corresponding Kamlet-Taft parameter.

All solvatochromic dye probes are susceptible to polarisation by the surrounding solvent molecules. If the probe also has a capacity for hydrogen-bonding, this will shift the band even further. In order to separate the hydrogen-bonding from the polarisability, two probes must be used, one that only responds to polarisation effects and one that responds to polarisation and either hydrogen-bond acidity or hydrogen-bond basicity of the solvent.

#### 3.1.1.1 Polarisability ( $\pi^*$ )

In order to measure the polarisability of a solvent, the probe molecule should be completely unable to donate or accept hydrogen bonds. The only remaining influence should be the solvent's permanent polarisation or polarisability. The dye that is used as  $\pi^*$  probe in this study is *N,N*-diethyl-4-nitroaniline (Figure 35). It is one of the  $\pi^*$  probes already used by Kamlet and Taft.<sup>109</sup>

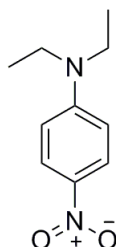


Figure 35: The  $\pi^*$  dye *N,N*-diethyl-4-nitroaniline

Although *N,N*-diethyl-4-nitroaniline is unable to donate hydrogen-bonds (as required for a  $\pi^*$  probe), it can actually accept hydrogen-bonds through the nitro group. However, the hydrogen-bonding is weak and is therefore neglected.

The  $\pi^*$  scale of Kamlet and Taft is normalised relative to two solvents. The position of the peak maximum of *N,N*-diethyl-4-nitroaniline in cyclohexane has been defined as zero. The second point of reference is the peak position in dimethylsulfoxide (DMSO) and the value 1 has been assigned to it.



$$\pi^* = \frac{\bar{\nu}_{\text{solvent}} - \bar{\nu}_{\text{cyclohexane}}}{\bar{\nu}_{\text{DMSO}} - \bar{\nu}_{\text{cyclohexane}}} \quad \text{Eq. 1}$$

### 3.1.1.2 Hydrogen-bond basicity ( $\beta$ )

The hydrogen-bonding basicity of a solvent can be measured using *N,N*-diethyl-4-nitroaniline and 4-nitroaniline (Figure 36 on the left). The dyes are a pair of homomorphs. Due to their similar structure, both dyes are similarly affected by the electrostatic polarisation of the solvent. Only 4-nitroaniline can donate hydrogen-bonds (HBD) to potential hydrogen-bond basic sites on the solvent.

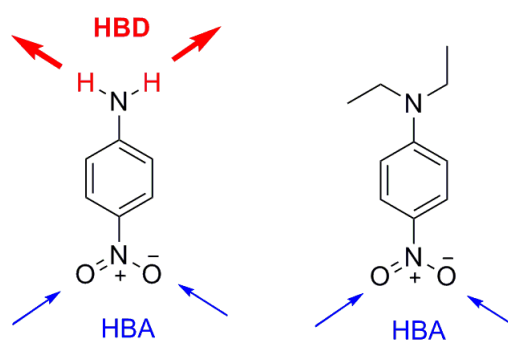


Figure 36: The  $\beta$  dye 4-nitroaniline and its homomorph  $\pi^*$  dye

To obtain  $\beta$ , the absorption spectra of both probes are measured and the positions of the peak maxima are determined. Using those, the enhanced solvatochromic shift ( $\Delta\nu$ ) can be calculated according to Equation 2.

$$\Delta\nu = \bar{\nu}_{4\text{-nitroaniline}} - \bar{\nu}_{N,N\text{-diethylnitroaniline}} \quad \text{Eq. 2}$$

The enhanced solvatochromic shift obtained for the solvent of choice is then related to the enhanced solvatochromic shift of two reference solvents. In the original publication, hexamethylphosphoramide (HMPA) was used to define the upper reference point for the  $\beta$  scale ( $\Delta\nu_{\text{HMPA}}=1$ ), because it displayed the largest enhanced solvatochromic shift and hence the strongest hydrogen-bond acceptor ability of all tested solvents.<sup>109</sup> However, HMPA is difficult to handle (it is hydrolytically unstable and corrosive), therefore dimethyl sulfoxide was chosen as a more convenient reference solvent in this study. This introduces the factor 0.76 into Equation 3 (which is the  $\beta$  value of DMSO). The  $\Delta\nu$  in

cyclohexane serves as second reference value, supplying  $\Delta\nu$  for a solvent that cannot accept hydrogen-bonds at all ( $\Delta\nu_{\text{hexane}}=0$ ).

$$\beta = 0.76 \frac{\Delta\bar{\nu}_{\text{solvent}} - \Delta\bar{\nu}_{\text{cyclohexane}}}{\Delta\bar{\nu}_{\text{DMSO}} - \Delta\bar{\nu}_{\text{cyclohexane}}} \quad \text{Eq. 3}$$

### 3.1.1.3 Hydrogen-bond acidity ( $\alpha$ )

The hydrogen-bond acidity of a solvent can be obtained in an analogous way to obtaining  $\beta$  with an enhanced solvatochromic shift.<sup>110</sup> The position of the peak maximum of *N,N*-diethyl-4-nitroaniline can be used to subtract the polarisation/polarisability component. The second probe must be able to accept hydrogen-bonds. However, there are no aniline dyes which absorb in the appropriate UV/Vis range and are good hydrogen-bond acceptors. Instead, the zwitterion 2,6-diphenyl-4-(2,4,6-triphenylpyridinium)phenoxide or Reichhardt's dye (RD) is used (Figure 37).

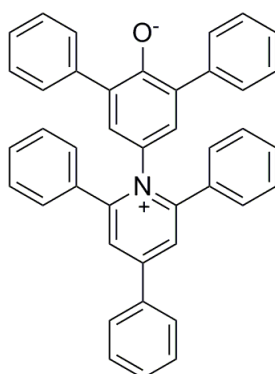


Figure 37: The  $\alpha$  dye 2,6-diphenyl-4-(2,4,6-triphenylpyridinium)phenoxide or Reichhardt's dye

Reichhardt's dye also has its merits, for example a very large solvatochromic shift. Moreover, a huge number of solvatochromic shifts measured with this dye are available in the literature, which can be used as references.<sup>112</sup> They are used for the widely known  $E_T(30)$  polarity scale. The  $E_T(30)$  parameter is calculated using Eq. 4.

$$E_T(30)(kcal/mol) = \frac{28591}{\lambda_{\text{max}}(RD)} \quad \text{Eq. 4}$$

Potential error is introduced by combining the measurement with two structurally different dyes, as each of them may experience the

polarisability of a solvent somewhat differently. This is typically neglected. Kamlet and Taft suggested calculating the enhanced solvatochromic shifts with the solvatochromic shift of Reichardt's dye and 4-nitroanisole (Figure 38) using Eq. 5.

$$\Delta\nu = \bar{\nu}_{\text{RD}} - \nu_{4\text{-nitroanisole}} \quad \text{Eq. 5}$$

The enhanced solvatochromic shift of the strongly hydrogen-bond donating solvent methanol has been defined to be 1 ( $\Delta\nu_{\text{MeOH}} = 1$ ) by Kamlet and Taft, while the enhanced solvatochromic shift of cyclohexane is defined as 0.<sup>110</sup>

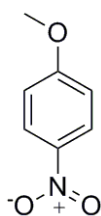


Figure 38: 4-nitroanisole, an alternative  $\pi^*$  probe

However, the  $\pi^*$  dye used for the original definition of  $\alpha$  by Kamlet and Taft is 4-nitroanisole and not *N,N*-diethyl-4-nitroaniline. The use of *N,N*-diethyl-4-nitroaniline would reduce the number of measurements that have to be taken, as its solvatochromic shift could be used for calculating both  $\beta$  and  $\alpha$ . However, since different dye probes have different sensitivity to the polarisation/polarisability of a solvent, the equation would need modification to compensate for the use of a *N,N*-diethyl-4-nitroaniline instead of the anisole (Eq. 6).

$$\alpha(\text{diethylnitroaniline}) = x \frac{\Delta\bar{\nu}_{\text{solvent}} - \Delta\bar{\nu}_{\text{cyclohexane}} - \gamma}{\Delta\bar{\nu}_{\text{MeOH}} - \Delta\bar{\nu}_{\text{cyclohexane}}} \quad \text{Eq. 6}$$

The Welton group has opted for not determining the modified equation, but uses a regression equation determined by Marcus (Eq. 7).<sup>112</sup> The regression equation requires  $E_T(30)$  and  $\pi^*$  which is determined with *N,N*-diethyl-4-nitroaniline.

$$\alpha = 0.0649E_T(30) - 2.03 - 0.72\pi^*_{N,N\text{-diethyl-4-nitroaniline}} \quad \text{Eq. 7}$$

#### 3.1.1.4 The Kamlet-Taft parameters of ionic liquids

The Kamlet-Taft polarity scales were first described decades ago and a large number of molecular solvents have been characterised this way.<sup>112</sup> However, only recently have they been used to determine the polarity of ionic liquids, because the ionic liquids which are used today were not available to Kamlet and Taft.<sup>113</sup>

The Kamlet-Taft parameters of several ionic liquids have been measured with the aforementioned set of dyes and are listed in Table 4. The values show that ionic liquids have a high polarisability (higher than DMSO). Ionic liquids with dialkylimidazolium cations have  $\alpha$  parameters of ca. 0.6. This relatively high hydrogen-bond acidity is thought to be due to the acidity of the proton bound to the C-2, which is the most electron-depleted site on the cation (due to the vicinity to two nitrogen atoms).<sup>67</sup> The  $\alpha$  value is significantly lower, when the C-2 site is capped with a methyl group or if the cation is changed into dialkylpyrrolidinium  $[\text{C}_n\text{C}_m\text{pyrr}]^+$ .

The  $\alpha$  value of 1,3-dialkylimidazolium ionic liquids is relatively high, in the range of formamide and benzyl alcohol. The apparent high acidity has been attributed to Reichhardt's dye being an anionic dye.<sup>97</sup> Due to the anionic nature it can interact more strongly with the imidazolium ring than a neutral dye probe. Hydrogen-bonding to the 1,3-dialkylimidazolium cation at the C-2 site has a destabilising effect, because the electron density is donated into anti-bonding orbitals. However, with a charged hydrogen-bond acceptor probe the destabilising effect is counteracted by a strong coulombic attraction between the charged species, resulting in what is called an "ionic" hydrogen bond.<sup>67</sup> A neutral dye will not be able to provide the stabilising coulombic contribution and thus indicate a significantly lower hydrogen-bond acidity.<sup>97</sup>

The  $\beta$  value is particularly susceptible to changes of the anion (Table 4). This has led to the general notion that the hydrogen-bonding acidity and basicity can be tuned independently from each other. This has been confirmed for ionic liquids of the form  $[\text{C}_n\text{C}_m\text{C}_j\text{im}][\text{anion}]$  or

$[C_nC_m\text{pyrr}][\text{anion}]$ .<sup>113</sup> However, a slight  $\beta$  dependence of  $\alpha$  has also been observed.<sup>113</sup>

Table 4: Kamlet-Taft parameters of selected non-protic imidazolium and pyrrolidinium ionic liquids. The values shaded in dark grey show the effect on  $\alpha$  upon changing the cation. Values shaded light grey show the impact on  $\beta$  when the anion is varied.<sup>113</sup>

	$\alpha$	$\beta$	$\pi^*$
$[C_4C_1\text{im}][\text{OTf}]$	0.63	0.46	1.01
$[C_4C_1\text{im}][\text{BF}_4]$	0.63	0.38	1.05
$[C_4C_1\text{im}][\text{NTf}_2]$	0.62	0.24	0.98
$[C_4C_1C_1\text{im}][\text{NTf}_2]$	0.38	0.24	1.01
$[C_4C_1\text{pyrr}][\text{NTf}_2]$	0.43	0.25	0.95

The ionic liquids for which the Kamlet-Taft parameters have been determined so far contained anions that have low or medium hydrogen-bonding basicity. It would be interesting to extend the characterisation of Kamlet-Taft parameters to ionic liquids with high hydrogen-bond basicity. These results are presented in this chapter.

### 3.1.2 Ionic liquid stability

The stability of ionic liquids is important for the development of processes employing ionic liquids. Elevated temperatures are always required for the ionic liquid pretreatment of lignocellulose. Several authors have performed pretreatment with  $[C_nC_1\text{im}][\text{MeCO}_2]$  and chloride based ionic liquids at temperature between 110 and 130°C.<sup>114-117</sup> Many pretreatment experiments mentioned in chapters 4, 5 and 6 have been conducted at 120°C. The stability of the ionic liquids at these significantly elevated temperatures must therefore be confirmed.

The stability of compounds can be characterised by thermogravimetric analysis. This technique correlates sample weight loss with temperature. A thermogravimetric analyser contains a sensitive balance with an inert sample holder, an oven and a thermocouple. The oven chamber is flushed with a stream of gas. The equipment requires a few milligrams of sample and detects weight changes in the microgram range.

During a typical experiment the temperature is increased at a constant rate while the sample weight is recorded. When a certain temperature is reached, decomposition into mostly volatile compounds will occur as demonstrated in Figure 39. Because the decomposition/weight loss is not instantaneous, the curve needs to be interpreted. A common method to determine the temperature of decomposition is the step-tangent method yielding the onset temperature of decomposition,  $T_{\text{onset}}$ . This temperature is obtained by fitting two tangents to the curve as depicted in Figure 39,  $T_{\text{onset}}$  being the temperature at which both tangents cross.

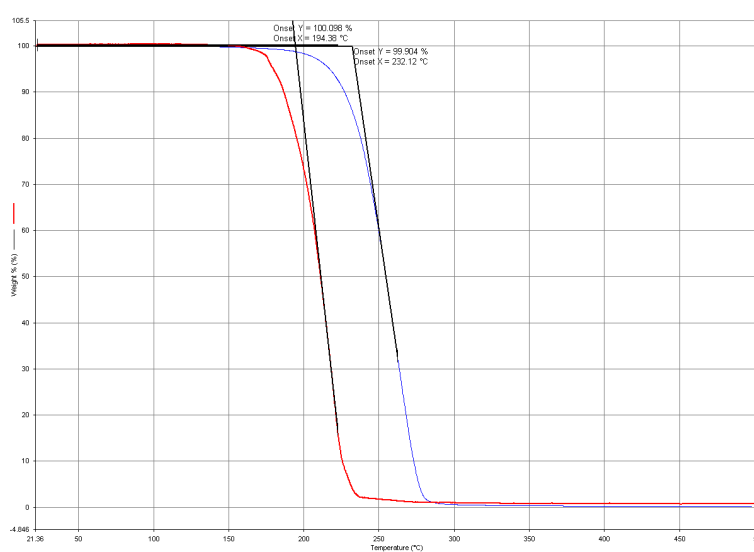


Figure 39: Determining  $T_{\text{onset}}$  of two ionic liquids by fitting tangents to the decomposition curves.

$T_{\text{onset}}$  is suitable for comparing the stability of different ionic liquids. It has been found that both the type of cation and anion influences the temperature of decomposition.<sup>118</sup> However, if the stability of an ionic liquid under certain process conditions is of interest,  $T_{\text{onset}}$  is only an indicator, as mass loss occurs below  $T_{\text{onset}}$ , as can be seen in Figure 39.

Therefore an alternative method has been suggested.<sup>119</sup> The amount of decomposition depends on the temperature as well as the time, so both need to be specified. Baranyi *et al.* have defined  $T_{0.01/10}$ , which is the temperature at which the ionic liquid degrades by 1% in 10 h.<sup>119</sup> Table 5 lists  $T_{\text{onset}}$  and  $T_{0.01/10}$  for selected ionic liquids. It shows that the ionic liquids show significant decomposition more than 100°C lower than the step-tangent method suggests. For the set of ionic liquids

investigated by Baranyi *et al.*, a linear relationship between both temperatures ( $T_{0.01/10} = 0.6902 T_{\text{onset}} + 56.829$ ) was found.<sup>120</sup>

Table 5:  $T_{0.01/10}$  and  $T_{\text{onset}}$  of various ionic liquids (in °C)<sup>120</sup>

Ionic liquid	$T_{\text{onset}}$	$T_{0.01/10}$
[C <sub>4</sub> C <sub>1</sub> pyrr][NTf <sub>2</sub> ]	435	271
[P <sub>66614</sub> ][N(CN) <sub>2</sub> ]	396	233
[C <sub>4</sub> C <sub>1</sub> pyrr][N(CN) <sub>2</sub> ]	283	170

In this work, the stability of selected hydrophilic ionic liquids was studied by the step-tangent method and by long-term thermal heating to find out whether these ionic liquids are stable under the conditions of lignocellulose pretreatment.

### 3.1.3 Hygroscopicity of ionic liquids

Although not all ionic liquids are miscible with water, even the hydrophobic ones have a certain affinity towards water. The moisture affects their chemical and physical properties,<sup>78</sup> therefore ionic liquids must always be dried *in vacuo* before use. There are also indications that the water content of ionic liquids influences the solubility<sup>117, 121</sup> and the reactivity<sup>122, 123</sup> of cellulose and lignocellulosic biomass.

So far, the nature of interactions of water with ionic liquids has only been investigated for 1-butyl-3-methylimidazolium ionic liquids with low and mid-range hydrogen-bonding anions, such as [PF<sub>6</sub>]<sup>-</sup>, [NTf<sub>2</sub>]<sup>-</sup> and [BF<sub>4</sub>]<sup>-</sup>. It has been shown that the amount of water absorbed is anion-dependent and is influenced by the strength of the hydrogen-bonding capabilities of the anion.<sup>96</sup> Crystal structures for solid ionic liquid hydrates of [C<sub>1</sub>C<sub>1</sub>im][HCO<sub>3</sub>]<sup>107</sup>, [C<sub>n</sub>C<sub>1</sub>im]Cl<sup>124</sup> and [C<sub>n</sub>C<sub>3</sub>C<sub>1</sub>C<sub>1</sub>N]Br<sup>125</sup> (where  $n \geq 10$ ) have been obtained. Usually, an interaction between the water molecules and the anion is observed, however, occasionally evidence for interactions between cation and the oxygen atom of water has been found.<sup>126</sup> The amount of water absorbed by the ionic liquid can be determined by Karl Fischer titration. IR-spectroscopy can provide

evidence for the strength of hydrogen-bonding *via* the peak positions of the OH stretching modes of water.<sup>96</sup>

In this study, the interactions of water with highly hydrophilic dialkylimidazolium ionic liquids were investigated, as they are of importance for the application in lignocellulose processing, which will be discussed in chapter 4.



## 3.2 Materials and Methods

### 3.2.1 *Materials*

Reichhardt's dye, 4-nitroaniline and *N,N*-diethyl-4-nitroaniline were purchased from Sigma-Aldrich and used as received. HPLC grade dichloromethane was purchased from VWR and used as received. 1-Butyl-3-methylimidazolium trifluoromethanesulfonate was kindly provided by Tom Wells and Matthew Lui.

### 3.2.2 *Karl Fischer titration*

The water content of ionic liquids was measured with a TitroLine KF trace titrator (Schott) using coulometric detection according to the manufacturer's instructions. The reagent was Hydranal Coulomat AG (Fluka). Typically 50-100 mg sample were injected using a 1 ml gas-tight plastic syringe.

### 3.2.3 *Determination of ionic liquid hygroscopicity*

500 mg dried ionic liquid were exposed to air for 3 days. The temperature in the lab was approximately 25°C. The quantity of moisture was determined by Karl Fischer titration. The ppm value was transformed into the water-to-ionic liquid ratio *via* the formula given below.

$$\frac{[H_2O]}{[IL]} = \frac{ppm}{18.015g/mol} \cdot \frac{M_W(IL)}{10^6 - ppm} \quad \text{Eq. 8}$$

### 3.2.4 *Spectroscopy*

IR-spectra were recorded with a Spectrum 100 IR machine (Perkin-Elmer) equipped with a universal ATR sampling accessory with diamond crystal. UV/Vis spectra were recorded using a PC-controlled Perkin Elmer Lambda 2 spectrometer with thermostatted sample holder. The spectrometer was calibrated with a holmium oxide standard. Spectra were recorded with a resolution of 0.2 nm.

### 3.2.5 *Measurement of Kamlet-Taft parameters*

Stock solutions of the Kamlet-Taft dyes (Reichhardt's dye, 4-nitroaniline and *N,N*-diethyl-4-nitroaniline) were prepared in dichloromethane and stored at 4°C in the dark. All ionic liquids were dried under vacuum until dry ( $\leq 3000$  ppm), unless stated otherwise.  $[\text{C}_4\text{C}_1\text{im}][\text{MeCO}_2]$  was dried at 50°C and  $[\text{C}_4\text{C}_1\text{im}][\text{Me}_2\text{PO}_4]$  at 100°C, all other ionic liquids at 40°C.

The dye solution was transferred into a quartz cuvette with 1 mm path length. The dichloromethane was evaporated, the ionic liquid added and the solution mixed by vigorous shaking or with help of an air-tight syringe. The spectra were recorded at 25°C. The maximum of the absorption peak was determined using Origin 7. A Gaussian function was fitted to a 40 nm wide region with the peak maximum in the centre. The solvatochromic shifts were transformed into the Kamlet-Taft parameters using the formulas in sections 3.1.1.1, 3.1.1.2 and 3.1.1.3. In cases where Reichhardt's dye was decolourised by the ionic liquid, more dye was added or a drop of triethylamine was mixed into the solution.

### 3.2.6 *Measuring the Kamlet-Taft parameters of ionic liquids with a melting point above room temperature*

This procedure was used for measuring the Kamlet-Taft polarity of  $[\text{C}_4\text{C}_1\text{im}]\text{Cl}$ , and  $[\text{C}_4\text{C}_1\text{im}][\text{MeSO}_3]$ , which are solid at room temperature. The stock solution of the dye was transferred into a small 5 ml round bottomed flask equipped with stir bar and a side-arm. The solvent was evaporated and the capped flask transferred into a glove box. 1 g of salt was added, the flask sealed and heated above its melting point under nitrogen atmosphere outside the glove box. The solution was mixed with the dye for 2-3 min. Because Reichhardt's dye was decolourised, a drop of triethylamine was added. In the glove box, the mixture was transferred into a cuvette with a Teflon cap. The solid was compacted carefully using the tip of a thin spatula. The cuvette was placed in the spectrometer with thermostatted sample holder and the spectra recorded after the salt had melted. For  $[\text{C}_4\text{C}_1\text{im}]\text{Cl}$  and  $[\text{C}_4\text{C}_1\text{im}][\text{MeSO}_3]$  the temperature was 75°C and 80°C, respectively.

### 3.2.7 Thermogravimetric analysis

Thermogravimetric analysis was performed on a Pyris 1 Thermogravimetric Analyzer (Perkin Elmer), using platinum sample holders. The Analyzer was calibrated using the Curie points of various metals. For decomposition experiments the samples were heated at 10°C/min to 500°C under a constant flow of nitrogen gas (20 ml/min). For long-term stability measurements, the samples were heated to 120°C and the weight loss monitored at 120°C for 60 h. The temperature of decomposition,  $T_{\text{onset}}$ , was determined using the step tangent method (described in section 3.1.2).

### 3.2.8 Kugelrohr distillation of $[C_4C_1py][MeCO_2]$

$[C_4C_1py][MeCO_2]$  (1.32 g) was placed in a glass bulb. A receiving bulb was connected and the stacked bulbs inserted into the Kugelrohr apparatus (Büchi). The apparatus was connected to a vacuum pump *via* a Schlenk line, the bulbs were evacuated and the oven temperature raised until the liquid started boiling (170°C). The distillate (0.82 g) was a colourless liquid at room temperature. The major product was identified as 4-(*N,N*-butylmethyl)aminobutyl acetate. Traces of 1-butylpyrrolidine were also present.

$^1\text{H-NMR}$  (400 MHz, DMSO- $d_6$ )  $\delta$ : 3.99 (2H, t,  $J=6.6$ ,  $-\text{CH}_2\text{-O}-$ ), 2.23 (4H, m,  $-\text{CH}_2\text{-N}$ ), 2.09 (3H, s,  $(\text{CH}_3\text{-C}(\text{O})\text{O}-)$ ), 1.98 (3H, s,  $\text{CH}_3\text{-N}$ ), 1.57 (2H, m,  $-\text{CH}_2-$ ), 1.43 (2H, m,  $-\text{CH}_2-$ ), 1.36 (2H, m,  $-\text{CH}_2-$ ) 1.28 (2H, m,  $\text{CH}_2-$ ), 0.87 (3H, t,  $J=7.3$ ,  $\text{N}-(\text{CH}_2)_3\text{-CH}_3$ ) ppm.  $^{13}\text{C}\{^1\text{H}\}\text{-NMR}$  (100 MHz, DMSO- $d_6$ )  $\delta$ : 170.48, 64.11, 57.36, 57.16, 42.01, 29.52, 26.8, 23.71, 20.89, 20.46, 14.17 ppm.  $m/z$  (EI $^+$ ): 201 (10%,  $\text{M}^+$ ), 158 (95%,  $[\text{M} - \text{CH}_3\text{C}=\text{O}]^+$ ), 100 (100%,  $\text{MeBuNCH}_2^+$ )

### 3.3 Results and Discussion

#### 3.3.1 Kamlet-Taft parameters of hydrophilic ionic liquids

##### 3.3.1.1 Accuracy of Kamlet-Taft values

Initially, a set of known Kamlet-Taft parameters was investigated. For this purpose the ionic liquid [C<sub>4</sub>C<sub>1</sub>im][OTf] was selected. The reproducibility of the measurement was very good (Table 6, first entry). The measured parameters were also in good agreement with previously published values using the same dye set (Table 6). However, when comparing the parameters from different sources, deviations of 5-10% were observed, much higher than the errors between single measurements.

Table 6: Kamlet-Taft parameters reported by different members of the Welton group in per-reviewed publications (standard deviation in brackets)

Abbreviation	$\alpha$	$\beta$	$\pi^*$
[C <sub>4</sub> C <sub>1</sub> im][OTf] <sup>127</sup>	0.634 (0.008)	0.483 (0.008)	0.974 (0.002)
[C <sub>4</sub> C <sub>1</sub> im][OTf] <sup>113</sup>	0.63	0.46	1.01
[C <sub>4</sub> C <sub>1</sub> im][OTf] <sup>128</sup>	0.62	0.46	1.01
[C <sub>4</sub> C <sub>1</sub> im][OTf] <sup>80</sup>	0.60	0.51	1.03

It was attempted to identify the cause(s) of these deviations. An important factor is the equation to calculate these values. In this work, the  $\pi^*$  and  $\beta$  scales were calibrated using cyclohexane and DMSO. Other researchers have or might have used regression equations calculated by Marcus<sup>112</sup> or Kamlet and Taft<sup>109, 111</sup>. When using regression curves of others, it must be ensured that the used spectrometer is well-calibrated, which might not be the case. However, the equations used are often not stated and details of the procedure are not given, as in the publication by Rinaldi.<sup>129</sup> As an example,  $\Delta\nu$  values of the standards used to normalise the  $\beta$  scale are shown in Table 7. The deviation between the standard  $\Delta\nu$  values from different sources is more than 10%. Additional error could be introduced when identifying the peak maximum in the absorption spectra,

as the peaks are broad and often not entirely symmetrical. For example, if a fitting program is used, the width of the fitting interval will have an impact on the value.

Table 7: Position of peak maxima of 4-nitroaniline (NA) and *N,N*-diethyl-4-nitroaniline (DENA) in reference solvents used to calculate  $\beta$  and  $\pi^*$ . Units are  $10^3 \text{ cm}^{-1}$ .

	NA in cyclohexane	DENA in cyclohexane	NA in DMSO	DENA in DMSO	$\Delta\nu$
Kamlet <i>et al.</i> 109	31.03	27.40	25.71	24.30	2.22
This work	30.85	27.46	25.67	24.22	1.94

### 3.3.2 Practical considerations for the use of Reichhardt's dye

Reichhardt's dye is an anionic dye. It is a phenolate with a  $pK_a$  of 8.65. This means that it can be protonated by solvents or substances with a lower  $pK_a$  value. Small quantities of acidic impurities are sufficient to interact with all dye molecules present in the solution ( $\approx 10 \mu\text{mol/ml}$ ). The acid-sensitivity of Reichhardt's dye is also the reason why it cannot be used to measure the hydrogen-bond acidity of acidic solvents. The procedure of the Welton lab to deal with acidic impurities in ionic liquids was to wash the ionic liquid with a dilute aqueous sodium hydroxide solution. However, for hydrophilic ionic liquids an aqueous washing step is not possible (see section 2.3.1 for details).

Two solutions were applied for this problem. Occasionally it helped to add more dye, until excess free phenolate ions are present (solution developed by Lorna Crowhurst). In other cases, a drop of triethylamine was used as an acid scavenger (developed by Guisepe Ranieri). The effect of triethylamine on the  $\alpha$  parameter was tested on  $[\text{C}_4\text{C}_1\text{im}][\text{N}(\text{CN})_2]$ , because Reichhardt's dye gave good absorbance without triethylamine. The triethylamine altered the  $\alpha$  value only slightly (0.542 before and 0.556 after addition, deviation by 2.6%). The increase may be due to residual moisture in the triethylamine.

An explanation for the difficulty of measuring  $\alpha$  in almost all of the hydrophilic ionic liquids could be the presence of moisture. It is very difficult to reduce the water content below 1000 ppm in ionic liquids such

as [C<sub>4</sub>C<sub>1</sub>im][Me<sub>2</sub>PO<sub>4</sub>] and [C<sub>4</sub>C<sub>1</sub>im][MeCO<sub>2</sub>]. It is known that the residual water molecules strongly hydrogen-bond to the anion,<sup>96</sup> which is likely to induce polarisation in the water molecules. This polarisation could be strong enough to protonate Reichardt's dye.

### 3.3.2.1 The effect of moisture on the Kamlet-Taft values

Kamlet-Taft parameters can be affected by impurities. One of the most prevalent impurities is water, which can be easily introduced by exposing ionic liquids to air. This is particularly important for ionic liquids with strongly hydrogen-bonding anions (as will be shown in section 3.3.5.2). In order to assess the effect that moisture has on hydrophilic ionic liquids, the Kamlet-Taft parameters of the ionic liquid [C<sub>4</sub>C<sub>1</sub>im][Me<sub>2</sub>PO<sub>4</sub>] were measured after the ionic liquid had been exposed to air for a few days (Table 8). The most pronounced effect was found for the  $\beta$  parameter which decreased significantly upon wetting. The  $\alpha$  and  $\pi^*$  values were not significantly affected.

Table 8: Effect of moisture on the Kamlet-Taft parameters of [C<sub>4</sub>C<sub>1</sub>im][Me<sub>2</sub>PO<sub>4</sub>]

	$\alpha$	$\beta$	$\pi^*$
[C <sub>4</sub> C <sub>1</sub> im][Me <sub>2</sub> PO <sub>4</sub> ], dried	0.452 (0.003)	1.118 (0.012)	0.970 (0.006)
[C <sub>4</sub> C <sub>1</sub> im][Me <sub>2</sub> PO <sub>4</sub> ], 8 wt% water	0.44	1.00	0.97

### 3.3.2.2 Thermochromism of solvatochromic dyes

Some of the "ionic liquids" investigated in this study are solids at room temperature, notably [C<sub>4</sub>C<sub>1</sub>im]Cl and [C<sub>4</sub>C<sub>1</sub>im][MeSO<sub>3</sub>]. A protocol was developed to mix the dyes with the ionic liquid without allowing moisture to enter. Because the substances must be transparent (and thus liquid), the UV/Vis spectra had to be recorded at elevated temperature. Unfortunately, the solvatochromic peak shifts are temperature-dependent, as demonstrated in Table 9.

Table 9: Thermochromatic effect on Kamlet-Taft parameters of [C<sub>4</sub>C<sub>1</sub>im][OTf],

	$\alpha$	$\beta$	$\pi^*$
[C <sub>4</sub> C <sub>1</sub> im][OTf], 25°C	0.634 (0.008)	0.483 (0.008)	0.974 (0.002)
[C <sub>4</sub> C <sub>1</sub> im][OTf], 75°C	0.60	0.47	0.93

Thermochromism has been demonstrated for the Kamlet-Taft parameters of [C<sub>4</sub>C<sub>1</sub>im][PF<sub>6</sub>].<sup>130</sup> In agreement with the results presented in Table 9, all values decreased with increasing the temperature. Therefore caution must be taken when comparing the Kamlet-Taft parameters of these ionic liquids with the Kamlet-Taft parameters measured at room temperature. However, as the deviations were relatively small, the thermochromism was neglected in this work.

### 3.3.3 Kamlet-Taft parameters of hydrophilic ionic liquids

The Kamlet-Taft parameters determined in this work are listed in Table 10, along with values found in the literature, where applicable. All ionic liquids were dried thoroughly before the measurements were taken.

The sometimes substantial deviations between different researchers (which have been discussed in 3.3.1.1) highlight the necessity to measure one's own Kamlet-Taft parameters and to make sure that the measurements are as accurate as possible.

Table 10: Kamlet-Taft parameters of hydrophilic 1-butyl-3-methylimidazolium ionic liquids (standard deviation in brackets) using the probes 4-nitroaniline, *N,N*-diethyl-4-nitroaniline and Reichhardt's dye. The values were determined at 25°C with dried ionic liquids, unless stated otherwise.

	$\alpha$	$\beta$	$\pi^*$
[C <sub>4</sub> C <sub>1</sub> im][OTf]	0.634 (0.008)	0.483 (0.008)	0.974 (0.002)
	0.63 <sup>113</sup>	0.46 <sup>113</sup>	1.01 <sup>113</sup>
[C <sub>4</sub> C <sub>1</sub> im][N(CN) <sub>2</sub> ]	0.543 (0.002)	0.596 (0.004)	1.052 (0.003)
[C <sub>4</sub> C <sub>1</sub> im][MeSO <sub>4</sub> ]	0.545 (0.006)	0.672 (0.009)	1.046 (0.002)
[C <sub>4</sub> C <sub>1</sub> im][HSO <sub>4</sub> ]	n/a	0.67	1.09
[C <sub>4</sub> C <sub>1</sub> im][MeSO <sub>3</sub> ] <sup>a</sup>	0.44	0.77	1.02
[C <sub>4</sub> C <sub>1</sub> im]Cl <sup>b</sup>	0.49	0.83	1.03
	0.44 <sup>131</sup>	0.84 <sup>131</sup>	1.14 <sup>131</sup>
[C <sub>4</sub> C <sub>1</sub> im][Me <sub>2</sub> PO <sub>4</sub> ]	0.452 (0.003)	1.118 (0.012)	0.970 (0.006)
[C <sub>4</sub> C <sub>1</sub> im][MeCO <sub>2</sub> ]	0.470 (0.012)	1.201 (0.017)	0.971 (0.007)
	0.43 <sup>132</sup>	1.05 <sup>132</sup>	1.04 <sup>132</sup>

<sup>a</sup>measured at 80°C; <sup>b</sup>measured at 75°C

### 3.3.3.1 The effect of hydrophilic anions on the Kamlet-Taft polarity of ionic liquids

The variation of the anion coincided with a large change of  $\beta$  (Figure 40). The ionic liquids [C<sub>4</sub>C<sub>1</sub>im][MeCO<sub>2</sub>] and [C<sub>4</sub>C<sub>1</sub>im][Me<sub>2</sub>PO<sub>4</sub>] extended the range of possible  $\beta$  values beyond 1.00, making them stronger hydrogen-bond acceptors than hexamethylphosphoramide. A less important but still significant effect of the anion on  $\alpha$  was also observed. The  $\alpha$  value dropped from 0.63 for [C<sub>4</sub>C<sub>1</sub>im][OTf] to around 0.45 for ionic liquids with strongly hydrogen-bond basic anions like [MeSO<sub>3</sub>]<sup>-</sup>, Cl<sup>-</sup>, [Me<sub>2</sub>PO<sub>4</sub>]<sup>-</sup> and [MeCO<sub>2</sub>]<sup>-</sup>. A decrease of  $\alpha$  with increasing  $\beta$  has also been observed with a different dye set by Spange *et.al.*<sup>133</sup>



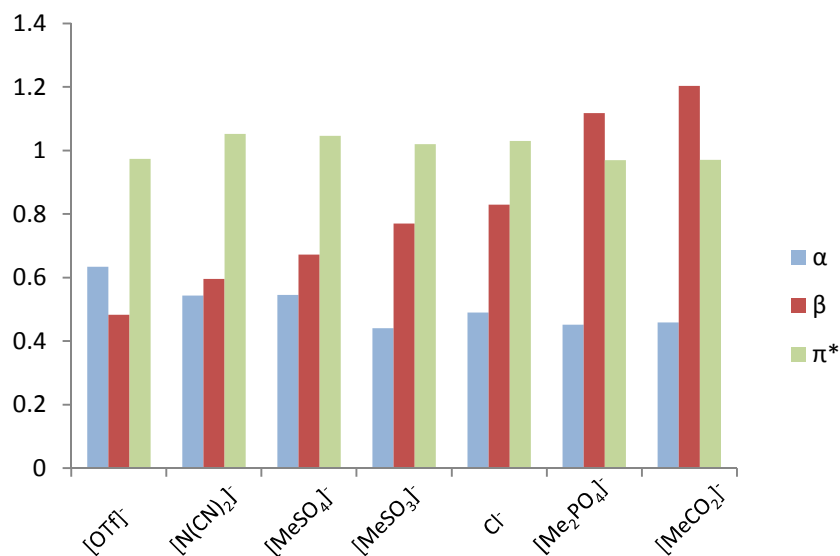


Figure 40: Kamlet-Taft parameters of dry hydrophilic 1-butyl-3-methylimidazolium ionic liquids. The parameter  $\beta$  varies widely, while  $\pi^*$  and  $\alpha$  are only slightly affected by the nature of the anion.

The dependency of the absorption of Reichardt's dye on the hydrogen-bond basicity is shown more clearly in Figure 41.

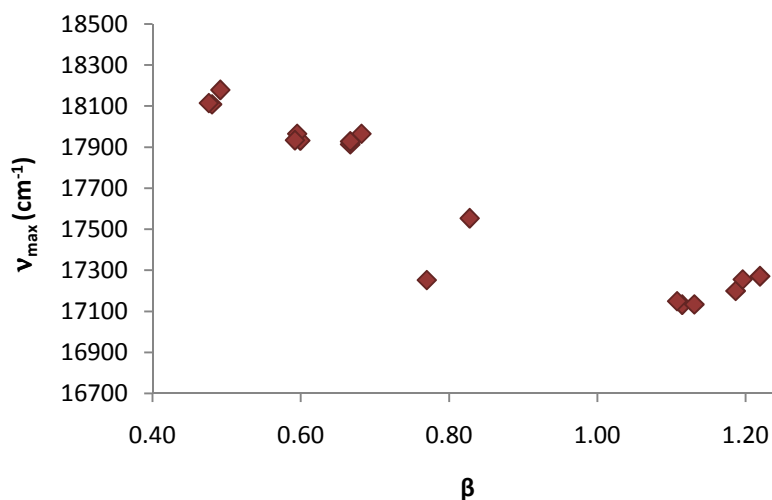


Figure 41: The influence of anion basicity of 1-butyl-3-methylimidazolium ionic liquids on the apparent hydrogen-bond acidity of the ionic liquid: the Kamlet-Taft  $\beta$  parameters of various ionic liquids were correlated with the position of the peak maximum of Reichardt's dye. A negative correlation can be observed.

The effect could be due to the strong hydrogen-bonds that highly basic anions can form with the cation *via* the C-2 proton (Figure 42). A sufficiently strong anion-cation hydrogen-bond could reduce coordination

of the phenolate oxygen on Reichardt's dye to this site. The dye would have to coordinate the less hydrogen-bond acidic C-4 and/or C-5 positions in this case, resulting in the measurement of lower  $\alpha$  values.

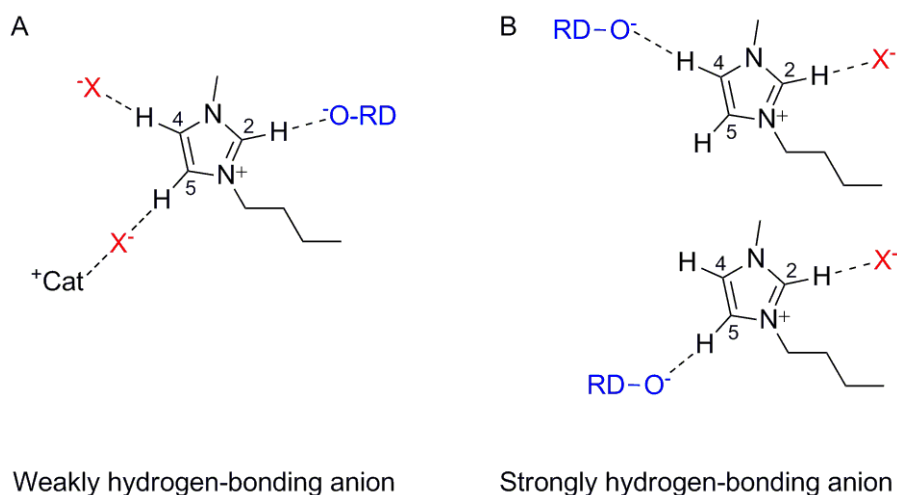


Figure 42: Possible cause of the reduction of the  $\alpha$  value with increasing hydrogen-bond basicity of the anion. A: Weakly hydrogen-bonding anions let Reichardt's dye with its phenoxide oxygen coordinate to the C-2 proton. B: Strongly hydrogen-bonding anions displace the dye from C-2 position and thus reduce the apparent hydrogen-bond acidity.

### 3.3.4 *The effect of hydrophilic anions on the hydrogen-bonding between cations and anions*

NMR shifts can be used to assess the strength of the hydrogen-bonds.<sup>134</sup> An anion effect on the ring protons in dialkylimidazolium ionic liquids has been reported before for 1-ethyl-3-methylimidazolium halides. It was shown that a more basic anion (chloride) will shift the C-2- signal downfield compared to the less hydrogen-bond basic anions (bromide or iodide).<sup>134</sup>

As part of this study, <sup>1</sup>H-NMR spectra were recorded to characterise the newly synthesised ionic liquids (section 2.2.3). A closer examination of the chemical shifts found for the 1-butyl-3-methylimidazolium revealed that the shift of the C-2 proton can vary by more than 1 ppm. Since the ionic liquids and the NMR-solvent (DMSO-d<sub>6</sub>) were dry when the spectra were recorded and the cation was the same in all cases, such significant differences are likely to be an effect of the anion. Although the ionic liquid concentration in the NMR samples was not controlled in this study, it is possible to obtain a very good correlation between the chemical shift of

the C-2 proton of hydrophilic ionic liquids and the values of the Kamlet Taft  $\beta$  parameter (Figure 43).

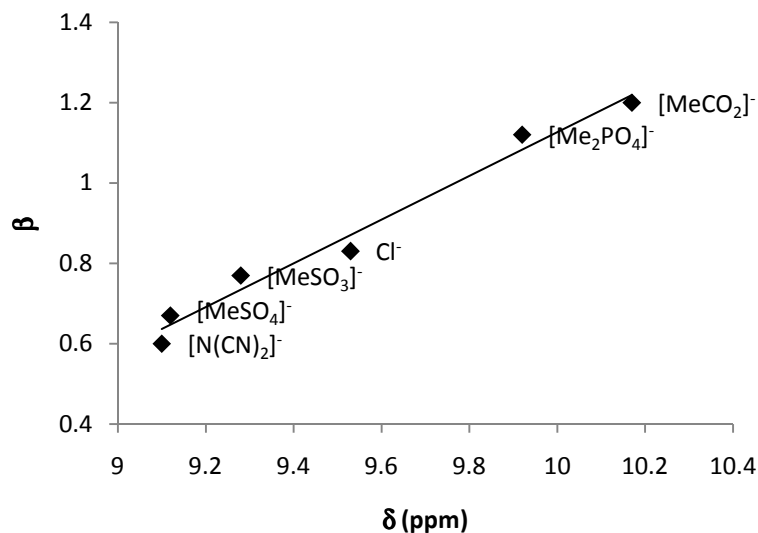


Figure 43: Correlation between the Kamlet-Taft parameter  $\beta$  of 1-butyl-3-methylimidazolium ionic liquids and the  $^1\text{H}$ -NMR chemical shift of the proton attached to carbon C-2 of the cation (in  $\text{DMSO-d}_6$ ). The higher the anion basicity was the larger was the chemical shift.  $R^2$  of the regression line is 0.978 and the p-value  $2 \cdot 10^{-4}$ .

Such a correlation indicates that basic anions interact strongly with the C-2 proton of the cation when they are in solution, forming hydrogen-bonded ion pairs. Lungwitz *et al.* have found a similar correlation when using a different dye set and a different NMR solvent ( $\text{CD}_2\text{Cl}_2$ )<sup>133</sup>

#### 3.3.4.1 The effect of salt impurities on the polarity parameters

The effect of other impurities such as inorganic salts was not investigated, although it was demonstrated that  $[\text{C}_4\text{C}_1\text{im}][\text{N}(\text{CN})_2]$  contained an unknown amount of residual sodium dicyanamide. The error introduced by an impurity depends on the strength of the interaction between the dye probes and the additional ions relative to the interaction between the probe and ionic liquid ions. It seems possible that the  $\alpha$  value is increased by the presence of salt because the smaller positive ions (in this case  $\text{Na}^+$ ) could interact more strongly with Reichardt's dye, as has been shown for 1% and 10% solution of  $\text{Li}^+$  ions in  $[\text{C}_4\text{C}_1\text{im}][\text{NTf}_2]$ .<sup>135</sup> In the case of  $[\text{C}_4\text{C}_1\text{im}][\text{N}(\text{CN})_2]$ , the value of the  $\alpha$  parameter is very similar to the value of  $\alpha$  of  $[\text{C}_4\text{C}_1\text{im}][\text{MeSO}_4]$  which is

made *via* a route (direct alkylation) that excludes contamination with salt impurities. This suggests that the  $\alpha$  parameter may have not been affected excessively. Nevertheless, an in-depth study of the effect of salt impurities would certainly be helpful.

### 3.3.5 *Physical properties that are affected by the hydrogen-bond basicity of the anion*

#### 3.3.5.1 Effect on the water-miscibility

The anion has a profound impact on the water-miscibility of ionic liquids. As it was shown earlier, this property has a profound impact on their synthesis and purification. Water miscibility depends on a variety of properties: size, the polarisability, the charge and the hydrogen-bonding. Kamlet-Taft polarity has not been developed to quantitatively predict water miscibility or miscibility with other solvents.

However, there is evidence that the  $\beta$  value has an effect on the water-miscibility and can be used qualitatively to predict whether an ionic liquid will be water miscible. This only applies if the other parameters do not change much. A bulky cation or a long lipophilic alkyl chain on the anion or cation may make the ionic liquid hydrophobic. Hydrogen-bond acidic functionalities increase the water-miscibility. The general rule is that the likelihood of obtaining a water-miscible ionic liquid is high when its hydrogen-bond basicity is high. This is due to the strong interaction of the anion with the hydrogen atoms in H<sub>2</sub>O, which has an impact on the solvation of the whole ion pair.

Table 11: Influence of the Kamlet-Taft  $\beta$  value on the water miscibility

	Ionic liquid anion	$\beta$ range	Group
Water immiscible	[NTf <sub>2</sub> ] <sup>-</sup> , [PF <sub>6</sub> ] <sup>-</sup> , [SbF <sub>6</sub> ] <sup>-</sup>	<0.25	1
Water miscible but can be extracted into dichloromethane	[BF <sub>4</sub> ] <sup>-</sup> , [OTf] <sup>-</sup> , [N(CN) <sub>2</sub> ] <sup>-</sup>	0.35-0.60	2
hydrophilic	[MeSO <sub>4</sub> ] <sup>-</sup> , [Me <sub>2</sub> PO <sub>4</sub> ] <sup>-</sup> , Cl <sup>-</sup> , [MeCO <sub>2</sub> ] <sup>-</sup> , [HCO <sub>2</sub> ] <sup>-</sup>	>0.65	3

### 3.3.5.2 Hygroscopicity of ionic liquids

While handling hydrophilic ionic liquids, it was noted that they can absorb substantial amounts of water. Drying for long periods and at elevated temperatures was required to reduce the moisture content to tolerable levels, indicating that water may be absorbed in larger quantities and may be bound more tightly than in less hydrophilic ionic liquids. In the case of [C<sub>4</sub>C<sub>1</sub>im][MeCO<sub>2</sub>], it was observed that the liquid warmed substantially when it was mixed with water.

To obtain further insight, the state of the water bound to ionic liquids was investigated using ATR-IR spectroscopy, as an extension to published work for “hydrophobic” and moderately hydrophilic ionic liquids.<sup>96</sup> The asymmetric ( $\nu_3$ ) and symmetric ( $\nu_1$ ) O-H stretching bands are strong peaks in the region around 3300 cm<sup>-1</sup>. They are absent in the dry ionic liquid (unless it contains hydroxyl groups) and grow with increasing moisture content (Figure 44).

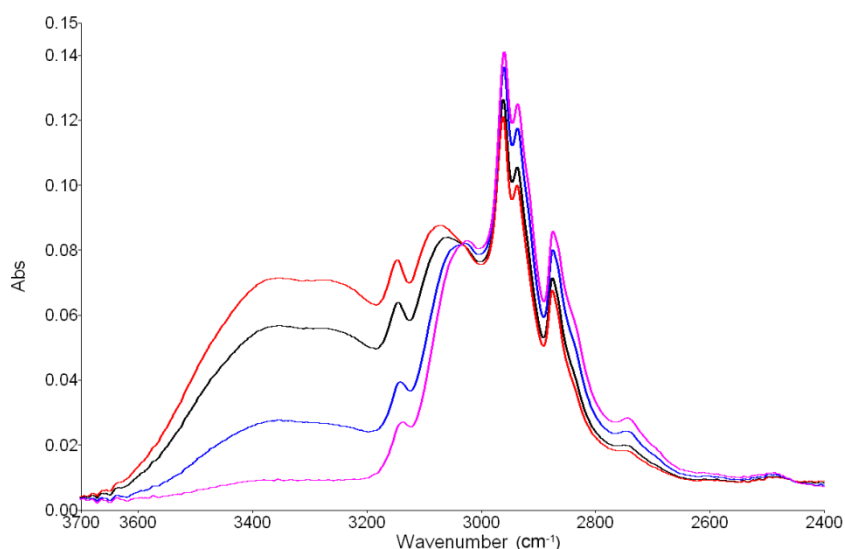


Figure 44: Moisture uptake by 1-butyl-3-methylimidazolium acetate monitored with ATR-IR spectroscopy. The uptake of water from the air is evidenced by an emerging broad band between  $3200\text{ cm}^{-1}$  and  $3500\text{ cm}^{-1}$ . Pink: dry ionic liquid (6500 ppm, 0.07 water molecules per ion pair), blue: 15 min, black: 45 min, red: 75 min.

While the peaks for the asymmetric and symmetric stretching vibrations are well separated in hydrophobic ionic liquids, they merge into a broad when the IR spectrum of hydrophilic ionic liquids is recorded.<sup>96</sup> This was observed for the ionic liquids synthesised in this study.

The second effect of the anion on the IR spectrum was a red-shift of the peak maximum for the merged peaks (Figure 45). Although the peaks were not deconvoluted, a red-shift could be observed for the hydrophilic ionic liquids used in this work in the order of the  $\beta$  value. For  $[\text{C}_4\text{C}_1\text{im}][\text{MeSO}_4]$ ,  $[\text{C}_4\text{C}_1\text{im}][\text{MeSO}_3]$ ,  $[\text{C}_4\text{C}_1\text{im}]\text{Br}$  and  $[\text{C}_4\text{C}_1\text{im}]\text{Cl}$ , the respective peak maxima were positioned at  $3492\text{ cm}^{-1}$ ,  $3444\text{ cm}^{-1}$ ,  $3413\text{ cm}^{-1}$  and  $3377\text{ cm}^{-1}$ , suggesting that the water is indeed more tightly bound if the anion has a higher hydrogen-bond basicity. The varying area of the OH-stretching band also indicates that more water can be absorbed by more hydrogen-bond basic ionic liquids when equilibrated with air.

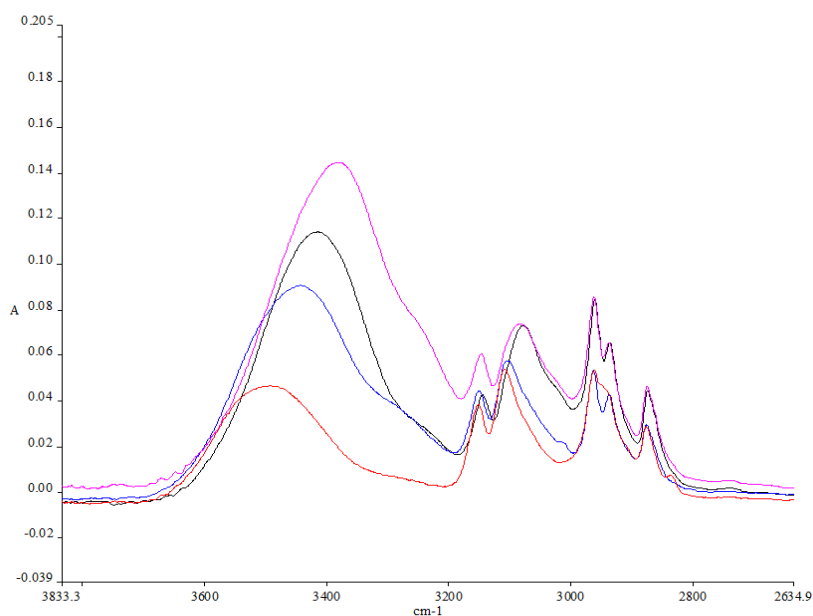


Figure 45: ATR-IR bands of the O-H stretching vibrations in moist  $[\text{C}_4\text{C}_1\text{im}][\text{MeSO}_4]$  (red),  $[\text{C}_4\text{C}_1\text{im}][\text{MeSO}_3]$  (blue),  $[\text{C}_4\text{C}_1\text{im}]\text{Br}$  (black) and  $[\text{C}_4\text{C}_1\text{im}]\text{Cl}$  (pink).

In addition, the amount of water taken up by various ionic liquids exposed to the laboratory air was determined by Karl Fischer titration of ionic liquids equilibrated with air. The results are shown in Table 12. A correlation of the moisture content with  $\beta$  is presented in Figure 46.

Some of the ionic liquids absorbed more than stoichiometric quantities of water, e.g.  $[\text{C}_4\text{C}_1\text{im}]\text{Br}$ ,  $[\text{C}_4\text{C}_1\text{im}][\text{MeSO}_3]$  and  $[\text{C}_4\text{C}_1\text{im}]\text{Cl}$  with  $\beta$  values around 0.8, and even more by the ionic liquids  $[\text{C}_4\text{C}_1\text{im}][\text{Me}_2\text{PO}_4]$  and  $[\text{C}_4\text{C}_1\text{im}][\text{MeCO}_2]$  with  $\beta$  values above 1.1. A strong linear correlation between the anion's hydrogen-bond basicity and the amount of water that an ionic liquid can absorb from air was found. The goodness of fit for the regression line was  $R^2=0.966$ .

Table 12: Moisture content of 1-butyl-3-methylimidazolium ionic liquids exposed to air

Ionic liquid anion	ppm ( $10^{-3}$ )	Water/IL ratio
[OTf] <sup>-</sup>	28	0.47
[N(CN) <sub>2</sub> ] <sup>-</sup>	71	0.87
[MeSO <sub>4</sub> ] <sup>-</sup>	70	1.05
[MeSO <sub>3</sub> ] <sup>-</sup>	130	1.95
Cl <sup>-</sup>	175	2.06
[Me <sub>2</sub> PO <sub>4</sub> ] <sup>-</sup>	169	2.98
[MeCO <sub>2</sub> ] <sup>-</sup>	241	3.49

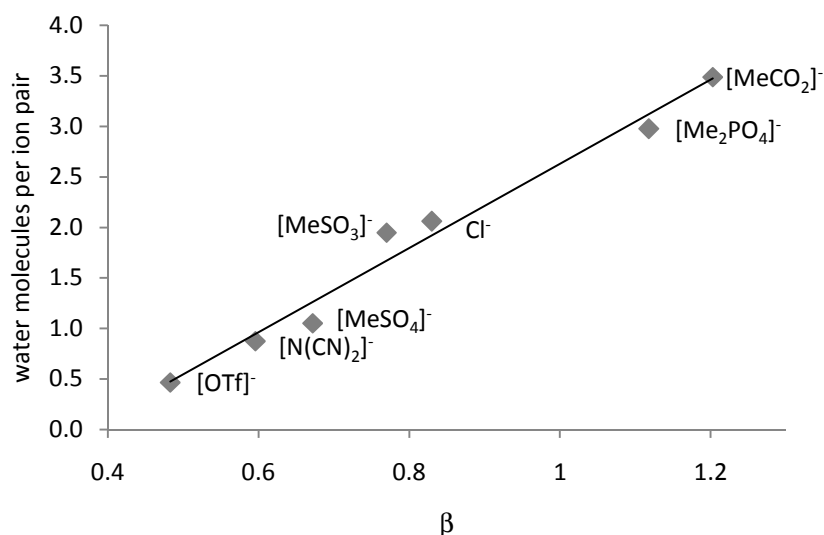


Figure 46: Correlation between the Kamlet-Taft  $\beta$  parameter of dry 1-butyl-3-methylimidazolium ionic liquids with the number of water molecules per ion pair when the ionic liquids are equilibrated with air. The fit of the trend line is  $R^2=0.966$ .

### 3.3.5.3 Ionic liquid stability at elevated temperatures

The stability of ionic liquids under conditions relevant to lignocellulose treatment was investigated by subjecting them to isothermal heating for 60 h. The temperature was set to 120°C, because this temperature has been frequently used for ionic liquid pretreatment of lignocellulosic biomass.<sup>136</sup> Most ionic liquids were stable under these conditions (Figure 47); however, it could be shown that mass loss occurs when the ionic liquids contains acetate anions. The weight of dry [C<sub>4</sub>C<sub>1</sub>im][MeCO<sub>2</sub>] was



8% lower after 60 h. The mass loss was rather dramatic for the pyrrolidinium based ionic liquid  $[C_4C_1\text{pyrr}][\text{MeCO}_2]$  and complete decomposition was observed at  $120^\circ\text{C}$  within less than 48 h.

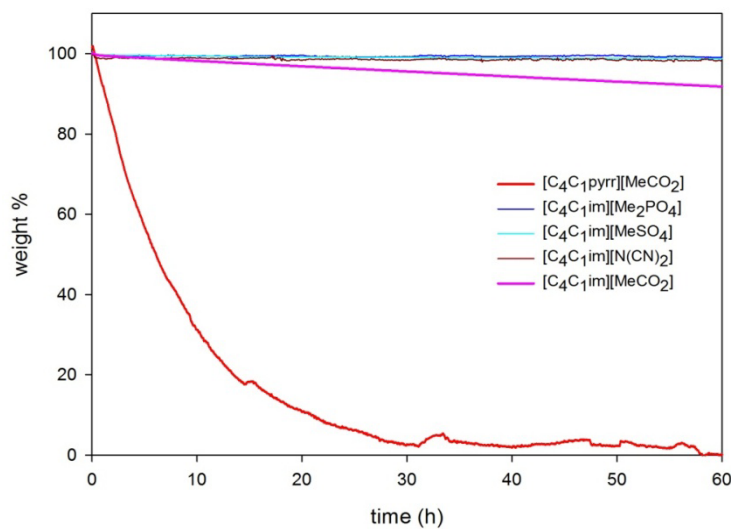


Figure 47: Long-term stability of hydrophilic ionic liquids at  $120^\circ\text{C}$

Interestingly, degradation products were not observed when analysing the  $[C_4C_1\text{im}][\text{MeCO}_2]$  that was left after the long-term stability experiment. This suggests that the volatile degradation products are removed by the gas stream flowing past the sample and the rate of removal is faster than the rate of degradation.

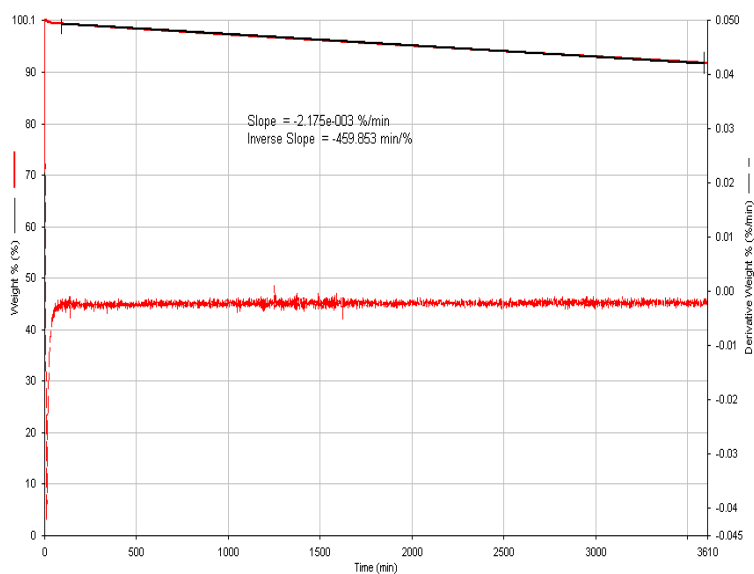


Figure 48: Decomposition of  $[C_4C_{1im}][MeCO_2]$  at  $120^\circ C$  and first derivative of the mass loss (red line).

The rate of mass loss for  $[C_4C_{1im}][MeCO_2]$  was linear over the observed time period (Figure 48). The time required for 1% weight loss of  $[C_4C_{1im}][MeCO_2]$  was 7.7 h. This could be significant, considering that ionic liquid pretreatment of lignocellulosic biomass is often in the range of hours. Moreover, ionic liquids are relatively expensive solvents and need to be reused many times to make an ionic liquid-based process economically viable.

The reduced thermostability of aliphatic ammonium ions was demonstrated by a more rapid weight loss of  $[C_4C_{1pyrr}][MeCO_2]$  compared to  $[C_4C_{1im}][MeCO_2]$  under the same conditions. Since  $[C_4C_{1pyrr}][MeCO_2]$  is high-melting with a temperature of  $> 50^\circ C$ , the temperature range where it is liquid and stable and therefore can be used as a solvent for reactions of biomass treatment must be small. It could be that this ionic liquid does not have a useful liquid range at all.

$T_{onset}$  was determined for selected ionic liquids using the step tangent method (Table 13). It shows that the ionic liquids that are stable at  $120^\circ C$  have a  $T_{onset}$  well above  $300^\circ C$ . For  $[C_4C_{1im}][MeCO_2]$ , the decomposition temperature was  $232^\circ C$ . This means that degradation occurs at least  $110^\circ C$  below the  $T_{onset}$ . Some experimenters have used  $[C_2C_{1im}][MeCO_2]$  at pretreatment temperatures up to  $160^\circ C$ <sup>136</sup> and

observed development of strong odour (personal communication Seema Singh, co-author of Arora *et al.*<sup>136</sup>). Therefore the instability of 1,3-dialkylimidazolium acetate ionic liquids over 100°C is an important message to the scientific community using ionic liquids for biomass processing. The influence of the moisture content remains to be investigated, as water might enhance the stability by reducing the nucleophilicity of the acetate anion. Because [C<sub>4</sub>C<sub>1</sub>im][MeCO<sub>2</sub>] is a liquid at room temperature, it can be useful for a number of low-temperature applications. However, its pronounced hygroscopicity needs to be taken into account, excluding this ionic liquid from applications that require strictly anhydrous conditions.

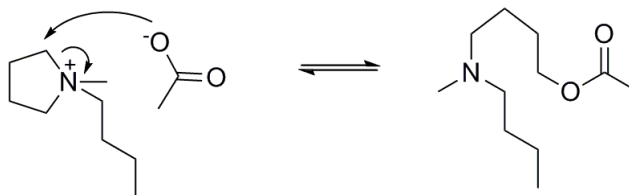
Table 13: Decomposition temperatures of selected ionic liquids

Ionic liquid	T <sub>onset</sub>
1,1-butylmethylpyrrolidinium acetate	194°C
1-butyl-3-methylimidazolium acetate	232°C
1-butyl-3-methylimidazolium methanesulfonate	349°C
1-butyl-3-methylimidazolium methyl sulfate	351°C
1-butyl-3-methylimidazolium hydrogen sulfate	358°C

#### 3.3.5.4 Decomposition mechanism for [C<sub>4</sub>C<sub>1</sub>pyrr][MeCO<sub>2</sub>]

An interesting observation was made during the drying of *N,N*-butylmethylpyrrolidinium acetate, [C<sub>4</sub>C<sub>1</sub>pyrr][MeCO<sub>2</sub>]. It was found that the ionic liquid started to boil under reduced pressure ( $\leq 5$  mbar) at around 100°C. The vapours would condense at the walls of the flask and, upon cooling, the liquid would solidify again. The NMR spectrum of the resolidified [C<sub>4</sub>C<sub>1</sub>pyrr][MeCO<sub>2</sub>] showed that it was mostly [C<sub>4</sub>C<sub>1</sub>pyrr][MeCO<sub>2</sub>], although the pungent smell of amine was also present. Kugelrohr distillation was used for an attempt to identify the volatile species. Unfortunately, the vacuum in the Kugelrohr apparatus was significantly lower than that of the Schlenk line, so boiling was only observed at 170°C. Nevertheless, a colourless liquid could be isolated in the second bulb, which was identified by liquid chromatography-mass spectrometry (LC-MS) and NMR spectroscopy as the ring-opened 4-

(*N,N*-methylbutyl)aminobutyl acetate (Scheme 15). Minor quantities of *N*-butylpyrrolidine were also present.



Scheme 15: Reversible decomposition of  $[C_4C_1\text{pyrr}][\text{MeCO}_2]$  at elevated temperatures and *in vacuo*.

Dealkylation of the cation has been established as a primary degradation route for ionic liquids of this type.<sup>119</sup> The low stability of *N,N*-butylmethylpyrrolidinium acetate corresponds well with the general trend that ionic liquid stability is strongly linked to the anion nucleophilicity.

It is suggested that the ring-opened product can revert to a salt upon reheating, which would explain the high purity of the ionic liquid even after elongated boiling, although the cyclisation of the isolated 4-*N,N*-methylbutylaminobutyl acetate was not demonstrated.

### 3.4 Summary

The Kamlet-Taft parameters of ionic liquids with a 1-butyl-3-methylimidazolium cation paired with various anions were determined. It was shown that hydrophilic 1,3-dialkylimidazolium ionic liquids have very similar polarisability, while the  $\beta$  value varies widely. This is in agreement with earlier postulates that, for this type of ionic liquid, the  $\beta$  parameter is mainly influenced by the anion.<sup>113</sup> An impact of the hydrogen-bond basicity on the  $\alpha$  parameter was also demonstrated, with a decrease in  $\alpha$  of up to one third for ionic liquids with very hydrogen-bond basic anions.

It was shown that  $\beta$  is the Kamlet-Taft parameter which is most sensitive to moisture, in agreement with the observation that water molecules hydrogen-bond more tightly to the anion than to the 1,3-dialkylimidazolium cation. The binding of water was shown to be tighter with more hydrogen-bond basic anions, demonstrated by the shift of the IR band of the OH stretching vibration.

A tighter ion pairing between strongly hydrogen-bond basic anions and the imidazolium cation was demonstrated by correlating the chemical  $^1\text{H}$ -NMR shift of the C-2 proton with the  $\beta$  parameter.

The hydrogen-bond basicity has also a profound effect on the stability and hygroscopicity of 1,3-dialkylimidazolium ionic liquids: the more hydrogen-bond basic the anion, the lower the stability of the ionic liquid and the more water was absorbed from the atmosphere.

Long-term stability under process relevant conditions was shown to be an issue for  $[\text{C}_4\text{C}_1\text{im}][\text{MeCO}_2]$  and particularly for  $[\text{C}_4\text{C}_1\text{pyrr}][\text{MeCO}_2]$ . It was shown that a major decomposition route of  $[\text{C}_4\text{C}_1\text{pyrr}][\text{MeCO}_2]$  is a nucleophilic attack of the anion on the cation, accompanied by ring opening.

## 4 Literature review: Solubilisation and pretreatment of lignocellulosic biomass with ionic liquids

### 4.1 Solubility of cellulose in ionic liquids

Cellulose is the most abundant component in lignocellulose. Only a few solvents are able to dissolve this crystalline polymer, for example *N*-methylmorpholine-*N*-oxide (NMO)<sup>137</sup> or concentrated phosphoric acid.<sup>47</sup> However, recently it was demonstrated that a range of ionic liquids, mostly containing 1,3-dialkylimidazolium as a cation, are effective cellulose solvents.<sup>74, 90, 131, 138-140</sup> Clear viscous solutions are obtained that show the typical behaviour of polymer solutions in general and cellulose solutions with other solvents in particular.<sup>141, 142</sup> Subsequently, homogenous chemical derivatisation of the cellulose dissolved in ionic liquids was also accomplished.<sup>143</sup> Cellulose dissolution is an industrially attractive application of ionic liquids due to the high solubility, improved stability of solvent and polymer (compared to the industrially used NMO) and the low toxicity (in the case of [C<sub>2</sub>C<sub>1</sub>im][MeCO<sub>2</sub>]).<sup>142</sup> Several patents have been granted in this field in the past few years.<sup>144</sup> The dissolved cellulose can be modified in solution or precipitated by adding water or protic organic solvents such as ethanol.<sup>74</sup> The crystallinity of the regenerated cellulose is reduced, which significantly accelerates its subsequent hydrolysis with cellulases.<sup>145</sup>

It has been observed that the ionic liquid anion plays an important role in determining an ionic liquid's ability to dissolve cellulose.<sup>74</sup> The cellulose dissolving ionic liquids contain anions that can form strong hydrogen bonds with hydroxyl groups, e.g. chloride, acetate, formate, dialkyl phosphates and dialkylphosphonates. NMR studies of ionic liquid solutions of glucose and cellobiose showed that the anion strongly

coordinates to the carbohydrate hydroxyl groups.<sup>146</sup> It has been shown that empirical Kamlet-Taft solvent descriptors can be used to predict cellulose solubility.<sup>129, 147</sup> Hydrogen-bond donating functionalities (e.g. hydroxyl groups) appear to reduce or prevent cellulose solubilisation.<sup>90, 148</sup> This observation indicates that the hydrogen-bond acidity, described by the  $\alpha$  parameter, needs to be below a certain threshold to obtain optimal cellulose solubility. Moisture also reduces cellulose solubility, probably for a similar reason.<sup>121</sup>

## 4.2 Solubility of lignocellulose in ionic liquids

Ionic liquids have also been used to dissolve lignocellulose. The partial dissolution of wood shavings in 1-butyl-3-methylimidazolium chloride was first described by Rogers and co-workers,<sup>149</sup> with the dissolution of wood saw dust and thermomechanical wood pulp in [C<sub>4</sub>C<sub>1</sub>im]Cl and in 1-allyl-3-methylimidazolium chloride being reported shortly afterwards.<sup>115</sup> Sun *et al.* were able to observe almost complete dissolution of 5 wt% softwood (southern yellow pine) and hard wood (red oak particles) in [C<sub>2</sub>C<sub>1</sub>im][MeCO<sub>2</sub>].<sup>117</sup> Solubilisation of switchgrass cross sections in [C<sub>2</sub>C<sub>1</sub>im][MeCO<sub>2</sub>] was followed by optical microscopy and it was shown that dissolution was complete after 2.5-3 h.<sup>150</sup> A link between the ability to dissolve cellulose and to partially or completely dissolve lignocellulose flour has been established by Zavrel *et al.* using light scattering (Figure 49).<sup>151</sup>

The rate of cellulase hydrolysis is proportional to the surface area of the substrate. Amorphous cellulose has a larger surface area and therefore glucose production is accelerated.<sup>152</sup> Decrystallisation of the cellulose portion of biomass after treatment with imidazolium chlorides and acetates was demonstrated by various groups.<sup>114, 115, 153</sup> Therefore, it is widely assumed that a major positive effect of ionic liquid pretreatment is the decrystallisation of cellulose.<sup>114</sup>

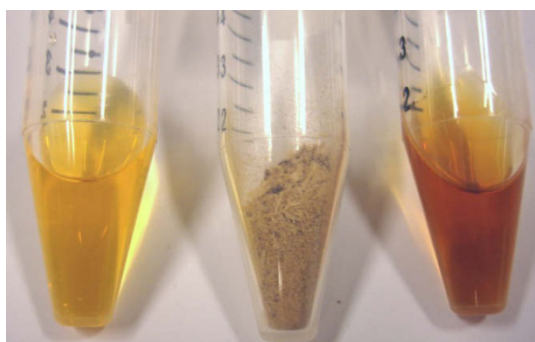


Figure 49: Dissolution of beech powder in  $[\text{C}_2\text{C}_1\text{im}][\text{MeCO}_2]$ <sup>151</sup>

Recently, an attempt was made to link the solvent properties of 1,3-dialkylimidazolium ionic liquids with their impact on lignocellulose, e.g. the extraction of lignin with the Hildebrand solubility parameter and the lignocellulose solubility with the Kamlet-Taft  $\beta$  parameter.<sup>114</sup> However, a numerical correlation was not attempted, probably due to the restricted number of 1,3-dialkylimidazolium ionic liquids investigated, the sole use of literature values and the lack of literature values for some of the important hydrophilic ionic liquids, such as  $[\text{C}_2\text{C}_1\text{im}][\text{MeCO}_2]$  and  $[\text{C}_4\text{C}_1\text{im}][\text{MeSO}_4]$ .

It has also been observed that adding water to  $[\text{C}_2\text{C}_1\text{im}][\text{MeCO}_2]$  prior to biomass pretreatment reduces the crystallinity index of the regenerated lignocellulose.<sup>154</sup> This indicates that water may also inhibit the solubilisation of lignocellulose. This is in agreement with the effect of water observed on cellulose solubility in ionic liquids.<sup>121</sup> However, it was also shown by others that it is not necessary to entirely dissolve biomass in this ionic liquid to improve the accessibility of cellulases to their substrate.<sup>135</sup>

### 4.3 Energy requirements for grinding lignocellulosic biomass

A grinding operation can increase the surface area of a lignocellulosic substrate, but it consumes significant amounts of energy.<sup>37</sup> For example, more than 10% of the energy contained in the biomass was used for grinding coarse air-dried willow chips to a particle size of  $<1$  mm.<sup>155</sup> The higher the ratio between initial and final particle size, the more



mechanical energy is required for the size reduction.<sup>156</sup> The energy input also depends on the type of biomass.<sup>156-158</sup>

The surface area of wood chips is small and diffusion of solvents and chemicals to the core of the chips is slow. A multi-scale model has been developed to help to optimise the energy consumption for aqueous acid pretreatment of grass lignocellulose by balancing grinding energy and pretreatment time (affected by diffusion of aqueous solvent and solubilised hemicellulose). The study predicted an optimum particle size of ca. 10 mm.<sup>158</sup> Therefore the effect of ionic liquid pretreatment on wood chips needs to be investigated in more detail.

Most reports on ionic liquid pretreatment or solubilisation of lignocellulose have focused on ground or even finely milled biomass. Very few reports have used wood chips as substrates. Incomplete dissolution of wood chips<sup>115</sup> and pine wood shavings<sup>149</sup> was reported by two early publications, but the issue was not addressed by most follow-up publications. One report showed that the particle size is one of the factors that influence the solubilisation of pine and oak wood in [C<sub>2</sub>C<sub>1</sub>im][MeCO<sub>2</sub>].<sup>117</sup> It was found that the use of larger particle sizes reduced the solubility of lignocellulose.

#### 4.4 Selective extraction of lignocellulose components during ionic liquid pretreatment

One way of characterising a lignocellulosic feedstock is to determine its composition. Different species contain varying amounts of cellulose, hemicellulose and lignin. The make-up of the hemicellulose fraction can vary. In *Miscanthus* and other herbaceous plants, the major hemicellulose sugar is xylose, while the prevailing hemicellulose sugar in pine is mannose. In addition, the biomass composition is often altered by chemical as well as biological pretreatment. Compositional analysis can give information about the effect of the pretreatment, e.g. if lignin, hemicellulose and/or cellulose are solubilised and to what extent.

In this study, standard protocols made publicly available by the US National Renewable Energy Laboratory (NREL) were used to assess the biomass composition. These protocols describe how the relative quantities of moisture and extractives, the quantities of the principal sugars (glucose, xylose, arabinose, mannose and galactose), lignin and an inorganic fraction called ash can be determined. This method was used in this work and is briefly described below.

The lignocellulosic biomass is first impregnated with concentrated acid to swell the cellulose. Subsequently, the cellulose and hemicellulose are hydrolysed at 120°C in dilute aqueous acid. The aqueous phase is analysed by HPLC for its carbohydrate content. The hydrolysate's absorption in the UV light is used to quantify the acid-soluble lignin. The acid-insoluble residue is dried and its weight determined. The acid-insoluble residue is then pyrolysed at 575°C and the remaining inorganic residue is quantified as ash content. The weight of the acid-soluble and acid-insoluble lignin combined is termed the Klason lignin content of the biomass.

#### *4.4.1 The effect of ionic liquid pretreatment on the composition of lignocellulosic biomass*

Data about the impact of ionic liquid pretreatment on the biomass composition have been published recently, at least for pretreatment with [C<sub>2</sub>C<sub>1</sub>im][MeCO<sub>2</sub>]. Both delignification and hemicellulose removal have been reported for various feedstocks after application of [C<sub>2</sub>C<sub>1</sub>im][MeCO<sub>2</sub>] (Table 14). Lignin solubilisation varied between 26% and 65%. The extent of hemicellulose removal varied between 22% and 83%. The variability is large in both cases, suggesting that both lignin and hemicellulose removal are susceptible to the pretreatment conditions, temperature, time and wood type, among others.

Table 14 Literature reports of lignin and hemicellulose removal by [C<sub>2</sub>C<sub>1</sub>im][MeCO<sub>2</sub>] pretreatment

Authors	Biomass	Temperature	Time	Lignin removed (%)	Hemicellulose removed (%)
Arora <i>et al.</i> <sup>136</sup>	Switchgrass	120°C	3 h	43	22
		160°C	3 h	65	83
Li <i>et al.</i> <sup>159</sup>	Switchgrass	160°C	3 h	38	53
Lee <i>et al.</i> <sup>114</sup>	Maple wood	130°C	1.5 h	52	26
Sun <i>et al.</i> <sup>117</sup>	Pine	110°C	16 h	26	Not measured
	Red oak	110°C	16 h	35	Not measured

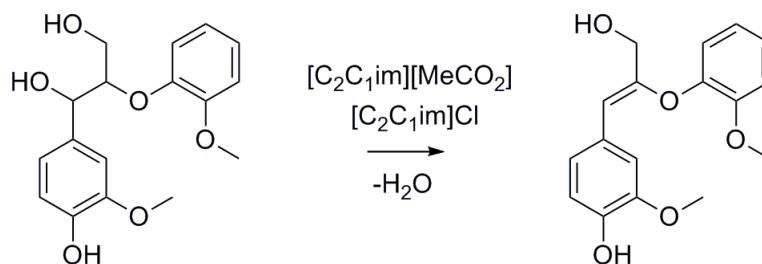
#### 4.4.2 Interactions of ionic liquids and lignin

The solubility of lignin preparations in ionic liquids varies substantially and seems to be considerably affected by the anion.<sup>75, 114</sup> 1,3-dialkylimidazolium ionic liquids with moderately to strongly hydrogen-bonding anions such as triflate, methyl sulfate and acetate anions have been reported to have particularly high lignin solubility. In a study using a Kraft pulp lignin, the solubilities of the preparation were highest in [C<sub>1</sub>C<sub>1</sub>im][MeSO<sub>4</sub>] and [C<sub>4</sub>C<sub>1</sub>im][MeSO<sub>4</sub>] at slightly elevated temperature (50°C), followed by [C<sub>4</sub>C<sub>1</sub>im][OTf].<sup>75</sup> However, various publications concluded that ionic liquids with methyl sulfate anions could not enhance the enzymatic digestibility of lignocellulosic biomass and the extraction of lignin was only modest.<sup>114, 136, 154, 160</sup> Ionic liquids with an aromatic side chain on the cation instead of an alkyl group have been designed to improve the lignin solubility - with moderate success.<sup>115</sup>

Tan *et al.* have demonstrated a very good recovery of lignin from sugar cane bagasse after treating the substrate with 1-ethyl-3-methylimidazolium alkylbenzenesulfonate [C<sub>2</sub>C<sub>1</sub>im][ABS] followed by a subsequent precipitation upon dilution.<sup>161</sup> [C<sub>2</sub>C<sub>1</sub>im][ABS] was synthesised using industrial grade sodium xylenesulfonate, which contains 26% of other anions (ethylbenzenesulfonate (13%),

cumenesulfonate (9%) and toluenesulfonate (4%)). It has been proposed by the authors of this publication that the aromatic nature of the alkylbenzenesulfonate anions is important for lignin solubility and a patent has been filed.<sup>161</sup> Lignin recovery after pretreatment with  $[\text{C}_2\text{C}_1\text{im}][\text{MeCO}_2]$  was achieved when it was extracted with a mixture of water and acetone and precipitated after the acetone was evaporated.<sup>75</sup>

Few studies on the structural changes of lignin during ionic liquid treatment have been published so far. The effect of ionic liquids on a lignin model compound featuring the most abundant linkage, the  $\beta$ -O-4 aryl ether, has been studied.<sup>162</sup> The compound was dissolved in  $[\text{C}_2\text{C}_1\text{im}]\text{Cl}$  and  $[\text{C}_2\text{C}_1\text{im}][\text{MeCO}_2]$  at 120°C. An  $\alpha,\beta$ -dehydration reaction was reported (Scheme 16), which is usually not observed under aqueous acidic or basic conditions. The conversion of the model compound was significantly faster in  $[\text{C}_2\text{C}_1\text{im}][\text{MeCO}_2]$  compared to the conversion in  $[\text{C}_2\text{C}_1\text{im}]\text{Cl}$ .



Scheme 16: Dehydration of the lignin model compound guaiacylglycerol- $\beta$ -guaiacyl ether in ionic liquids.<sup>162</sup>

A recent investigation of the residual lignin in  $[\text{C}_2\text{C}_1\text{im}][\text{MeCO}_2]$  pretreated maple wood with 2-dimensional NMR revealed various changes: increase of syringyl to guaiacyl unit ratio, decrease of the  $\beta$ -ether content (which are both signs of lignin depolymerisation), acetylation at the  $\gamma$ -position of the lignin subunit and deacetylation of xylan.<sup>163</sup>

The solubility of lignin in ionic liquids has been used for catalytic transformation of lignin into value-added chemicals. The catalytic oxidation of organosolv beech lignin in ionic liquids using molecular oxygen has been demonstrated by Stärk *et al.*<sup>72</sup> The main product was

2,6-dimethoxy-1,4-benzoquinone, besides vanillin, syringaldehyde and other oxidised lignin fragments. The fragments could be partially extracted into organic solvents.

## 4.5 Carbohydrates in ionic liquids

### 4.5.1 Carbohydrate depolymerisation

Before cellulose can be utilised as a substrate for fermentation it needs to be depolymerised into soluble components, ideally glucose. Glucose can be used by most fermentative microorganisms. The depolymerisation of cellulose to glucose is called saccharification and can be catalysed either enzymatically or chemically; both have been used in conjunction with ionic liquid pretreatment.

#### 4.5.1.1 Chemical depolymerisation in ionic liquids

Chemical hydrolysis is fast and the catalyst is considerably cheaper than enzymes. Performing the chemical hydrolysis of cellulose dissolved in ionic liquids has the advantage that the glycosidic bonds are more accessible to the acid catalyst. The *in situ* chemical hydrolysis of pure cellulose and the cellulose (and hemicellulose) contained in biomass has been attempted by various researchers.<sup>122, 164-166</sup> In most studies, a lignocellulose solubilising ionic liquid such as [C<sub>4</sub>C<sub>1</sub>im]Cl and catalytic amounts of a strong acid were used. Brønsted-acidic ionic liquids have also been used for this purpose. For example, one study accomplished the simultaneous dissolution and hydrolysis of cellulose in ionic liquids containing hydrogen sulfate anions.<sup>167, 168</sup>

The most comprehensive study of the chemical hydrolysis of lignocellulose by Sievers *et al.* used pine flour, [C<sub>4</sub>C<sub>1</sub>im]Cl and sulfuric acid.<sup>122</sup> Solubilisation of the cellulose and hemicellulose fractions was observed. Although the conversions were high, the yield of monomeric sugars was very low.<sup>122</sup> The addition of small quantities of water enhanced the monomer yield slightly, but larger amounts of water lowered it. This was probably due to a decrease of the cellulose

solubility. In addition, the sugars were partially transformed into degradation products such as HMF and furfural.

The two-sided role of water (required for hydrolysis but reduces cellulose solubility), led to the application of a modified strategy by Binder *et al.*<sup>164</sup> They dissolved cellulose and the carbohydrate fraction of corn stover with [C<sub>2</sub>C<sub>1</sub>im]Cl containing catalytic amounts of HCl. Water was added incrementally during the hydrolysis to maintain a balance between hydrolysis and solubility of the cellulose polymers (the shorter the polymer the more water was tolerated). Using corn stover as a substrate, the yield of glucose under optimised conditions was 70-80% and the HMF yield was below 10%. As an alternative to soluble acids, solid acid catalysts have been used in ionic liquids.<sup>169</sup> The best solid acid catalyst identified by this study achieved cleavage into short cellulose oligomers which could be precipitated upon dilution with water. However, another study showed that the acidic protons contained in the solid catalyst are released into the ionic liquid and that the hydrolysis rate is proportional to the H<sup>+</sup> concentration in the liquid.<sup>170</sup> This hampers effective separation of catalyst and ionic liquid for recycling and makes the use of a heterogeneous catalysis obsolete.

The anion-dependency of the glucose yield during chemical saccharification of cellulose was investigated by Binder *et al.*<sup>164</sup> While a number of ionic liquids containing chloride anions were effective in generating glucose from cellulose, the application of the ionic liquids [C<sub>2</sub>C<sub>1</sub>im][NO<sub>3</sub>], [C<sub>4</sub>C<sub>1</sub>mim][BF<sub>4</sub>], [C<sub>1</sub>C<sub>1</sub>im][Me<sub>2</sub>PO<sub>4</sub>] and [C<sub>2</sub>C<sub>1</sub>im][MeCO<sub>2</sub>] did not result in the formation of detectable amounts of glucose. For the first two ionic liquids, it was suggested that their inability to dissolve the polymer prevents access of the acid catalyst to the glycosidic bonds and thus hydrolysis. The latter two ionic liquids can dissolve cellulose, but the relatively high pK<sub>a</sub> values of dimethyl phosphoric acid (1.29<sup>171</sup>) and acetic acid (4.76) reduced the acidity (pK<sub>a</sub> (HCl) = -8, pK<sub>a</sub> (H<sub>3</sub>O<sup>+</sup>) = -2) to an extent that prevented detectable glucose production. In agreement, another group has observed inertness of the glycosidic bond in cellobiose against hydrolysis in [C<sub>2</sub>C<sub>1</sub>im][MeCO<sub>2</sub>] with added acid.<sup>170</sup>

#### 4.5.1.2 Enzymatic saccharification

Enzymatic saccharification is slow and the biological catalyst more expensive. However, the use of enzymes avoids the formation of sugar degradation products, thus increases the yield and decreases the formation of toxic sugar degradation products.

Several groups have therefore attempted to combine cellulose dissolution and enzymatic hydrolysis. However, it was observed that cellulases are deactivated by the hydrophilic ionic liquids needed for cellulose dissolution (e.g. [C<sub>4</sub>C<sub>1</sub>im]Cl). Deactivation occurs even at low concentrations of these ionic liquids (in mixtures with water), when cellulose is no longer soluble.<sup>91, 172, 173</sup> It was shown that the reduction was only partly due to enhanced viscosity and increased ionic strength.<sup>172, 173</sup> Screening for cellulases with higher tolerance towards cellulose dissolving ionic liquids led to the discovery of enzymes with improved stability.<sup>174, 175</sup> Nevertheless, the activity of these enzymes was significantly decreased in the presence of 30 vol% ionic liquid and higher.

This suggests that it might be best to conduct enzymatic hydrolysis of cellulose and hemicellulose after separating it from the ionic liquid liquor. Cellulose reprecipitated from ionic liquids is hydrolysed faster by cellulases than crystalline cellulose by cellulases.<sup>145, 172</sup> Enhanced absorption of enzymes onto regenerated cellulose was observed which is an indication that the surface area is increased.<sup>145</sup>

Various papers on the enzymatic saccharification of ionic liquid pretreated lignocellulose were also published in the past few years. The ionic liquids used for lignocellulose pretreatment are miscible with water and polar solvents (e.g. methanol, ethanol or a mixture of water and acetone)<sup>153</sup> and the solvents can be used to separate the biomass from the ionic liquid.

Generally, the accessibility of enzymes to the carbohydrate fraction is increased after ionic liquid pretreatment. Representative examples of glucose and xylose yields are listed in Table 15. Studies which used ball-milled wood samples are not included; fine milling improves cellulose digestibility significantly without a pretreatment,<sup>176</sup> however, the use of

fine powders as feedstock is not economical (see section 4.3).<sup>156</sup> Studies using 3,5-dinitrosalicylic acid (DNS) which is used for measuring the reducing sugar content were also not considered (e.g. Lee *et al.*<sup>114</sup>) because the assay is not specific for glucose. Glucose yields from lignocellulose are therefore often overestimated. The entries in Table 15 show that the glucose yields were higher than expected from untreated biomass. However, they were not quantitative under the conditions used.

Table 15: Saccharification yields from ionic liquid pretreated biomass reported in the literature. Glu: glucose, Xyl: Xylose.

Author	Biomass	Ionic liquid	Pretreatment conditions	Glu yield	Xyl yield
Doherty <i>et al.</i> <sup>154</sup>	Ground maple	[C <sub>4</sub> C <sub>1</sub> im][MeCO <sub>2</sub> ]	90°C, 24 h	74%	64%
		[C <sub>2</sub> C <sub>1</sub> im][MeCO <sub>2</sub> ]	90°C, 24 h	70%	64%
Li <i>et al.</i> <sup>176</sup>	eucalyptus	[AllylC <sub>1</sub> im]Cl	120°C, 5 h	15%	<i>n.d.</i>
Li <i>et al.</i> <sup>177</sup>	Wheat straw	[C <sub>2</sub> C <sub>1</sub> im][Et <sub>2</sub> PO <sub>4</sub> ]	130°C, 30 min	55%	<i>n.d.</i>

In addition, the saccharification yield after [C<sub>4</sub>C<sub>1</sub>im][MeCO<sub>2</sub>] pretreatment for various lengths of time has been correlated with the crystallinity index of the cellulose in the pulp and with the delignification.<sup>114</sup> Both curves were S-shaped. Doherty *et al.*, correlated the saccharification yield with the Kamlet-Taft parameter  $\beta$  of [C<sub>4</sub>C<sub>1</sub>im][MeSO<sub>4</sub>] and [C<sub>4</sub>C<sub>1</sub>im][MeCO<sub>2</sub>] mixtures.<sup>154</sup> A negative impact of water on the glucose yield was also reported by these authors.

#### 4.5.2 Other reactions of sugars in ionic liquids

A number of ionic liquids have high solubility for highly functionalised molecules such as carbohydrates,<sup>178, 179</sup> due to their high polarisability and due to the high hydrogen-bond basicity some provide.

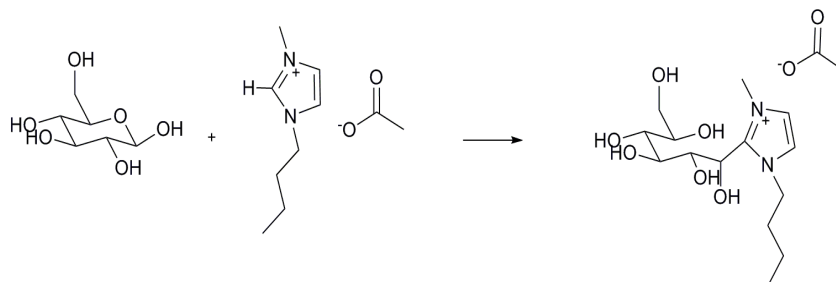
Recently, very good conversion of fructose to HMF in 1-methylimidazolium chloride, [C<sub>1</sub>Him]Cl, was reported.<sup>180</sup> The high yields are ascribed to the high solubility of fructose in this ionic liquid and the water-free environment provided. The production of HMF in an aqueous environment is a challenge, because HMF is transformed into more



stable products (details in section 1.7.2.2 on page 54). The reported HMF yield was high but not quantitative, probably due to the release of water during HMF formation.

More recently, high yielding transformation of glucose into HMF in ionic liquids was reported.<sup>181</sup> The metal catalyst  $\text{CrCl}_2$  showed superior selectivity compared to various other metal and protic acid catalysts. It is proposed that the  $\text{CrCl}_2$  facilitates the isomerisation of aldoses into ketoses, while the fairly anhydrous conditions in the ionic liquid stabilise the HMF. In a second study, HMF could be generated directly from cellulose, using catalytic quantities of  $\text{CrCl}_2$  in  $[\text{C}_2\text{C}_1\text{im}]\text{Cl}$  achieving yields of up to 54%.<sup>182</sup>

As a side-reaction, a condensation reaction between the 1,3-dialkylimidazolium cation in  $[\text{C}_4\text{C}_1\text{im}][\text{MeCO}_2]$  and the reducing ends of sugars and carbohydrate polymers was reported (Scheme 17).<sup>183</sup> The adduct slowly hydrolysed in the presence of water.



Scheme 17: Condensation of glucose with a 1,3-dialkylimidazolium cation under basic conditions.

## 5 The impact of the ionic liquid anion on the swelling and dissolution of wood chips

The energy consumption for particle size reduction prior to a pretreatment can be substantial, particularly for hardwood and softwood, but also for grasses.<sup>155</sup> Therefore, coarsely chipped biomass should be a more economical substrate. In contrast to this, almost all publications concerned with ionic liquid pretreatment of lignocellulosic biomass have used ground or even finely milled lignocellulose to date. Often, the biomass was also pre-dried in an oven. This chapter describes the impact that the choice of ionic liquid anion may have on the treatment of chip-sized biomass. The impact of biomass type, temperature and moisture was also examined.

### 5.1 Materials and Methods

Cellulose, fibrous, long was obtained from Sigma. HPLC grade methanol was from VWR. The ionic liquids used in this study were prepared as described in section 2.2.3.

#### 5.1.1 Preparation of wood chips

Pine (*Pinus radiata*) sapwood was obtained from a 15 year old tree harvested at Silwood Park, Ascot in June 2008. All wood was taken from material sawn from the main trunk. Wood chips of dimensions 10x10 x5 mm were prepared. Specimens were stored air-dried in plastic bags at normal temperature. The moisture content of the pine wood was 9% on an oven-dried basis. *Miscanthus x giganteus* internodes ( $\varnothing = 11$  mm) were cut into discs of 5 mm height to obtain *Miscanthus* chips. Willow branches of 2 cm diameter were cut into discs of 5 mm height. Square chips of 10 mm x 10 mm were excised from the discs with a saw. Both

*Miscanthus* and willow chips were used air-dried (which means 5-10% moisture content).

### 5.1.2 Swelling experiments

Wide-mouthed Pyrex glass culture tubes ( $\varnothing=25$  mm) with screw cap and Teflon lining were used as reaction vessels. Experiments were performed in triplicate to account for sample heterogeneity.

The ionic liquids were thoroughly dried before use at 40°C under vacuum and overnight, except for  $[\text{C}_4\text{C}_1\text{im}][\text{MeCO}_2]$  and  $[\text{C}_4\text{C}_1\text{im}][\text{Me}_2\text{PO}_4]$ , which were dried at 50°C and 100°C, respectively. The residual water content was 200 ppm for  $[\text{C}_4\text{C}_1\text{im}][\text{OTf}]$ , 400 ppm for  $[\text{C}_4\text{C}_1\text{im}][\text{MeSO}_4]$ , 3100 ppm for  $[\text{C}_4\text{C}_1\text{im}][\text{N}(\text{CN})_2]$ , 1200 ppm for  $[\text{C}_4\text{C}_1\text{im}][\text{Me}_2\text{PO}_4]$  and 1600 ppm for  $[\text{C}_4\text{C}_1\text{im}][\text{MeCO}_2]$ , according to Karl Fisher titration using the Titroline trace (Schott) with Hydranal Coulomat AG solution (Fluka), unless stated otherwise.

A wide-mouthed Schlenk flask with rubber septum was used as a soaking apparatus. A culture tube containing a single wood sample was inserted into a large wide Schlenk flask and the flask sealed with the septum. Ionic liquid (1.5-2 ml) was injected through the septum with a syringe until the chip was completely immersed in ionic liquid. Vacuum was applied until the chip appeared to be fully soaked (usually 2-3 min). The tube was tightly sealed and the sample stored at 4°C up for to 5 hours until preparation of the remaining samples was finished. Prepared samples were heated in an oven to the desired temperature. For measurements, the vials were removed from the oven and left to cool. The timing was stopped while samples were outside the oven (ca. 1 h). Trial experiments had shown that the swelling process at room temperature is extremely slow and therefore this was an acceptable simplification. The ionic liquid was drained from the wood chips and their surface wiped dry with a paper towel. The dimensions of the wood chips were measured with a calliper ( $\pm 0.01$  mm) and the samples placed back into the glass vial as quickly as possible.

For swelling under anhydrous conditions, pine wood chips were dried under reduced pressure at room temperature. The samples were handled in a glove box or under a nitrogen atmosphere at all times. 2 g of  $[\text{C}_4\text{C}_1\text{im}]\text{Cl}$  or 1.5 ml of dry  $[\text{C}_4\text{C}_1\text{im}][\text{Me}_2\text{PO}_4]$  and  $[\text{C}_4\text{C}_1\text{im}][\text{MeCO}_2]$  were transferred into Schlenk flasks, the pine specimens added and the Schlenk flask evacuated to allow filling of the wood pores. The samples were heated to 120°C for 15 h.

### 5.1.3 *Dissolution of pine flour*

Pine wood was ground for 5 min in a water cooled bench top grinding machine. Part of the flour was dried under vacuum at 50°C for 5 h. The dried pine flour was transferred into the glove box for storage. 30 mg of wet or dried wood flour was mixed with 1.0 g of  $[\text{C}_4\text{C}_1\text{im}][\text{MeCO}_2]$  or  $[\text{C}_4\text{C}_1\text{im}]\text{Cl}$ . The flasks were kept under a nitrogen atmosphere at all times. The mixtures were heated to 90°C while stirring.

### 5.1.4 *Pine chip processing*

Each pine chip was dried under vacuum at room temperature prior to the treatment. It was then immersed in  $[\text{C}_4\text{C}_1\text{im}][\text{MeCO}_2]$  with 7 wt% moisture content and incubated for 18 h in total. The surface was scraped with a blunt spatula to remove the softened material. At the end of the pretreatment, 10 ml methanol were added and the mixture stirred for 24 h. The suspension was centrifuged and the chip washed twice with 10 ml methanol. The chip was air-dried for the 3 days. The enzymatic saccharification was performed according to LAP "Enzymatic saccharification of lignocellulosic biomass" (NREL/TP-510-42629). Commercial enzyme preparations were used: Celluclast (*T. reesei* cellulase mix) and Novozyme 188 ( $\beta$ -glucosidase), which contain hemicellulolytic activity and allow the hydrolysis of hemicellulose polymers (both from Sigma). The samples were analysed for glucose and hemicellulose monomer release (xylose, arabinose, mannose and galactose, which are not resolved) on a Jasco HPLC system with refractive index detector equipped with an Aminex HPX-87H column

(Biorad). The mobile phase was 10 mM sulfuric acid, the column oven temperature 35°C, the flow rate 0.6 ml/min and the acquisition time 25 min. Glucose and hemicellulose yields were calculated based on the glucose and hemicellulose contents of the untreated biomass, respectively. It was assumed that the oven-dried pine wood was 46% cellulose and 27% hemicellulose, which is typical for this *Pinus radiata*.<sup>184</sup>

## 5.2 Results and Discussion

### 5.2.1 *Experimental design*

A range of ionic liquids containing the popular 1-butyl-3-methylimidazolium cation,  $[\text{C}_4\text{C}_1\text{im}]^+$ , was screened for their effect on wood chips. The cation was chosen because most ionic liquids reported to affect lignocellulose and its components used 1,3-dialkylimidazolium cations.

Air-dried wood was used because rigorous drying of biomass requires energy input, which is undesirable in terms of the energy efficiency of the process. The ionic liquids were dried under vacuum, to provide identical conditions in terms of moisture content, because ionic liquids have varying uptake rates and equilibrium contents for moisture (details on ionic liquid hygroscopicity in section 3.3.5.1, p. 115). The residual moisture contents of the ionic liquids are listed in the experimental section.

Wide-mouthed culture flasks with screw caps and Teflon liners were used as reaction vessels (Figure 67, p. 170), because they are guaranteed to withstand temperatures of up to 120°C. The Teflon lining also ensured chemical resistance and tight capping and the wide mouth was required to accommodate the wood chips. The effect on pine chips was monitored at three different temperatures, 60°C, 90°C and 120°C.

The initial observation was that, under the conditions used, none of the ionic liquids investigated was able to completely disintegrate the pine wood specimens. Instead, a more or less pronounced change of dimensions was observed. Hence it was decided to measure the specimens' size changes during the pretreatment.

The structure of wood results in anisotropic expansion when it is contacted with solvents. Therefore the specimens were cut in a specific orientation to obtain consistent results (Figure 50). The three dimensions were defined as follows. The expansion in direction *a*, also called tangential direction, was measured parallel to growth rings. Length *b* was

oriented perpendicular to the growth rings (radial direction) and direction *c* had axial orientation.

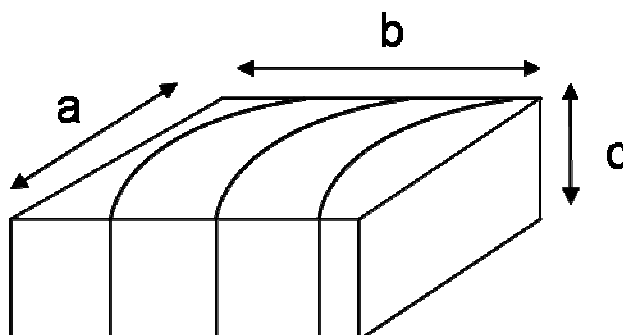


Figure 50: Schematic depiction of a pine chip with 3 growth rings. Definition of lengths *a* (tangential), *b* (radial) and *c* (axial) relative to growth rings.

The same definitions were applied to willow chips. Due to the rotational symmetry of *Miscanthus* chips, only two dimensions had to be defined: the radial length *a* (disc diameter) and the axial length *c* (disc height). Examples of biomass chips used in this study are shown in Figure 51.

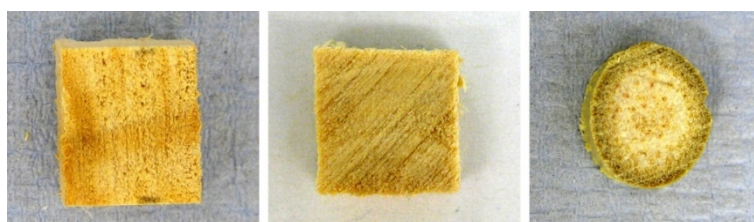


Figure 51: Wood chips used for swelling experiments: pine (left), willow (middle) and *Miscanthus* (right).

This study focussed on pine chips. Softwood is a wood type that is particularly recalcitrant to various pretreatment options and is therefore a challenging substrate.<sup>53</sup> Specimens with a mass of 0.15-0.20 g were immersed in 1.5-2.0 g of ionic liquid (ca. 10% biomass by weight). The ionic liquid was added under mild vacuum, which enabled the rapid filling of all the wood voids in the specimens. Trial experiments had shown that such a preparation was necessary to obtain uniform swelling across all orientations and more consistent results.

In general, solvents which have the capability to swell wood (e.g. water) increase the tangential length (length *a*) more than the other lengths. This is due to the orientation of the cellulose fibrils in the cell

walls, which are mostly oriented in axial direction.<sup>18</sup> When the solvents penetrate the lignocellulosic matrix and weaken the hydrogen bonds in the cellulose fibrils, allowing the polymer strands to move further apart and increase the fibrils' diameters. Expansion perpendicular to the growth ring (length  $b$ ) is usually less pronounced. This is due to the existence of radial cell pores, which restrict swelling. Swelling in the axial direction is usually least pronounced, due to the orientation of the cellulose fibrils. After immersing air-dried pine chips in water the profile shown in Figure 52 was obtained. The water increased the chips' lengths by ca. 5% in tangential direction, while they were expanded by ca. 3% in the radial and axial directions. The length of  $c$  (axial) was slightly variable and decreased slightly from 3% to 1%, indicating that some cell wall material is lost during incubation at 90°C.

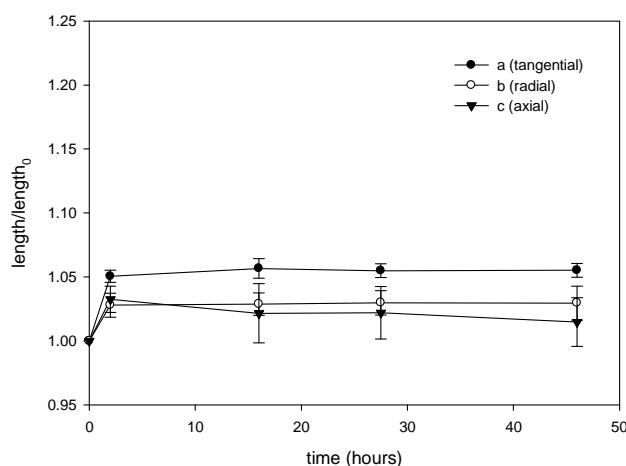


Figure 52: Swelling of pine chips incubated in distilled water at 90°C in the 3 directions defined in Figure 50.

### 5.2.2 Swelling and dissolution of pine wood chips

Three responses of air-dried pine chips to the incubation in dried ionic liquids were observed:

- non-swelling
- swelling, but non-dissolving
- dissolving



*Non-swelling:* the ionic liquids  $[\text{C}_4\text{C}_1\text{im}][\text{NTf}_2]$ ,  $[\text{C}_4\text{C}_1\text{im}][\text{PF}_6]$  and  $[\text{C}_4\text{C}_1\text{im}][\text{OTf}]$  induced no or very limited swelling in all directions, even at high temperatures and after prolonged heating. This could be due to poor interaction of the ionic liquid with the chemical functionalities of the cell wall polymers. An example is the ionic liquid  $[\text{C}_4\text{C}_1\text{im}][\text{OTf}]$ , whose profile is shown in Figure 53a.

*Swelling, but non-dissolving:* the ionic liquids  $[\text{C}_4\text{C}_1\text{im}][\text{N}(\text{CN})_2]$  and  $[\text{C}_4\text{C}_1\text{im}][\text{MeSO}_4]$  showed a second type of response: swelling of the wood specimens in all directions in the expected order:  $a > b > c$  (Figure 52b). The expansion was slightly more pronounced than the swelling in water. While water induced expansion of length  $a$  by 5% (at 60°C and 90°C), ionic liquids of the described type expanded  $a$  by 8%. This type of profile is a good example for favourable interactions of the ionic liquid with the cell wall material, but lacking the ability to disintegrate the cell wall matrix.  $[\text{C}_4\text{C}_1\text{im}][\text{N}(\text{CN})_2]$  is known to dissolve monomeric or oligomeric carbohydrates,<sup>185</sup> but cannot dissolve cellulose.<sup>127, 186</sup>

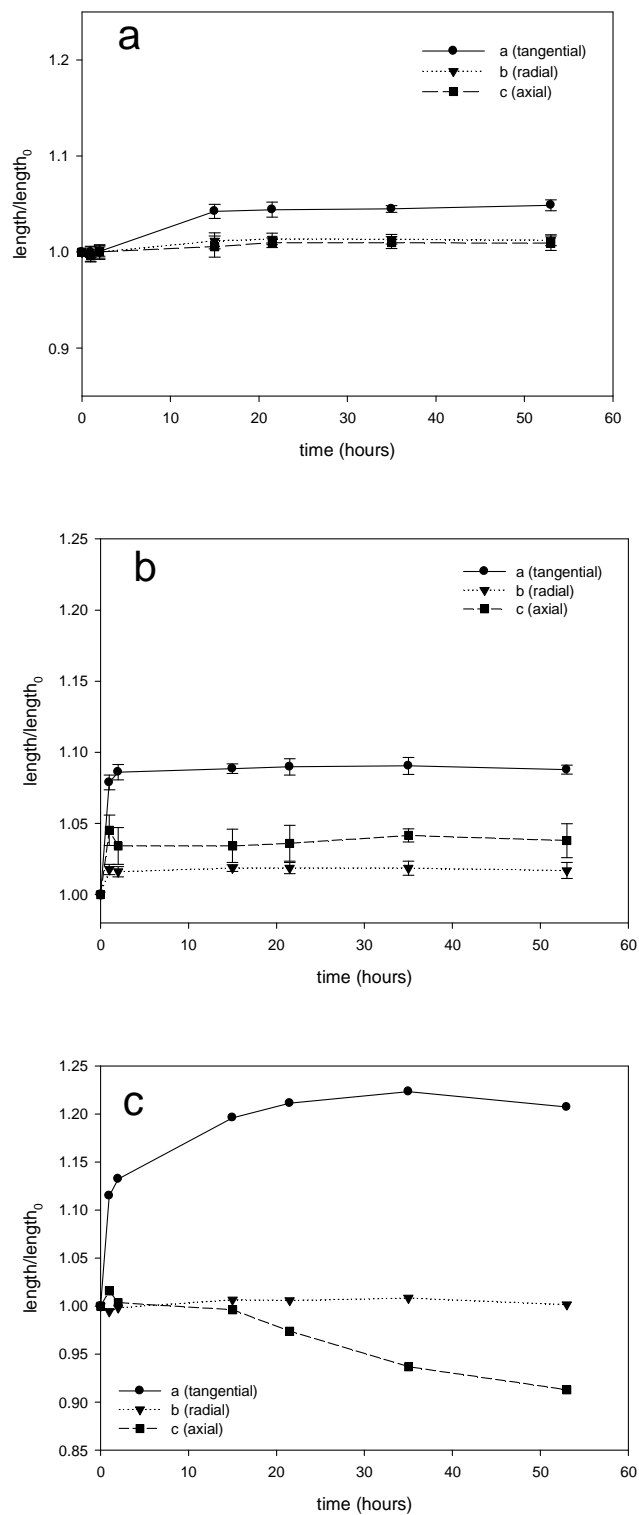


Figure 53: Swelling of pine chips treated at 120°C with: a [C<sub>4</sub>C<sub>1</sub>im][OTf], b [C<sub>4</sub>C<sub>1</sub>im][N(CN)<sub>2</sub>], c [C<sub>4</sub>C<sub>1</sub>im][MeCO<sub>2</sub>]. The expansion is relative to length

*Dissolving:* the ionic liquids  $[C_4C_{1im}][Me_2PO_4]$ ,  $[C_4C_{1im}]Cl$  and  $[C_4C_{1im}][MeCO_2]$  induced strong swelling in direction *a*, little change in *b* direction and significant shrinkage in *c* direction (Figure 53c). This type of profile is ascribed to the ability of the ionic liquid to disintegrate the cell wall matrix and to dissolve lignocellulosic material. The decrease of length *c* is ascribed to dissolution of cell wall material. The reason for the dissolution being mainly observed in the *c* direction could be a combination of two factors:

- A larger surface area of the *a*·*b* sides (rougher surface due to wood pores)
- A lower tendency of wood chips to swell in axial direction (swelling might compensate for removal of cell wall material by the ionic liquid)

Lignocellulosic components, particularly the carbohydrate polymers, are rich in hydroxyl groups. Ionic liquid anions that can strongly coordinate to these hydroxyl groups are able to weaken the hydrogen-bonding interactions in the wood matrix and allow the chips to expand. The lateral swelling of thin cross sections of poplar wood in  $[C_2C_{1im}][MeCO_2]$  has been observed under the microscope and used to incorporate nanoparticles into the cell walls of poplar.<sup>187</sup>

Some of the specimens incubated in  $[C_4C_{1im}][MeCO_2]$  at 120°C cracked along the growth ring. It is suggested that the strong swelling exerted considerable tension on the tissue structure of the wood, which ultimately led to breaking.

It was shown in Chapter 3 that  $[C_4C_{1im}][MeCO_2]$  is not entirely stable at 120°C (pp. 119). However, the decomposition at this temperature is slow (ca. 1% in 8 h) and although degradation products such as imidazole will be present and alter the composition of the solvent, it seems acceptable that this issue was neglected during this study. At lower temperatures, significantly less swelling and dissolution was observed, indicating that the higher temperature compensates for the gradual reduction of ionic liquid purity. For an industrial application the stability of the ionic liquids will be an important consideration and it may turn out that the

dialkylimidazolium acetates are not applicable at temperatures that allow swelling and dissolution of wood chips.

A summary of the 3 types of observed swelling behaviour of ionic liquids is given in Table 16.

Table 16: Classification of ionic liquids according to their impact on wood chips

Group	Solvents
Non-swelling	[C <sub>4</sub> C <sub>1</sub> im][NTf <sub>2</sub> ], [C <sub>4</sub> C <sub>1</sub> im][PF <sub>6</sub> ], [C <sub>4</sub> C <sub>1</sub> im][OTf]
Swelling but non-dissolving	Water, [C <sub>4</sub> C <sub>1</sub> im][N(CN) <sub>2</sub> ], [C <sub>4</sub> C <sub>1</sub> im][MeSO <sub>4</sub> ]
Swelling and dissolving	[C <sub>4</sub> C <sub>1</sub> im]Cl, [C <sub>4</sub> C <sub>1</sub> im][Me <sub>2</sub> PO <sub>4</sub> ], [C <sub>4</sub> C <sub>1</sub> im][MeCO <sub>2</sub> ]

The ionic liquids were clear and colourless prior to the treatment. During treatment with [C<sub>4</sub>C<sub>1</sub>im][MeCO<sub>2</sub>], the liquid became strongly coloured (Figure 54). Discolouration of the ionic liquid upon lignocellulose dissolution has been frequently observed,<sup>164</sup> suggesting that not only physical dissolution takes place, but also chemical modifications, resulting in the release of coloured compounds. These coloured compounds could stem from the degradation of the ionic liquid or be generated when lignin or carbohydrates are modified/degraded.

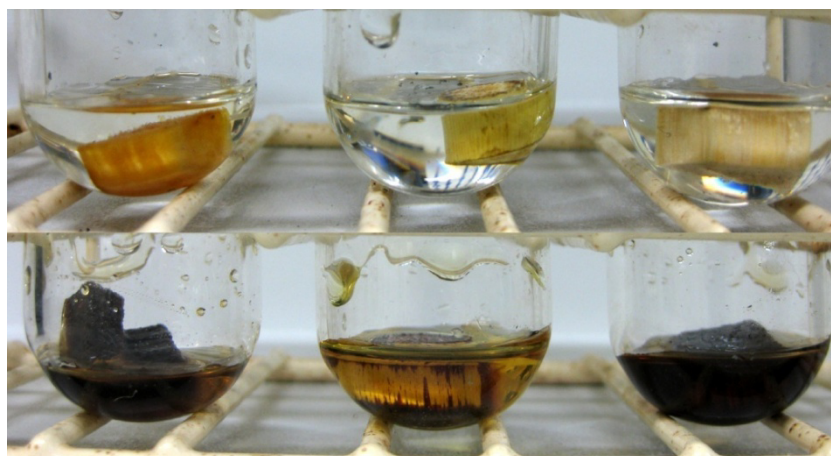


Figure 54: Wood chips (pine, *Miscanthus*, willow) immersed in [C<sub>4</sub>C<sub>1</sub>im][MeCO<sub>2</sub>]. Top: before pretreatment. Bottom: after 70 min pretreatment at 120°C.

Nevertheless, both Figure 53 and Figure 54 demonstrate that wood chips do not disintegrate easily - even in "wood-dissolving" ionic liquids. Although it was not necessarily expected that a homogenous solution would be obtained, it was anticipated that the chips would disintegrate.

### 5.2.3 *The influence of moisture on the disintegration of pine chips*

It has been shown that cellulose solubility is affected by moisture in the ionic liquids, and water in sufficient concentrations will inhibit or reverse the dissolution process.<sup>121</sup> Therefore, the effect of water wood chip solubility was explored in more detail. Dissolution of larger wood particles such as chips or shavings has only been investigated in a few studies. Sun *et al.* reported 92.6% dissolution of 0.5-1 mm pine particles in [C<sub>2</sub>C<sub>1</sub>im][MeCO<sub>2</sub>] at 110°C after 16 h.<sup>117</sup> These particles had been dried at 90°C overnight prior to the dissolution and vigorous stirring had been applied.

It is possible that the lignocellulose dissolution may also be inhibited by water and may be responsible for the reduced solubility of wood chips. Moisture can be introduced by the biomass and by the ionic liquid. Biomass contains significant amounts of moisture, 8-15 wt% when air-dried, and more than 50 wt% when freshly harvested. In addition, all ionic liquids are more or less hygroscopic.<sup>96</sup> Ionic liquids such [C<sub>4</sub>C<sub>1</sub>im][MeCO<sub>2</sub>] or [C<sub>4</sub>C<sub>1</sub>im][Me<sub>2</sub>PO<sub>4</sub>] can absorb large amounts of moisture when exposed to air (demonstrated in section 3.2.2 of this study). Lee *et al.* could not observe dissolution of wood particles of 250 µm in [C<sub>2</sub>C<sub>1</sub>im][MeCO<sub>2</sub>] at slightly lower temperature (90°C) but longer incubation time (24 h).<sup>114</sup> No drying of the biomass or the ionic liquid is reported, suggesting that moisture may be present in the pretreatment liquor. This shows that investigating the water sensitivity of the swelling process is important.

In order to test the hypothesis that moisture inhibits the disintegration of wood chips, pretreatment of thoroughly dried wood specimens was carried out. The samples were handled under a nitrogen atmosphere at all times to prevent moisture uptake during incubation. The pine cubes

were dried under high vacuum at room temperature, immersed in the dry ionic liquids and the impregnation with liquid was aided by evacuating the sample vial. The temperature was then raised to 120°C.



Figure 55: Dry pine specimens treated at 120°C for 15 h with  $[\text{C}_4\text{C}_1\text{im}][\text{Me}_2\text{PO}_4]$  (left),  $[\text{C}_4\text{C}_1\text{im}][\text{MeCO}_2]$  (middle) and  $[\text{C}_4\text{C}_1\text{im}]\text{Cl}$  (right). The specimen in the middle is a meshed pine chip.

Interestingly, the performance of  $[\text{C}_4\text{C}_1\text{im}][\text{MeCO}_2]$  improved greatly under these conditions, resulting in softening and disintegration of the pine specimen at 120°C in less than 15 hours. To demonstrate that the reduction of the moisture content was responsible for the improved disintegration, the samples were exposed to air. It was found that the structure rehardened (Figure 55). Interestingly, dried pine specimens treated with dried  $[\text{C}_4\text{C}_1\text{im}][\text{Me}_2\text{PO}_4]$  and  $[\text{C}_4\text{C}_1\text{im}]\text{Cl}$  remained intact during pretreatment and no softening was observed.

An exemplary calculation shows that the air-dried biomass introduced the greater part of the moisture into the system. Measurement of the water content of  $[\text{C}_4\text{C}_1\text{im}][\text{Me}_2\text{PO}_4]$  and  $[\text{C}_4\text{C}_1\text{im}][\text{MeCO}_2]$  (before adding wood chips) showed that 1.5 ml ionic liquid contained 2.1 mg and 2.5 mg water, respectively. The pine chips contained 9 wt% water. A typical wood specimen of 150 mg would therefore add 14 mg water. It was also shown that even wood chips which have been dried under vacuum increase the water content of the ionic liquid substantially, as shown in Figure 56.

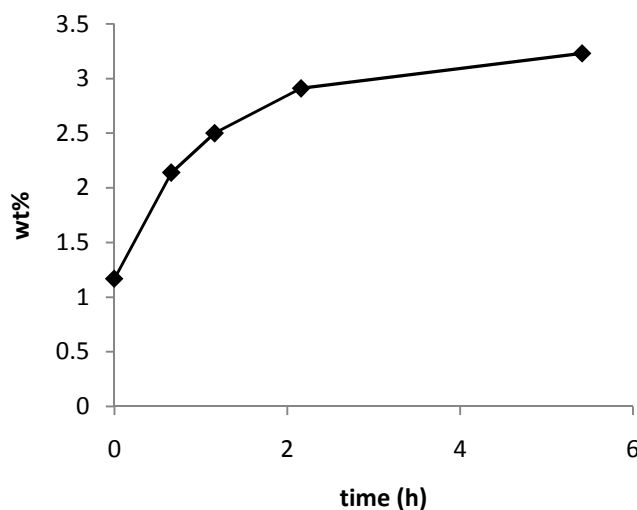


Figure 56: The water content of  $[\text{C}_4\text{C}_{1\text{im}}][\text{MeCO}_2]$  during the swelling of a dried willow chip at  $120^\circ\text{C}$  determined by Karl Fischer titration.

These results suggest that varying moisture contents of ionic liquids and/or biomass may be responsible for the large variability of wood solubility in  $[\text{C}_2\text{C}_{1\text{im}}][\text{MeCO}_2]$  reported in the literature.<sup>114, 117</sup> Therefore, it is advised to monitor the water content during dissolution experiments. This water-sensitivity is also of particular significance for the practical application of ionic liquids in biomass processing, as the feedstock will contain a proportion of bound water and, when freshly harvested, appreciable quantities of free water. An industrial process that is based on dissolving lignocellulose in ionic liquids will have to deal with additional energy requirements for drying the substrate as well as the ionic liquid, which may hamper the industrial viability of ionic liquid pretreatment.

#### 5.2.4 The influence of the anion basicity

The observation that the ionic liquid anion had a profound impact on the swelling (Figure 57), triggered the attempt to correlate the chip swelling with the Kamlet-Taft parameter  $\beta$ , which is a property of the anion in the in case of 1,3-dialkylimidazolium ionic liquids (shown by Crowhurst *et al.*<sup>113</sup>, see also section 3.3.3).

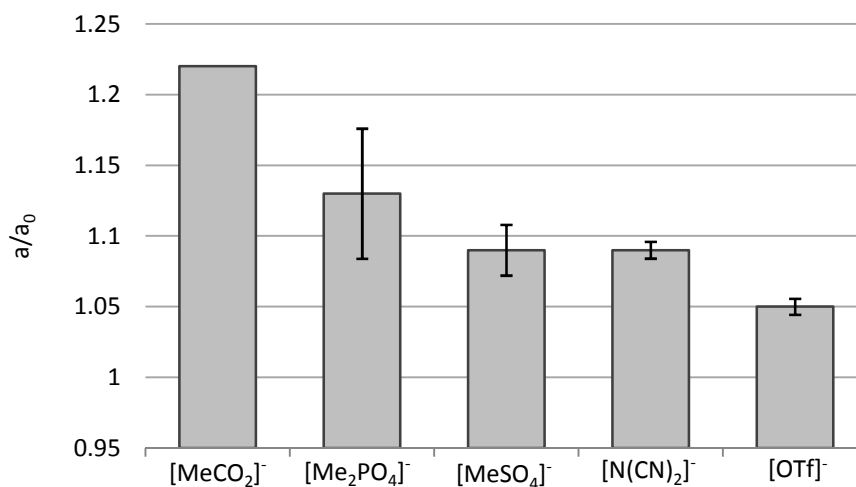


Figure 57: Swelling of pine chips after immersion in various 1-butyl-3-methylimidazolium ionic liquids. The relative expansion in tangential direction ( $a/a_0$ ) is shown, which is the ratio between the length after swelling ( $a$ ) and the length before immersion of the chips in ionic liquid ( $a_0$ ). The expansion shown was measured after 35 h incubation at 120°C.

The plot of the  $\beta$  value against the swelling in the various dimensions is shown in Figure 58. For the tangential length  $a/a_0$ , a higher  $\beta$  parameter coincided with a more pronounced swelling in the longitudinal direction  $a$ . A regression line was fitted with the equation  $a/a_0 = 0.153\beta + 0.978$  and  $R^2 = 0.760$  and  $p = 0.054$ . The regression analysis shows that a correlation is possible, although the  $p$  value is relatively high. The correlation might be improved by increasing the number of ionic liquids included in the correlation.



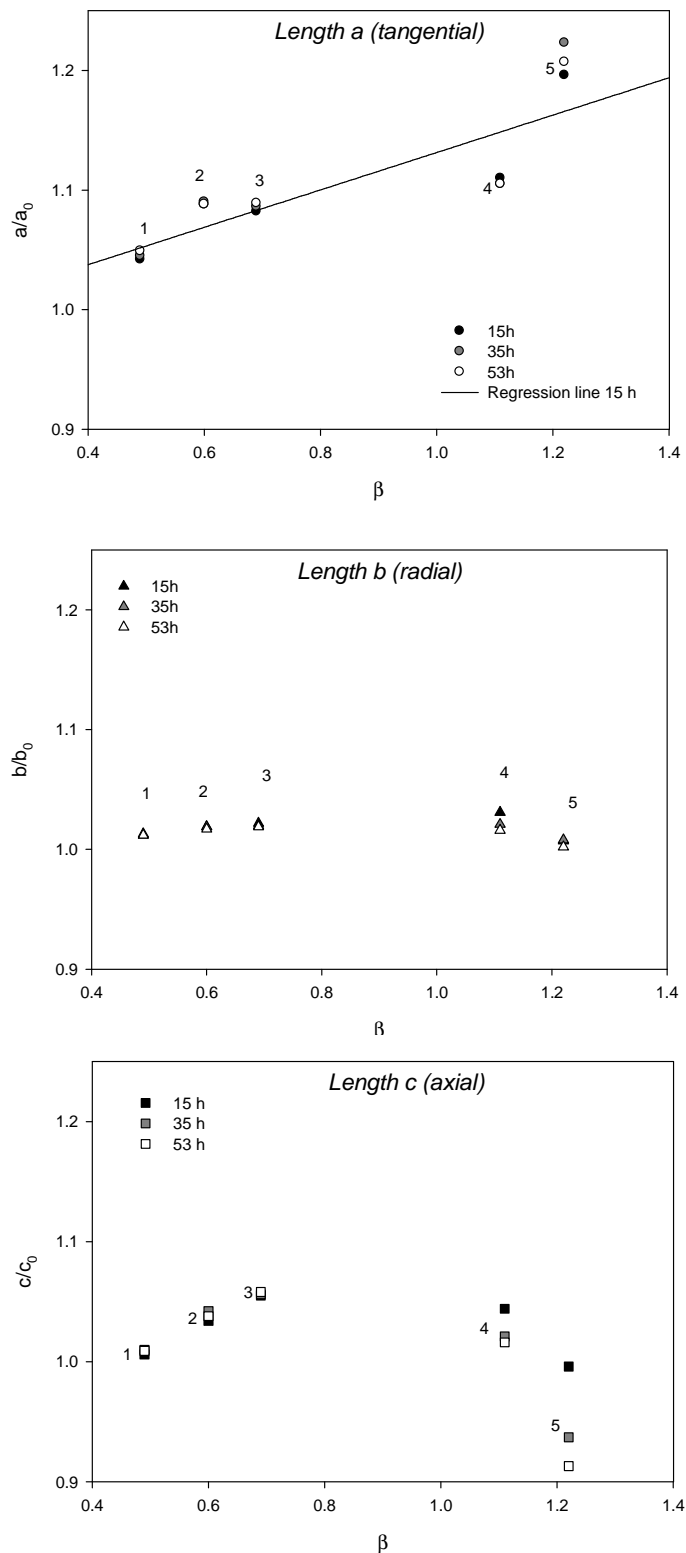


Figure 58: Correlation of pine chip swelling and dissolution in the tangential (a), radial (b) and axial (c) direction in 1-butyl-3-methylimidazolium ionic liquids at 120°C with the Kamlet-Taft parameter  $\beta$ . Expansion and shrinkage at 3 time-points is shown.

---

Anions 1 - [OTf], 2 - [N(CN)<sub>2</sub>], 3 - [MeSO<sub>4</sub>], 4 - [Me<sub>2</sub>PO<sub>4</sub>], 5 - [MeCO<sub>2</sub>].  $R^2 = 0.760$  and  $\rho = 0.054$  for the regression line shown for  $a/a_0$ .

Figure 58 also shows the swelling of length  $b$  plotted against the  $\beta$  parameter. The swelling in direction  $b$  was small, regardless of the hydrogen-bond basicity of the ionic liquid. A correlation between length  $b$  and the polarity parameter  $\beta$  does not reveal much information. A small decrease of length  $b$  was seen in the case of the application of [C<sub>4</sub>C<sub>1</sub>im][Me<sub>2</sub>PO<sub>4</sub>], suggesting that dissolution prevails over expansion for this ionic liquid.

The correlation between length  $c$  and  $\beta$  was more complex. For ionic liquids with a lower  $\beta$  value, expansion of  $c$  seemed to correlate with an increased  $\beta$  value. However, for ionic liquids with  $\beta > 1.0$ , less expansion was seen after short incubation times. More significantly, a reduction of the axial length  $c$  was observed. The reduction of the axial length was time-dependent. The longer the chips were incubated in the ionic liquids [C<sub>4</sub>C<sub>1</sub>im][Me<sub>2</sub>PO<sub>4</sub>] and [C<sub>4</sub>C<sub>1</sub>im][MeCO<sub>2</sub>] the more length  $c$  decreased. For the ionic liquid with the highest  $\beta$  value, [C<sub>4</sub>C<sub>1</sub>im][MeCO<sub>2</sub>], a reduction by 10% compared to the initial air-dried length was observed.

In summary, these data demonstrate that  $\beta$  has an important effect on both the swelling and the dissolution of pine wood chips. A high  $\beta$  value coincides with increased swelling in the tangential direction and with size reduction in the axial direction. The correlation between wood chip swelling and the  $\beta$  parameter is likely to be due to the high abundance of hydroxyl groups in the biomass. The hydroxyl groups are coordinated by ionic liquid anions, thus weakening intermolecular hydrogen-bonds and allowing expansion. At high  $\beta$  values, the interaction with the hydroxyl groups is so strong that the solubility of the carbohydrate polymers is high enough to cause partial dissolution of the wood chips.

### 5.2.5 *The influence of the pretreatment temperature*

Expansion in the tangential direction (length  $a$  in Figure 50) was chosen as the principal indicator to measure the temperature

dependence of swelling. Pine chips were treated with ionic liquid at three temperatures 60°C, 90°C and 120°C (Figure 59).

Generally, the ionic liquid anion had a significant impact on the temperature-dependency of wood chip swelling. [C<sub>4</sub>C<sub>1</sub>im][OTf] had the lowest  $\beta$  value (0.49) among the ionic liquids tested and was a poor swelling agent. It did not induce swelling at 60°C or 90°C and very limited swelling at 120°C. This could be assigned to the high thermal energy enabling the ionic liquid to interact more favourable with the wood matrix (allowing intercalation into the material) than at lower temperature. It could also mean that the thermal energy is high enough to allow reactions between the lignocellulosic material (possibly the lignin) and the ionic liquid, weakening the structure and allowing its expansion. To resolve this further investigations would be required.

The ionic liquids with mid-range  $\beta$  values, [C<sub>4</sub>C<sub>1</sub>im][N(CN)<sub>2</sub>] and [C<sub>4</sub>C<sub>1</sub>im][MeSO<sub>4</sub>] (0.60 and 0.67 respectively), were able to swell the wood by *ca.* 8%. This exceeded the swelling induced by water, which expanded air-dried pine chips by 5% at 60°C and 90°C. Interestingly, the maximal specimen swelling achievable in [C<sub>4</sub>C<sub>1</sub>im][N(CN)<sub>2</sub>] and [C<sub>4</sub>C<sub>1</sub>im][MeSO<sub>4</sub>] was not affected by temperature.

The chip swelling in the ionic liquids [C<sub>4</sub>C<sub>1</sub>im][Me<sub>2</sub>PO<sub>4</sub>] and [C<sub>4</sub>C<sub>1</sub>im][MeCO<sub>2</sub>] exceeded 8%, correlating well with their high  $\beta$  values of 1.12 and 1.20, respectively. The swelling in these ionic liquids was temperature dependent. [C<sub>4</sub>C<sub>1</sub>im][MeCO<sub>2</sub>] swelled the specimens by 15% at 90°C. At 120°C, the induced expansion was more than 20%.

At low temperature, the swelling was slower for ionic liquids, although significant differences could be observed. Although the ionic liquids [C<sub>4</sub>C<sub>1</sub>im][Me<sub>2</sub>PO<sub>4</sub>] or [C<sub>4</sub>C<sub>1</sub>im][MeSO<sub>4</sub>] were able to swell the chips even at low temperature, the time for reaching the maximal swelling was particularly long (> 60 h). This ascribed to the relatively high viscosity of these liquids (*e.g.* 700 mPa s for [C<sub>4</sub>C<sub>1</sub>im][Me<sub>2</sub>PO<sub>4</sub>] at 20°C)<sup>83</sup>. The size of the anion could also play a role, as the ionic liquid ion pairs must not only diffuse into the wood pores but also into the dense cell wall matrix (and the cellulose fibrils) to interact with the available hydroxyl groups.

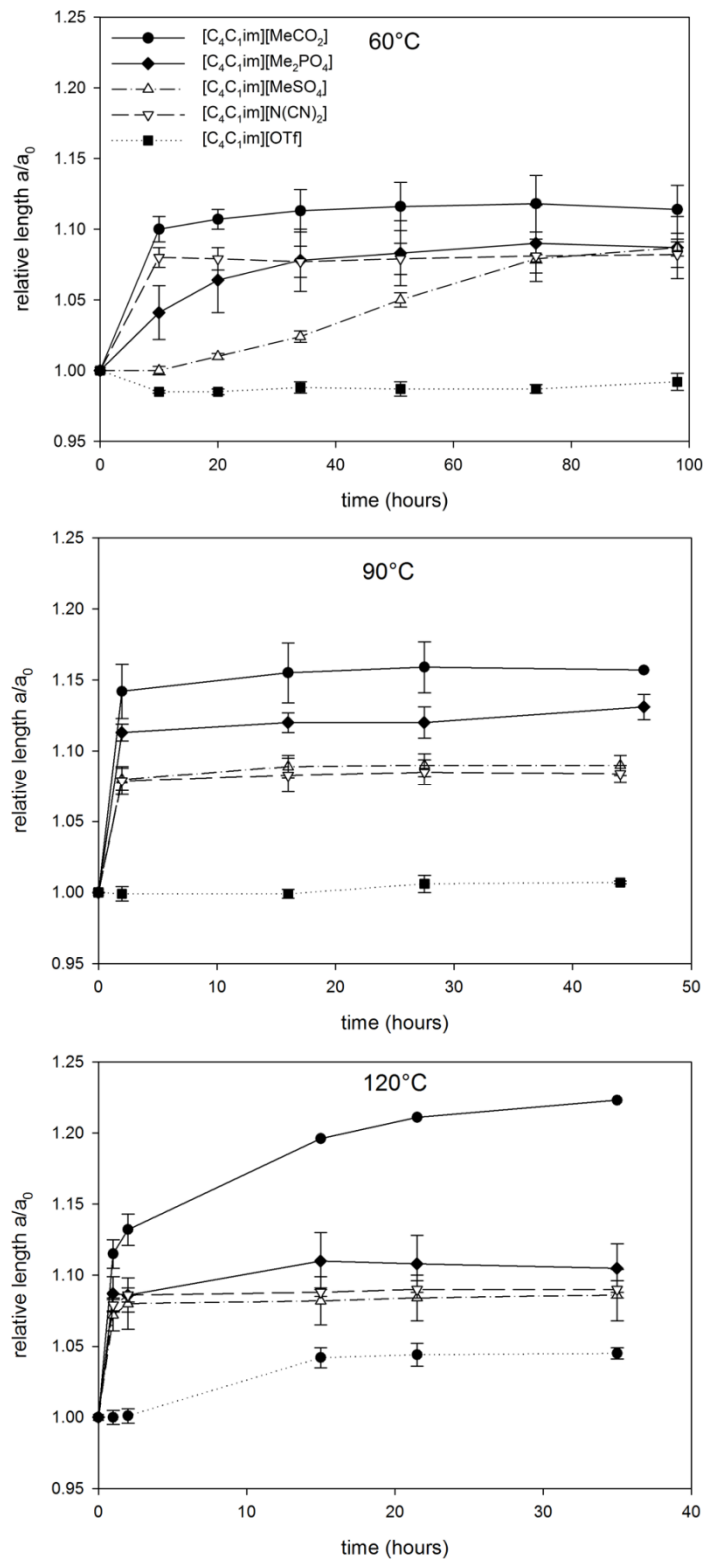


Figure 59: Expansion of pine chips immersed in 1-butyl-3-methylimidazolium ionic liquids at various temperatures (60, 90 and 120°C) in the direction tangential to the growth rings. The expansion depends on the ionic liquid and the temperature.

### 5.2.6 Wood chip regeneration

The effect of regeneration on the chip dimensions from  $[\text{C}_4\text{C}_1\text{im}][\text{MeCO}_2]$  was investigated in more detail. A pine chip was pretreated for 18 h at 120°C and the water content of the ionic liquid prior the treatment was 7 wt%. The swelled wood chip was contacted with methanol to yield regenerated lignocellulose (Figure 60). It was observed that some cell wall material had gone into solution and was regenerated as flakes. Subsequently the chip and the flakes were washed and dried on the laboratory bench and contacted with cellulose and hemicellulose hydrolysing enzymes to measure the sugar release after pretreatment and the impact of the enzymatic treatment on the dimensions of the wood specimen.



Figure 60: Pine chip regeneration in methanol after 18 h treatment with  $[\text{C}_4\text{C}_1\text{im}][\text{MeCO}_2]$ .

The length changes of the undissolved wood chip portion (after washing and air-drying) are shown in Figure 61. During the treatment with  $[\text{C}_4\text{C}_1\text{im}][\text{MeCO}_2]$ , the typical expansion in the tangential direction  $a$  and a decrease of the axial length  $c$  was observed. The subsequent regeneration combined with drying decreased the lengths of the lateral directions  $a$  and  $b$ . Length  $a$  was reduced to 70% of the original air-dried size, and length  $b$  was reduced to 65%. The length of the axial length  $c$  decreased during pretreatment, but was hardly affected by regeneration and drying. It is concluded that the 10% reduction in  $c$  are mainly due to solubilisation of cell wall material. The prolonged immersion in water during the saccharification led to a renewed swelling, which is ascribed to the general ability of water to interact with dried lignocellulose. Length  $c$  also slightly decreased during the saccharification, which is ascribed to

action of the hydrolytic enzymes solubilising cell wall polymers from the surface of the chip.

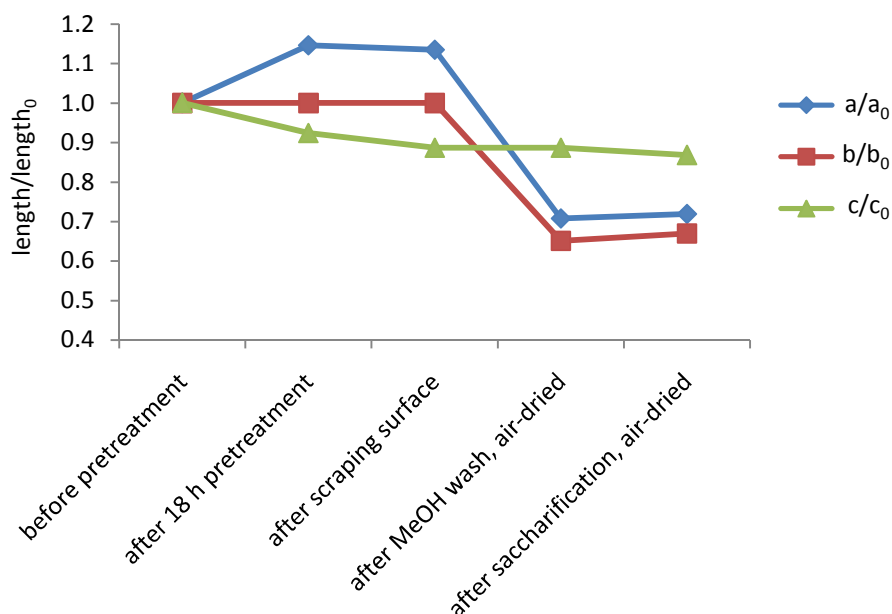


Figure 61: The dimensions of pine chips over the course of ionic liquid pretreatment with [C<sub>4</sub>C<sub>1</sub>im][MeCO<sub>2</sub>] at 120°C followed by regeneration and washing in methanol, drying and incubation with cellulose and hemicellulose hydrolysing enzymes.

That a fraction of the cell wall material went into solution during the treatment and the enzymatic saccharification is supported by the weight changes observed (Table 17). The weight of the chip was reduced by 10% during treatment and additional 15% during saccharification.

Table 17: Weight changes of a pine chip before and after treatment with [C<sub>4</sub>C<sub>1</sub>im][MeCO<sub>2</sub>] (oven-dried weight, ODW)

Stage	Chip weight (mg, ODW)	%
Untreated chip	190	100.0
Treated chip (washed and dried)	171	90.0
Chip after saccharification	140	74.0

The reason for the reduction of length *a* and *b* could be partially due to solubilisation, but also due to the collapse of the wood pores. A collapse of the porous structure has been observed for switchgrass (on a microscopic scale).<sup>150</sup> Interestingly, other researchers could not observe

significant changes in the pore size of eucalyptus flour treated with  $[\text{C}_2\text{C}_1\text{im}][\text{MeCO}_2]$  at  $120^\circ\text{C}$  for 3 h.<sup>163</sup> This could be due to the different type of biomass, the shorter pretreatment time or a higher water content in the system.

The dried pine specimen was also subjected to enzymatic saccharification. The amount of glucose released from the regenerated wood chip was only moderate. 8.5% of the original glucose was released by the enzymes and 10.1% of the hemicellulose. Although these data indicate that the sugar yield is increased by the ionic liquid treatment, the compact structure of the chip (which might have been enhanced by the collapse of the wood pores) seems to have prevented diffusion of the enzymes to the inside, preventing effective disintegration of the chip.

### 5.2.7 *The effect of the biomass type*

The swelling and dissolution profiles that have been presented so far were obtained with pine specimens. For comparison, the swelling of other lignocellulose feedstocks, willow chips (a hardwood) and *Miscanthus* discs (a perennial grass), was also investigated. The ionic liquid  $[\text{C}_4\text{C}_1\text{im}][\text{MeCO}_2]$  was used for the comparative study, as it has been identified as the most effective swelling agent in earlier experiments. The procedure was analogous to the treatment of pine chips, the ionic liquid had been dried *in vacuo* and the wood was used air-dried.

The swelling profile of willow chips (Figure 62) displayed the same features as observed for the swelling of pine chips (see Figure 53c). The expansion of length *a* was large, while dissolution became apparent in direction *c*. However, the swelling of willow was more pronounced. After 40 h, length *a* had expanded by 47%, which is twice as much as observed for pine chips, and length *b* by 15% (compared to 0% found for pine). The reduction in *c* was similar to the one seen for pine chips: *c* decreased by 8% within 40 h regardless of the wood type.

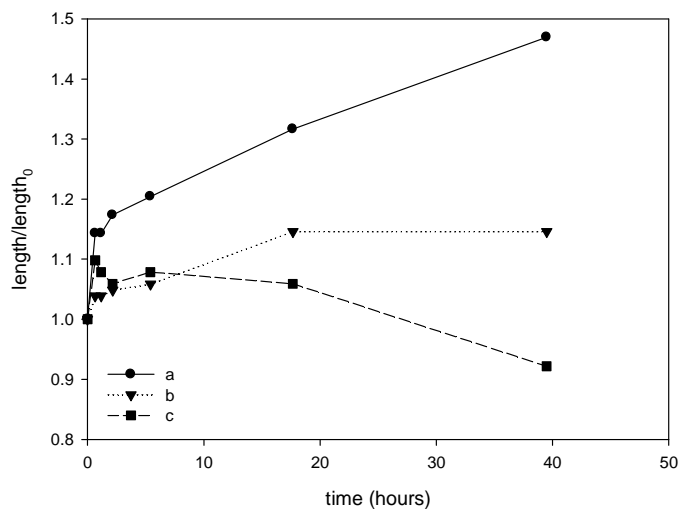


Figure 62: Swelling profile of a willow chip immersed in  $[C_4C_{1im}][MeCO_2]$  containing 1.2 wt% moisture at  $120^\circ C$ .

In contrast, the swelling/dissolution profile of *Miscanthus* chips was different (Figure 63). The disc diameter *a* was hardly affected by the ionic liquid treatment. A reduction in axial direction *c* was also not observed. Nevertheless, after 6 h, the *Miscanthus* chips disintegrated, preventing further measurements of the chip size but also demonstrating that the ionic liquid had a profound effect, though not visible as expansion or size reduction.

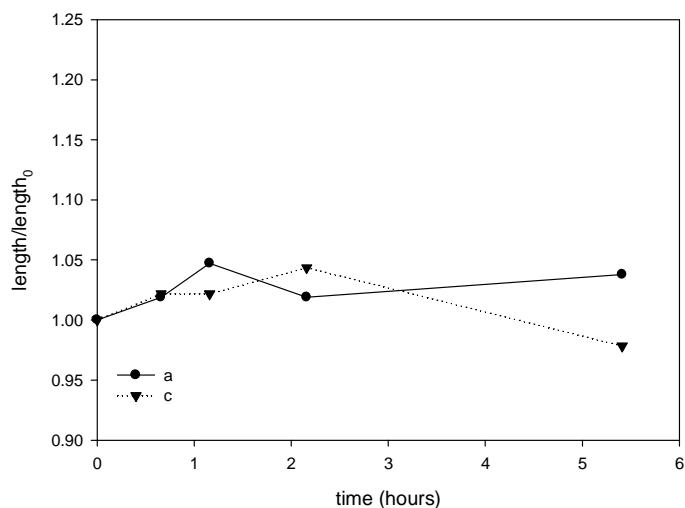


Figure 63: Swelling profile of a *Miscanthus* chip immersed in  $[C_4C_{1im}][MeCO_2]$  containing 1.2 wt% moisture.



It is suggested that the thin walls of the inner pith of *Miscanthus* stems, can deform relatively easily, particularly when the wall matrix is softened by a cellulose solubilising ionic liquid. This deformation could have accommodated the swelling of the cell walls in the pith as well as in the more rigid outer ring and therefore an over-all expansion to the outside was not detected. Such deformation of parenchyma cells has been observed for switchgrass cross sections (Figure 64).<sup>150</sup> In addition, this study reported disintegration of the cell wall structure in the ionic liquid [C<sub>2</sub>C<sub>1</sub>im][MeCO<sub>2</sub>] within a couple of hours for cross sections of the structurally and compositionally similar switchgrass.

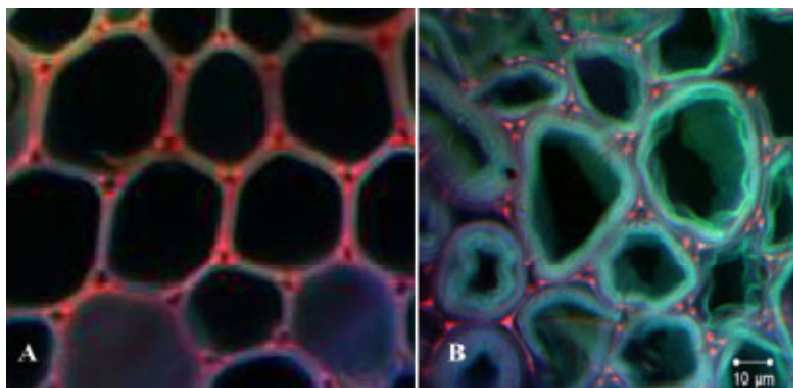


Figure 64: Deformation of switchgrass cell walls in [C<sub>2</sub>C<sub>1</sub>im][MeCO<sub>2</sub>] observed with fluorescence confocal microscopy. A: before treatment, B: after 10 min treatment at 120°C.<sup>150</sup>

The data also show that, out of all lignocellulosic substrates used in this study, *Miscanthus* chips exhibit the least resistance to disintegration. This is probably due to the larger pores and thinner cell walls. It may also suggest a higher susceptibility of lignocellulosic matrix found in herbaceous plants towards ionic liquid pretreatment.

### 5.3 Summary

The swelling of wood chips in various 1,3-dialkylimidazolium ionic liquids has been investigated. The effects of ionic liquids on the structural integrity of wood chips ranged from hardly any swelling/dissolution to pronounced swelling, partial dissolution particularly in axial direction and cracking of the chips. A correlation between the Kamlet-Taft  $\beta$  parameter of the ionic liquid and the swelling and dissolution behaviour was

established. This work shows shown that the small surface to volume ratio of chips results in long reaction times to achieve dissolution.

The disintegration of air-dried hardwood and softwood chips in dried [C<sub>4</sub>C<sub>1</sub>im][MeCO<sub>2</sub>] was not possible at 120°C (without stirring). In contrast to this, it was demonstrated that complete dissolution of air-dried *Miscanthus* chips under the conditions used is possible; suggesting that grass lignocellulose may be more amenable to ionic liquid pretreatment. It has also been shown that the presence of even small quantities of water (e.g. the 9 wt% residual moisture in air-dried pine chips) considerably affects the swelling and the dissolution of wood chips. It is concluded that additional mechanical force may be required to achieve comminution of hardwood and softwood chips on a time-scale that is relevant to industry (minutes instead of hours/days without requiring complete dryness). In addition, the water-tolerance of ionic liquid pretreatment may require improvement.

The experiments presented here do not relate chip swelling and partial solubilisation with enhanced enzymatic digestibility of the cellulose and hemicellulose portion, which is the ultimate goal of a pretreatment operation. It is postulated that complete dissolution (which includes the cellulose portion) may not be required to enhance the digestibility of the carbohydrate portion in lignocellulosic biomass. The relationship between the anion present in 1,3-dialkylimidazolium ionic liquids and the enzymatic digestibility will therefore be presented in the next chapter, however, ground biomass was mostly used for the study.

## 6 Pretreatment of lignocellulosic biomass with ionic liquid water mixtures

While investigating the dissolution behaviour of wood chips (presented in chapter 5) a wide range of ionic liquids was tested. Certain observations made during this screening provided the start pointing for the discovery of ionic liquids which have not been used successfully in lignocellulose pretreatment before. These ionic liquids are known and even commercially available.

Whilst exploring lignocellulose pretreatment using these and known pretreatment liquids, it turned out that they are able to address current limitations of ionic liquid pretreatment, such as ionic liquid stability at process-relevant temperatures and the water-sensitivity of the process. To further characterise the effect of these ionic liquids, the fate of the main lignocellulosic components was investigated. The composition of pretreated biomass (*Miscanthus*, willow and pine) was determined and it was attempted to investigate the solubilised biomass portion. Although most results in this chapter were obtained using ground biomass (0.18-0.85 mm fraction), so that effects of the particle size could be excluded, data on the use of chips are also presented at the end.

### 6.1 Materials and Methods

#### 6.1.1 Materials

The ground lignocellulosic biomass used in this study was pine sapwood (*Pinus sylvestris*, variety SCOES) from East Sussex, de-barked mixed stems of willow (*Salix viminalis*, variety TORA) and *Miscanthus x giganteus* whole stems. The biomass was air-dried, ground and sieved (0.18-0.85 mm, -20+80 of US mesh scale) before use. The moisture content of untreated lignocellulose was 8.0% (*Miscanthus*), 8.9% (pine)

and 7.6% (willow) based on oven-dried weight. The biomass was stored in plastic bags at room temperature. Chip-sized *Miscanthus* and willow biomass was prepared as described in section 5.1.1 on page 137. 1-Butyl-3-methylimidazolium methyl sulfate was purchased from Sigma and 1-ethyl-3-methylimidazolium acetate was a gift from BASF and both used as received (apart from drying). The other ionic liquids were prepared as described in section 2.2.3. All ionic liquids were dried to a water content >3000 ppm prior to use. Elemental analysis was performed by the London Metropolitan University Service.

### 6.1.2 *Enhanced liquid uptake of Miscanthus chips at 80 °C*

*Miscanthus x giganteus* chips (a=b = 11 mm, c= 5 mm) were soaked in ionic liquid under reduced pressure and pre-incubated in snap-top glass vials with plastic cap at room temperature for 26 days. Subsequently, the samples were heated to 80°C for a few hours and the soaked chips weighed afterwards. The enhanced liquid uptake at 80°C was calculated according to equation 9 with  $m_{80^{\circ}\text{C}}$  being the mass after the incubation at 80°C,  $m_{ps}$  the mass of the pre-incubated chips before heating at 80°C and  $\rho$  the ionic liquid density at 25°C (literature values).

$$v_{\text{uptake}} = \frac{m_{80^{\circ}\text{C}} - m_{ps}}{m_{ps} \cdot \rho} \quad \text{Eq. 9}$$

### 6.1.3 *Determination of biomass moisture content*

To determine the oven-dried weight, 100-200 mg air-dried ground or chip-sized biomass was wrapped in aluminium foil of known weight and dried in an oven at 105°C overnight. The samples were transferred into a desiccator with activated silica and the weight determined after 5 min. The moisture content was calculated according to equation 10.

$$\text{moisture (\%)} = \frac{m_{\text{air dried}} - m_{\text{oven dried}}}{m_{\text{oven dried}}} \cdot 100\% \quad \text{Eq. 10}$$

#### 6.1.4 *Ionic liquid pretreatment and isolation of pretreated pulp*

0.500 g lignocellulosic biomass (on an oven-dried weight basis) was transferred into wide-mouthed pyrex culture tubes with screw cap and Teflon-lining. Pure ionic liquid or ionic liquid water mixtures (5 ml in total) were added. The samples were incubated without stirring in an oven at 120°C for various lengths of time. After the pretreatment, the samples were cooled to room temperature and mixed with 10 ml methanol. Other solvents were tested (e.g. ethanol, isopropanol, acetone or water) but the process was optimal with methanol. After 2 h, the suspension was filtered through cellulose filter papers (Whatman 541 or equivalent). The supernatant was set aside for precipitation of the dissolved lignin. The pulp was rinsed with methanol from a wash bottle and incubated with 10 ml fresh methanol overnight. The suspension was filtered again, rinsed with methanol from a wash bottle and the solids air-dried on the filter paper overnight. The air-dried weight was recorded and the samples transferred into re-sealable air-tight sample bags. The moisture content was determined according to section 6.1.3, which allowed calculation of the oven-dried biomass (pulp) yield.

#### 6.1.5 *Lignin isolation*

The supernatant obtained after pretreatment (diluted with methanol) was dried under mild vacuum at 40°C using a Carousel 12 (Radleys, UK) equipped with a temperature-controlled hotplate, glass reaction vessels and 10 mm oval rare earth metal stir bars (purchased from Sigma-Aldrich), to remove the organic wash solvent. Subsequently, 10 ml of water were added to the dried liquor to precipitate the lignin as a fine suspension. The precipitate was washed 3 times with distilled water, air-dried for several days and dried *in vacuo* at room temperature. The weight of the dried precipitate was recorded and the sample stored in a glass vial with plastic cap. The precipitate yield was reported as relative percentage of the Klason lignin content of untreated biomass.

### 6.1.6 *Enzymatic saccharification*

The enzymatic saccharification was performed according to LAP “Enzymatic saccharification of lignocellulosic biomass” (NREL/TP-510-42629), which can be downloaded from <http://www.nrel.gov/biomass/pdfs/42629.pdf>. Pretreated biomass was washed and air-dried prior to the saccharification as described in section 6.1.4. Ca. 150 mg of treated and untreated were added to 50 ml cylindrical plastic vials and buffer, antibiotics and enzyme preparation as described in the standard protocol. Commercial enzyme preparations were used: Celluclast (*T. reesei* cellulase mix) and Novozyme 188 ( $\beta$ -glucosidase, both from Sigma) at 50°C for up to 96 h, which contain hemicellulolytic activity and allow the hydrolysis of hemicellulose polymers (both from Sigma). If a pretreatment condition was run in duplicate or triplicate, one saccharification experiment per sample was performed. If the pretreatment condition was not replicated, the saccharification was performed in duplicate. The samples were analysed for glucose and hemicellulose monomers (xylose, arabinose, mannose and galactose) on a Jasco HPLC system with refractive index detector equipped with an Aminex HPX-87H column (Biorad). The mobile phase was 10 mM sulfuric acid, the column oven temperature 35°C, the flow rate 0.6 ml/min and the acquisition time 25 min. Glucose and hemicellulose yields were calculated based on the glucose and hemicellulose contents of the untreated biomass, respectively.

### 6.1.7 *Determination of extractives*

The extractives from untreated pine and willow biomass were removed by a one-step automated solvent extraction with 95% ethanol using an ASE 300 accelerated solvent extractor (Dionex) according to the LAP “Determination of extractives” (NREL/TP-510-42619), issue date 7/17/2005, which can be downloaded from <http://www.nrel.gov/biomass/pdfs/42619.pdf>. Extractives from untreated *Miscanthus* were removed by a two-step solvent extraction, initially with deionised water and subsequently with 95% ethanol according to the LAP.

### 6.1.8 Compositional analysis

Compositional analysis (determination of Klason lignin, carbohydrate and ash content) was performed according to the laboratory analytical procedure (LAP) "Determination of structural carbohydrates and lignin in biomass" (NREL/TP-510-42618). 300 mg of oven-dried biomass were used per experiment. HPLC analysis of glucose and hemicellulose sugars was performed on an Agilent 1200 system with refractive index detector equipped with an Aminex HPX-87P column (Biorad), a de-ashing column and a Carbo-P guard column. The mobile phase was de-ionised water. The column temperature was set to 80°C and the flow rate was 0.6 ml/min.

### 6.1.9 Calculating the delignification

The removal of lignin or delignification (delign.) was calculated from the Klason lignin content of the untreated lignocellulosic biomass and the Klason lignin content of the pulp according to Eq. 11.

$$\text{Delign. (\%)} = \frac{\text{Klason lignin (untreated)} - \text{Klason lignin (pulp)}}{\text{Klason lignin (untreated)}} \cdot 100\% \quad \text{Eq. 11}$$

### 6.1.10 Quantification of solubilised sugars and furfurals

The concentrations of 2-furaldehyde, 5-(hydroxymethyl)-2-furaldehyde (HMF), glucose and monomeric hemicellulose sugars in the ionic liquid supernatant were analysed on a Jasco HPLC system equipped with an Aminex HPX-87H column (Biorad), a refractive index and a UV detector with 10 mM sulfuric acid as mobile phase. The column oven temperature was 55°C, the flow rate 0.6 ml/min, the acquisition time 55 min. 200 µl of the pretreatment liquor after lignin precipitation (40 v/v% ionic liquid-water mixture) were mixed with 600 µl deionised water in a 1.5 ml plastic cup, vortexed and centrifuged for 10 min at 13 000 rpm using a table-top centrifuge. The supernatant was transferred into a clean cup and centrifuged for 10 min. The clear liquid was analysed by HPLC.

Standards of HMF and 2-furaldehyde (both from Sigma-Aldrich) with 0.01-0.4 mg/ml were prepared. The peak areas were plotted against the

concentrations to obtain the calibration factor  $f_c(S)$ . The fraction of biomass dissolved in the liquor (and converted, in the case HMF or furfural) were calculated equation 12. The transformation factor  $F_t$  accounting for the differences in molecular weight of the original biomass components and the product, was 1.37 for furfural, 1.28 for HMF, 0.91 for glucose and 0.88 for hemicellulose sugars.

$$\text{wt}\%(S) = \frac{A_{\text{HPLC}} \cdot F_D \cdot V_{\text{PL}} \cdot F_T(S)}{F_{\text{HPLC}}(S) \cdot m_{\text{biomass}} \cdot F_C} \cdot 100\% \quad \text{Eq. 12}$$

$A_{\text{HPLC}}$ : area of HPLC peak,  $F_{\text{HPLC}}(S)$ : HPLC calibration factor for substance S,  $F_D$ : dilution factor,  $V_{\text{PL}}$ : volume of pretreatment liquor in ml,  $m_{\text{biomass}}$ : biomass (oven-dried weight) in mg,  $F_C$ : fraction of glucan or hemicellulose sugars in untreated biomass as determined by compositional analysis,  $F_T(S)$ : transformation factor accounting for molecular mass differences between starting material and product.

### 6.1.11 Ionic liquid treatment of cellulose

300 mg of air-dried cellulose were incubated with 5 ml pure ionic liquid or an 80/20 vol% ionic liquid water mixture at 120°C for 22 h. After 15 h, the samples were stirred using a spatula. At the end of the treatment samples were cooled to room temperature and 15 ml distilled water were added to the ionic liquid cellulose suspension/solutions in order to regenerate solubilised cellulose. The cellulose incubated with  $[\text{C}_4\text{C}_1\text{im}][\text{MeSO}_4]$ ,  $[\text{C}_4\text{C}_1\text{im}][\text{HSO}_4]$  and the water control was separated from the liquid phase by centrifugation. The solids were washed twice with 15 ml distilled water and centrifuged. Cellulose incubated in  $[\text{C}_2\text{C}_1\text{im}][\text{MeCO}_2]$  and  $[\text{C}_4\text{C}_1\text{im}][\text{MeCO}_2]$  was isolated by filtration through a Buchner funnel and washing with water. The solids were washed with distilled water until the wash water was clear. The solids were dried on filter paper or in the centrifugation tubes. The air-dried yield was determined and 100 mg of the sample subjected to saccharification using LAP “Enzymatic saccharification of lignocellulosic biomass” (NREL/TP-510-42629) as described in section 6.1.6 on page 165. Some ionic liquid treated samples had to be powdered using a pestle and a mortar prior to the saccharification, due to their gummy consistency.



## 6.2 Results and Discussion

### 6.2.1 Treatment of *Miscanthus* chips with $[C_4C_1im][MeSO_4]$

Initial experiments that explored the swelling of *Miscanthus* wood chips in a variety of ionic liquids, revealed that the ionic liquid 1-butyl-3-methylimidazolium methyl sulfate,  $[C_4C_1im][MeSO_4]$ , had an unusual effect on this substrate. When the chips immersed in this ionic liquid were heated to 80°C, they shrank instead of the expected swelling. The chips also absorbed significantly more liquid than chips immersed in all other ionic liquids and even water (Figure 65).

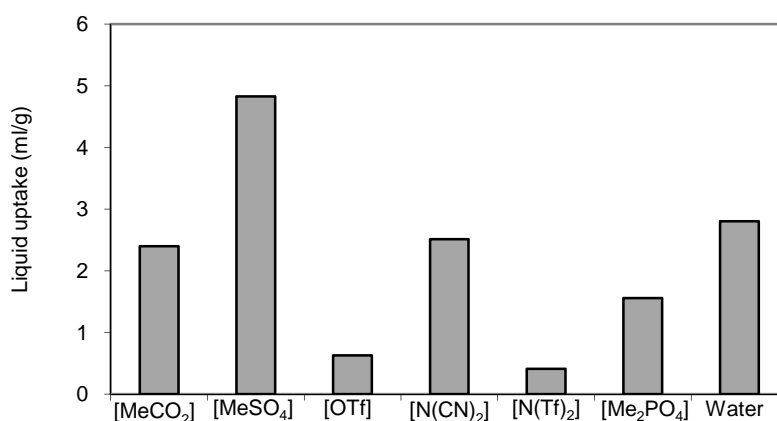


Figure 65: The uptake of various 1-butyl-3-methylimidazolium ionic liquids and water into *Miscanthus* chips at 80°C. Ionic liquid anions (left to right): acetate, methyl sulfate, triflate, dicyanamide, bis(trifluoromethylsulfonyl)imide, dimethyl phosphate

The lignocellulose structure became soft and, upon stirring the suspension, the chips visibly 'dissolved'. The solution was examined under the microscope and revealed the presence of separated parenchyma and fibre cell walls (Figure 66). Such a process is called maceration, the meshing of a tissue without complete destruction.

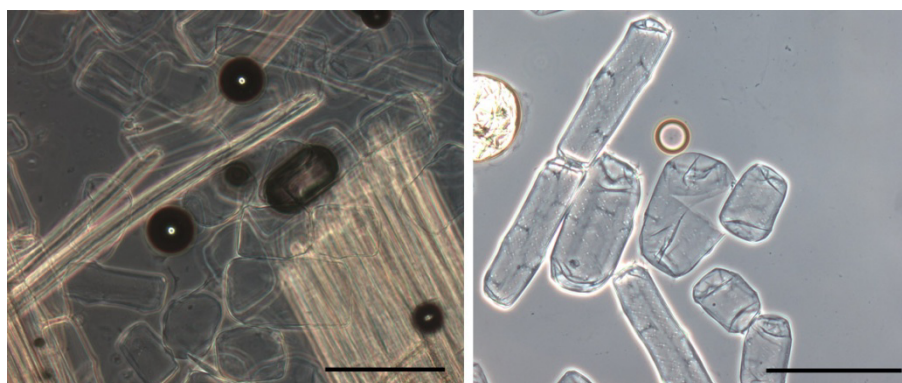


Figure 66: Images of *Miscanthus* wood dissolved in wet  $[C_4C_1im][MeSO_4]$  using light transmission microscopy. Left: outer part with fibre cells; right: parenchyma cells. Scale bar corresponds to 100  $\mu m$ .

These observations suggested that the middle lamella, the “glue” between the cell walls, may have been compromised by the ionic liquid treatment. The middle lamella contains hemicelluloses and pectins and, in mature tissues, it is heavily lignified.

These observations not only suggest that the surface area of *Miscanthus* chips could be vastly enhanced using a relatively mild treatment. It also hinted at the possibility that  $[C_4C_1im][MeSO_4]$  treatment may enhance the digestibility of the lignocellulose by altering lignin and/or hemicelluloses. However, such an idea contradicted the findings of various research groups who had used methyl sulfate containing ionic liquids or biomass pretreatment and concluded that such ionic liquids do not enhance the digestibility of maple wood or corn cob (Table 18).<sup>114, 136, 154, 188</sup>

Table 18: Studies that have used methylsulfate based ionic liquids for biomass

Reference	Ionic liquid	Biomass	Observation
Lee <i>et al.</i> <sup>114</sup>	$[C_1C_1im][MeSO_4]$	Ground maple wood (250 $\mu m$ )	No lignin extraction, no enhanced saccharification yield
Doherty <i>et al.</i> <sup>154</sup>	$[C_4C_1im][MeSO_4]$	Ground maple wood	19% lignin extracted, lower saccharification yield than untreated wood
Li <i>et al.</i> <sup>187</sup>	$[C_1C_1im][MeSO_4]$	Corn cob	Only slightly elevated saccharification yield, other ILs were picked to be more effective

### 6.2.2 Design of pretreatment experiment

The wide-mouthed culture glass tubes used for the chip swelling experiments were also used in the pretreatment of ground biomass (Figure 67). Hungate tubes, which are normally used for anaerobic culture of microbes, were also used occasionally. The pretreatment temperature was selected to be 120°C, because more pronounced pretreatment was observed at this temperature than at 100°C.<sup>189</sup> In order to minimise ionic liquid use, small batches of 500 mg (oven-dried weight) biomass was used per experiment. This was enough material to determine the oven-dried weight after pretreatment and also subject some of it to enzymatic saccharification. More biomass (1-1.5 g) was needed if compositional analysis of the pretreated material was to be performed. The typical solid loading used was 0.1 g/ml. This was just enough to cover the ground *Miscanthus* without compressing it.



Figure 67: Capped glass tubes used for the ionic liquid pretreatment of ground lignocellulosic biomass: *Miscanthus* (left), willow (middle) and pine (right).

When using the new experimental set-up, the treatment of air-dried *Miscanthus* flour with pure  $[C_4C_{1im}][MeSO_4]$  at 120°C for 6 h or longer resulted in a gummy ionic liquid biomass composite (Figure 68 left).



Figure 68: *Miscanthus* flour after pretreatment with  $[C_4C_{1im}][MeSO_4]$ . Left: pretreated at  $120^\circ C$  for 6 h with pure ionic liquid (experiment performed by Julian Giannuzzi). Right: pretreated at  $120^\circ C$  for 22 h with 80/20 vol% ionic liquid water mixtures after washing.

The release of sugars by hydrolytic enzymes from this gummy composite was measured by MSci student Julian Giannuzzi and turned out to be very low.<sup>189</sup> However, application of a mixture of ionic liquid and water yielded a liquid fraction and a beige pulp. The liquid was almost black after the pretreatment. Upon separation of the liquid and solid fraction, a beige pulp was obtained (Figure 68 right). Preliminary testing of the enzymatic saccharification indicated that high glucose yields could be obtained from this pulp, even after an extended period of heating.

Based on these findings, a pretreatment experiment was designed that would allow more precise quantification of the compositional changes and saccharification yields. The flow scheme according to which the lignocellulosic biomass was processed is depicted in Figure 69.

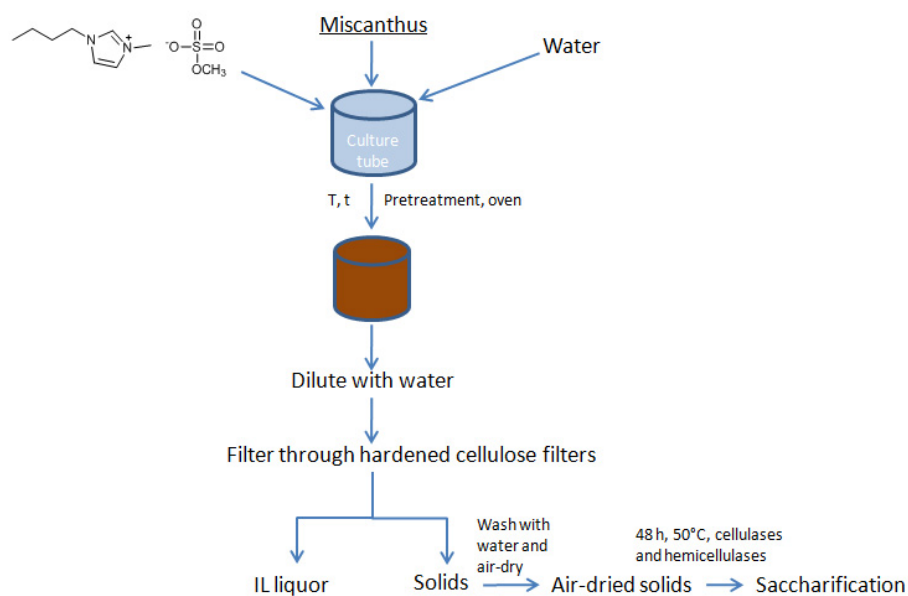


Figure 69: The experimental setup for pretreatment of *Miscanthus* flour with  $[C_4C_{1im}][MeSO_4]$  water mixtures.

### 6.2.3 The notation for ionic liquid water mixtures

To facilitate discussion of the following results, a notation is devised which indicates the amount of ionic liquid contained in the ionic liquid water mixtures. A subscript is added to the ionic liquid notation, indicating the ionic liquid content in volume percent (v/v % or vol%), with the remainder being water. An example is  $[C_4C_{1im}][MeSO_4]_{80\%}$ , which contains 80 vol%  $[C_4C_{1im}][MeSO_4]$  and 20 vol% water. Normally, the volume of a solution is not equal to the sum of the volumes of the pure components, but this is neglected throughout this thesis. Where volume percent is used it has been calculated as follows:

$$\text{vol\%} = \frac{\text{volume of ionic liquid}}{\text{volume of ionic liquid} + \text{volume of water}} \cdot 100\% \quad \text{Eq. 12}$$

### 6.2.4 *Miscanthus* composition

The composition of the untreated *Miscanthus* feedstock was determined by compositional analysis. 43.6% of the oven-dried biomass was glucan, 18.3% was xylan and 6 % were the other hemicellulose sugars (arabinose, mannose and galactose). This means that 75% of the hemicellulose sugars were xylose. The Klason lignin content was 26.5%.

### 6.2.5 Sugar yields after pretreatment of *Miscanthus* with 1-butyl-3-methylimidazolium methyl sulfate water mixtures

An experiment was carried out to investigate the influence of water on the pulp's enzymatic digestibility in more detail. The *Miscanthus* flour was treated with six ionic liquid water mixtures. The mixture with the highest ionic liquid content contained was 98 vol%  $[\text{C}_4\text{C}_1\text{im}][\text{MeSO}_4]$ , the mixture with the lowest content 20 vol% of this ionic liquid, while temperature and pretreatment time were the same for all samples. A set of control samples was treated with deionised water.

After thoroughly washing and air-drying the pretreated *Miscanthus* biomass, the pulp was subjected to enzymatic saccharification with standard commercial cellulase preparations. The glucose and hemicellulose yield obtained after pretreatment with ionic liquid water mixtures are shown in Figure 70. The highest glucose yields were obtained with liquors containing 90-60 vol% ionic liquid. Up to 92% of the glucose contained in the original biomass was released during the saccharification. These saccharification yields come close to the industrially desired sugar recovery of  $>80\%$ <sup>190</sup> and are significantly higher than some of the yields reported by other researchers for their pretreatment experiments (listed in Table 15 on page 135).

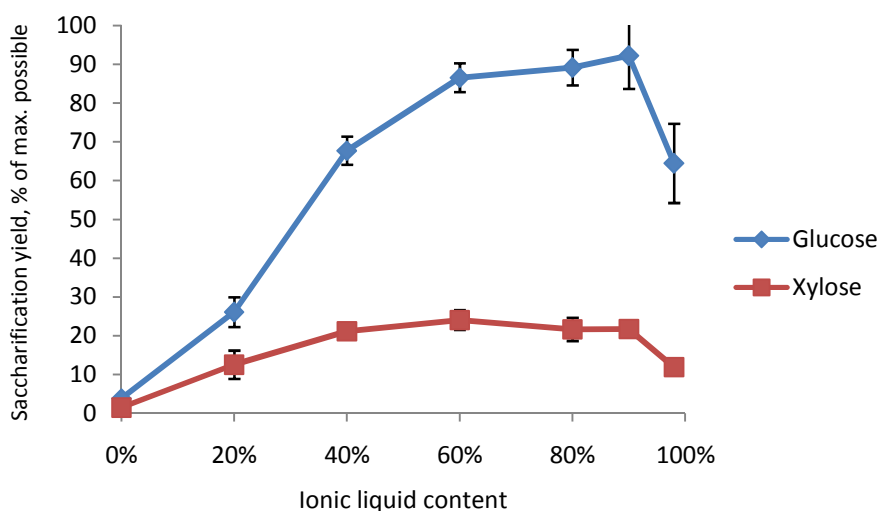


Figure 70: Saccharification yields after 22 h/120°C pretreatment of ground *Miscanthus* with  $[\text{C}_4\text{C}_1\text{im}][\text{MeSO}_4]$  water mixtures.

The release of glucose from samples treated with ionic liquid water mixtures was always better than the yield obtained from water-treated controls. This suggests that treatment with aqueous  $[\text{C}_4\text{C}_1\text{im}][\text{MeSO}_4]$  solution can substantially increase the accessibility of the cellulose fraction. Although a higher ionic liquid content improves the yield under the conditions used, a relatively high water content of up to 40% did not significantly reduce the glucose yields. A low water content decreased the saccharification yield, corroborating the observation that a certain amount of water is necessary to obtain the best possible sugar release.

The xylose recovery from pretreated samples was comparatively low. Only 20-25% of the original hemicellulose fraction was released during the saccharification. Nevertheless, the xylose yield after treatment with any ionic liquid water mixtures was higher than after treatment with pure water.

The data shown in Figure 70 were obtained with a HPLC system equipped with an Aminex HPX-87P column (Bio-rad). This HPLC column can resolve individual hemicellulose sugars, such as xylose, arabinose, mannose and galactose, while the other column used in this study, the Aminex HPX-87H, can individually resolve only glucose and arabinose while the others elute at the same time. Using the Aminex HPX-87P, it could be shown that after pretreatment, the quantities of hemicellulose sugars other than xylose, such as arabinose, mannose and galactose, were below the detection limit. Subsequently, it was deemed suitable to use the HPLC system with Aminex HPX-87H column, and to assume that all hemicellulose sugars recovered during saccharification were xylose.

Figure 71 shows samples after the completed saccharification. While the volume of untreated *Miscanthus* hardly changed during saccharification, the treated material was almost entirely solubilised by the hydrolytic enzymes, leaving behind a powdery brown residue.

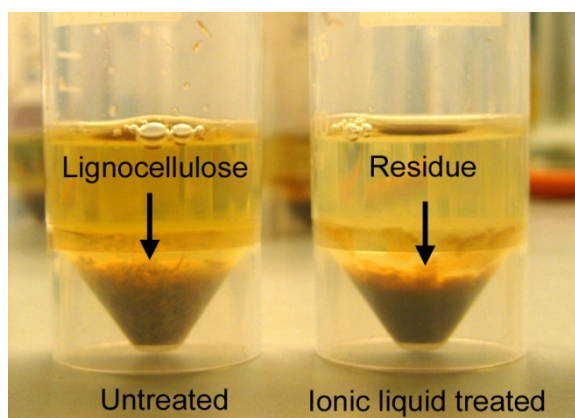


Figure 71: Saccharification samples after completed enzyme hydrolysis of untreated and pretreated *Miscanthus*. Complete solubilisation of the fibrous biomass was achieved after pretreatment and only a fine brown residue was left behind (right vial). Pretreatment conditions:  $[\text{C}_4\text{C}_1\text{im}][\text{MeSO}_4]_{80\%}$  at  $120^\circ\text{C}$  for 22 h.

### 6.2.6 The impact of the solid loading

The solid to liquid ratio is an important economical factor for biomass pretreatment. A high solid content is desirable, as this means less chemical input. Very high solid-to-liquid ratios can be achieved with AFEX pretreatment (up to 60%),<sup>191</sup> while most of the currently published studies on ionic liquid pretreatment only used solid loadings of 5 wt%. Poplar has been pretreated with ionic liquid at a biomass loading of 30% without reduction of saccharification yield.<sup>192</sup>

The data displayed in Figure 70 were obtained with using 0.1 g air-dried ground *Miscanthus* per 1 ml of pretreatment solvent. This corresponds to a solid to liquid ratio of 8.6 wt%. The impact of higher and lower solid content on the saccharification yield was examined. The results are shown in Figure 72. It is shown that a lower solid loading increased the glucose yield slightly but decreased the xylose yield. A 50% increase of the solid loading had almost no effect on the yield. However, when the solid loading during pretreatment was doubled to 0.2 g/ml or 17 wt%, the glucose yield dropped.



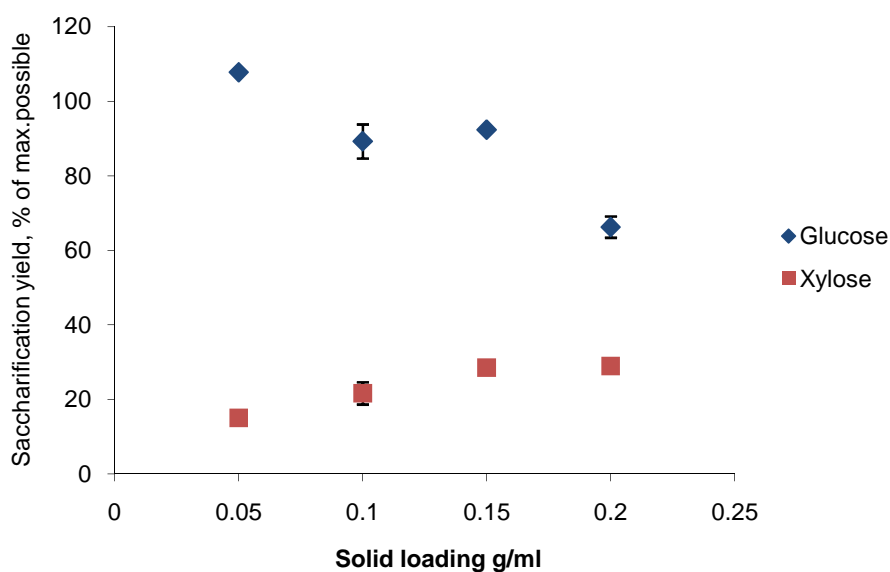


Figure 72: Saccharification yields obtained after ionic liquid pretreatment of ground *Miscanthus* at various solid loadings. Conditions:  $[C_4C_{1im}][MeSO_4]_{80\%}$ , 22 h, 120°C, saccharification time was 48 h.

The reduced yield at higher solid concentration can be explained with a decreased wetting of the biomass. The effect was probably enhanced by the lack of stirring. It is anticipated that stirring and compression of the biomass will improve the saccharification yield at high solid-to-liquid ratios.

### 6.2.7 *The influence of the wash solvent on biomass recovery and fractionation*

After pretreatment, the liquor was intensely coloured, which suggests that part of the lignin had been solubilised into the ionic liquid (Figure 73). Native lignin is not coloured, however, when lignin is chemically modified, it often turns dark.



Figure 73: Ionic liquid pretreatment liquor diluted with methanol.

During washing the pulp with water, it was observed that the diluted liquor would become hazy and a fine precipitate would settle after some time. It was speculated that this precipitate was lignin. It was further rationalised that washing with an organic wash solvent could help to improve the separation of lignin from the pulp, as it would not precipitate during washing. Short chain alcohols were deemed as appropriate, as the solubility of Kraft lignin is high in methanol (Sigma Aldrich data sheet) and many organosolv processes use ethanol.<sup>48</sup>

Apart from methanol and ethanol, the use of isopropanol and the non-protic polar solvent acetone was investigated. Initially, a 1,4-dioxane water mixture was also applied, because it is frequently used to solubilise lignin. This was abandoned, because dioxane would promote phase separation in the presence of ionic liquid and water which was hard to control. In addition, 1,4-dioxane is a suspected carcinogen, which makes it difficult to handle, and has a high boiling point, which makes it difficult to remove.

The influence of the wash solvent on the biomass recovery after washing is shown in Figure 74. The biomass recovery after pretreatment was significantly affected by the choice of wash solvent. After washing with water, 55% of the original biomass weight was recovered in the solid fraction, while the use of methanol and ethanol resulted in a higher mass recovery (62% and 80%, respectively). Unexpectedly, the recovered

mass after washing with isopropanol and acetone exceeded the weight of the original biomass (112% and 125%).

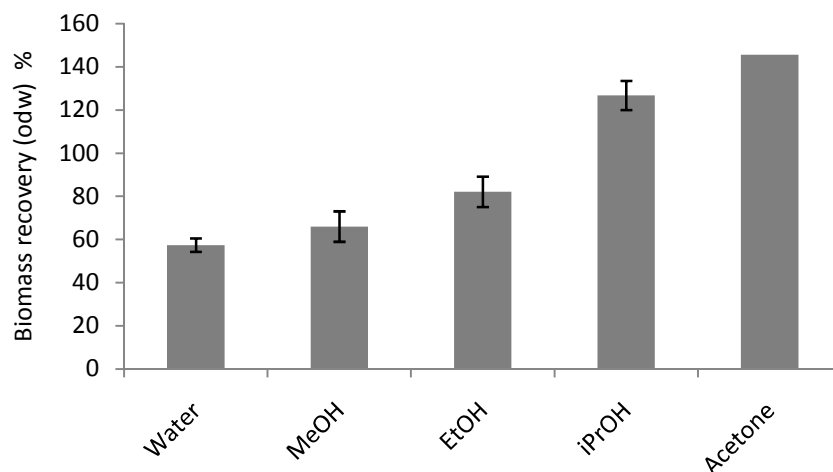


Figure 74: Influence of wash solvent on the biomass recovery after pretreatment with  $[\text{C}_4\text{C}_1\text{im}][\text{MeSO}_4]_{80\%}$  for 22 h at  $120^\circ\text{C}$ . All experiments were performed in triplicate, except for the washing with acetone.

IR spectra of the pulps were recorded and are shown in Figure 75. The sharp peaks at  $3000\text{ cm}^{-1}$  are caused by C-H stretching vibrations typically observed for the 1,3-dialkylimidazolium cation. This shows that residual ionic liquid was present. The water and methanol washed biomass contained only small amounts of ionic liquid, suggesting that the ionic liquid had been removed more thoroughly.

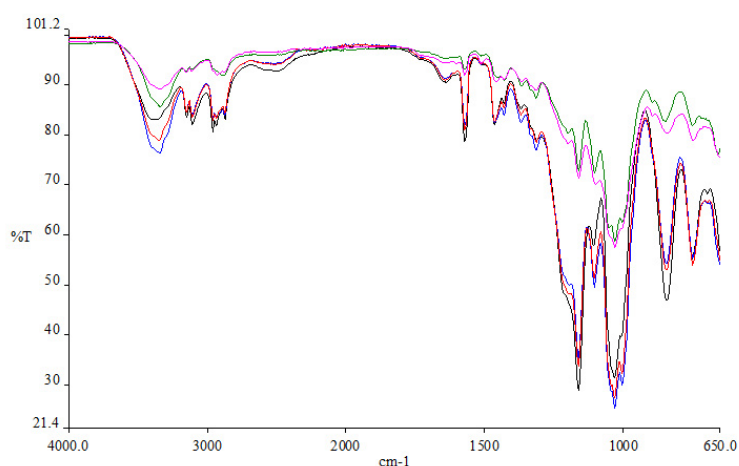


Figure 75: ATR-IR spectra of *Miscanthus* pulp recovered after a pretreatment with  $[\text{C}_4\text{C}_1\text{im}][\text{MeSO}_4]_{80\%}$  for 22 h at  $120^\circ\text{C}$ . Wash solvents: water (pink), methanol (green), acetone (black), isopropanol (red) and ethanol (blue).

One of the samples that had been washed with isopropanol was Soxhlet extracted (with iso-propanol) to achieve complete removal of the ionic liquid. The ATR-IR spectra in Figure 76 show that the ionic liquid was indeed successfully removed during the extraction. This suggests that removal of the ionic liquid by isopropanol is possible, but is slower.

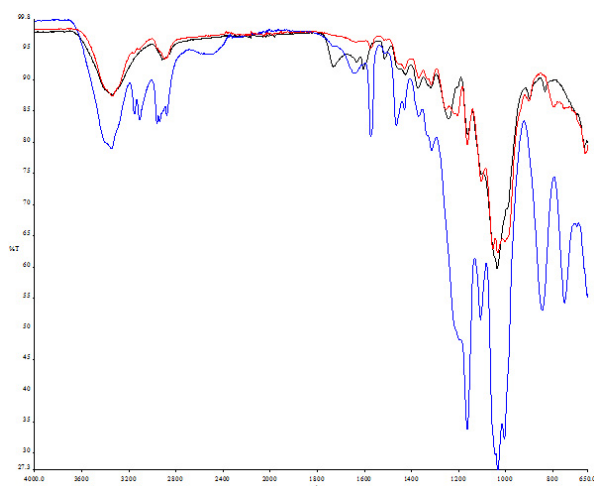


Figure 76: ATR-IR spectrum of ground *Miscanthus*: untreated (black), pretreated with [C<sub>4</sub>C<sub>1</sub>im][MeSO<sub>4</sub>]<sub>80%</sub> at 120°C and washed with isopropanol (blue) and pretreated and Soxhlet extracted with isopropanol (red).

The ability of a solvent to wash away the ionic liquid may be correlated with the solvent polarity. Solvents that provide a combination of a high polarisability ( $\pi^*$ ) and hydrogen-bond donor ability ( $\alpha$ ) should be the most effective wash solvents, e.g. water and methanol. Isopropanol and acetone have lower  $\pi^*$  values and acetone has a particularly low  $\alpha$  value.

After washing with organic solvents and water the pulp was subjected to saccharification (Figure 77). The saccharification yields after washing with methanol and ethanol were not affected. However, glucose yields were reduced for biomass washed with isopropanol or acetone. This could be due to a deactivation of the hydrolytic enzymes (or part of them as cellulose hydrolysis requires a range of enzymes) by the residual ionic liquid. The xylose yields do not appear to be significantly affected.

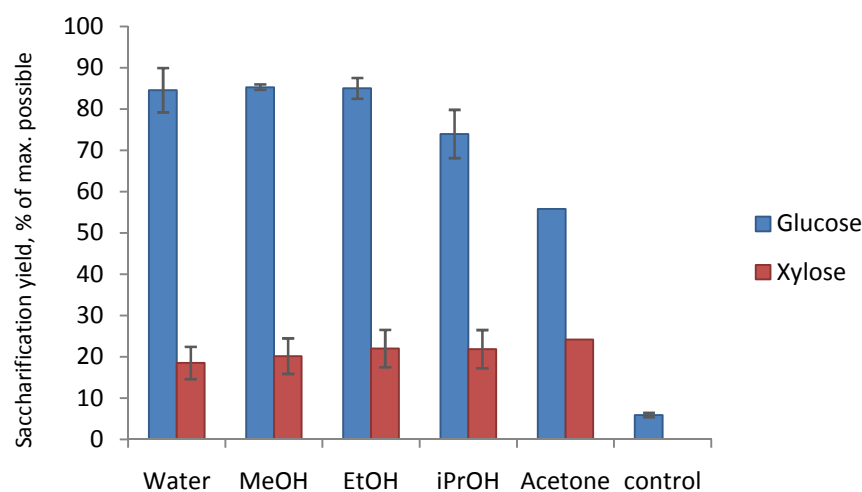


Figure 77: Influence of the wash solvent on the saccharification yield. Pretreatment with  $[\text{C}_4\text{C}_1\text{im}][\text{MeSO}_4]_{80\%}$  was performed at  $120^\circ\text{C}$  for 22 h, the saccharification for 48 h.

### 6.2.8 Lignin precipitation and the impact of the wash solvent on the yield

The precipitate was isolated and the yield determined in order to find out if washing with organic solvents would improve the final yield. The solvents were evaporated from the diluted ionic liquid liquor and 200 vol% water added to induce precipitation. The precipitate was washed with water and dried.

In order to characterise the precipitate, the carbon, nitrogen and hydrogen content of untreated *Miscanthus*, of the pulp and the precipitate were determined (Figure 78). A low carbon content is indicative of a higher oxygen content in the fraction. Therefore a fraction containing mainly highly oxygenated carbohydrates will have a lower carbon content than a fraction that is rich in the unsaturated polymer lignin. The pulp had the lowest carbon content of all fractions and the precipitate had the highest, suggesting that the lignin content was high in the precipitate and low in the pulp.

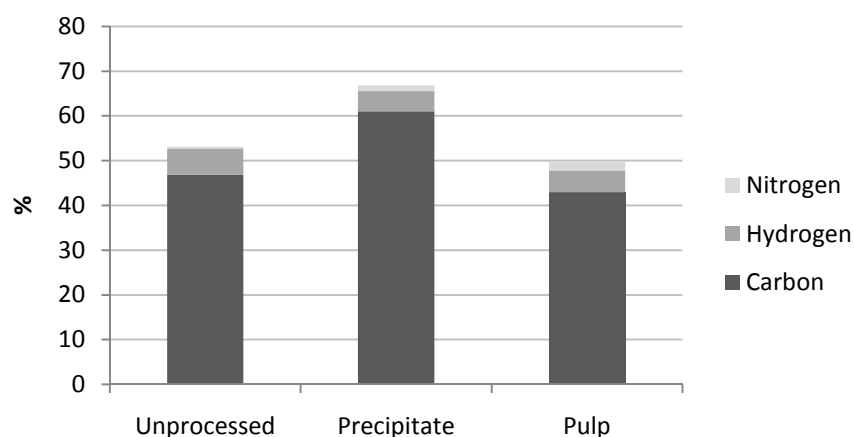


Figure 78: Elemental composition of fractions after exhaustive solvent washing with isopropanol. The carbon content was the highest in the precipitate, which is attributed to the lower abundance of oxygenated carbon in lignin.

Nevertheless, elemental analysis cannot show conclusively that the precipitate is lignin. However, the analysis of the Klason lignin content in untreated and treated *Miscanthus* (presented in section 6.2.11, see specifically Figure 83) also supports the conclusions that lignin has been removed from the pulp. AT-IR gives further confirmation that the precipitate is largely lignin (Figure 79).

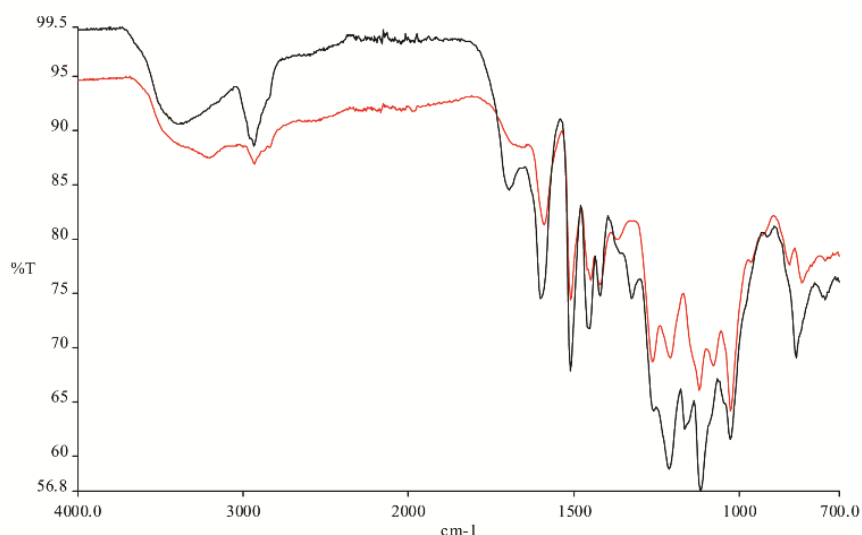


Figure 79: AT-IR spectrum of precipitate isolated from a  $[C_4C_{1im}][HSO_4]_{80\%}$  liquor after treatment of ground *Miscanthus* at 120°C for 22 h upon dilution with water (black line). The precipitate was washed with water and dried prior to the analysis. For comparison, the AT-IR spectrum of a reference lignin (alkali lignin, Aldrich) was recorded (red line).

The purified precipitate obtained after the various solvent washes was weighed to determine the yield. These yields, relative to the lignin content of untreated *Miscanthus*, are shown in Figure 80.

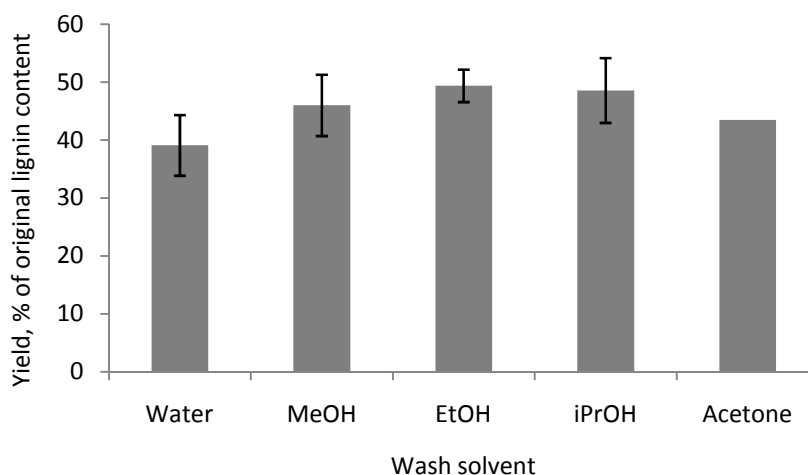


Figure 80: Lignin yield after application of various solvent for separating solid and liquid fractions. Water was used for the precipitation ( $[\text{C}_4\text{C}_1\text{im}][\text{MeSO}_4]_{80\%}$ , 120°C, 22 h).

Yields between 40% and 50% relative to the lignin content in untreated *Miscanthus* were achieved. A slightly lower yield was obtained when water was used as wash solvent. However, the errors of the measurements were relatively large. Therefore differences between the yields after methanol, ethanol, isopropanol and acetone treatment are of little significance. It should be noted that the precipitate might not only contain lignin but also so-called pseudo-lignins, which are insoluble sugar degradation products. Formation of pseudo-lignins has been observed under acidic pretreatment conditions and that pseudo-lignin can be extracted with organic solvents.<sup>193</sup>

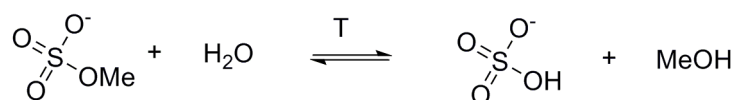
The use of an organic wash solvent seems to improve the fractionation and the lignin recovery. However, the improved lignin recovery needs to be balanced with the reduced ability of organic solvents to separate the ionic liquid from the pulp. Methanol was selected as wash solvent for further experiments, because it combines high solubility for the ionic liquid with improved precipitate recovery. The elemental analysis data provided early confirmation that lignin could be separated from the pulp,

in a similar fashion to the way organosolv lignin is isolated from the ethanol containing liquor.

### 6.2.9 Recycling of $[C_4C_1im][MeSO_4]$

Ionic liquids must be recycled to be economically viable. Therefore recovery of the ionic liquid was attempted, after the pretreatment was finished. The water was evaporated under mild heating and the remaining liquid submitted for  $^1H$ -NMR analysis. The signals of dialkylimidazolium cation could be identified as expected, but the peak integral for the methyl group of the anion was significantly diminished. In the negative mass spectrum of the recovered ionic liquid, a prominent peak at  $m/z=97$  was discovered, which was only a minor peak in the mass spectrum of fresh  $[C_4C_1im][MeSO_4]$ .

The methyl sulfate anion contains an ester bond which is susceptible to hydrolysis in the presence of water. Hydrolysis of this bond would result in the formation of hydrogen sulfate anions (Scheme 18). The reduction of the NMR integral of the methyl group is therefore attributed to the formation of hydrogen sulfate. The hydrolysis is expected to reach equilibrium in a closed system (such as the capped vessels used for the pretreatment experiments).



Scheme 18: Equilibrium between methyl sulfate and hydrogen sulfate at elevated temperatures in the presence of water and methanol

The extent of ester hydrolysis for each of the ionic liquid water mixtures is shown in Figure 81. At 2 vol% water content, 70% of the anions were present as methyl sulfate. Anion hydrolysis reached a maximum at 40 vol% water content; from this mixture, only 20% of anions were recovered as methyl sulfate.



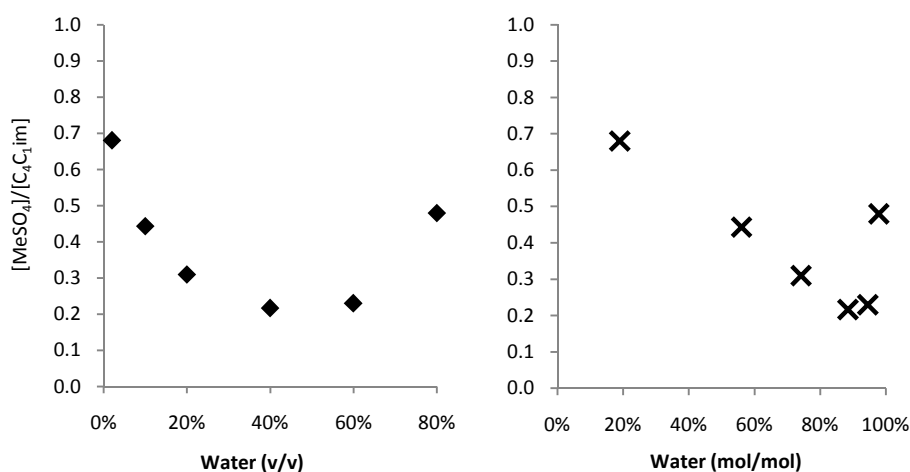


Figure 81: Ratio of cation to  $[\text{MeSO}_4^-]$  anions in the ionic liquid recovered after pretreatment of *Miscanthus* in ionic liquid/water mixtures for 22 h at 120°C.

### 6.2.10 Enzymatic digestibility after pretreatment with $[\text{C}_4\text{C}_1\text{im}][\text{HSO}_4^-]$ -water mixtures

The discovery that the binary ionic liquid water mixtures turn into quaternary mixtures under the conditions of the pretreatment triggered the question of whether all or only some of the components are required to obtain the high saccharification yields observed earlier. It was decided to investigate pretreatment of *Miscanthus* with aqueous mixtures of  $[\text{C}_4\text{C}_1\text{im}][\text{HSO}_4^-]$ , excluding methyl sulfate and methanol from the mixture.

Interestingly, the saccharification yields for both glucose and xylose after pretreatment with  $[\text{C}_4\text{C}_1\text{im}][\text{HSO}_4^-]$  water mixtures were very similar to the yields obtained after pretreatment with  $[\text{C}_4\text{C}_1\text{im}][\text{MeSO}_4^-]$ -water mixtures (Figure 82). Glucose yields were close to 90% for the liquors containing 10-40 vol% water. This was achieved in a shorter time (13 h) than previously used for the  $[\text{C}_4\text{C}_1\text{im}][\text{MeSO}_4^-]$  treatment (22 h). This suggests that either the increased concentrations of hydrogen sulfate anions accelerated the pretreatment or that a pretreatment time shorter than 22 h was sufficient to obtain high cellulose digestibility.

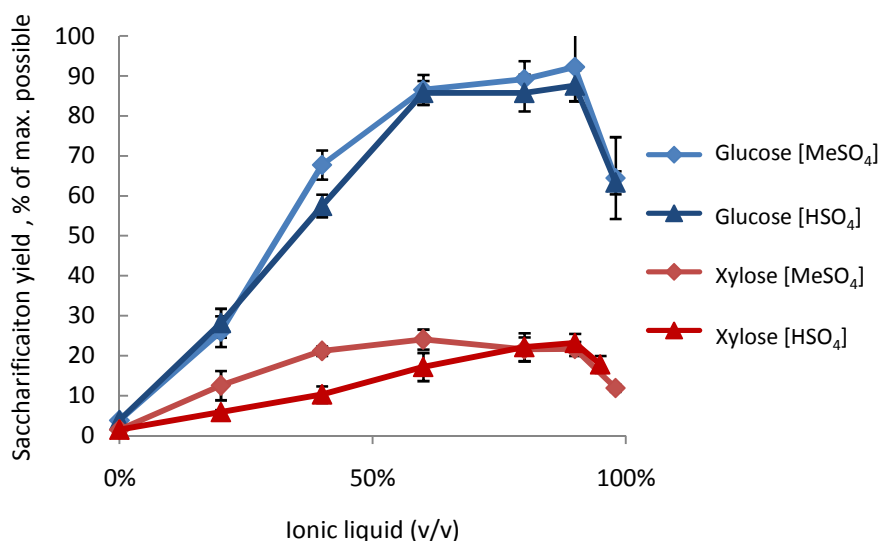


Figure 82: Saccharification of *Miscanthus* pulp after pretreatment with  $[C_4C_1im][HSO_4]$  water and  $[C_4C_1im][MeSO_4]$  water mixtures. The conditions were  $120^\circ C$  and 13 h or 22 h pretreatment time, respectively.

### 6.2.11 Biomass composition after pretreatment with $[C_4C_1im][MeSO_4]$ and $[C_4C_1im][HSO_4]$ -water mixtures

The solubilisation of up to half of the original weight coupled with a high glucose yield obtained from this non-solubilised fraction suggests that the cellulose content of the pulp had been significantly enhanced by the ionic liquid treatment. To confirm this, the composition of *Miscanthus* before and after pretreatment was determined. The investigated samples were *Miscanthus* pulps pretreated at  $120^\circ C$  with either  $[C_4C_1im][HSO_4]_{80\%}$  or  $[C_4C_1im][MeSO_4]_{80\%}$ . The pretreatment time was 2 h or 22 h. The 2 h incubation falls into the 'active' phase, when mass loss and saccharification yield change rapidly with time (will be discussed later). Therefore the composition of the biomass at 2 h may offer a glimpse into the mechanism of the pretreatment.

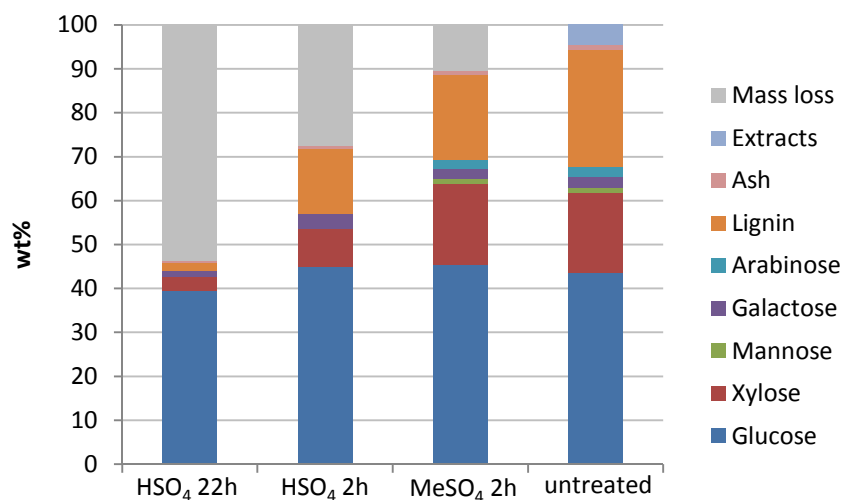


Figure 83: Effect of pretreatment with  $[C_4C_1im][MeSO_4]_{80\%}$  and  $[C_4C_1im][HSO_4]_{80\%}$  at  $120^\circ C$  on the composition of ground *Miscanthus* for various lengths of time.

Figure 83 shows that a  $[C_4C_1im][MeSO_4]_{80\%}$  pretreatment for 2 h resulted in only 10% mass loss. The hemicellulose content was nearly unchanged, while the lignin content was slightly reduced. The mass loss was significantly higher after a 2 h pretreatment with  $[C_4C_1im][HSO_4]_{80\%}$ . The mass loss was caused by the solubilisation of lignin and the removal of hemicellulose. The hemicellulose content was halved within the 2 h.

The composition after a 22 h pretreatment with  $[C_4C_1im][HSO_4]_{80\%}$  is also shown in Figure 83. Only 46% of the original biomass was recovered as a solid after the long treatment. In this solid, 85% of the material was glucan. This means that 91% of the original glucan was recovered with the pulp, suggesting that only 9% of the glucose had been solubilised into the liquor. The losses may include glucose that was part of the hemicellulose, but may also contain glucose that was part of cellulose. During saccharification, 86% of the original glucose was released. This means that 94% of glucan in the pulp was accessible to enzymes during saccharification. The hemicellulose content was very low, accounting for 9% of the solid fraction. This translates into a solubilisation of 80% of the (non-glucose) hemicellulose sugars. The lignin content of the solid was only 4%, implying that 93% of the lignin was solubilised during the treatment. This is in accordance with the results obtained by elemental analysis (Figure 78 on page 181).

### 6.2.12 Precipitate yield from $[C_4C_1im][HSO_4]$ water mixtures

The precipitation of lignin from the  $[C_4C_1im][HSO_4]$  water liquors was also investigated. Figure 84 shows how the precipitate yield was affected by the ionic liquid content of the liquor. Generally, the higher the ionic liquid content was the more precipitate could be isolated. The yield decreased almost linearly between 95 vol% and 40 vol% ionic liquid. A sharper drop was observed when the ionic liquid content decreased from 40 vol% to 20 vol%. This could be due to reduced delignification at low ionic liquid content.

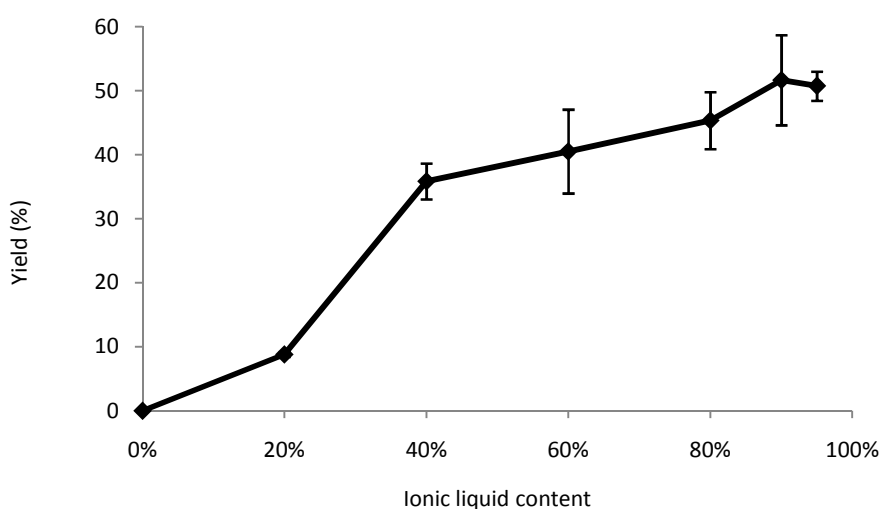


Figure 84: Lignin recovery after pretreatment with  $[C_4C_1im][HSO_4]$  water mixtures at 120°C for 13 h.

### 6.2.13 The time dependency of the saccharification yield

In the last section, the pretreatment effect of ionic liquid-water mixtures was investigated, either containing  $[C_4C_1im][HSO_4]$  or  $[C_4C_1im][MeSO_4]$ . It was found that  $[C_4C_1im][MeSO_4]$  was converted into a mixture of methyl sulfate and hydrogen sulfate anions under pretreatment conditions. Interestingly, although the data in Figure 82 were collected after different lengths of pretreatment, 22 h for the methyl sulfate pretreatment and 13 h for the hydrogen sulfate pretreatment, the saccharification yields were very similar. Therefore, the increase of the saccharification yields over time was investigated in more detail.

The  $[\text{C}_4\text{C}_1\text{im}][\text{MeSO}_4]_{80\%}$  and  $[\text{C}_4\text{C}_1\text{im}][\text{HSO}_4]_{80\%}$  liquors were chosen as examples. Figure 85 shows the development of the biomass recovery. It is demonstrated that the majority of the biomass solubilisation occurred within 4 h after the start of the pretreatment, accounting for 90% of the mass loss. The rest of the mass loss occurred in the remaining ~20 h. It was also demonstrated that  $[\text{C}_4\text{C}_1\text{im}][\text{HSO}_4]_{80\%}$  solubilised hemicellulose and lignin slightly faster in the early stage of the pretreatment (45 min and 90 min time points), but in the later stages, the effect of pretreatment liquor composition on the mass loss was negligible.

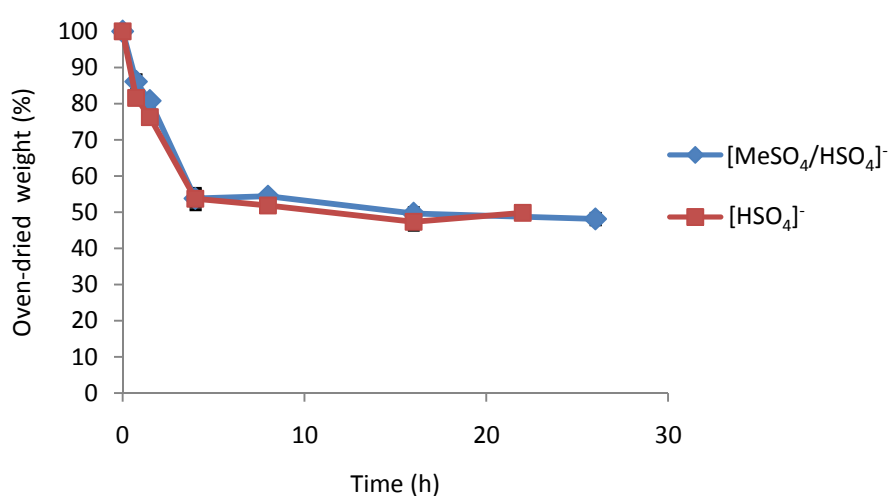


Figure 85: Mass loss during pretreatment with  $[\text{C}_4\text{C}_1\text{im}][\text{MeSO}_4]_{80\%}$  or  $[\text{C}_4\text{C}_1\text{im}][\text{HSO}_4]_{80\%}$  liquors at 120°C.

The development of the saccharification yield and the recovery of the precipitate yield are shown in Figure 86. The glucose yield rose steeply in the first 8 h, peaked around 15 h and then remained more or less constant. The xylose yield reached a maximum around 30% at 8 h, and then declined to 20% towards the end of the pretreatment.

The lignin yield followed a similar trend, increasing rapidly within the first 8 h and only slowly afterwards. Although the majority of mass loss occurred within the first 4 hours, the glucose yields were significantly improved by prolonging the pretreatment to 8 h. This suggests that the removal of hemicelluloses and lignin needs to be relatively advanced before the hydrolytic enzymes used in this study have full access to their substrate.

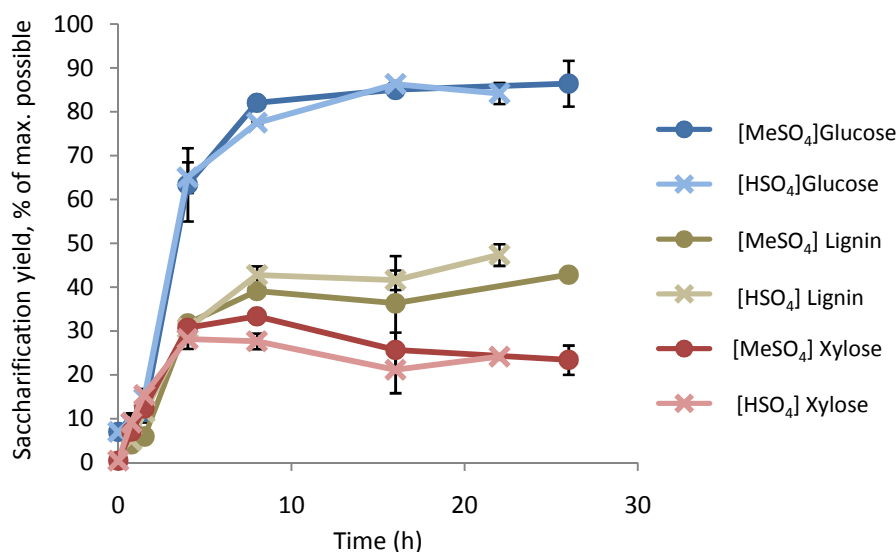


Figure 86: Time course study of saccharification and lignin yields obtained from ground *Miscanthus*. Pretreatment with  $[\text{C}_4\text{C}_1\text{im}][\text{MeSO}_4]_{80\%}$  and  $[\text{C}_4\text{C}_1\text{im}][\text{HSO}_4]_{80\%}$  mixtures was performed at  $120^\circ\text{C}$  for up to 26 h.

In conclusion, the data suggest that the pretreatment does not need to last for 22 h or even 13 h. 8-10 h are sufficient to obtain the maximum glucose yields. Prolonging the pretreatment does not seem to have a significant impact on the glucose yield, while the xylose yield decreases.

#### 6.2.14 Solubilised sugars and sugar degradation products

The fate of the solubilised carbohydrates was also investigated. The glucose and the other sugars contained in the ionic liquid liquor were quantified by HPLC. The analysis of sugars in the presence of ionic liquid is fairly new. HPLC columns are relatively expensive, so adverse effects on the columns resin must be avoided. A method has been reported for analysing sugar monomers dissolved in  $[\text{C}_4\text{C}_1\text{im}]\text{Cl}$  using the Aminex HPX-87H column.<sup>122</sup> The ionic liquid solution was diluted several fold before the HPLC analysis and the sample centrifuged to remove components that would precipitate in the (aqueous) mobile phase. The drawback of using the Aminex HPX-87H column is its inability to resolve hemicellulose sugars. While glucose gives a distinct peak, the sugars xylose, arabinose, mannose and galactose have very similar elution times and their respective peaks merge into one. As the largest fraction

of the hemicellulose in *Miscanthus* is xylose (75%), the assumption was made that all hemicellulose monomers are xylose. The putative extinction coefficient of *Miscanthus* hemicellulose, calculated from the hemicellulose sugar content of untreated biomass (including xylose, arabinose, mannose and galactose) is similar to the extinction coefficient of pure xylose. The deviation was calculated and was less than 2%. Therefore the error introduced by the over-lapping of the peaks can be neglected. However, the hemicellulose composition in the liquor may be different from the hemicellulose composition in the original biomass, which was not taken into account. For example, it may be possible that the hexoses become enriched relative to the pentoses, as hexoses degrade less readily than pentoses.<sup>35, 122</sup>

Despite these short-comings, the content of monomeric glucose and hemicellulose in the ionic liquid liquor was determined for both  $[C_4C_1im][MeSO_4]_{80\%}$  and  $[C_4C_1im][HSO_4]_{80\%}$  pretreatment and is shown in Figure 87. The amount of dissolved glucose was around 0.5% for both pretreatment liquors. The glucose content rose within the first hour of the pretreatment and remained unchanged thereafter.

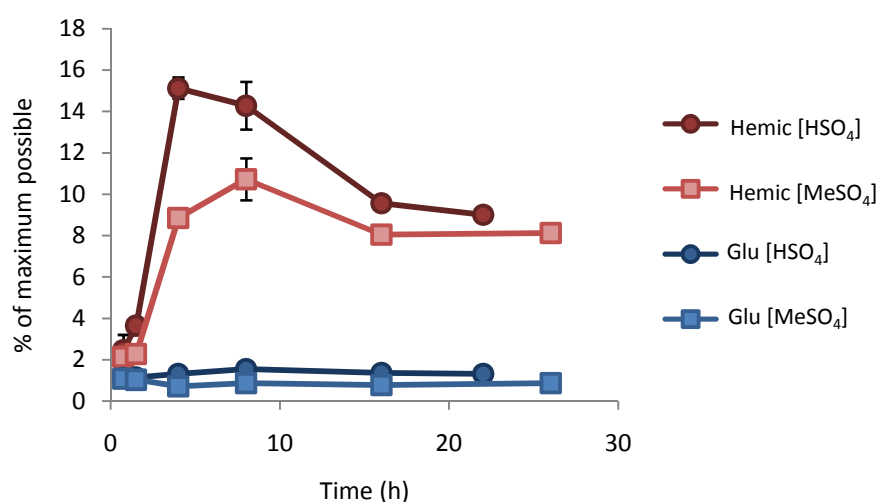


Figure 87: Sugar monomers (hemicellulose sugars and glucose) in  $[C_4C_1im][HSO_4]_{80\%}$  and  $[C_4C_1im][MeSO_4]_{80\%}$  pretreatment liquors released from *Miscanthus* during pretreatment at 120°C.

The amount of hemicellulose monomers peaked around 4 h for  $[C_4C_1im][HSO_4]_{80\%}$ , and around 8 h for  $[C_4C_1im][MeSO_4]_{80\%}$ , and decreased afterwards. This suggests that the solubilised hemicellulose

monomers are converted into other compounds. Xylan hydrolysis is faster than the conversion of xylose to furfural, therefore a transient accumulation of xylose can be expected.<sup>61</sup> In approximation, the xylose concentration at a certain time can be described by the following equation (with  $k_0 > k_1$ ).

$$\frac{d[Xyl]}{dt} = k_0[Xylan] - k_1[Xylose] \quad \text{Eq. 13}$$

An analogous rate law can be written for the formation of HMF from glucose, mannose and other hexoses. The ionic liquid liquor was therefore also analysed for furfural and HMF content and the results are shown in Figure 88. The HMF content increased during the first 30 min and remained practically unchanged afterwards. It can be seen that less than 2% of the original glucan were found as HMF at any time point. The quantity of HMF in the liquor was also very similar for both pretreatment solvents.

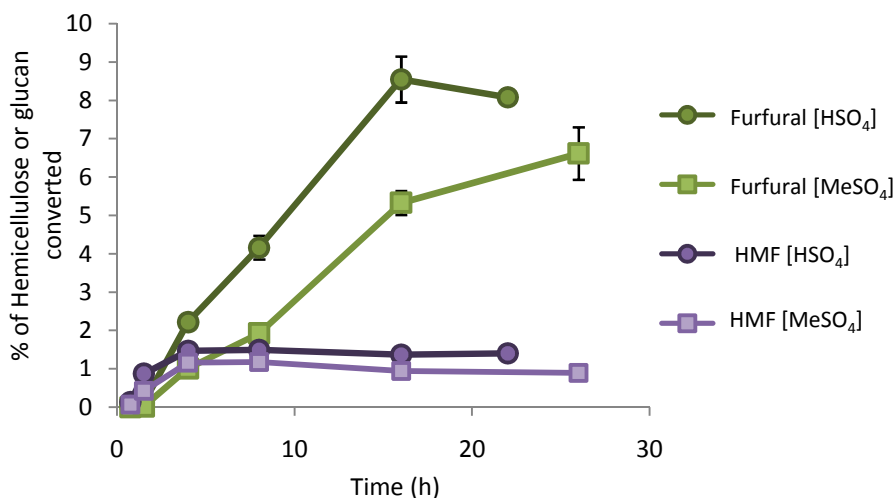


Figure 88: Amount of furfural and 5-hydroxymethylfurfural found in the pretreatment liquor (per biomass). The data were collected after lignin precipitation.

In the case of furfural, the composition of the pretreatment liquor made a significant difference. More 2-furaldehyde was formed during pretreatment with  $[C_4C_1im][HSO_4]_{80\%}$ . This could be due to the higher concentration of acidic anions in this liquor. In the  $[C_4C_1im][MeSO_4]_{80\%}$  liquor, around a third of anions are non-acidic  $[MeSO_4]^-$  (see Figure 81 on p. 184), reducing the amount of available protons in the liquor. It has been shown that both temperature and acid concentration influence the



rate of furfural formation.<sup>61</sup> The lower concentration of acid in [C<sub>4</sub>C<sub>1</sub>im][MeSO<sub>4</sub>]<sub>80%</sub> may therefore slow down the acid-catalysed transformation of xylose into furfural ( $k_1$  in Eq. 13). In addition, it should also decelerate the hydrolysis of xylan to xylose ( $k_0$  in Eq. 13).

The standard deviations for furfural are significantly larger than the deviations seen for HMF. This is unusual, as the data for both substances were obtained using the same chromatograms. Both peaks were well-separated and symmetrically shaped. With the  $R^2$  value being 0.998, the calibration curve for furfural was consistent. This suggests that the HPLC system was capable of quantifying this compound reliably. Therefore a problem with the sample preparation is suspected, which affects the accuracy of furfural quantification but does not interfere with HMF.

The liquor samples that were used for HMF and furfural quantification were taken after precipitating the lignin. This means that the liquor had been subjected to a number of processing steps, *e.g.* methanol had been added during the washing step and removed *via* evaporation before the lignin precipitation. Furfural is volatile, but has a high boiling point of 160°C. The methanol was distilled out under mild vacuum and mild heating (40°C). However, furfural can form an azeotrope with water which boils at 98°C (at atmospheric pressure).<sup>61</sup> This azeotrope contains 45% furfural. Information about a possible methanol furfural azeotrope could not be obtained. Since water was present in the pretreatment liquor, removal of furfural *via* the azeotrope is a likely explanation for the large error bars. HMF, which is even less volatile than furfural, was not affected by the sample processing. If this is true, the furfural content before distillation is expected to be significantly higher than determined in Figure 88.

For selected conditions, the furfural quantification was performed on samples before the evaporation and the amounts of sugar monomer and furfural without the bias are shown in Figure 89. These data show that the furfural formation was limited in the first two hours of the pretreatment, but increased significantly when the pretreatment time was

extended. 33% of all hemicelluloses had been converted to furfural after 22 h, while 8% of the hemicellulose was present as monomers.

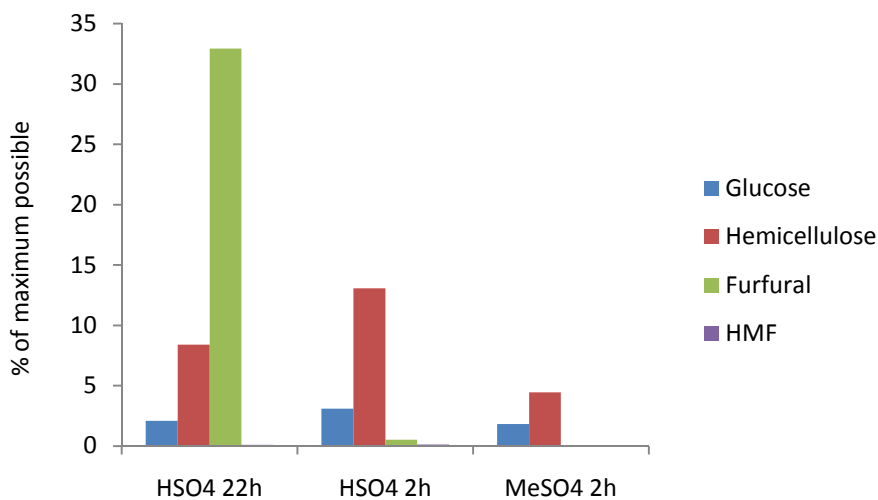


Figure 89: Amount of sugar monomers and furfurals dissolved in the ionic liquid liquor  $[\text{C}_4\text{C}_1\text{im}][\text{HSO}_4]_{80\%}$  or  $[\text{C}_4\text{C}_1\text{im}][\text{MeSO}_4]_{80\%}$ . Samples were taken immediately after the pretreatment, before the lignin precipitation.

These furfural yields are higher than reported by others. Sievers *et al.* obtained a furfural yield of 13% when treating xylose in  $[\text{C}_4\text{C}_1\text{im}]\text{Cl}$  which had been acidified with catalytic quantities of  $\text{H}_2\text{SO}_4$ . 21% of the xylose was converted into solid degradation products.<sup>123</sup> The fate of the remaining xylose (66%) was not investigated. Tao *et al.* have reported better conversion, claiming a 91% conversion of xylose into furfural in mixture of water and the ionic liquid 1-(4-sulfonic acid)butyl-3-methylimidazolium hydrogen sulfate.<sup>194</sup> This shows that the presence of water may increase the furfural yield. The furfural was recovered by distillation after the ionic liquid pretreatment.<sup>194</sup> Extraction with ethyl acetate or other water-immiscible organic solvents has also been employed.<sup>195</sup> Tao *et al.* found that other Lewis or Brønsted acid catalysts (e.g. simple sulfuric acid) in place of the ionic liquid gave slightly lower but comparable yields,<sup>194</sup> questioning whether an “expensive ionic liquid-based acid catalyst is necessary to obtain furfural.

The low HMF yield obtained in this study can be explained by the propensity of this compound to be converted to levulinic and formic acids in the presence of water (for the reaction mechanism see section 1.7.2.2 on p. 54). In order to obtain a more realistic picture of the degradation of

hexoses, the levulinic acid and formic acid should be quantified, which was not accomplished in this study.

In conclusion, the fate of 59% of the total hemicellulose could be traced: 18% were recovered with the pulp and released during saccharification, while 8% appeared as sugar monomers or as furfurals (33%) in the liquor. The remaining 41% could be present in the pretreatment liquor as oligomers or as degradation products other than HMF or furfural.

### 6.2.15 *The influence of the ionic liquid anion*

The effect of the ionic liquid anion on biomass processing has already been a focus in the previous chapter. It was shown that the nature of the anion is an important factor in promoting wood chip swelling and dissolution and it affects other properties such as stability or hygroscopicity. This chapter focuses on the enzymatic digestibility of the cellulose and hemicellulose fraction and the biomass fractionation. Exploration of the anion effect on the glucose yield and pulp composition will complement the data already obtained. The effectiveness of the pretreatment with  $[\text{C}_4\text{C}_1\text{im}][\text{MeSO}_4]_{80\%}$  and  $[\text{C}_4\text{C}_1\text{im}][\text{HSO}_4]_{80\%}$  was compared to the pretreatment with mixtures of water and other 1,3-dialkylimidazolium ionic liquids.

The effectiveness of a pretreatment depends on many variables, for example temperature, time, feedstock and particle size. Therefore a comparison between different ionic liquids is best conducted using identical conditions and the same feedstock. The condition that has been investigated most thoroughly so far was the pretreatment of *Miscanthus* with a mixture of 80 vol% ionic liquid and 20 vol% water at 120°C for 22 h. This condition was also selected for investigating the anion effect on the saccharification yields. The ionic liquid anions investigated were acetate, chloride, methanesulfonate and triflate. Acetate and chloride based ionic liquids have been used for pretreatment previously, particularly  $[\text{C}_2\text{C}_1\text{im}][\text{MeCO}_2]$ .<sup>114, 117, 136, 163</sup> Methanesulfonate,  $[\text{MeSO}_3]^-$ , can be regarded as a hydrolytically stable analogue of methylsulfate,  $[\text{MeSO}_4]^-$ . It resembles the methyl sulfate anion structurally and has

similar hydrogen-bond basicity (slightly higher). It also contains a sulfonyl functionality, which was part of the anions in the ionic liquid (mixture) 1-ethyl-3-methylimidazolium alkylbenzenesulfonate,  $[\text{C}_2\text{C}_1\text{im}][\text{ABS}]$ .  $[\text{C}_2\text{C}_1\text{im}][\text{ABS}]$ ;<sup>161</sup> this ionic liquid mixture has been successfully applied for the fractionation of sugar cane bagasse.  $[\text{C}_4\text{C}_1\text{im}][\text{OTf}]$  has been reported to have high lignin solubility, but did not show particularly strong interactions with the cell wall material in the experiments presented in Chapter 5.

#### 6.2.15.1 The effect of the anion on the composition

The biomass composition and the mass loss after pretreatment with various ionic liquid water mixtures are depicted in Figure 90. The data are ordered according to the hydrogen-bond basicity ( $\beta$  parameter) of the ionic liquids, with high values on the left. The figure shows that  $[\text{C}_4\text{C}_1\text{im}][\text{HSO}_4]_{80\%}$  caused the greatest mass loss, concomitant with a extended removal of lignin and hemicellulose.

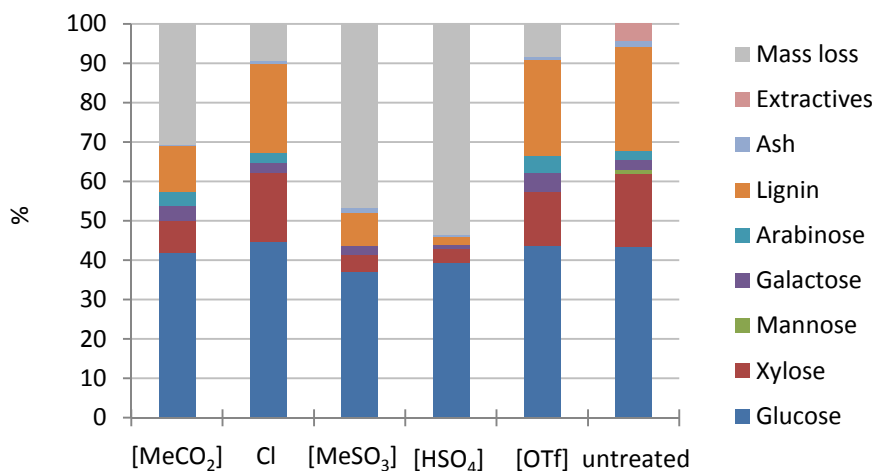


Figure 90: The impact of pretreatment with 80/20% dialkylimidazolium ionic liquid water mixtures on the composition of *Miscanthus*. The anions are ordered according to their  $\beta$  parameter (high values on the left). The cation was 1-butyl-3-methylimidazolium, except for  $[\text{C}_2\text{C}_1\text{im}][\text{MeCO}_2]$ .

The second best cellulose fractionation was observed with  $[\text{C}_4\text{C}_1\text{im}][\text{MeSO}_3]_{80\%}$ . The hemicellulose content was reduced to similar levels, but the lignin content was significantly higher compared to the  $[\text{C}_4\text{C}_1\text{im}][\text{HSO}_4]_{80\%}$  pulp.

A significant reduction of the hemicellulose and lignin content was observed after pretreatment with  $[\text{C}_2\text{C}_1\text{im}][\text{MeCO}_2]_{80\%}$ . However, the fractionation was significantly less advanced than after  $[\text{C}_4\text{C}_1\text{im}][\text{MeSO}_3]_{80\%}$  and after  $[\text{C}_4\text{C}_1\text{im}][\text{HSO}_4]_{80\%}$  treatment. The effect of  $[\text{C}_4\text{C}_1\text{im}]\text{Cl}_{80\%}$  on the biomass composition was surprisingly small. The least impact on the composition was exerted by  $[\text{C}_4\text{C}_1\text{im}][\text{OTf}]_{80\%}$ .

#### 6.2.15.2 The effect of the anion on the enzymatic digestibility

The highest glucose yields were obtained after pretreatment of *Miscanthus* with  $[\text{C}_4\text{C}_1\text{im}][\text{MeSO}_3]_{80\%}$  and  $[\text{C}_4\text{C}_1\text{im}][\text{HSO}_4]_{80\%}$  and a subsequent enzymatic saccharification (Figure 91). Pretreatment with  $[\text{C}_2\text{C}_1\text{im}][\text{MeCO}_2]_{80\%}$  resulted in good glucose yields, but did not induce the same level of digestibility. The glucose yields obtained after treatment with  $[\text{C}_4\text{C}_1\text{im}]\text{Cl}_{80\%}$  and  $[\text{C}_4\text{C}_1\text{im}][\text{OTf}]_{80\%}$  were very low, not higher than the yields obtained from untreated biomass.

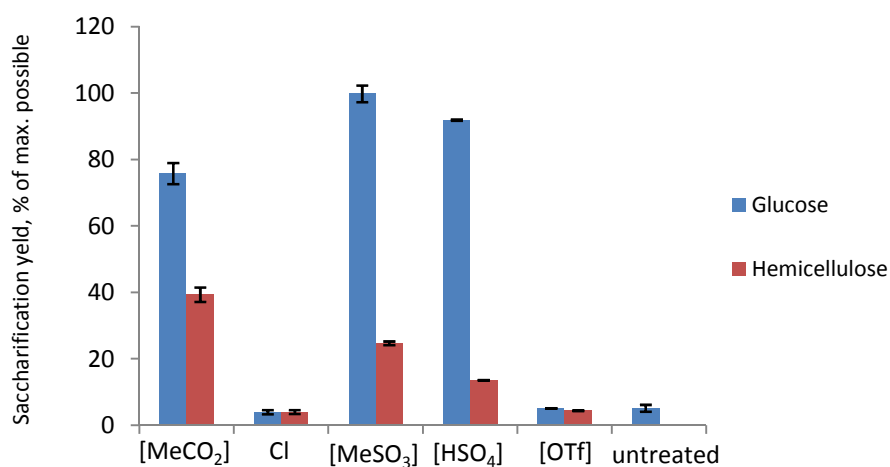


Figure 91: Anion effect of saccharification yields after pretreatment with 80/20% mixtures of 1,3-dialkylimidazolium ionic liquid and water at 120°C for 22 h. Yields were determined after 96 h of saccharification. The cation was  $[\text{C}_4\text{C}_1\text{im}]^+$ , with exception of  $[\text{C}_2\text{C}_1\text{im}][\text{MeCO}_2]$ .

A closer look at saccharification yields reported in the literature obtained with chloride based ionic liquids, such as  $[\text{C}_4\text{C}_1\text{im}]\text{Cl}$  and 1-allyl-3-methylimidazolium chloride,  $[\text{C}=\text{C}_2\text{C}_1\text{im}]\text{Cl}$ , reveals that the yields are only moderate in many cases. A glucose yield of around 20% was reported from regenerated ground eucalyptus after pretreatment with the

chloride based ionic liquid  $[\text{C}=\text{C}_2\text{C}_1\text{im}]\text{Cl}$  at  $120^\circ\text{C}$  for 5 h.<sup>176</sup> Better yields have been obtained from corn stover, releasing glucose almost quantitatively.<sup>192</sup> It should be noted, however, that corn stover is relatively digestible, even when it has received no pretreatment at all ( $\approx 25\%$  of glucose released from untreated corn stover).<sup>192</sup> The high water content in  $[\text{C}_4\text{C}_1\text{im}]\text{Cl}_{80\%}$  could be responsible for the particularly low saccharification yields observed in this study and suggests that water might be more deactivating for chloride based ionic liquids than for others.

A slightly different pattern was observed for the hemicellulose yield. The highest hemicellulose yield was achieved with  $[\text{C}_2\text{C}_1\text{im}][\text{MeCO}_2]_{80\%}$ . 39% of the original hemicellulose was enzymatically released. 63% of hemicellulose was recovered in the  $[\text{C}_2\text{C}_1\text{im}][\text{MeCO}_2]_{80\%}$  pretreated pulp, so roughly two thirds of the hemicellulose was accessible to the hemicellulose hydrolases. Hemicellulose recovery after  $[\text{C}_4\text{C}_1\text{im}][\text{MeSO}_3]_{80\%}$  and  $[\text{C}_4\text{C}_1\text{im}][\text{HSO}_4]_{80\%}$  pretreatment was 25% and 14%. This means that almost all of the hemicellulose recovered with the pulp was accessible to hemicellulose hydrolases (residual hemicellulose content in the pulp was 27% and 18%, respectively). The hemicellulose release from  $[\text{C}_4\text{C}_1\text{im}]\text{Cl}_{80\%}$  and  $[\text{C}_4\text{C}_1\text{im}][\text{OTf}]_{80\%}$  pretreated pulp was low. This suggests, together with the low glucose yields and the small changes compositional changes, that the liquors containing chloride and trifluoromethanesulfonate ions have very little effect on the features referring recalcitrance to the cell wall structure. The improved accessibility of hemicellulose after treatment with  $[\text{C}_2\text{C}_1\text{im}][\text{MeCO}_2]_{80\%}$ ,  $[\text{C}_4\text{C}_1\text{im}][\text{MeSO}_3]_{80\%}$  and  $[\text{C}_4\text{C}_1\text{im}][\text{HSO}_4]_{80\%}$  is could be due to the removal of the lignin, while the removal of acetyl groups from the xylan backbone may also help. The deacetylation of xylan has been observed for treatment of maple wood with  $[\text{C}_2\text{C}_1\text{im}][\text{MeCO}_2]$ .<sup>163</sup> The cleavage of lignin-carbohydrate complexes would also increase the accessibility to hemicellulose.

The mentioned alterations may be more complete in the presence of methanesulfonate and hydrogen sulfate anions than in the presence of acetate anion, explaining the superior yields obtained with  $[\text{C}_4\text{C}_1\text{im}][\text{MeSO}_3]_{80\%}$  and  $[\text{C}_4\text{C}_1\text{im}][\text{HSO}_4]_{80\%}$ .

### 6.2.15.3 The effect of the anion on the sugar solubilisation and the generation of furfurals

The effect of the anion on the carbohydrates which were solubilised during the ionic liquid treatment was also explored. The results are shown in Figure 92. Pretreatment with  $[\text{C}_2\text{C}_1\text{im}][\text{MeCO}_2]$  generated very low amounts of monomers and practically no furfurals. Since a significant portion of the hemicellulose had been solubilised during pretreatment (Figure 90), the low abundance of monomers could be due to the solubilised sugars being mostly in oligomeric form. This is in agreement with the observations of Arora *et al.* who investigated the presence of monomers and oligomers in the  $[\text{C}_2\text{C}_1\text{im}][\text{MeCO}_2]$  supernatant after pretreatment of switchgrass at 120°C for 5 days.<sup>136</sup> Analysis with high-performance anion-exchange chromatography (HPAC) revealed that even after such a long pretreatment almost all solubilised carbohydrates were still in oligomeric form. Statistically, the probability of xylose oligomers breaking is higher in the middle of the chain than at the ends,<sup>196</sup> so even if hydrolysis occurs, the abundance of monomers should be low until the oligomers hydrolysis has sufficiently advanced.

Substantial quantities of monomers and furfurals were found in the methanesulfonate and hydrogen sulfate containing liquors. 47.0% and 41.3% of the hemicellulose, respectively, was detected as hemicellulose monomers or 2-furaldehyde in these liquors. The product ratio varied considerably. Monomeric sugars prevailed in the methanesulfonate liquor, while the majority of the monomers had been converted to furfural in the hydrogen sulfate liquor. Again, this can be explained by the differing acidity of the ionic liquids.

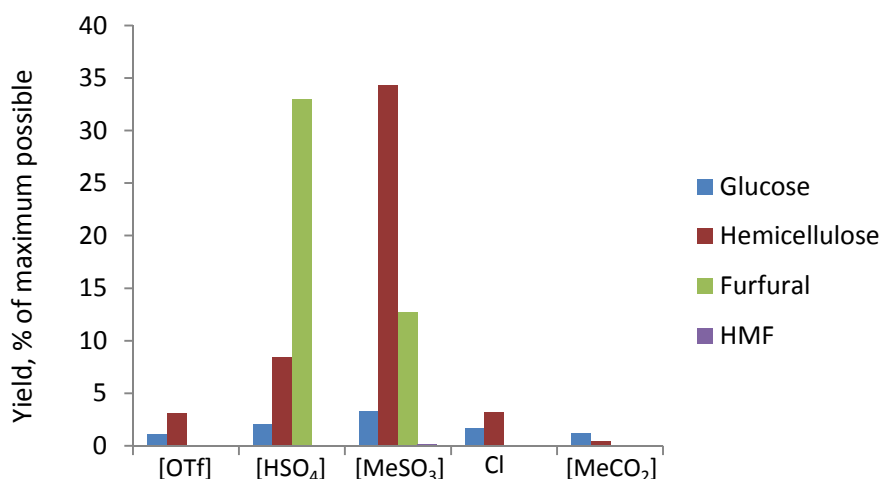


Figure 92: Concentrations of solubilised sugars and sugar dehydration products in 80 vol% ionic liquid liquors after pretreatment of *Miscanthus*.

Both  $[\text{C}_4\text{C}_1\text{im}]\text{Cl}_{80\%}$  and  $[\text{C}_4\text{C}_1\text{im}][\text{OTf}]_{80\%}$  liquors displayed a low abundance of monomers and dehydration products, which does not come as a surprise, given the negligible solubilisation of carbohydrates achieved by these liquors (see also Figure 90).

In aqueous media, the activation energy of HMF formation from hexoses is greater than the activation energy of HMF decomposition to levulinic acid and formic acid (see section 1.7.2.2). This makes it difficult to isolate HMF in high yields<sup>197</sup> and would also explain the low amount of HMF (<1%) found in all ionic liquid liquors (irrespective of the anion).

#### 6.2.15.4 The effect of the anion on the lignin recovery

The anion also had an effect on the amount of precipitate that could be recovered and on the extent of lignin removal (delignification). Both the delignification and the precipitate yield are shown in Figure 93. Generally, delignification and precipitate yield appeared to be linked. The more lignin was removed from the biomass, the more precipitate was obtained. The precipitate yield was generally lower than the delignification.

The lignin recovery was best from  $[\text{C}_4\text{C}_1\text{im}][\text{HSO}_4]_{80\%}$ . The amount of isolated precipitate was 64% of the original lignin content. This was



followed by a 31% recovery from  $[\text{C}_4\text{C}_1\text{im}][\text{MeSO}_3]_{80\%}$  and a 18% recovery from  $[\text{C}_4\text{C}_1\text{im}][\text{MeCO}_2]_{80\%}$ .

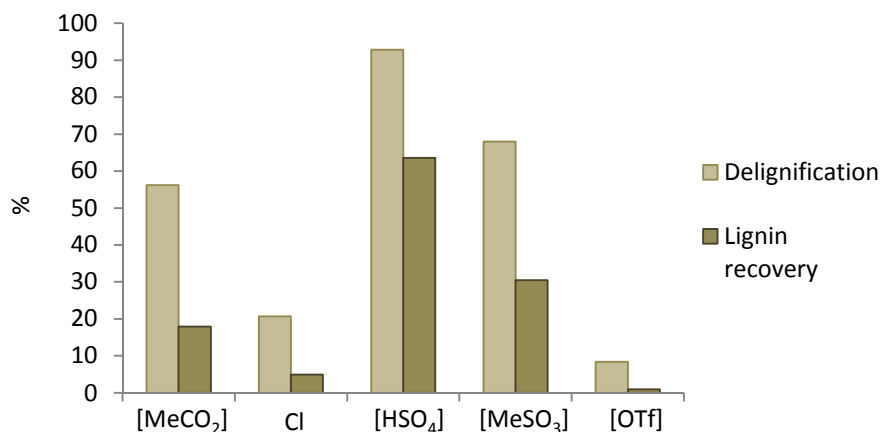


Figure 93: The influence of the anion of 1,3-dialkylimidazolium ionic liquids on the delignification and the lignin yield. *Miscanthus* flour was pretreated with ionic liquid water mixtures at 120°C for 22 h. The ionic liquid cation was  $[\text{C}_4\text{C}_1\text{im}]^+$ , except in  $[\text{C}_2\text{C}_1\text{im}][\text{MeCO}_2]$ .

Kraft pulp lignin has been reported to be soluble in  $[\text{C}_4\text{C}_1\text{im}][\text{OTf}]$ .<sup>75</sup> However, delignification with this ionic liquid was poor, albeit in an ionic liquid water mixture, not pure. A reason for these conflicting observations could be that solubilisation of a chemically altered lignin preparation is different from the extraction of native lignin from biomass. A picture of purified and dried precipitate is shown in Figure 94.



Figure 94: *Miscanthus* lignin precipitated from the pretreatment liquor. Left: after 22 h from  $[\text{C}_4\text{C}_1\text{im}][\text{HSO}_4]_{80\%}$ ; middle: after 22 h from  $[\text{C}_4\text{C}_1\text{im}][\text{MeSO}_3]_{80\%}$ ; right: after 2 h from  $[\text{C}_4\text{C}_1\text{im}][\text{HSO}_4]_{80\%}$ .

### 6.2.16 The effect of the Kamlet-Taft parameter $\beta$ on the saccharification yield

The Kamlet-Taft parameter  $\beta$  is a measure for the hydrogen-bond basicity of solvents, including ionic liquids. It served well to predict wood chip swelling (chapter 5) and cellulose solubility<sup>147</sup> in ionic liquids, but fails to reliably predict the enhancement of biomass digestibility (Figure 95).

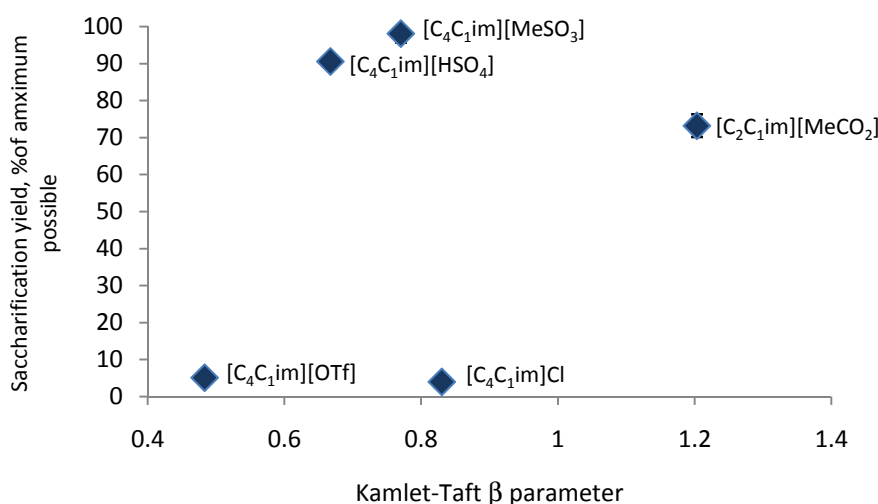


Figure 95: The Kamlet-Taft  $\beta$  parameter of the pure ionic liquid plotted against the glucose yield after enzymatic saccharification of the pulp after pretreatment with 80/20vol% ionic liquid water mixtures at 120°C for 22 h. A correlation between the glucose yield and the Kamlet-Taft parameter, which represents the hydrogen-bond basicity of the ionic liquid anion, cannot be established.

Instead, it will be shown in this section that efficient enzymatic saccharification of the cellulose fraction is (inversely) related to the lignin and hemicellulose content (Figure 96 left). The S-shaped dependency between saccharification yield and lignin removal by ionic liquid treatment has been observed by others.<sup>154</sup> The enzymatic digestibility was also correlated with residual hemicellulose content (Figure 96, on the right). It is, however, less clear than the correlation with the lignin content. Lignin and hemicellulose form a covalently cross-linked coating around the cellulose fibrils (Figure 5 on p. 34), impeding access of the enzymes to the fibrils. Therefore it seems logical that the removal of both components should increase the enzymatic digestibility of cellulose. These results suggest that ionic liquids properties other than the anion's

hydrogen-bond basicity are (also) responsible for the enhancement of lignocellulose digestibility after ionic liquid pretreatment.

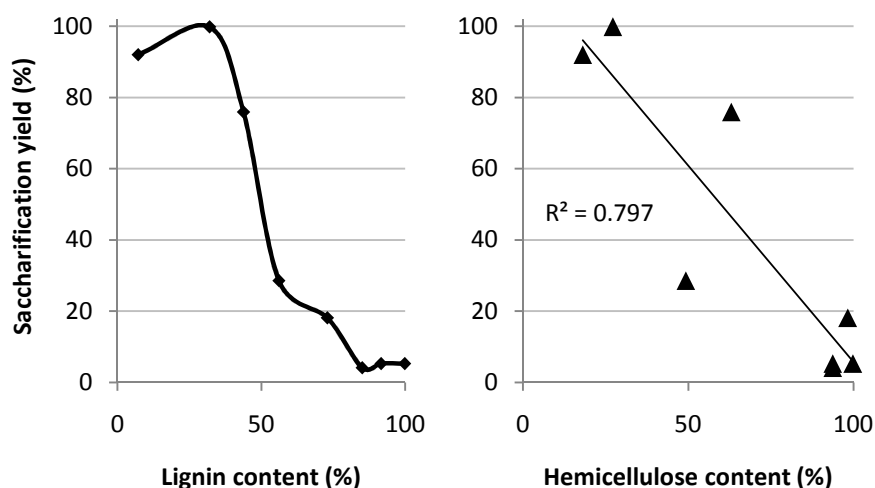


Figure 96: Correlation between lignin removal and hemicellulose content in *Miscanthus* pulp after pretreatment with 1,3-dialkylimidazolium ionic liquids and the enzymatic cellulose digestibility.

### 6.2.17 The effect of the lignocellulose type: pretreatment of willow and pine with $[C_4C_1im][HSO_4]_{80\%}$ and $[C_2C_1im][MeCO_2]_{80\%}$

So far, the pretreatment of *Miscanthus* was the focus of this work. However, a desired characteristic of an industrially relevant pretreatment option is that it can cope with a range of feedstocks. Therefore the treatment of wood lignocellulose (hardwood and softwood) was examined to establish the effectiveness of  $[C_4C_1im][HSO_4]_{80\%}$  treatment on more recalcitrant substrates. As a comparison, the use of  $[C_2C_1im][MeCO_2]_{80\%}$  was also investigated.

#### 6.2.17.1 The composition of willow and pine before and after pretreatment

The effect of  $[C_4C_1im][HSO_4]_{80\%}$  treatment at 120°C for 22 h on ground willow and pine is shown in Figure 97. The removal of lignin and hemicellulose from willow was extensive, while delignification and hemicellulose removal with  $[C_4C_1im][HSO_4]_{80\%}$  were less complete in the case of pine wood.

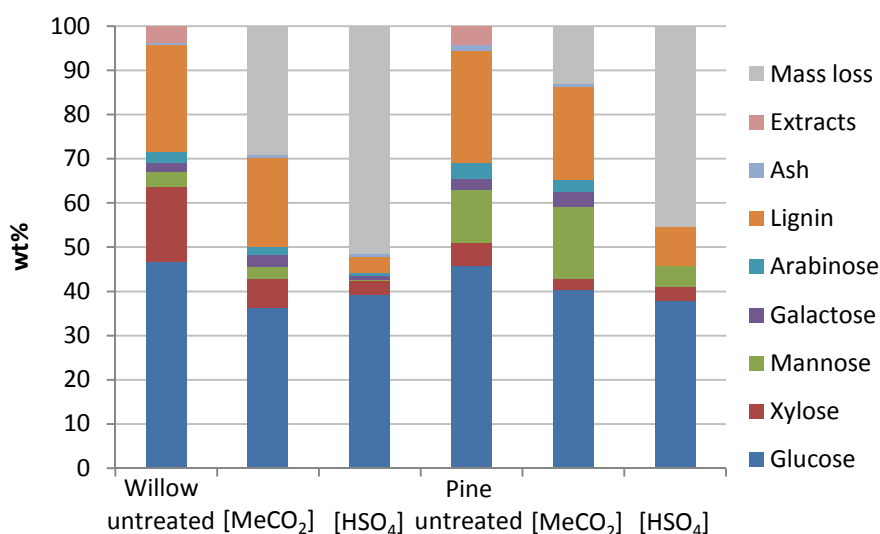


Figure 97: Composition of willow and pine flour before and after pretreatment with  $[C_4C_1im][HSO_4]_{80\%}$  and  $[C_2C_1im][MeCO_2]_{80\%}$ .

Figure 97 also shows the effect of  $[C_2C_1im][MeCO_2]_{80\%}$  pretreatment on pine and willow. Reduced delignification and hemicellulose removal was observed compared to  $[C_4C_1im][HSO_4]_{80\%}$  pretreatment for both biomass types. In fact, the  $[C_2C_1im][MeCO_2]_{80\%}$  liquor had surprisingly little impact on the composition of pine. Although the trend established for ionic liquids (hydrogen sulfate based ionic liquid more effective than acetate based ionic liquid) seems to be also valid for biomass types other than *Miscanthus*, it is shown that the type of biomass can have a significant impact on the effectiveness of the pretreatment. The reasons for this are thought to be the thicker cell walls of wood lengthening the pretreatment time and the more hydrolysis resistant guaiacyl-rich lignin in softwood in particular.<sup>39</sup> The fractionation achieved with softwood under experimental conditions used in this study is not satisfying and requires substantial optimisation.

#### 6.2.17.2 The effect of the biomass type on the glucose yield

The glucose yields obtained after enzymatic saccharification of willow and pine pulps shown are in Figure 98. They reflect roughly the amount of delignification and hemicellulose removal brought about by the ionic liquid treatment. Overall, *Miscanthus* pretreated with  $[C_4C_1im][HSO_4]_{80\%}$

exhibited the highest cellulose digestibility. The second best yield was obtained from willow after  $[\text{C}_4\text{C}_1\text{im}][\text{HSO}_4]_{80\%}$  pretreatment.

The order of glucose yields was *Miscanthus*/ $[\text{C}_4\text{C}_1\text{im}][\text{HSO}_4]_{80\%}$  > willow/ $[\text{C}_4\text{C}_1\text{im}][\text{HSO}_4]_{80\%}$  > *Miscanthus*/ $[\text{C}_2\text{C}_1\text{im}][\text{MeCO}_2]_{80\%}$  > willow/ $[\text{C}_2\text{C}_1\text{im}][\text{MeCO}_2]_{80\%}$  > pine/ $[\text{C}_4\text{C}_1\text{im}][\text{HSO}_4]_{80\%}$  > pine/ $[\text{C}_2\text{C}_1\text{im}][\text{MeCO}_2]_{80\%}$ . This suggests that ionic liquid pretreatment is particularly effective with *Miscanthus*. The saccharification yields from pretreated pine were surprisingly low in both cases. Significant delignification (66%) and hemicellulose removal (69%) of pine were accomplished with  $[\text{C}_4\text{C}_1\text{im}][\text{HSO}_4]_{80\%}$  pretreatment (Figure 97), however, the glucose yield was only 30% of the theoretically possible yield.

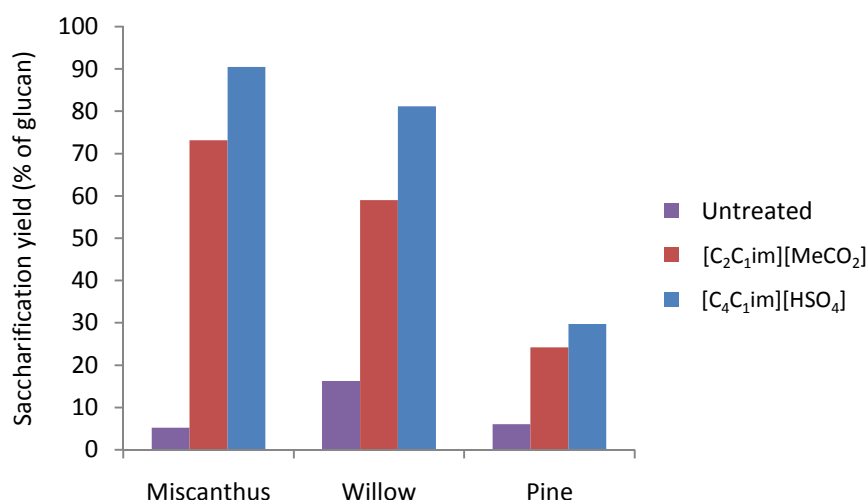


Figure 98: Glucose yield after enzymatic hydrolysis of various feedstocks pretreated with  $[\text{C}_4\text{C}_1\text{im}][\text{HSO}_4]_{80\%}$  at 120°C for 22 h (96 h saccharification).

The saccharification yield obtained from willow pretreated with  $[\text{C}_2\text{C}_1\text{im}][\text{MeCO}_2]_{80\%}$  is in good agreement with published yields obtained for poplar using the same ionic liquid water mixture. The treatment resulted in the release of 49% of the glucose.<sup>192</sup> The same authors reported that the glucose yield was 85%, when no extra water was added. A similar reduction of the glucose yield upon addition of 20 vol% water to  $[\text{C}_2\text{C}_1\text{im}][\text{MeCO}_2]$  was observed by Doherty *et al.*<sup>154</sup>

The time course of the enzymatic saccharification reaction is depicted in Figure 99. It shows that the saccharification of ground *Miscanthus* was completed after 96 h, while liberation of glucose from pretreated willow and pine still continued. It appears that the final glucose yield obtained from willow could be in the same range as the yield from *Miscanthus*.

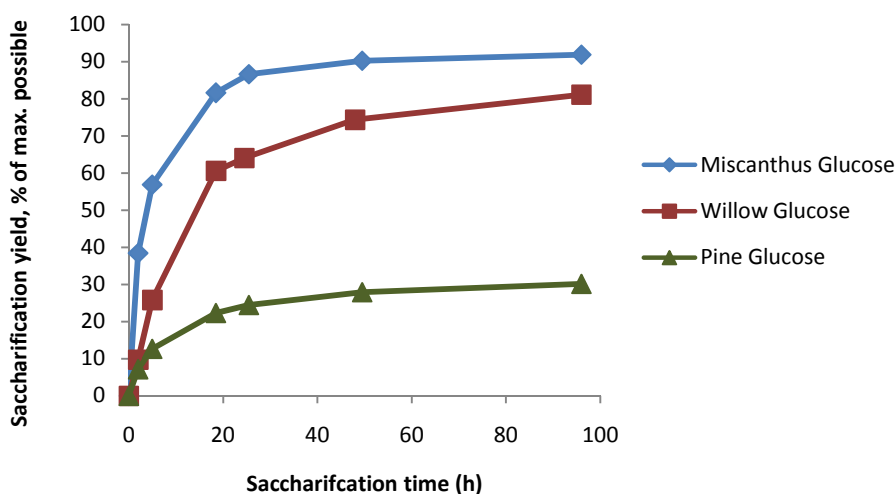


Figure 99: Enzymatic saccharification of various lignocellulose pulps obtained after pretreatment with  $[C_4C_{1im}][HSO_4]_{80\%}$  at 120°C for 22 h.

### 6.2.17.3 The effect of the biomass type on the concentration of solubilised sugars and furfurals

The amounts of solubilised sugar monomers and furfurals in the ionic liquid liquor after pretreatment of willow and pine flour are displayed in Figure 100.

The combined quantities of solubilised monomeric hemicellulose and furfurals present in the pretreatment liquor were similar for all biomass types. 41% of the hemicellulose in *Miscanthus*, 34% of the willow hemicellulose and 36% of the pine hemicellulose were detected as either monomers or 2-furaldehyde.

Compared to the *Miscanthus* liquor, less furfural was detected in the willow and pine pretreatment liquors. Instead, more intact hemicellulose monomers were found. This could be due to the varying hemicellulose composition. Hard- and softwoods contain less pentoses than grasses. Particularly, pine wood contains large amounts of mannose (12%) and little pentoses (9%) compared to *Miscanthus* (1% and 20%).

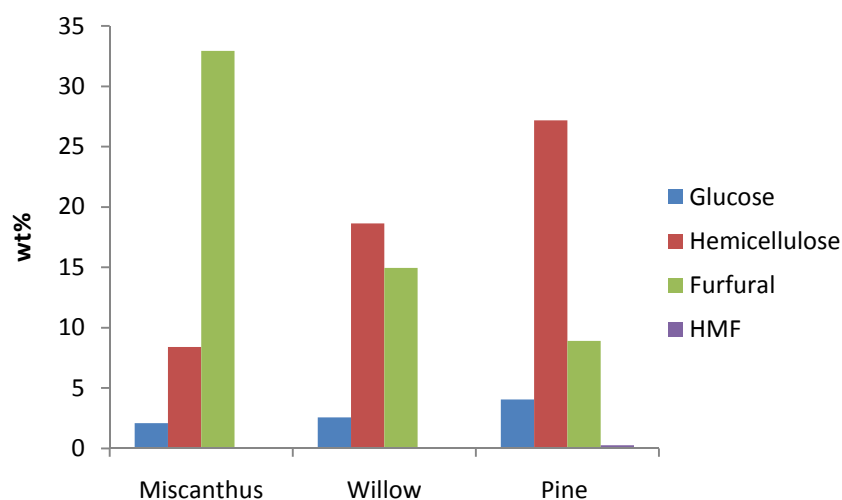


Figure 100: Sugar monomers and furfurals found in the  $[C_4C_1im][HSO_4]_{80\%}$  pretreatment liquor after pretreatment of various lignocellulose feedstocks at  $120^\circ C$  for 22 h.

#### 6.2.17.4 The effect of the biomass type on the delignification and the lignin recovery

The delignification and precipitate yield are shown in Figure 101. The delignification was generally better with  $[C_4C_1im][HSO_4]_{80\%}$  than with  $[C_2C_1im][MeCO_2]_{80\%}$ . Lignin recovery was generally higher from the  $[C_4C_1im][HSO_4]_{80\%}$  liquors. This is probably due to the more extensive delignification, but could also be affected by the pH of the liquor. Lowering the pH of ionic liquid liquors has been shown to improve lignin recovery.<sup>161</sup> Under acidic conditions, more hemicellulose could have been converted into pseudo-lignins, also contributing to the yield of precipitate.

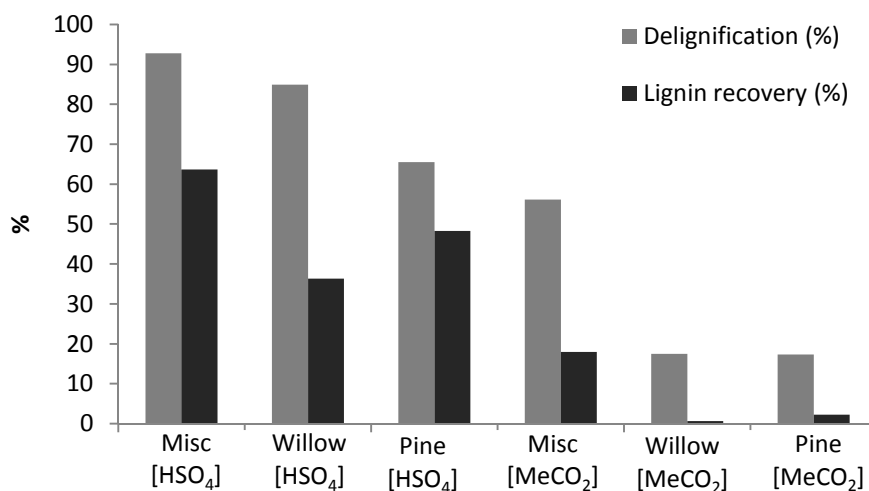


Figure 101: Delignification and recovery of lignin after pretreatment of various feedstocks with 80/20% ionic liquid/water mixtures at 120°C for 22 h. The pretreatment liquors were [C<sub>4</sub>C<sub>1</sub>im][HSO<sub>4</sub>]<sub>80%</sub> and [C<sub>2</sub>C<sub>1</sub>im][MeCO<sub>2</sub>]<sub>80%</sub>. Only one sample per measurement was processed. Misc: *Miscanthus*.

The comparably low level of delignification with [C<sub>2</sub>C<sub>1</sub>im][MeCO<sub>2</sub>]<sub>80%</sub> could be due to the water sensitivity of this liquor, which has been shown reduce delignification. A negative correlation between the water content and lignin removal from maple wood flour by [C<sub>2</sub>C<sub>1</sub>im][MeCO<sub>2</sub>] pretreatment has been reported by Doherty *et al.*<sup>154</sup>

### 6.2.18 Pretreatment of *Miscanthus* and willow chips with [C<sub>4</sub>C<sub>1</sub>im][HSO<sub>4</sub>]<sub>80%</sub>

Both *Miscanthus* and willow appeared to be suitable substrates for pretreatment with [C<sub>4</sub>C<sub>1</sub>im][HSO<sub>4</sub>]<sub>80%</sub>. In most experiments mentioned in this chapter, ground biomass was used as substrate. However, a truly energy-efficient pretreatment process is likely to use chipped biomass. Therefore the pretreatment of chip-sized willow and *Miscanthus* was also carried out. The phenomenological impact of the pretreatment is illustrated in Figure 102. For *Miscanthus* chips, substantial disintegration of the less recalcitrant inner pith was observed. A fine powder settled on the filter paper during filtration, which is in agreement with the effect observed after the very first [C<sub>4</sub>C<sub>1</sub>im][MeSO<sub>4</sub>] treatment (section 6.2.1).





Figure 102: *Miscanthus* and willow chips pretreated with  $[\text{C}_4\text{C}_1\text{im}][\text{HSO}_4]_{80\%}$  at  $120^\circ\text{C}$  for 22 h.

Willow chips also underwent significant changes upon pretreatment. In addition to the discoloration, the chips were significantly easier to break up into smaller pieces (Figure 102, a blunt spatula was used for breaking this chip). This suggests that the ionic liquid may generally weaken the lignocellulose structure. This could be exploited and pretreatment of chips with  $[\text{C}_4\text{C}_1\text{im}][\text{HSO}_4]_{80\%}$  prior to grinding could reduce the energy required for comminution. An untreated and a pretreated willow chip are shown in Figure 103. The collapse of the woody structure is less pronounced than observed for pine chips after  $[\text{C}_4\text{C}_1\text{im}][\text{MeCO}_2]$  treatment (Figure 61), probably due to preservation of the fibrous structure of cellulose.

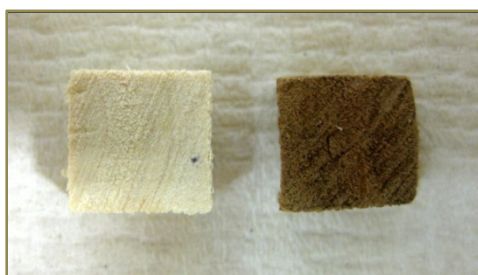


Figure 103: Air-dried willow chips before and after  $[\text{C}_4\text{C}_1\text{im}][\text{HSO}_4]_{80\%}$  pretreatment at  $120^\circ\text{C}$  for 22 h.

The glucose yields obtained after incubating chipped lignocellulose with cellulose enzymes are depicted in Figure 104. The hydrolysis of *Miscanthus* pulp proceeded faster than the hydrolysis of willow, but came to a halt after 48 h. Only 70% of the glucose was liberated during enzymatic saccharification, compared to >85% obtained from ground

material. A visible check of the residue showed that the left-over material stemmed from the outer ring, which features thicker cell walls than the pith. The saccharification yield from willow chips was surprisingly good, reaching levels that were comparable to that of ground biomass (84% glucose yield compared to 81% from ground willow). The denser cell wall structure of hardwood and the reduced surface area of chips were probably responsible for the slower saccharification.

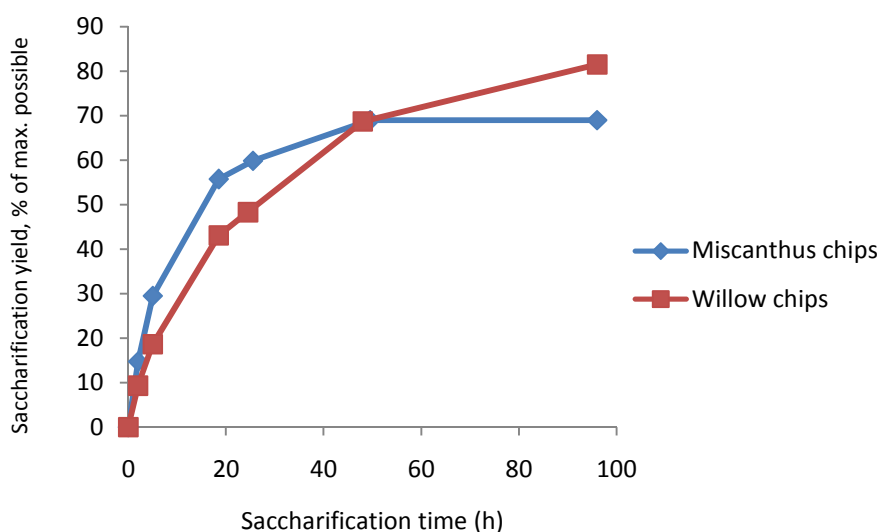


Figure 104: Saccharification of *Miscanthus* and willow chips after pretreatment with  $[C_4C_{1im}][HSO_4]_{80\%}$  for 22 h at 120°C

### 6.2.19 Treatment of cellulose with $[C_4C_{1im}][HSO_4]$ and $[C_4C_{1im}][MeSO_4]$

In Chapter 5, it was reported that 1-butyl-3-methylimidazolium methyl sulfate,  $[C_4C_{1im}][MeSO_4]$ , could not induce strong swelling and dissolution of pine chips as could  $[C_4C_{1im}][MeCO_2]$  and  $[C_4C_{1im}][Me_2PO_4]$ , which suggests that it cannot dissolve cellulose. To confirm the insolubility of cellulose in this ionic liquid as well as in  $[C_4C_{1im}][HSO_4]$ , microcrystalline cellulose (Avicel) was treated in these ionic liquids. For comparison, Avicel was also pretreated with the cellulose-solubilising ionic liquids  $[C_4C_{1im}][MeCO_2]$  and  $[C_2C_{1im}][MeCO_2]$ . The conditions were chosen to be comparable with the lignocellulose pretreatment primarily used in this chapter: 120°C and 22

h. Vacuum-dried ionic liquids were used as well as mixtures containing 20% water.

Homogenous cellulose solutions were only obtained in pure  $[\text{C}_2\text{C}_1\text{im}][\text{MeCO}_2]$  and  $[\text{C}_4\text{C}_1\text{im}][\text{MeCO}_2]$ . However, upon addition of the antisolvent water, a voluminous precipitate was also observed for the cellulose immersed in the mixture of  $[\text{C}_2\text{C}_1\text{im}][\text{MeCO}_2]$  with 20% water (Table 19). This suggests that a certain degree of cellulose swelling and decrystallisation can occur even when cellulose is not homogeneously solubilised.

Table 19: Solubility of cellulose in 1,3-dialkylimidazolium ionic liquids containing methyl sulfate, hydrogen sulfate and acetate anions; the solubility in dried ionic liquid (IL) and ionic liquid mixed with 20 vol% water was investigated.

IL content	$[\text{C}_4\text{C}_1\text{im}][\text{HSO}_4]$	$[\text{C}_4\text{C}_1\text{im}][\text{MeSO}_4]$	$[\text{C}_2\text{C}_1\text{im}][\text{MeCO}_2]$	$[\text{C}_4\text{C}_1\text{im}][\text{MeCO}_2]$
100%	-	-	+	+
80%	-	-	(+)	<i>Not measured</i>

All liquors containing 100% ionic liquid turned black during the long treatment, irrespective of the anion (Figure 105). This suggests that cellulose degradation occurred in all tested ionic liquids. The 80% samples were less coloured (yellowish), suggesting that the presence of water may reduce the degradation of the cellulose under the conditions used.

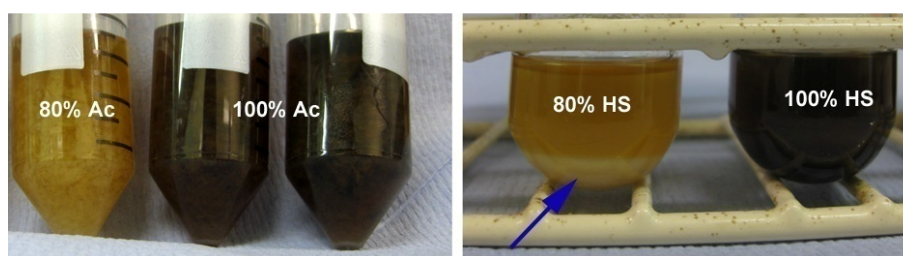


Figure 105: Regenerated cellulose pretreated in 80% and 100%  $[\text{C}_2\text{C}_1\text{im}][\text{MeCO}_2]$  (left). Note the voluminous cellulose flakes in the 80% sample. Cellulose in undiluted  $[\text{C}_4\text{C}_1\text{im}][\text{HSO}_4]$  (right). The dark colour of 100% samples is a sign of cellulose degradation.

Cellulose dissolution was not observed in the pure methyl sulfate and hydrogen sulfate ionic liquids, in agreement with their lower  $\beta$  values

(0.67 respectively). However, it was noted that the cellulose recovered from these liquors was difficult to wash, because the fibrils dispersed in water, which complicated the separation. This was neither observed for untreated or water-treated cellulose nor for the respective 80/20% ionic liquid water mixtures. It was also not observed for cellulose precipitated from the 100%  $[\text{C}_4\text{C}_1\text{im}][\text{MeCO}_2]$  and  $[\text{C}_2\text{C}_1\text{im}][\text{MeCO}_2]$  liquors. The dispersion of the fibrils suggests that the affinity of  $[\text{C}_4\text{C}_1\text{im}][\text{MeSO}_4]_{100\%}$  and  $[\text{C}_4\text{C}_1\text{im}][\text{HSO}_4]_{100\%}$  treated Avicel to water was increased compared to before the treatment and also compared to the amorphous cellulose precipitated from acetate ionic liquids.

The treatment with  $[\text{C}_4\text{C}_1\text{im}][\text{MeSO}_4]_{100\%}$  and  $[\text{C}_4\text{C}_1\text{im}][\text{HSO}_4]_{100\%}$  had a profound impact on the enzymatic hydrolysis (Figure 106). Reduced saccharification yields were observed for the cellulose incubated in pure  $[\text{C}_4\text{C}_1\text{im}][\text{MeSO}_4]$  and  $[\text{C}_4\text{C}_1\text{im}][\text{HSO}_4]$ . A decreased glucose release was not observed for cellulose incubated in the 80/20% ionic liquid water mixtures. The cellulose treated with the pure  $[\text{C}_2\text{C}_1\text{im}][\text{MeCO}_2]$  was also digestible.

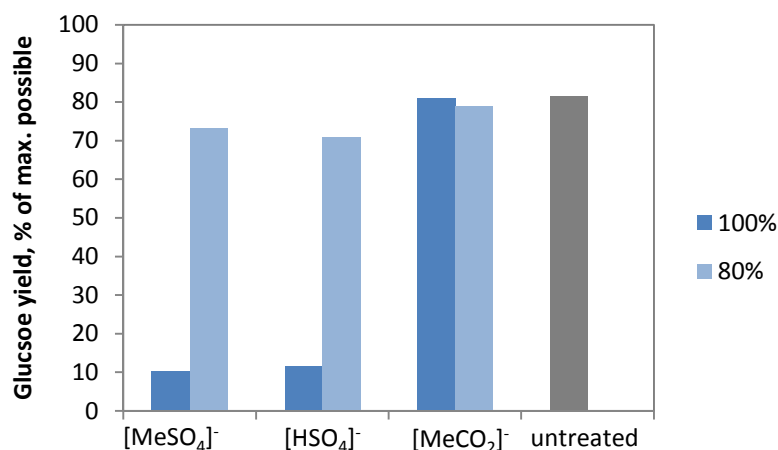
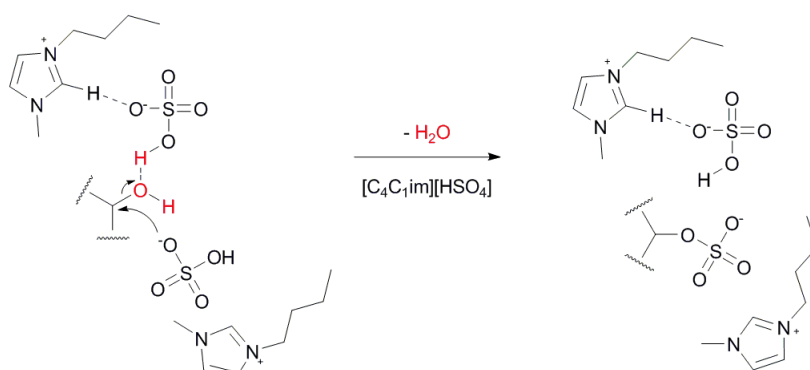


Figure 106: Enzymatic saccharification of Avicel cellulose after treatment with pure 1,3-dialkylimidazolium ionic liquids and 80/20% ionic liquid/water mixtures at 120°C for 22 h. The yield was determined after a 48 h saccharification.

It is suggested that the reduced digestibility after treatment with anhydrous  $[\text{C}_4\text{C}_1\text{im}][\text{HSO}_4]$  and  $[\text{C}_4\text{C}_1\text{im}][\text{MeSO}_4]$  is due to sulfation of the hydroxyl groups on the fibril surface, a reaction that is not favoured in the presence of water because the sulfate ester is a high energy bond. The reaction that would lead to such a modification is shown in Scheme

19. The negative charges on the surface would make the cellulose more hydrophilic and contribute to the dispersion of fibrils in water. The charged surface could also be responsible for the reduced enzymatic digestibility, as the hydrolases would not be able to recognise their substrate.



Scheme 19: Putative sulfation of cellulose in [C<sub>4</sub>C<sub>1</sub>im][HSO<sub>4</sub>]

These results also provide a possible explanation for the composite formation between ionic liquid and the biomass in pure [C<sub>4</sub>C<sub>1</sub>im][MeSO<sub>4</sub>] (Figure 68). It is suggested that it is formed because the ionic liquid reacts with the hydroxyl groups in the lignocellulose, binding the ionic liquid to the biomass through covalent bonds and coulombic forces.

### 6.3 Summary

The usefulness of the ionic liquids [C<sub>4</sub>C<sub>1</sub>im][MeSO<sub>4</sub>], [C<sub>4</sub>C<sub>1</sub>im][HSO<sub>4</sub>] and [C<sub>4</sub>C<sub>1</sub>im][MeSO<sub>3</sub>] in the pretreatment of lignocellulosic biomass has been established for the first time. It has been shown that these ionic liquids are effective in the presence of significant quantities of water. The requirement for water addition is also a likely explanation for the little success other groups had using [C<sub>4</sub>C<sub>1</sub>im][MeSO<sub>4</sub>] for lignocellulose pretreatment. It is thought that water is necessary to prevent sulfation of the biomass by the ionic liquid and for the hydrolysis of bonds in hemicellulose and lignin.

The ionic liquid pretreatment resulted in solubilisation of lignin and of hemicellulose, leaving a solid residue that was highly enriched in cellulose. The cellulose in the pulp fraction was highly susceptible to

enzymatic saccharification and glucose yields in excess of 90% could be obtained, which is an improvement compared to many reports found in the literature. The hemicellulose was partially recovered with the solid and also readily hydrolysable. A significant portion of the hemicellulose was detected in the pretreatment liquor as sugar monomers as well as the dehydration products HMF and 2-furaldehyde. In addition, upon dilution of the pretreatment liquor with water, a precipitate could be recovered, which appears to contain part of the solubilised lignin.

Comparison of the effect obtained with ionic liquid water mixtures containing other anions showed that  $[\text{C}_4\text{C}_1\text{im}][\text{HSO}_4]_{80\%}$  and  $[\text{C}_4\text{C}_1\text{im}][\text{MeSO}_3]_{80\%}$  liquors achieve superior fractionation and glucose yields compared to  $[\text{C}_4\text{C}_1\text{im}][\text{MeCO}_2]_{80\%}$  under the conditions of the pretreatment. The yields after  $[\text{C}_4\text{C}_1\text{im}]\text{Cl}_{80\%}$  and  $[\text{C}_4\text{C}_1\text{im}][\text{OTf}]_{80\%}$  pretreatment were very low. This shows that the anion of 1,3-dialkylimidazolium ionic liquids plays a vital role for the fractionation, the enzymatic digestibility and the tolerance towards water. A straightforward correlation between pretreatment effectiveness and anion basicity, as found for cellulose solubility or wood chip swelling, could not be found. However, the saccharification yields can be correlated with the delignification and hemicellulose removal, as already suggested by others.

While willow treated with  $[\text{C}_4\text{C}_1\text{im}][\text{MeCO}_2]_{80\%}$  and particularly  $[\text{C}_4\text{C}_1\text{im}][\text{HSO}_4]_{80\%}$  was also highly susceptible to saccharification, pretreated pine lignocellulose gave only moderate yields, irrespective of the ionic liquid used. Willow and Miscanthus chips were also susceptible to disintegrated by the ionic liquid water mixtures, size reduction before the saccharification is required to enhance the surface area and speed up enzymatic saccharification.

## 7 General summary, outlook and conclusions

In this chapter, the data obtained in this study are combined with results published in patent and peer-reviewed literature and used for a more general discussion of ionic liquid pretreatment. Suggestions for further experiments are put forward.

### 7.1 The importance of (ligno)cellulose solubility in ionic liquid pretreatment

Cellulose decrystallisation has been regarded as a very important effect of ionic liquid pretreatment. Several authors have emphasised decrystallisation as a major contributor to the effectiveness of ionic liquid pretreatment.<sup>115, 154</sup> This reasoning seems to be partly historical; the use of ionic liquids for lignocellulose pretreatment branched off from the investigation of cellulose solubilisation in ionic liquids. This was merged with the fact that less crystalline cellulose has a larger surface area and accelerates hydrolysis.<sup>198</sup> The focus of ionic liquid pretreatment research has begun to shift from achieving total biomass solubilisation to optimisation of the glucose yield.<sup>114,161</sup>

The results presented in chapter 6 under-pin this development. This work shows that neither complete wood solubilisation nor cellulose decrystallisation is essential to obtain effective ionic liquid pretreatment. Chapter 6 shows that effective pretreatment can be achieved with the ionic liquids  $[\text{C}_4\text{C}_1\text{im}][\text{MeSO}_4]$ ,  $[\text{C}_4\text{C}_1\text{im}][\text{HSO}_4]$  and  $[\text{C}_4\text{C}_1\text{im}][\text{MeSO}_3]$ , which are not able to dissolve cellulose. It should be noted that many pretreatment processes achieve the essential improvements in cellulose accessibility without cellulose decrystallisation (with the exception of concentrated acid treatments). Cellulases have evolved to deal with a crystalline substrate,<sup>199</sup> while an intact lignin-hemicellulose shield certainly limits access to the fibrils' surface.

The fractionative pretreatment presented in this work does not only reduce the necessity of complete biomass solubilisation. The treatment with [C<sub>4</sub>C<sub>1</sub>im][HSO<sub>4</sub>] and [C<sub>4</sub>C<sub>1</sub>im][MeSO<sub>3</sub>] water mixtures relies on the fact that the cellulose remains crystalline in them, its compact structure protecting most of the glycosidic bonds from hydrolysis.

## 7.2 Comparison with other pretreatment options

The primary purpose of a pretreatment is to improve the accessibility of the cellulose fraction in a cost and energy efficient manner. However, there are secondary material streams that may affect the economics, such as recovery of the hemicellulose and the valorisation of lignin. A qualitative comparison of ionic liquid pretreatment as it is currently known with other pretreatment operations is attempted in the next section. Features that are common to ionic liquid pretreatment and other pretreatment options as well as differences are discussed in order to highlight which aspects of biomass processing may be improved by ionic liquid pretreatment and also to highlight where the short-comings of this process (currently) are.

### 7.2.1 *Advantages of using ionic liquids*

*Excellent fractionation:* ionic liquids, particularly some of those presented in this work, can achieve a very good separation of cellulose from the other components. This could be particularly useful for the biorefinery approach, where cellulose is used as a source of fermentable glucose, while lignin and to some extent the hemicellulose are converted chemically into other products. For example, a good fractionation cannot be achieved with dilute acid pretreatment, because most of the lignin will continue to adhere to the cellulose fibrils after the treatment. The removal of lignin, soluble lignin fragments and sugar degradation products should have a positive impact on the saccharification step, reducing required enzyme loadings and boosting the growth of fermentative microorganisms.



*Safety:* The hazard for workers and the environment due to air-pollution and the potential for explosion are problems associated with organosolv pretreatment<sup>49</sup> which are reduced when using ionic liquid. The non-volatility of ionic liquids should also facilitate the recovery, improving the economics by reducing solvent losses.

*Separation steps:* The non-volatility of ionic liquids could allow separations which are not possible in aqueous systems, such as distilling out volatile value-added products or biphasic extraction of compounds from the ionic liquid liquor into an organic solvent.

*Reduction of energy use:* The non-volatility of the pretreatment liquor could reduce the requirement for pressure equipment. Performing pretreatment at lower pressure is currently only feasible for a small number of processes such as base pretreatment or biological pretreatment. Although the temperature dependence was not investigated as part of this thesis, the temperature at which good pretreatment is observed in literature reports is usually around 100°C.<sup>117, 154, 163, 192</sup> Such temperatures are comparatively low. Another advantage is the lack of unpleasant odours, which are an issue in Kraft pulping (which uses sulfide salts) that requires rigorous containment of the liquor.

### 7.2.2 *Disadvantages/challenges of ionic liquid pretreatment*

The following section lists the aspects of ionic liquid pretreatment that require attention in the future. Further investigation will help to determine whether the difficulties are inherent disadvantages or can be improved upon by optimisation or technical innovation.

*Price:* Ionic liquids are likely to be the most expensive solvents that are currently under investigation for biomass pretreatment. Therefore the prices of applicable ionic liquids need to be reduced. The use of protic ionic liquids could be beneficial, as they are by orders of magnitude cheaper than their alkylated counterparts.

*Pretreatment time:* The best pretreatment time ( $\approx 8$  h) determined for  $[\text{C}_4\text{C}_1\text{im}][\text{HSO}_4]_{80\%}$  in this study is significantly longer than the time many other pretreatment operations require. Higher temperatures could be

used to shorten the time, but must be balanced against limited ionic liquid stability and degradation reactions affecting the sugar yield.

*Ionic liquid purity:* Volatile solvents such as ethanol or ammonia can be recovered and purified by distillation after the pretreatment. This is not possible for most of the currently used ionic liquids. The non-volatility of the employed ionic liquids has important implications for ionic liquid recycling and the hemicellulose recovery, among others. Carbohydrate monomers and oligomers, furfurals, organic acids, lignin fragments, inorganic salts and other solutes are released into the ionic liquid and may accumulate within a few cycles unless they are removed. The colour changes that accompany ionic liquid pretreatment are evidence for chemical reactions in the ionic liquor. The application of distillable acid-base ionic liquids may be a solution to this problem. Otherwise a sequence of separation procedures, such as solvent extraction and chromatography needs to be put in place that will ensure the ionic liquid remains sufficiently clean for repeated recycling.

*Loss of ionic liquid through incorporation into biomass:* Even if cheaper ionic liquids can be designed in the future, they will only be cost-effective pretreatment solvents if high recovery is possible. Therefore the reactivity of ionic liquids towards the major lignocellulose components needs to be investigated in more detail. For example, the incorporation of ionic liquid components into lignin or cellulose pulp could hamper the economical viability of ionic liquid pretreatment.<sup>161, 163</sup>

*Recovery of solubilised biomass components:* The solubilised sugars and other organic compounds released during pretreatment are also valuable and should be retrieved. Usually around 25% of the biomass is hemicellulose; therefore the use of the hemicellulose fraction will improve the process economics of lignocellulose utilisation. This is another reason to improve separation of ionic liquid from dissolved components. Separation of [C<sub>2</sub>C<sub>1</sub>im]Cl from non-volatile sugars with ion exclusion chromatography has been suggested.<sup>164</sup> However, dilution with large quantities of water may be required and the energy needed for reconcentration could be substantial.

*Hemicellulose degradation:* The monomeric pentoses have the tendency to be converted into furfural, particularly in an acidic environment, such as [C<sub>4</sub>C<sub>1</sub>im][HSO<sub>4</sub>]. This transformation could be reduced by using less acidic ionic liquids such as [C<sub>4</sub>C<sub>1</sub>im][MeSO<sub>3</sub>]. Another option would be the selective extraction of the hemicellulose sugars, using a mild pre-hydrolysis step with dilute aqueous acid. This has been suggested for various other pretreatment options such as organosolv pretreatment,<sup>200</sup> paper pulping,<sup>201</sup> aqueous ammonia (post-hydrolysis)<sup>202</sup> and ammonia fibre expansion (AFEX)<sup>203</sup>. The pre-hydrolysis step would solubilise the accessible portion of hemicellulose under conditions that limit degradation reactions, before harsher conditions are applied to remove the lignin. If the production of 2-furfuraldehyde is desired, exploitation of the water furfural azeotrope may be an interesting opportunity that combines high furfural yields and purification of the ionic liquid.

*Particle size:* In many cases, the biomass used in ionic liquid pretreatment studies has not had economically acceptable particle sizes. The work described has attempted to address this aspect, but more research is required.

### 7.3 Comparison of different ionic liquids

One focus of this work was the comparison of different ionic liquids and their effect on biomass. The following summarises the differences that are relevant for a process (for ionic liquid water mixtures).

*Hemicellulose recovery:* Using the ionic liquid with acetate anion results in a higher hemicellulose recovery in the solid. Reduced solubilisation of hemicellulose is desirable for fermentation, as the hemicellulose sugars can also be fermented, resulting in increased product yields.

*Hemicellulose degradation:* The [C<sub>4</sub>C<sub>1</sub>im][HSO<sub>4</sub>] water mixtures have provided the most advanced cellulose lignin fractionation. However, this comes at a price of reduced hemicellulose and glucose retention in the solid and the degradation of hemicellulose to furfural (and likely to

levulinic acid). The use of the non-acidic ionic liquids with acetate and methanesulfonate anions seems to significantly reduce furfural formation.

*Delignification and lignin recovery:* Substantial differences in the extent of delignification and lignin recovery have been observed. Delignification will improve enzymatic saccharification and fermentation by reducing the lignin content of the biomass, a high lignin yield will be beneficial for biorefineries. In this respect  $[\text{C}_4\text{C}_1\text{im}][\text{HSO}_4]$  is better compared to  $[\text{C}_4\text{C}_1\text{im}][\text{MeCO}_2]$ .

*Equipment requirements:* The ionic liquids  $[\text{C}_n\text{C}_1\text{im}][\text{MeCO}_2]$  are basic and non-corrosive as well as non-toxic.<sup>a</sup> The ionic liquid  $[\text{C}_4\text{C}_1\text{im}][\text{HSO}_4]$  is acidic, so expensive equipment that is resistant to corrosion might be required.

*Thermal stability.*  $[\text{C}_4\text{C}_1\text{im}][\text{HSO}_4]$  and  $[\text{C}_4\text{C}_1\text{im}][\text{MeSO}_3]$  are thermally stable under the process conditions, while 1,3-dialkylimidazolium acetates are significantly less stable (Section 0 on p. 119). Temperatures of 160°C (used by Arora *et al.*<sup>136</sup>) or higher will result in significant ionic liquid degradation and formation of toxic and odorous amines and should be avoided.

A general advantage of using ionic liquid water mixtures in contrast to pure ionic liquids could be the reduction of liquor viscosity.<sup>78</sup> A high viscosity hampers stirring and separation. However, water has a great influence on the viscosity and small quantities are sufficient to reduce the viscosity of the ionic liquid dramatically.<sup>78</sup> Moreover, mixing ionic liquids with the cheap and readily available solvent water will reduce the cost of the pretreatment liquor.

## 7.4 A putative ionic liquid process

On the basis of the data presented here and earlier considerations, a putative process is devised in Figure 107. The central aspect is the cycling of the ionic liquid, which is essential for a viable ionic liquid

---

<sup>a</sup> MSDS Sigma Aldrich for 1-ethyl-3-methylimidazolium acetate

pretreatment process. This is due to the high solvent cost compared to the solvent cost in hydrothermal pretreatment options.

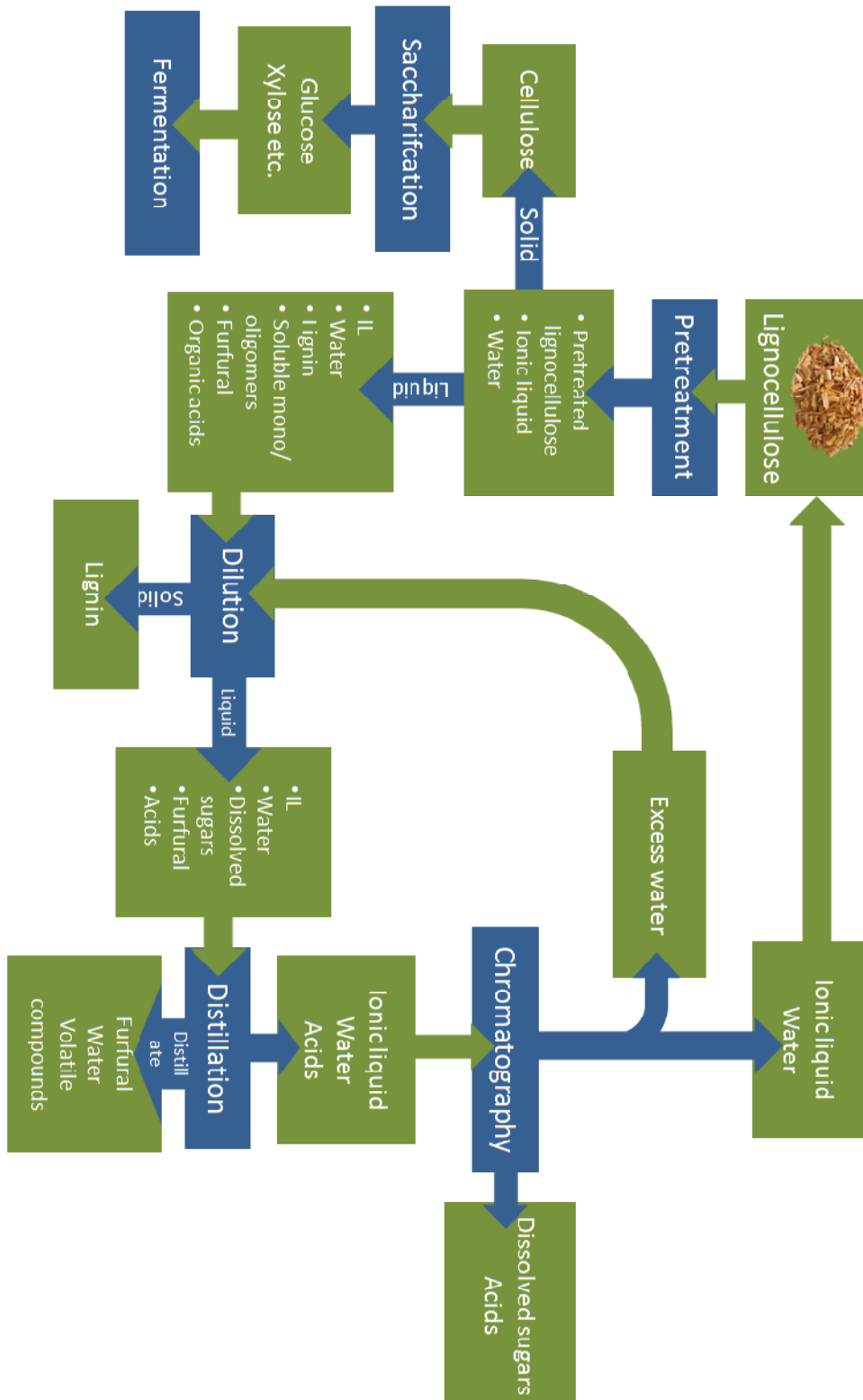


Figure 107: Suggested pretreatment process using ionic liquids that fractionate biomass.

The process is initiated by fractionating the lignocellulose into a solid cellulose enriched pulp (roughly 50% of the original wood) and a fraction that dissolves in the ionic liquid liquor during the pretreatment. After the cellulose pulp has been isolated, the liquor can be diluted with water to yield the lignin-containing precipitate. Volatile compounds are subsequently separated from the liquor by distillation, as in the case of furfural. The furfural could be distilled during the ionic liquid treatment to optimise furfural yields (semi-batch operation). Non-volatiles are separated by chromatography, resulting in a purified ionic liquid stream and a stream containing hydrophilic compounds such as organic acids and soluble monomeric or oligomeric carbohydrates. Alternatively, hydrophobic non-volatiles could be extracted with an organic solvent. For example, the extraction of HMF from 1-methylimidazolium chloride into diethyl ether has been demonstrated.<sup>180</sup> The use of volatile flammable organic solvents needs to be reviewed and alternatives to a harmful and very flammable solvent such as diethyl ether must be found. The water content of the ionic liquid liquor is adjusted before it is contacted with fresh biomass.

Some parts of this process are based on speculation and need detailed research. These are, for example, the distillation, the solvent extraction and the chromatographic separation. In addition to detailed quantification of the material streams, the energy requirements and equipment cost need to be estimated to allow further evaluation of the process viability.

## 7.5 Further work

### 7.5.1 *Ionic liquid synthesis*

The ionic liquid synthesis involving a methyl carbonate intermediate could be improved by using an automatic titrator to ensure exact and reliable combination of precursor and acid, measuring either the pH or the conductivity of the solution. The purification method of the precursor described in this work will make sure that pure ionic liquids are obtained.

### 7.5.2 *Stability of dialkylimidazolium acetate ionic liquids*

It was shown that the thermal stability of acetate ionic liquids is low compared to other ionic liquids. However, the mass loss during isothermal heating at 120°C could be investigated in more detail, establishing whether the mass loss was due to the supposed volatility of the neutral carbene acid complex of  $[\text{C}_4\text{C}_1\text{im}][\text{MeCO}_2]^{100}$  or decomposition by dealkylation. The influence of water on stability of ionic liquids with anions such as acetate could also be investigated; it is anticipated that water could increase the stability of these ionic liquids.

### 7.5.3 *Ionic liquid pretreatment*

#### 7.5.3.1 Optimisation of ionic liquid composition

It would be interesting to find a highly effective but very inexpensive cation anion combination. The hydrogen sulfate anion is a very good example of a cheap (and non-toxic) anion, as it may be derived from sulfuric acid, a cheap commodity chemical. Anions such as acetate or chloride can also be produced from cheap precursors. There is also room for cation optimisation. The use of 1-butylimidazolium,  $[\text{HC}_4\text{im}]^+$ , or 1-methylimidazolium,  $[\text{HC}_1\text{im}]^+$ , cations could be attempted. The absence of the second alkylation and the straight-forward combination of sulfuric acid and the amine, e.g. in  $[\text{HC}_1\text{im}][\text{HSO}_4]$ , will reduce the cost significantly, compared to  $[\text{C}_4\text{C}_1\text{im}][\text{HSO}_4]$ . These ionic liquids also offer the opportunity to modify the acidity of the ionic liquid by changing the acid/base ratio.

#### 7.5.3.2 Hemicellulose recovery

Furfural formation is slower than the hydrolysis of xylan to xylose, therefore it is expected that the monomer to furfural ratio can be optimised. The use of the non-acidic  $[\text{C}_4\text{C}_1\text{im}][\text{MeSO}_3]$  may achieve repression of furfural formation.

Engineering the ratio of neutral anions to acidic anions could also be used to improve selectivity of hemicellulose hydrolysis. Using mixtures of methyl sulfate and hydrogen sulfate is possible, but is constrained by the



chemical equilibrium between them and water. Another possible combination is a combination of methanesulfonate with hydrogen sulfate, which should not suffer from this limitation.

#### 7.5.3.3 Optimising other process variables

This work has already investigated certain process variables such as time and water content. Other variables would also need attention, particularly the pretreatment temperature, but also the effect of stirring.

#### 7.5.3.4 Investigation of separations involving ionic liquids and biomass

The chromatographic separation of sugars (and other polar components) could be investigated. The best type of chromatographic column needs to be identified (size exclusion, ion exchange column) and the economic feasibility established. The potential of solvent extraction and distillation to retrieve solubilised components needs to be investigated, too.

#### 7.5.3.5 Grinding after ionic liquid pretreatment

The effect of particle size must be investigated in more detail. The dissolution of wood is expected to have two major advantages: size reduction and cellulose decrystallisation. However, it was shown in this work, that complete dissolution is difficult, particularly for wood chips. Based on this observation, it is suggested that using the cell wall swelling to reduce the grinding energy could be more promising. The potential to reduce the energy requirement for grinding has been noted for sulfite pretreatment (SPORL).<sup>204</sup> The collapse of the wood pores upon removal of the biomass swelling ionic liquids suggests that the grinding should be performed while the wood chips are immersed in ionic liquid and the cell walls are swollen.

#### 7.5.3.6 Characterisation of soluble carbohydrate oligomers

The fate of the solubilised sugars needs more detailed investigation. In this study, only sugar monomers could be quantified, although short oligomers (up to 30 sugar units) are also soluble in water.<sup>196</sup> In the

presence of ionic liquids, the solubility of oligomers could extend to higher molecular weight oligomers. Therefore, selective precipitation of hemicellulose upon dilution of the ionic liquid may be possible; a process has been patented which describes dilution of the liquor with water to precipitate cellulose and precipitation of the dissolved hemicellulose by adding ethanol afterwards.<sup>205</sup> The effect of ionic liquids on the degree of polymerisation of cellulose is also of interest. Particularly acidic ionic liquids could promote chain shortening, which may have an effect on the speed of the enzymatic saccharification.

#### 7.5.3.7 Determining the yield of organic acids

The yield of organic acids such as acetic acid and hydroxycinnamic acids could be investigated, particularly for *Miscanthus* which contains substantial amounts of these acids. In addition, the concentrations of levulinic acid and formic acid, the degradation products of HMF, could also be determined in order to obtain a better understanding of the degradation reactions taking place.

#### 7.5.3.8 Characterisation of isolated lignin

More detailed analysis of the precipitate is required. For example, investigating the degree of polymerisation of the isolated lignin could give insight into the amount of recondensation reactions occurring. The incorporation of ionic liquid into lignin needs to be investigated. For example, the cationic intermediates formed during acid-catalysed ether-bond hydrolysis could react with the anions. It would also be interesting to find out if lignin solubility is also dependent on hydrogen-bond acidity ( $\alpha$  parameter), as it contains many ether bonds. The influence of cation aromaticity on lignin solubility would also be an aspect worth investigating.

## 7.6 Over-all conclusions

The application of ionic liquids for the thermal treatment of lignocellulosic biomass has been investigated in this study. The suitability of various ionic liquids based on the 1,3-dialkylimidazolium

cation combined with a wide range of anions for lignocellulose fractionation and enhancement of the enzymatic hydrolysis of the carbohydrate polymers has been examined.

The synthesis of sufficiently clean 1-butyl-3-methylimidazolium ionic liquids with hydrogen-bond basic anions was the first goal of this study. The applied strategies were direct alkylation, the silver salt route and the methyl carbonate route. High quality, colour-less or only slightly coloured liquids or, in some cases, low-melting solids were obtained. The purification of dialkylimidazolium methyl carbonate or hydrogen carbonate salts, promising intermediates for synthesis of highly hydrophilic ionic liquids, was investigated.

The measurements of selected process-relevant physicochemical properties showed that certain ionic liquids, in particular the acetate containing 1-butyl-3-methylimidazolium ionic liquids as well as the pyrrolidinium-based analogue, are not sufficiently stable at process-relevant temperatures. The generally lower stability of cellulose dissolving ionic liquids has been attributed to the presence of strongly hydrogen-bond basic anions which are required to achieve dissolution but also reduce the stability of the ionic liquids due to their high nucleophilicity. It was also demonstrated that dialkylimidazolium ionic liquids with hydrogen-bond basic anions can attract more than stoichiometric quantities of water when exposed to air, showing that pretreatment with such ionic liquids under anhydrous conditions requires extensive drying of the ionic liquids, the biomass and exclusion of moisture during the dissolution process.

In order to improve the industrial relevance of lignocellulose dissolution in ionic liquids, air-dried pine wood chips were used for biomass dissolution. The effects of ionic liquids on the structural integrity of wood chips ranged from hardly any swelling/dissolution even at elevated temperatures to pronounced swelling, partial dissolution particularly in axial direction and cracking of the chips. It was shown that under such conditions dissolution is anisotropic and incomplete. The absence of softening even after long hours of treatment is attributed to residual moisture introduced with the biomass. Despite this, the swelling of air-

dried pine wood chips could be correlated with the hydrogen-bond basicity of the ionic liquids, which was described by the Kamlet-Taft parameter  $\beta$ . Dissolution studies with willow and *Miscanthus* chips showed that they are more amenable to swelling and gradual dissolution than pine, the required treatment time being long nevertheless. It is concluded that the small surface to volume ratio of chips results in long reaction times to achieve dissolution and smaller particle size may be required.

Pretreatment of lignocellulosic biomass, particularly *Miscanthus* with the 1-butyl-3-methylimidazolium methyl sulfate, 1-butyl-3-methylimidazolium hydrogen sulfate and 1-butyl-3-methylimidazolium methanesulfonate was explored. For the first time, high saccharification yields after treatment with these ionic liquids were reported, the optimised yields being higher than after treatment with analogous 1-ethyl-3-methylimidazolium acetate liquors. Effective pretreatment with the sulfate based ionic liquids could only be achieved when a certain amount of water was added. It was subsequently shown that the use of these ionic liquids not only requires water but also that they are highly water-tolerant. 10-40 vol% water was tolerated without significant loss of saccharification yields. In contrast, the yields after treatment with 1,3-dialkylimidazolium chlorides was greatly reduced when 20% water were present. The requirement for water addition is also a likely explanation for the little success other groups had using  $[\text{C}_4\text{C}_1\text{im}][\text{MeSO}_4]$  for lignocellulose pretreatment. It is thought that the water is needed to prevent sulfation of the biomass by the ionic liquid and for the hydrolysis of bonds in hemicellulose and lignin.

Effective separation of the lignocellulose components into an insoluble cellulose fraction, a soluble hemicellulose fraction and a lignin containing precipitate was demonstrated. The influence of the water content, pretreatment time and biomass type on the enzymatic saccharification yield as well as production and conversion of the solubilised sugar monomers into dehydration products was investigated. It was demonstrated that *Miscanthus* (a perennial grass) and willow (a hardwood) are very amenable to pretreatment with  $[\text{C}_4\text{C}_1\text{im}][\text{HSO}_4]$  water mixtures, while the use of pine resulted in less complete fractionation

and incomplete enzymatic cellulose digestion. Willow and *Miscanthus* chips could be successfully pretreated and high saccharification yields obtained, showing that larger particles may be equally suitable to the fractionative pretreatment with ionic liquid water mixtures.

A straightforward correlation between pretreatment effectiveness and anion basicity, as found for cellulose solubility or wood chip swelling, could not be found. However, the saccharification yields can be correlated with the delignification and hemicellulose removal.

Further optimisation of the entire process is required to harness the optimum performance of these hardly volatile and non-flammable pretreatment liquors.

## 8 References

1. Solomon, S.; Qin, D.; Manning, M.; Z. Chen, M. M.; Averyt, K. B.; Tignor, M.; Miller, H. L., *Contribution of Working Group I to the Fourth Assessment Report of the Intergovernmental Panel on Climate Change 2007: The Physical Science Basis*. Cambridge University Press: Cambridge, United Kingdom and New York, NY, USA, 2007.
2. United States National Oceanic and Atmospheric Administration <http://www.ncdc.noaa.gov/sotc/global/2008/ann> (accessed 25 July).
3. U.S. Energy Information Administration *International Energy Outlook 2010, DOE/EIA-0484*; 2010.
4. European Environment Agency Final energy consumption by sector in the EU-27, 1990-2006. [http://www.eea.europa.eu/data-and-maps/figures/ds\\_resolveuid/F2B9A83D-A26F-46A0-93EA-776C13D18750](http://www.eea.europa.eu/data-and-maps/figures/ds_resolveuid/F2B9A83D-A26F-46A0-93EA-776C13D18750) (accessed 26th July).
5. Pickett, J. *Sustainable biofuels: prospects and challenges*; The Royal Society: London, 2008.
6. Searchinger, T.; Heimlich, R.; Houghton, R. A.; Dong, F.; Elobeid, A.; Fabiosa, J.; Tokgoz, S.; Hayes, D.; Yu, T.-H., Use of U.S. Croplands for Biofuels Increases Greenhouse Gases Through Emissions from Land-Use Change. *Science* **2008**, 319 (5867), 1238-1240.
7. U.S. Department of Energy Genome Programs image gallery <http://genomics.energy.gov> (accessed 22 February).
8. Perlack, R. D.; Wright, L. L.; Turhollow, A. F.; Graham, R. L.; Stokes, B. J.; Erbach, D. C. *Biomass as a feedstock for a bioenergy and bioproducts industry: the technical feasibility of a billion-ton annual supply*; U.S. Department of Energy and U.S. Department of Agriculture: 2005.
9. Schmer, M. R.; Vogel, K. P.; Mitchell, R. B.; Perrin, R. K., Net energy of cellulosic ethanol from switchgrass. *Proceedings of the National Academy of Sciences* **2008**, 105 (2), 464-469.
10. Worldwatch Institute, *Biofuels for Transport: Global Potential and Implications for Sustainable Energy and Agriculture*. Earthscan: 2007.
11. Clifton-Brown, J. C.; Lewandowski, I.; Andersson, B.; Teixeira, F.; Basch, G.; Christian, D. G.; Kjeldsene, J. B.; Jorgensene, U.; Mortensene, J. V.; Tiched, A. B.; Schwarze, K.-U.; Tayebic, K., Performance of 15 Miscanthus genotypes at five sites in Europe. 2001.
12. DOE, U. S. *Breaking the Biological Barriers to Cellulosic Ethanol: A Joint Research Agenda*; DOE/SC-0095; 2006.
13. Mosier, N.; Wyman, C.; Dale, B.; Elander, R.; Lee, Y. Y.; Holtzapple, M.; Ladisch, M., Features of promising technologies for pretreatment of lignocellulosic biomass. *Bioresour. Technol.* **2005**, 96 (6), 673-686.

14. Moore; Collins; Davies, *Chemistry*. McGraw-Hill Companies: 1978.
15. Jørgensen, H.; Kristensen, J.; Felby, C., Enzymatic conversion of lignocellulose into fermentable sugars: challenges and opportunities. *Biofuels, Bioproducts and Biorefining* **2007**, 1 (2), 119-134.
16. Wikipedia Cellulose hydrogen bonding. [http://en.wikipedia.org/wiki/File:Cellulose\\_strand.jpg](http://en.wikipedia.org/wiki/File:Cellulose_strand.jpg) (accessed 20 July).
17. Ding, S.-Y.; Himmel, M. E., The Maize Primary Cell Wall Microfibril: A New Model Derived from Direct Visualization. *Journal of Agricultural and Food Chemistry* **2006**, 54 (3), 597-606.
18. Eaton, R. A.; Hale, M. D. C., *Wood decay, pests and protection*. 151 ed.; Chapman and Hall: London, 1993.
19. Boerjan, W.; Ralph, J.; Baucher, M., Lignin Biosynthesis. *Annual Review of Plant Biology* **2003**, 54 (1), 519-546.
20. Donaldson, L. A., Lignification and lignin topochemistry -- an ultrastructural view. *Phytochemistry* **2001**, 57 (6), 859-873.
21. Donaldson, L. A., Mechanical constraints on lignin deposition during lignification. *Wood Science and Technology* **1994**, 28 (2), 111-118.
22. El Hage, R.; Brosse, N.; Chrusciel, L.; Sanchez, C.; Sannigrahi, P.; Ragauskas, A., Characterization of milled wood lignin and ethanol organosolv lignin from *miscanthus*. *Polymer Degradation and Stability* **2009**, 94 (10), 1632-1638.
23. Grabber, J. H., How do lignin composition, structure, and cross-linking affect degradability? A review of cell wall model studies. *Crop Science* **2005**, 45 (3), 820-831.
24. Wikipedia Structure of lignin. <http://en.wikipedia.org/wiki/File:LigninStructure.png> (accessed 20 July).
25. Berlin, A.; Balakshin, M.; Gilkes, N.; Kadla, J.; Maximenko, V.; Kubo, S.; Saddler, J., Inhibition of cellulase, xylanase and [beta]-glucosidase activities by softwood lignin preparations. *J. Biotechnol.* **2006**, 125 (2), 198-209.
26. Myton, K. E.; Fry, S. C., Intraprotoplasmic feruloylation of arabinxylans in *Festuca arundinacea* cell cultures. *Planta* **1994**, 193 (3), 326-330.
27. Ralph, J.; Grabber, J. H.; Hatfield, R. D., Lignin-ferulate cross-links in grasses: active incorporation of ferulate polysaccharide esters into ryegrass lignins. *Carbohydr. Res.* **1995**, 275 (1), 167-178.
28. Grabber, J. H.; Hatfield, R. D.; Ralph, J., Diferulate cross-links impede the enzymatic degradation of non-lignified maize walls. *Journal of the Science of Food and Agriculture* **1998**, 77 (2), 193-200.

29. Lawoko, M.; Henriksson, G.; Gellerstedt, G., Characterization of lignin-carbohydrate complexes from spruce sulfite pulp. *Holzforschung* **2006**, *60* (2), 162-165.
30. Lewandowski, I.; Clifton-Brown, J.; Scurlock, J.; Huisman, W., Miscanthus: European experience with a novel energy crop. *Biomass & bioenergy* **2000**, *19* (4), 209-227.
31. University of Illinois Miscanthus photo. [http://miscanthus.illinois.edu/?page\\_id=11](http://miscanthus.illinois.edu/?page_id=11) (accessed 26th July).
32. Beale, C. V.; Long, S. P., Seasonal dynamics of nutrient accumulation and partitioning in the perennial C4-grasses *Miscanthus x giganteus* and *Spartina cynosuroides*. *Biomass and Bioenergy* **1997**, *12* (6), 419-428.
33. Brereton, N. J. B.; Pitre, F. E.; Ray, M. J.; Karp, A.; Murphy, R. J., Investigation of tension wood formation and 2,6-dichlorobenzonitrile application in short rotation coppice willow composition and enzymatic saccharification. *Biotechnology for Biofuels* **2011**, *4* (13).
34. Aylott, M. J.; Casella, E.; Tubby, I.; Street, N. R.; Smith, P.; Taylor, G., Yield and spatial supply of bioenergy poplar and willow short-rotation coppice in the UK. *New Phytologist* **2008**, *178* (2), 358-370.
35. Saeman, J. F., Kinetics of Wood Saccharification - Hydrolysis of Cellulose and Decomposition of Sugars in Dilute Acid at High Temperature. *Industrial & Engineering Chemistry* **1945**, *37* (1), 43-52.
36. Polčin, J.; Bezúch, B., Investigation on enzymic hydrolysis of lignified cellulosic materials. *Wood Science and Technology* **1977**, *11* (4), 275-290.
37. Zhu, J.; Pan, X.; Zalesny, R., Pretreatment of woody biomass for biofuel production: energy efficiency, technologies, and recalcitrance. *Applied Microbiology and Biotechnology* **2010**, *87* (3), 847-857.
38. Wyman, C. E.; Dale, B. E.; Elander, R. T.; Holtzapple, M.; Ladisch, M. R.; Lee, Y. Y.; Mitchinson, C.; Saddler, J. N., Comparative sugar recovery and fermentation data following pretreatment of poplar wood by leading technologies. *Biotechnology Progress* **2009**, *25* (2), 333-339.
39. McDonough, T. J., The chemistry of organosolv delignification. *Tappi J* **1993**, 186-193.
40. Ragauskas A.J.; Nagy M.; Kim D.H.; Eckert C.A.; Hallett J.P.; C.L., L., From wood to fuels. *Ind. Biotechnol.* **2006**, *2*, 55-65.
41. Pingali, S. V.; Urban, V. S.; Heller, W. T.; McGaughey, J.; O'Neill, H.; Foston, M.; Myles, D. A.; Ragauskas, A.; Evans, B. R., Breakdown of Cell Wall Nanostructure in Dilute Acid Pretreated Biomass. *Biomacromolecules* **2010**, *11* (9), 2329-2335.



42. Jørgensen, H.; Olsson, L., Production of cellulases by *Penicillium brasilianum* IBT 20888--Effect of substrate on hydrolytic performance. *Enzyme and Microbial Technology* **2006**, *38* (3-4), 381-390.
43. Eriksson, T.; Börjesson, J.; Tjerneld, F., Mechanism of surfactant effect in enzymatic hydrolysis of lignocellulose. *Enzyme and Microbial Technology* **2002**, *31* (3), 353-364.
44. Zhu, J.; Zhu, W.; Obryan, P.; Dien, B.; Tian, S.; Gleisner, R.; Pan, X., Ethanol production from SPORL-pretreated lodgepole pine: preliminary evaluation of mass balance and process energy efficiency. *Applied Microbiology and Biotechnology* **2010**, *86* (5), 1355-1365.
45. Sjöström, E., *Wood chemistry: fundamentals and applications*. 2nd ed.; Academic Press: London and San Diego, 1993.
46. Farone, W.; Cuzens, J. Method of Producing Sugars Using Strong Acid Hydrolysis of Cellulosic and Hemicellulosic Materials. US 5,562,777, 1996.
47. Zhang, Y. H. P.; Ding, S. Y.; Mielenz, J. R.; Cui, J. B.; Elander, R. T.; Laser, M.; Himmel, M. E.; McMillan, J. R.; Lynd, L. R., Fractionating recalcitrant lignocellulose at modest reaction conditions. *Biotechnology and Bioengineering* **2007**, *97* (2), 214-223.
48. Zhao, X.; Cheng, K.; Liu, D., Organosolv pretreatment of lignocellulosic biomass for enzymatic hydrolysis. *Applied Microbiology and Biotechnology* **2009**, *82* (5), 815-27.
49. Zhao, X.; Cheng, K.; Liu, D., Organosolv pretreatment of lignocellulosic biomass for enzymatic hydrolysis. *Applied Microbiology and Biotechnology* **2009**, *82* (5), 815-827.
50. Pan, X.; Gilkes, N.; Kadla, J.; Pye, K.; Saka, S.; Gregg, D.; Ehara, K.; Xie, D.; Lam, D.; Saddler, J., Bioconversion of hybrid poplar to ethanol and co-products using an organosolv fractionation process: Optimization of process yields. *Biotechnology and Bioengineering* **2006**, *94* (5), 851-861.
51. Sannigrahi, P.; Miller, S. J.; Ragauskas, A. J., Effects of organosolv pretreatment and enzymatic hydrolysis on cellulose structure and crystallinity in Loblolly pine. *Carbohydr. Res.* **2010**, *345* (7), 965-970.
52. El Hage, R.; Brosse, N.; Sannigrahi, P.; Ragauskas, A., Effects of process severity on the chemical structure of *Miscanthus* ethanol organosolv lignin. *Polymer Degradation and Stability* **2010**, *95* (6), 997-1003.
53. Kumar, P.; Barrett, D. M.; Delwiche, M. J.; Stroeve, P., Methods for Pretreatment of Lignocellulosic Biomass for Efficient Hydrolysis and Biofuel Production. *Ind. Eng. Chem. Res.* **2009**, *48* (8), 3713-3729.
54. Balan, V.; Sousa, L. d. C.; Chundawat, S. P. S.; Marshall, D.; Sharma, L. N.; Chambliss, C. K.; Dale, B. E., Enzymatic digestibility and pretreatment degradation products of AFEX-treated hardwoods (*Populus nigra*). *Biotechnology Progress* **2009**, *25* (2), 365-375.

55. Kim, T. H.; Lee, Y. Y., Pretreatment and fractionation of corn stover by ammonia recycle percolation process. *Bioresour. Technol.* **2005**, *96* (18), 2007-2013.
56. Le Ngoc Huyen, T.; Rémond, C.; Dheilly, R. M.; Chabbert, B., Effect of harvesting date on the composition and saccharification of *Miscanthus x giganteus*. *Bioresour. Technol.* **2010**, *101* (21), 8224-8231.
57. Sticklen, M. B., Plant genetic engineering for biofuel production: towards affordable cellulosic ethanol. *Nat Rev Genet* **2008**, *9* (6), 433-443.
58. Fernando, S., Biorefineries: current status, challenges, and future direction. *Energy & Fuels* **2006**, *20* (4), 1727.
59. Werpy, T.; Petersen, G. *Top Value Added Chemicals from Biomass. Volume 1 - Results of Screening for Potential Candidates from Sugars and Synthesis Gas.*; Produced by the Staff at Pacific Northwest National Laboratory (PNNL); National Renewable Energy Laboratory (NREL), Office of Biomass Program (EERE): 2004.
60. Antal, M. J.; Leesomboon, T.; Mok, W. S.; Richards, G. N., Kinetic studies of the reactions of ketoses and aldoses in water at high temperature. 3. Mechanism of formation of 2-furaldehyde from D-xylose. *Carbohydr. Res.* **1991**, *217*, 71-85.
61. Zeitsch, K. J., *The Chemistry and Technology of Furfural and its Many By-Products*. Elsevier: 2000; p 1-376.
62. Girisuta, B.; Janssen, L. P. B. M.; Heeres, H. J., Kinetic Study on the Acid-Catalyzed Hydrolysis of Cellulose to Levulinic Acid. *Ind. Eng. Chem. Res.* **2007**, *46* (6), 1696-1708.
63. Román-Leshkov, Y.; Chheda, J. N.; Dumesic, J. A., Phase Modifiers Promote Efficient Production of Hydroxymethylfurfural from Fructose. *Science* **2006**, *312* (5782), 1933-1937.
64. Sheldon, R. A., The E Factor: 15 years on. *Green Chemistry* **2007**, *9* (12), 1273-1283.
65. Yang, B.; Wyman, C. E., Pretreatment: the key to unlocking low-cost cellulosic ethanol. *Biofuels, Bioproducts and Biorefining* **2008**, *2* (1), 26-40.
66. Wilkes, J. S.; Zaworotko, M. J., Air and water stable 1-ethyl-3-methylimidazolium based ionic liquids. *J. Chem. Soc.-Chem. Commun.* **1992**, (13), 965-967.
67. Hunt, P. A.; Kirchner, B.; Welton, T., Characterising the electronic structure of ionic liquids: An examination of the 1-butyl-3-methylimidazolium chloride ion pair. *Chemistry-a European Journal* **2006**, *12* (26), 6762-6775.
68. Niedermeyer, H.; Ab Rani, M. A.; Lickiss, P. D.; Hallett, J. P.; Welton, T.; White, A. J. P.; Hunt, P. A., Understanding siloxane functionalised ionic liquids. *Physical Chemistry Chemical Physics* **2010**, *12* (8), 2018-2029.

69. Pringle, J. M.; Golding, J.; Baranyai, K.; Forsyth, C. M.; Deacon, G. B.; Scott, J. L.; MacFarlane, D. R., The effect of anion fluorination in ionic liquids - physical properties of a range of bis(methanesulfonyl)amide salts. *New Journal of Chemistry* **2003**, 27 (10), 1504-1510.
70. Pérez Arlandis, J. M. The solvent properties of ionic liquids and their effect on amination reactions. Imperial College London, London, 2006.
71. Plechkova, N. V.; Seddon, K. R., Applications of ionic liquids in the chemical industry. *Chemical Society Reviews* **2008**, 37 (1), 123-150.
72. Stärk, K.; Taccardi, N.; Bösmann, A.; Wasserscheid, P., Oxidative Depolymerization of Lignin in Ionic Liquids. *ChemSusChem* **2010**, 3 (6), 719-723.
73. Hallett, J. P.; Liotta, C. L.; Ranieri, G.; Welton, T., Charge Screening in the S(N)2 Reaction of Charged Electrophiles and Charged Nucleophiles: An Ionic Liquid Effect. *J. Org. Chem.* **2009**, 74 (5), 1864-1868.
74. Swatloski, R. P.; Spear, S. K.; Holbrey, J. D.; Rogers, R. D., Dissolution of cellulose with ionic liquids. *Journal of the American Chemical Society* **2002**, 124 (18), 4974-4975.
75. Pu, Y. Q.; Jiang, N.; Ragauskas, A. J., Ionic liquid as a green solvent for lignin. *Journal of Wood Chemistry and Technology* **2007**, 27 (1), 23-33.
76. Stoimenovski, J.; Izgorodina, E. I.; MacFarlane, D. R., Ionicity and proton transfer in protic ionic liquids. *Physical Chemistry Chemical Physics* **2010**, 12 (35), 10341-10347.
77. Hallett, J. P.; Welton, T., Room-Temperature Ionic Liquids: Solvents for Synthesis and Catalysis. 2. *Chem. Rev.* **2011**, 5 (111), 3508-3576.
78. Seddon, K. R.; Stark, A.; Torres, M. J., Influence of chloride, water, and organic solvents on the physical properties of ionic liquids. *Pure Appl. Chem.* **2000**, 72 (12), 2275-2287.
79. Schleicher, J. C.; Scurto, A. M., Kinetics and solvent effects in the synthesis of ionic liquids: imidazolium. *Green Chemistry* **2009**, 11 (5), 694-703.
80. Wells, T. P.; Hallett, J. P.; Williams, C. K.; Welton, T., Esterification in ionic liquids: The influence of solvent basicity. *J. Org. Chem.* **2008**, 73 (14), 5585-5588.
81. Earle, M. J.; Gordon, C. M.; Plechkova, N. V.; Seddon, K. R.; Welton, T., Decolorization of ionic liquids for spectroscopy. *Analytical Chemistry* **2007**, 79 (2), 758-764.
82. Holbrey, J. D.; Reichert, W. M.; Swatloski, R. P.; Broker, G. A.; Pitner, W. R.; Seddon, K. R.; Rogers, R. D., Efficient, halide free synthesis of new, low cost ionic liquids: 1,3-dialkylimidazolium salts containing methyl- and ethyl-sulfate anions. *Green Chemistry* **2002**, 4 (5), 407-413.

83. Kuhlmann, E.; Himmler, S.; Giebelhaus, H.; Wasserscheid, P., Imidazolium dialkylphosphates - a class of versatile, halogen-free and hydrolytically stable ionic liquids. *Green Chemistry* **2007**, *9* (3), 233-242.
84. Cassol, C.; Ebeling, G.; Ferrera, B.; Dupont, J., A Simple and Practical Method for the Preparation and Purity Determination of Halide-Free Imidazolium Ionic Liquids. *Advanced Synthesis & Catalysis* **2006**, *348* (1-2), 243-248.
85. Bonhôte, P.; Dias, A.-P.; Papageorgiou, N.; Kalyanasundaram, K.; Grätzel, M., Hydrophobic, Highly Conductive Ambient-Temperature Molten Salts. *Inorganic Chemistry* **1996**, *35* (5), 1168-1178.
86. Shi, C.; Ge, Q.; Zhou, F.; Cai, M.; Wang, X.; Fang, X.; Pan, X., An improved preparation of 3-ethyl-1-methylimidazolium trifluoroacetate and its application in dye sensitized solar cells. *Solar Energy* **2009**, *83* (1), 108-112.
87. Himmler, S.; Hormann, S.; van Hal, R.; Schulz, P. S.; Wasserscheid, P., Transesterification of methylsulfate and ethylsulfate ionic liquids-an environmentally benign way to synthesize long-chain and functionalized alkylsulfate ionic liquids. *Green Chemistry* **2006**, *8* (10), 887-894.
88. Holleman, A. F.; Wiberg, N., *Lehrbuch der anorganischen Chemie*. 33 ed.; Walter de Gruyter & Co: Berlin, 1985.
89. Fukumoto, K.; Yoshizawa, M.; Ohno, H., Room temperature ionic liquids from 20 natural amino acids. *Journal of the American Chemical Society* **2005**, *127* (8), 2398-2399.
90. Zhao, H.; Baker, G. A.; Song, Z. Y.; Olubajo, O.; Crittle, T.; Peters, D., Designing enzyme-compatible ionic liquids that can dissolve carbohydrates. *Green Chemistry* **2008**, *10* (6), 696-705.
91. Holbrey, J. D.; Rogers, R. D.; Shukla, S. S.; Wilfred, C. D., Optimised microwave-assisted synthesis of methylcarbonate salts: a convenient methodology to prepare intermediates for ionic liquid libraries. *Green Chemistry* **2010**, *12* (3), 407-413.
92. Mori, S.; Ida, K.; Ue, M. Process for producing quaternary salts 4,892,944, 1988.
93. Sakakura, T.; Kohno, K., The synthesis of organic carbonates from carbon dioxide. *Chemical Communications* **2009**, (11), 1312-1330.
94. Gattow, G.; Behrendt, W., Methyl hydrogen carbonate. *Angewandte Chemie (International ed. in English)* **1972**, *11* (6), 534.
95. Adelwohrer, C.; Yoneda, Y.; Takano, T.; Nakatsubo, F.; Rosenau, T., Synthesis of the perdeuterated cellulose solvents N-methylmorpholine N-oxide (NMMO-d(11) and NMMO-N-15-d(11)), N,N-dimethylacetamide (DMAc-d(9) and DMAc-N-15-d(9)), 1-ethyl-3-methylimidazolium acetate (EMIM-OAc-d(14)) and 1-butyl-3-methylimidazolium acetate (BMIM-OAc-d(18)). *Cellulose* **2009**, *16* (1), 139-150.

96. Cammarata, L.; Kazarian, S. G.; Salter, P. A.; Welton, T., Molecular states of water in room temperature ionic liquids. *Physical Chemistry Chemical Physics* **2001**, 3 (23), 5192-5200.
97. McIntosh, A. J. S. Hydrogen bonding effects in ionic liquids. Final year project report, Imperial College London, London, 2008.
98. Gerhard, D.; Alpaslan, S. C.; Gores, H. J.; Uerdingen, M.; Wasserscheid, P., Trialkylsulfonium dicyanamides - a new family of ionic liquids with very low viscosities. *Chemical Communications* **2005**, (40), 5080-5082.
99. Lin, I. J. B.; Vasam, C. S., Silver(I) N-heterocyclic carbenes. *Comments Inorganic Chem.* **2004**, 25 (3-4), 75-129.
100. Hollóczki, O.; Gerhard, D.; Massone, K.; Szarvas, L.; Németh, B.; Veszprémi, T.; Nyulászi, L., Carbenes in ionic liquids. *New Journal of Chemistry* **2010**, (34), 3004-3009.
101. Denk, M. K.; Rodezno, J. M.; Gupta, S.; Lough, A. J., Synthesis and reactivity of subvalent compounds Part 11. Oxidation, hydrogenation and hydrolysis of stable diamino carbenes. *Journal of Organometallic Chemistry* **2001**, 617 (1), 242-253.
102. Holbrey, J. D.; Reichert, W. M.; Tkatchenko, I.; Bouajila, E.; Walter, O.; Tommasi, I.; Rogers, R. D., 1,3-dimethylimidazolium-2-carboxylate: the unexpected synthesis of an ionic liquid precursor and carbene-CO<sub>2</sub> adduct. *Chemical Communications* **2003**, (1), 28-29.
103. Smiglak, M.; Holbrey, J. D.; Griffin, S. T.; Reichert, W. M.; Swatloski, R. P.; Katritzky, A. R.; Yang, H. F.; Zhang, D. Z.; Kirichenko, K.; Rogers, R. D., Ionic liquids via reaction of the zwitterionic 1,3-dimethylimidazolium-2-carboxylate with protic acids. Overcoming synthetic limitations and establishing new halide free protocols for the formation of ILs. *Green Chemistry* **2007**, 9 (1), 90-98.
104. Fischer, J.; Siegel, W.; Bomm, V.; Fischer, M.; Munding, K. Process for the preparation of 1,3-dimethylimidazolium-4-carboxylate. 6175019 B1, 1999.
105. Picquet, M.; Poinot, D.; Stutzmann, S.; Tkatchenko, I.; Tommasi, I.; Wasserscheid, P.; Zimmermann, J., Ionic Liquids: Media for Better Molecular Catalysis. *Topics in Catalysis* **2004**, 29 (3), 139-143.
106. Bosamia, H. H. The halide-free synthesis of ionic liquids of ionic liquids. MSci Project thesis, Imperial College London, London, 2010.
107. Bridges, N. J.; Hines, C. C.; Smiglak, M.; Rogers, R. D., An intermediate for the clean synthesis of ionic liquids: Isolation and crystal structure of 1,3-dimethylimidazolium hydrogen carbonate monohydrate. *Chemistry-a European Journal* **2007**, 13 (18), 5207-5212.
108. Reichardt C; Welton T, *Solvents and solvent effects in organic chemistry*. 4 ed.; Wiley-VCH: Weinheim, 2010.

109. Kamlet, M. J.; Taft, R. W., Solvatochromic comparison method. 1.  $\beta$ -scale of solvent hydrogen-bond acceptor (HBA) basicities. *Journal of the American Chemical Society* **1976**, *98* (2), 377-383.
110. Taft, R. W.; Kamlet, M. J., Solvatochromic comparison method. 2. The  $\alpha$ -scale of solvent hydrogen-bond donor (HBD) acidities. *Journal of the American Chemical Society* **1976**, *98* (10), 2886-2894.
111. Kamlet, M. J.; Abboud, J. L.; Taft, R. W., Solvatochromic comparison method. 6.  $\Pi^*$  scale of solvent polarities. *Journal of the American Chemical Society* **1977**, *99* (18), 6027-6038.
112. Marcus, Y., The properties of organic liquids that are relevant to their use as solvating solvents. *Chemical Society Reviews* **1993**, *22* (6), 409-416.
113. Crowhurst, L.; Mawdsley, P. R.; Perez-Arlandis, J. M.; Salter, P. A.; Welton, T., Solvent-solute interactions in ionic liquids. *Physical Chemistry Chemical Physics* **2003**, *5* (13), 2790-2794.
114. Lee, S. H.; Doherty, T. V.; Linhardt, R. J.; Dordick, J. S., Ionic liquid-mediated selective extraction of lignin from wood leading to enhanced enzymatic cellulose hydrolysis. *Biotechnology and Bioengineering* **2009**, *102* (5), 1368-1376.
115. Kilpeläinen, I.; Xie, H.; King, A.; Granstrom, M.; Heikkinen, S.; Argyropoulos, D. S., Dissolution of wood in ionic liquids. *Journal of Agricultural and Food Chemistry* **2007**, *55*, 9142-9148.
116. Miyafuji, H.; Miyata, K.; Saka, S.; Ueda, F.; Mori, M. In *Reaction behavior of wood in an ionic liquid, 1-ethyl-3-methylimidazolium chloride*, 58th Annual Meeting of the Japan-Wood-Research-Society, Tsukuba, JAPAN, Mar; Springer Tokyo: Tsukuba, JAPAN, 2008; pp 215-219.
117. Sun, N.; Rahman, M.; Qin, Y.; Maxim, M. L.; Rodriguez, H.; Rogers, R. D., Complete dissolution and partial delignification of wood in the ionic liquid 1-ethyl-3-methylimidazolium acetate. *Green Chemistry* **2009**, *11* (5), 646-655.
118. Fredlake, C. P.; Crosthwaite, J. M.; Hert, D. G.; Aki, S.; Brennecke, J. F., Thermophysical properties of imidazolium-based ionic liquids. *J. Chem. Eng. Data* **2004**, *49* (4), 954-964.
119. Baranyai, K. J.; Deacon, G. B.; MacFarlane, D. R.; Pringle, J. M.; Scott, J. L., Thermal Degradation of Ionic Liquids at Elevated Temperatures. *Australian Journal of Chemistry* **2004**, *57* (2), 145-147.
120. Wooster, T. J.; Johanson, K. M.; Fraser, K. J.; MacFarlane, D. R.; Scott, J. L., Thermal degradation of cyano containing ionic liquids. *Green Chemistry* **2006**, *8* (8), 691-696.
121. Mazza, M.; Catana, D. A.; Vaca-Garcia, C.; Cecutti, C., Influence of water on the dissolution of cellulose in selected ionic liquids. *Cellulose* **2009**, *16* (2), 207-215.

122. Sievers, C.; Valenzuela-Olarte, M. B.; Marzioletti, T.; Musin, D.; Agrawal, P. K.; Jones, C. W., Ionic-Liquid-Phase Hydrolysis of Pine Wood. *Ind. Eng. Chem. Res.* **2009**, *48* (3), 1277-1286.
123. Sievers, C.; Musin, I.; Marzioletti, T.; Olarte, M.; Agrawal, P.; Jones, C., Acid-Catalyzed Conversion of Sugars and Furfurals in an Ionic-Liquid Phase. *ChemSusChem* **2009**, *2* (7), 665-671.
124. Downard, A.; Earle, M. J.; Hardacre, C.; McMath, S. E. J.; Nieuwenhuyzen, M.; Teat, S. J., Structural Studies of Crystalline 1-Alkyl-3-Methylimidazolium Chloride Salts. *Chemistry of Materials* **2003**, *16* (1), 43-48.
125. Taga, T.; Machida, K.; Kimura, N.; Hayashi, S.; Umemura, J.; Takenaka, T., Structure of dodecyldimethylpropylammonium bromide hemihydrate. *Acta Crystallogr. Sect. C-Cryst. Struct. Commun.* **1987**, *43*, 1204-1206.
126. Mele, A.; Tran, C. D.; De Paoli Lacerda, S. H., The Structure of a Room-Temperature Ionic Liquid with and without Trace Amounts of Water: The Role of C-H...O and C-H...F Interactions in 1-n-Butyl-3-Methylimidazolium Tetrafluoroborate. *Angewandte Chemie International Edition* **2003**, *42* (36), 4364-4366.
127. Brandt, A.; Hallett, J. P.; Leak, D. J.; Murphy, R. J.; Welton, T., The effect of the ionic liquid anion in the pretreatment of pine wood chips. *Green Chemistry* **2010**, *12* (4), 672-679.
128. Ranieri, G.; Hallett, J. P.; Welton, T., Nucleophilic reactions at cationic centers in ionic liquids and molecular solvents. *Ind. Eng. Chem. Res.* **2008**, *47* (3), 638-644.
129. Rinaldi, R., Instantaneous dissolution of cellulose in organic electrolyte solutions. *Chemical Communications* **2011**, *47* (1), 511-513.
130. Baker, S. N.; Baker, G. A.; Bright, F. V., Temperature-dependent microscopic solvent properties of 'dry' and 'wet' 1-butyl-3-methylimidazolium hexafluorophosphate: correlation with ET(30) and Kamlet-Taft polarity scales. *Green Chemistry* **2002**, *4*, 165-169.
131. Fukaya, Y.; Sugimoto, A.; Ohno, H., Superior solubility of polysaccharides in low viscosity, polar, and halogen-free 1,3-dialkylimidazolium formates. *Biomacromolecules* **2006**, *7* (12), 3295-3297.
132. Wu, Y. S.; Sasaki, T.; Kazushi, K.; Seo, T.; Sakurai, K., Interactions between spiropyran and room-temperature ionic liquids: Photochromism and solvatochromism. *J. Phys. Chem. B* **2008**, *112* (25), 7530-7536.
133. Lungwitz, R.; Friedrich, M.; Linert, W.; Spange, S., New aspects on the hydrogen bond donor (HBD) strength of 1-butyl-3-methylimidazolium room temperature ionic liquids. *New Journal of Chemistry* **2008**, *32* (9), 1493-1499.
134. Avent, A. G.; Chaloner, P. A.; Day, M. P.; Seddon, K. R.; Welton, T., Evidence for hydrogen bonding in solutions of 1-ethyl-3-methylimidazolium

halides, and its implications for room-temperature halogenoaluminate(III) ionic liquids. *Journal of the Chemical Society, Dalton Transactions* **1994**, (23), 3405-3413.

135. Ab Rani, M. A.; Brandt, A.; Crowhurst, L.; Dolan, A.; Hallett, J. P.; Hassan, N. H.; Hunt, P. A.; Lui, M.; Niedermeyer, H.; Perez-Arlandis, J. M.; Schrems, M.; To, T. Q.; Welton, T.; Wilding, R., Understanding the polarity of ionic liquids. *Physical Chemistry Chemical Physics* **2011**, *13* (37), 16831-16840.

136. Arora, R.; Manisseri, C.; Li, C.; Ong, M.; Scheller, H.; Vogel, K.; Simmons, B.; Singh, S., Monitoring and Analyzing Process Streams Towards Understanding Ionic Liquid Pretreatment of Switchgrass (*Panicum virgatum*). *BioEnergy Research* **2010**, *3* (2), 134-145.

137. Kuo, C. H.; Lee, C. K., Enhanced enzymatic hydrolysis of sugarcane bagasse by N-methylmorpholine-N-oxide pretreatment. *Bioresour. Technol.* **2009**, *100* (2), 866-871.

138. Wu, J.; Zhang, J.; Zhang, H.; He, J. S.; Ren, Q.; Guo, M., Homogeneous acetylation of cellulose in a new ionic liquid. *Biomacromolecules* **2004**, *5* (2), 266-268.

139. Fukaya, Y.; Hayashi, K.; Wada, M.; Ohno, H., Cellulose dissolution with polar ionic liquids under mild conditions: required factors for anions. *Green Chemistry* **2008**, *10* (1), 44-46.

140. Köhler, S.; Liebert, T.; Schöbitz, M.; Schaller, J.; Meister, F.; Günther, W.; Heinze, T., Interactions of ionic liquids with polysaccharides 1. Unexpected acetylation of cellulose with 1-ethyl-3-methylimidazolium acetate. *Macromolecular Rapid Communications* **2007**, *28* (24), 2311-2317.

141. Gericke, M.; Schluffer, K.; Liebert, T.; Heinze, T.; Budtova, T., Rheological Properties of Cellulose/Ionic Liquid Solutions: From Dilute to Concentrated States. *Biomacromolecules* **2009**, *10* (5), 1188-1194.

142. Sescousse, R.; Le, K. A.; Ries, M. E.; Budtova, T., Viscosity of Cellulose-Imidazolium-Based Ionic Liquid Solutions. *The Journal of Physical Chemistry B* **2010**, *114* (21), 7222-7228.

143. Pinkert, A.; Marsh, K. N.; Pang, S.; Staiger, M. P., Ionic Liquids and Their Interaction with Cellulose. *Chemical Reviews* **2009**, *109* (12), 6712-6728.

144. Swatloski, R. P.; Rogers, R. D.; Holbrey, J. D. Dissolution and processing of cellulose using ionic liquids. US 6824599 B2, 30/11/2004, 2004.

145. Zhao, H.; Jones, C. I. L.; Baker, G. A.; Xia, S.; Olubajo, O.; Person, V. N., Regenerating cellulose from ionic liquids for an accelerated enzymatic hydrolysis. *J. Biotechnol.* **2009**, *139* (1), 47-54.

146. Remsing, R. C.; Hernandez, G.; Swatloski, R. P.; Masefski, W. W.; Rogers, R. D.; Moyna, G., Solvation of carbohydrates in N,N '-



dialkylimidazolium ionic liquids: A multinuclear NMR spectroscopy study. *J. Phys. Chem. B* **2008**, *112* (35), 11071-11078.

147. Xu, A. R.; Wang, J. J.; Wang, H. Y., Effects of anionic structure and lithium salts addition on the dissolution of cellulose in 1-butyl-3-methylimidazolium-based ionic liquid solvent systems. *Green Chemistry* **2010**, *12* (2), 268-275.

148. Pinkert, A.; Marsh, K. N.; Pang, S., Alkanolamine Ionic Liquids and Their Inability To Dissolve Crystalline Cellulose. *Ind. Eng. Chem. Res.* **2010**, *49* (22), 11809-11813.

149. Fort, D. A.; Remsing, R. C.; Swatloski, R. P.; Moyna, P.; Moyna, G.; Rogers, R. D., Can ionic liquids dissolve wood? Processing and analysis of lignocellulosic materials with 1-n-butyl-3-methylimidazolium chloride. *Green Chemistry* **2007**, *9* (1), 63-69.

150. Singh, S.; Simmons, B. A.; Vogel, K. P., Visualization of Biomass Solubilization and Cellulose Regeneration During Ionic Liquid Pretreatment of Switchgrass. *Biotechnology and Bioengineering* **2009**, *104* (1), 68-75.

151. Zavrel, M.; Bross, D.; Funke, M.; Buchs, J.; Spiess, A. C., High-throughput screening for ionic liquids dissolving (ligno-)cellulose. *Bioresour. Technol.* **2009**, *100* (9), 2580-2587.

152. Levine, S. E.; Fox, J. M.; Blanch, H. W.; Clark, D. S., A Mechanistic Model of the Enzymatic Hydrolysis of Cellulose. *Biotechnology and Bioengineering* **2010**, *107* (1), 37-51.

153. Sun, X.-F.; Sun; Fowler, P.; Baird, M. S., Extraction and Characterization of Original Lignin and Hemicelluloses from Wheat Straw. *Journal of Agricultural and Food Chemistry* **2005**, *53* (4), 860-870.

154. Doherty, T. V.; Mora-Pale, M.; Foley, S. E.; Linhardt, R. J.; Dordick, J. S., Ionic liquid solvent properties as predictors of lignocellulose pretreatment efficacy. *Green Chemistry* **2010**, *12* (11), 1967-1975.

155. Miao, Z.; Grift, T. E.; Hansen, A. C.; Ting, K. C., Energy requirement for comminution of biomass in relation to particle physical properties. *Industrial Crops and Products* **2011**, *33* (2), 504-513.

156. Cadoche, L.; López, G. D., Assessment of size reduction as a preliminary step in the production of ethanol from lignocellulosic wastes. *Biological Wastes* **1989**, *30* (2), 153-157.

157. Mani, S.; Tabil, L. G.; Sokhansanj, S., Grinding performance and physical properties of wheat and barley straws, corn stover and switchgrass. *Biomass and Bioenergy* **2004**, *27* (4), 339-352.

158. Hosseini, S. A.; Shah, N., Multiscale modelling of hydrothermal biomass pretreatment for chip size optimization. *Bioresour. Technol.* **2009**, *100* (9), 2621-2628.

159. Li, C.; Knierim, B.; Manisseri, C.; Arora, R.; Scheller, H. V.; Auer, M.; Vogel, K. P.; Simmons, B. A.; Singh, S., Comparison of dilute acid and ionic

liquid pretreatment of switchgrass: Biomass recalcitrance, delignification and enzymatic saccharification. *Bioresour. Technol.* **2010**, *101* (13), 4900-4906.

160. Li, Q.; Jiang, X.; He, Y.; Li, L.; Xian, M.; Yang, J., Evaluation of the biocompatible ionic liquid 1-methyl-3-methylimidazolium dimethylphosphite pretreatment of corn cob for improved saccharification. *Applied Microbiology and Biotechnology* **2010**, *87* (1), 117-126.

161. Tan, S. S. Y.; MacFarlane, D. R.; Upfal, J.; Edey, L. A.; Doherty, W. O. S.; Patti, A. F.; Pringle, J. M.; Scott, J. L., Extraction of lignin from lignocellulose at atmospheric pressure using alkylbenzenesulfonate ionic liquid. *Green Chemistry* **2009**, *11* (3), 339-345.

162. Kubo, S.; Hashida, K.; Yamada, T.; Hishiyama, S.; Magara, K.; Kishino, M.; Ohno, H.; Hosoya, S., A Characteristic Reaction of Lignin in Ionic Liquids; Glycelol Type Enol-Ether as the Primary Decomposition Product of  $\beta$ -O-4 Model Compound. *Journal of Wood Chemistry and Technology* **2008**, *28* (2), 84 - 96.

163. Çetinkol, Ö.; Dibble, D. C.; Cheng, G.; Kent, M. S.; Knierim, B.; Manfred, A.; E, W. D.; G, P. J.; Melnichenko, Y. B.; Ralph, J.; A, S. B.; M, H. B., Understanding the impact of ionic liquid pretreatment on eucalyptus. *Biofuels* **2010**, *1* (1), 33-46.

164. Binder, J. B.; Raines, R. T., Fermentable sugars by chemical hydrolysis of biomass. *Proceedings of the National Academy of Sciences* **2010**, *107* (10), 4516-4521.

165. Li, C.; Wang, Q.; Zhao, Z. K., Acid in ionic liquid: An efficient system for hydrolysis of lignocellulose. *Green Chemistry* **2008**, *10* (2), 177-182.

166. Massonne, K. B. D., (DE), D'Andola, Giovanni (Heidelberg, DE), Stegmann, Veit (Mannheim, DE), Mormann, Werner (Siegen, DE), Wezstein, Markus (Kirchhunden, DE), Leng, Wei (Siegen, DE) Method for breaking down cellulose in solution. 2007/101812 A1, 2007.

167. Fanselow, M.; Holbrey, J.; Seddon, K. R.; Vanoye, L.; Zheng, A. Conversion method. 2009/030949 A1, 2009.

168. Massonne, K.; D'Andola, G.; Stegmann, V.; Mormann, W.; Wezstein, M.; Leng, W. Method for breaking down cellulose in solution. 2007/101811 A1, 2007.

169. Rinaldi, R.; Palkovits, R.; Schüth, F., Depolymerization of Cellulose Using Solid Catalysts in Ionic Liquids. *Angewandte Chemie International Edition* **2008**, *47* (42), 8047-8050.

170. Dwiatmoko, A. A.; Choi, J. W.; Suh, D. J.; Suh, Y.-W.; Kung, H. H., Understanding the role of halogen-containing ionic liquids in the hydrolysis of cellobiose catalyzed by acid resins. *Applied Catalysis A: General* **2010**, *387* (1-2), 209-214.

171. Kumler, W. D.; Eiler, J. J., The Acid Strength of Mono and Diesters of Phosphoric Acid. The n-Alkyl Esters from Methyl to Butyl, the Esters of

Biological Importance, and the Natural Guanidine Phosphoric Acids. *Journal of the American Chemical Society* **1943**, 65 (12), 2355-2361.

172. Engel, P.; Mladenov, R.; Wulfhorst, H.; Jäger, G.; Spiess, A. C., Point by point analysis: how ionic liquid affects the enzymatic hydrolysis of native and modified cellulose. *Green Chemistry* **2010**, 12 (11), 1959-1966.

173. Engel, P.; Mladenov, R.; Wulfhorst, H.; Jager, G.; Spiess, A. C., Point by point analysis: how ionic liquid affects the enzymatic hydrolysis of native and modified cellulose. *Green Chemistry* **2010**, 12 (11), 1959-1966.

174. Datta, S.; Holmes, B.; Park, J. I.; Chen, Z.; Dibble, D. C.; Hadi, M.; Blanch, H. W.; Simmons, B. A.; Sapro, R., Ionic liquid tolerant hyperthermophilic cellulases for biomass pretreatment and hydrolysis. *Green Chemistry* **2010**, 12 (2), 338-345.

175. Pottkämper, J.; Barthen, P.; Ilmberger, N.; Schwaneberg, U.; Schenk, A.; Schulte, M.; Ignatiev, N.; Streit, W. R., Applying metagenomics for the identification of bacterial cellulases that are stable in ionic liquids. *Green Chemistry* **2009**, 11 (7), 957-965.

176. Li, B.; Asikkala, J.; Filpponen, I.; Argyropoulos, D. S., Factors Affecting Wood Dissolution and Regeneration of Ionic Liquids. *Ind. Eng. Chem. Res.* **2010**, 49 (5), 2477-2484.

177. Li, Q.; He, Y.-C.; Xian, M.; Jun, G.; Xu, X.; Yang, J.-M.; Li, L.-Z., Improving enzymatic hydrolysis of wheat straw using ionic liquid 1-ethyl-3-methyl imidazolium diethyl phosphate pretreatment. *Bioresour. Technol.* **2009**, 100 (14), 3570-3575.

178. Zakrzewska, M. E.; Bogel-Łukasik, E.; Bogel-Łukasik, R., Solubility of Carbohydrates in Ionic Liquids. *Energy & Fuels* **2010**, 24 (2), 737-745.

179. Guo, Z.; Lue, B.-M.; Thomasen, K.; Meyer, A. S.; Xu, X., Predictions of flavonoid solubility in ionic liquids by COSMO-RS: experimental verification, structural elucidation, and solvation characterization. *Green Chemistry* **2007**, 9 (12), 1362-1373.

180. Moreau, C.; Finiels, A.; Vanoye, L., Dehydration of fructose and sucrose into 5-hydroxymethylfurfural in the presence of 1-H-3-methyl imidazolium chloride acting both as solvent and catalyst. *Journal of Molecular Catalysis A: Chemical* **2006**, 253 (1-2), 165-169.

181. Zhao, H.; Holladay, J. E.; Brown, H.; Zhang, Z. C., Metal Chlorides in Ionic Liquid Solvents Convert Sugars to 5-Hydroxymethylfurfural. *Science* **2007**, 316 (5831), 1597-1600.

182. Su, Y.; Brown, H. M.; Huang, X.; Zhou, X.-d.; Amonette, J. E.; Zhang, Z. C., Single-step conversion of cellulose to 5-hydroxymethylfurfural (HMF), a versatile platform chemical. *Applied Catalysis A: General* **2009**, 361 (1-2), 117-122.

183. Ebner, G.; Schiehser, S.; Potthast, A.; Rosenau, T., Side reaction of cellulose with common 1-alkyl-3-methylimidazolium-based ionic liquids. *Tetrahedron Letters* **2008**, 49 (51), 7322-7324.

184. Atwell, B. J.; Henery, M. L.; Whitehead, D., Sapwood development in *Pinus radiata* trees grown for three years at ambient and elevated carbon dioxide partial pressures. *Tree Physiology* **2003**, *23* (1), 13-21.
185. Liu, Q. B.; Janssen, M. H. A.; van Rantwijk, F.; Sheldon, R. A., Room-temperature ionic liquids that dissolve carbohydrates in high concentrations. *Green Chemistry* **2005**, *7* (1), 39-42.
186. Laus, G.; Bentivoglio, G.; Schottenberger, H.; Kahlenberg, V.; Kopacka, H.; Röder, T.; Sixta, H., Ionic liquids: current developments, potential and drawbacks for industrial applications. *Lenzinger Berichte* **2005**, *84*, 71-85.
187. Lucas, M.; Macdonald, B. A.; Wagner, G. L.; Joyce, S. A.; Rector, K. D., Ionic Liquid Pretreatment of Poplar Wood at Room Temperature: Swelling and Incorporation of Nanoparticles. *ACS Applied Materials & Interfaces* **2010**, *2* (8), 2198-2205.
188. Li, Q.; Jiang, X. L.; He, Y. C.; Li, L. Z.; Xian, M.; Yang, J. M., Evaluation of the biocompatible ionic liquid 1-methyl-3-methylimidazolium dimethylphosphite pretreatment of corn cob for improved saccharification. *Applied Microbiology and Biotechnology* **2010**, *87* (1), 117-126.
189. Giannuzzi, J. L. T. Mechanisms for Improved Saccharification of Lignocellulosic Biomass for Bio-Fuel Production: Pre-treatment Methods to Enhance Glucose Yields from *Miscanthus giganteus*. Imperial College London, London, 2009.
190. Lynd, L. R., Overview and Evaluation of Fuel Ethanol From Cellulosic Biomass: Technology, Economics, the Environment, and Policy. *Annual Review of Energy and the Environment* **1996**, *21* (1), 403-465.
191. Lau, M.; Gunawan, C.; Dale, B., The impacts of pretreatment on the fermentability of pretreated lignocellulosic biomass: a comparative evaluation between ammonia fiber expansion and dilute acid pretreatment. *Biotechnology for Biofuels* **2009**, *2* (1), 30.
192. Varanasi, S.; Schall, C. A.; Dadi, A. P.; Anderson, J.; Rao, K.; Paripati, R. P.; Kumar, G. Biomass Pretreatment. 112291 A2, 2008.
193. Li, J.; Henriksson, G.; Gellerstedt, G., Lignin depolymerization/repolymerization and its critical role for delignification of aspen wood by steam explosion. *Bioresour. Technol.* **2007**, *98* (16), 3061-3068.
194. Tao, F. R.; Song, H. L.; Chou, L. J., Efficient process for the conversion of xylose to furfural with acidic ionic liquid. *Can. J. Chem.-Rev. Can. Chim.* **2011**, *89* (1), 83-87.
195. Playne, M. J.; Wallis, A. F. A., Determination of pentose sugars in fermentation solutions by a simple gas chromatographic procedure. *Biotechnology Letters* **1982**, *4* (10), 679-684.

196. Hosseini, S. A.; Lambert, R.; Kucherenko, S.; Shah, N., Multiscale Modeling of Hydrothermal Pretreatment: From Hemicellulose Hydrolysis to Biomass Size Optimization. *Energy & Fuels* **2010**, *24* (9), 4673-4680.
197. Chang, C.; Ma, X.; Cen, P., Kinetics of Levulinic Acid Formation from Glucose Decomposition at High Temperature. *Chinese Journal of Chemical Engineering* **2006**, *14* (5), 708-712.
198. Sun, N.; Rodriguez, H.; Rahman, M.; Rogers, R. D., Where are ionic liquid strategies most suited in the pursuit of chemicals and energy from lignocellulosic biomass? *Chemical Communications* **2011**, *47* (5), 1405-1421.
199. Beguin, P.; Aubert, J. P., The biological degradation of cellulose. *Fems Microbiology Reviews* **1994**, *13* (1), 25-58.
200. Lee, Y.-H.; Robinson, C. W.; Moo-Young, M., Evaluation of organosolv processes for the fractionation and modification of corn stover for bioconversion. *Biotechnology and Bioengineering* **1987**, *29* (5), 572-581.
201. Frederick Jr, W. J.; Lien, S. J.; Courchene, C. E.; DeMartini, N. A.; Ragauskas, A. J.; Lisa, K., Co-production of ethanol and cellulose fiber from Southern Pine: A technical and economic assessment. *Biomass and Bioenergy* **2008**, *32* (12), 1293-1302.
202. Oh, K. K.; Kim, Y. S.; Yoon, H. H.; Tae, B. S., Pretreatment of lignocellulosic biomass using combination of ammonia recycled percolation and dilute-acid process. *J. Ind. Eng. Chem.* **2002**, *8* (1), 64-70.
203. Brosse, N.; Sannigrahi, P.; Ragauskas, A., Pretreatment of *Miscanthus x giganteus* Using the Ethanol Organosolv Process for Ethanol Production. *Ind. Eng. Chem. Res.* **2009**, *48* (18), 8328-8334.
204. Zhu, J. Y.; Pan, X. J.; Wang, G. S.; Gleisner, R., Sulfite pretreatment (SPORL) for robust enzymatic saccharification of spruce and red pine. *Bioresour. Technol.* **2009**, *100* (8), 2411-2418.
205. Rahman, M.; Qin, Y.; Maxim, M. L.; Rogers, R. D. Ionic liquid systems for the processing of biomass, their components and/or derivatives, and mixtures thereof. 2010/056790 A1, 2010.